

The copyright of this thesis vests in the author. No quotation from it or information derived from it is to be published without full acknowledgement of the source. The thesis is to be used for private study or non-commercial research purposes only.

Published by the University of Cape Town (UCT) in terms of the non-exclusive license granted to UCT by the author.

**An investigation into the biocatalytic
application of the thermostable nitrile
hydratase from the thermophilic strain
Geobacillus pallidus RAPc8**

by

Idan Chiyanzu

BSc (UNZA), MSc (UCT)

**Thesis Presented for the Degree of
DOCTOR OF PHILOSOPHY
in the Department of Chemical Engineering
UNIVERSITY OF CAPE TOWN**



December 2008

An investigation into the of biocatalytic application of the thermostable nitrile hydratase from the thermophilic strain *Geobacillus pallidus* RAPc8

Abstract:

Nitrile hydratases (NHases) are bacterial metalloenzymes that catalyze the hydration of nitriles to their corresponding amides. The enzymes have been found in several microorganisms and participate in the metabolism of nitrile compounds as source of carbon and nitrogen. The commercial use of NHases is well recognized and has prompted research interest as well as the application of the enzymes in the manufacture of commodity amide chemicals. This has largely been due to the versatile nature of the enzymes, associated with their physiochemical properties and broad substrate specificity. However, the widespread application of nitrile-converting enzymes in the industrial processes has been restricted in part by the thermal instability of the mesophilic-derived enzymes, and thus there is an increased focus on NHases from thermophilic microorganisms.

A novel moderately thermophilic microorganism, *Geobacillus pallidus* RAPc8, was isolated by our collaborators (Pereira and co-workers, 1998). The strain has an optimal growth temperature of 65°C and constitutively expresses a thermostable nitrile hydratase. The gene cluster containing the nitrile hydratase were cloned, sequenced, and inducibly expressed in *E. coli* BL21 (DE3) to levels of approximately 49 U/mg. The NHase was purified by four steps including heat treatment, ammonium sulfate precipitation, hydrophobic interaction chromatography and ion exchange chromatography.

In the present study, the enzyme was purified by 5-fold increase, with a 66.7% yield from the cell-free extract of the *E. coli* BL21 (DE3) strain. The purified NHase was found to consist of two subunits (α -subunit, 28 kDa; β -subunit, 29 kDa) and showed a maximum activity at 60°C and a pH 7. In the presence of positive monovalent metal ions (K^+) and positive bivalent metal ions (Ba^{2+} , Mg^{2+} , Co^{2+} , and Fe^{2+}), the NHase activity was enhanced; however, transition metal ions (Mn^{2+} , Zn^{2+} and Cu^{2+}) inhibited the enzyme activity at the concentrations tested. The inhibition by Cu^{2+} and Zn^{2+} on the NHase appears to be partly due to the high affinity of the metal ions for

cysteine residues that are present in the enzyme active site and are essential for activity. The effects of monophasic and biphasic organic/aqueous cosolvent systems were studied in view of the practical usefulness of organic solvents for application of nitrile hydratase in a variety of industrially-important reactions. In the presence of 10% non-polar (water-immiscible) cosolvents such as ethyl acetate, toluene and benzene, NHase activity was enhanced. Formaldehyde, methanol, 1, 4-dioxane, and ethanol, employed as water-miscible cosolvents, caused decreases in the NHase activity. The highest deleterious effect was observed in formaldehyde (with relative activity of 20 %). The influence of substrate concentration on the NHase activity showed that enzyme activity increased with increase in substrate concentration until a maximum at 100 mM, and thereafter the high substrate concentrations inhibited the enzyme activity. The substrate inhibition constant was estimated to be $K_i = 101.0$ mM, while kinetic parameters for the *G. pallidus* RAPc8 where $K_m = 10.2$ mM, $V_{max} = 48.1 \mu\text{mol.mL}^{-1}.\text{min}^{-1}$ and $k_{cat} = 629.9 \text{ s}^{-1}$ using 3-cyanopyridine substrate.

In their native form, NHases are generally labile. In order to develop practical biocatalysts for use in amide production, it is therefore desirable to improve the stability of the NHase. In this regard, immobilization of enzymes is considered a valuable modification for industrial application, as the biocatalysts can be re-used, easily separated from reaction mixtures, are convenient to handle, and their activity is retained. In the present study, the purified *G. pallidus* RAPc8 NHase was immobilized on a wide variety of support materials (Eupergit[®]C, Amberlite XAD-4, Sepabeads Series EC, SE-Sephadex, DEAE-Sephadex A 50, Dowex, and Super-Q-Toyopearl, Controlled Pore Glass beads, and Bio-Beads) using different techniques including covalent binding, adsorption, entrapment and cross-linking. The biocatalyst in which the NHase was immobilized on Eupergit[®]C and cross-linked with EDAC exhibited the best immobilization efficiency (92.3 %) among all the biocatalysts studied. It was found that immobilization of NHase on supports was not sufficient, and cross-linking was required to allow multipoint attachment that would stabilize the three-dimensional structure. A comparative study of the properties of the soluble and the immobilized enzyme was conducted, in which pH, temperature, thermostability, operational stability, organic solvents, reusability profiles and kinetic parameters were examined. Both the soluble and immobilized NHase showed similar optimum temperature (60°C) and pH (7.0), although the immobilized NHase was found to be more stable than the soluble enzyme. For

example, operational pH and temperature ranges were broader for Eupergit[®]C-EDAC NHase, and the thermoinactivation of the Eupergit[®]C-immobilized NHase was slower than that of the soluble enzyme; the immobilized NHase activity was retained at more than 80% of the original level, at 60°C after 1 hour. In repeated usage, 85.7 % of initial activity was retained after re-use in 8 batch cycles. Moreover, the Eupergit[®]C-immobilized NHase converted 3-cyanopyridine at concentrations of up to 300 mM, a reaction which was not observed in the soluble counterpart. Immobilization resulted in an increase in the K_m to 17.7 mM and a decrease in V_{max} to 4.5 $\mu\text{mol}/\text{min}$ determined at 50°C using 3-cyanopyridine as substrate. Moreover, the immobilized NHase showed higher relative activities than those of the soluble NHase in the presence of 10% (v/v) monophasic and biphasic solvent systems, especially solvents such as ethyl acetate, toluene, cyclohexane, methanol, acetone and ethanol, all had relative values above 100%. Study of thermal deactivation kinetics at four temperatures (40, 50, 60 and 70°C) revealed that immobilization of the biocatalyst resulted in appreciable stabilization. By comparison of the half-life ($t_{1/2}$) values obtained at 60°C, it can be concluded that the immobilized NHase was almost 6-fold more stable than the soluble NHase. These properties indicated that the Eupergit[®]C-EDAC NHase could find application in industrial hydration of nitriles to their corresponding amides.

The biocatalyst was further applied in a packed-bed reactor and results expressed in terms of substrate conversion (δ) and volumetric productivity (Q). It was found that while substrate conversion decreased with increase in substrate feed concentration, on the other hand, the volumetric productivity increased with increase in feed substrate concentration when the flow rate and reactor volume were kept constant. The substrate conversion (%) decreased with increased flow rate, while volumetric productivity increased with increase in flow rate at all the substrate concentrations tested. Bioreactor studies of the immobilized enzyme revealed maximum volumetric productivity of 48.7 g/L/h for a system with a flow rate of 3 mL/min, substrate concentration of 15.6 g/L, using a packed bed volume of 7.54 mL (equivalent to 5 g biocatalyst). A kinetic model of the hydrolysis process was developed and gave a good fit with experimental results. This work illustrates that understanding biocatalyst properties is key in the development of improved biocatalysts needed in industrial chemistry.

Table of Contents

CONTENTS	PAGE
Abstract.....	i
Table of contents.....	iv
List of Figure.....	xiii
List of Tables.....	xxii
List of Schemes.....	xxiv
List of Abbreviations.....	xxv
Acknowledgements.....	xxvii
Declaration.....	xxviii
Outputs.....	xxix

CHAPTER ONE: INTRODUCTION

1.1 Introduction and problem statement.....	1
1.2 Motivation.....	4
1.3 Hypothesis.....	5
1.4 Objectives.....	5
1.5 Experimental Methodology.....	6
1.6 Organization of Thesis.....	6

CHAPTER TWO: LITERATURE REVIEW

2.1 INTRODUCTION.....	8
2.2 BIOCATALYSIS.....	9
2.3 DEVELOPMENT OF A BIOCATALYSIS PROCESS.....	10
2.3.1 Biocatalytic development cycle.....	10
2.3.2 Biocatalyst selection for a chemical synthesis.....	11
2.3.3 Biocatalyst production by fermentation in a suitable expression systems.....	12
2.3.4 Biocatalyst characterisation for optimal reaction.....	12
2.3.5 Immobilization and performance of the immobilized biocatalysts.....	13
2.3.6 Immobilized enzyme reactors.....	14
2.3.7 Downstream processing of synthesized products in biocatalytic processes.....	17

2.4 NITRILE OR CYANO-CONTAINING COMPOUNDS.....	17
2.4.1 Occurrence and roles of nitrile-converting enzymes.....	18
2.5 ENZYMOLOGY OF NITRILE HYDRATASE (NHase).....	21
2.5.1 Molecular size of the NHases.....	22
2.5.2 Cofactors for the NHase.....	22
2.5.3 Structure of the NHase.....	22
2.5.4 Structure of the active centre of the NHase.....	23
2.5.5 Mechanism of action for the NHase.....	24
2.5.6 Substrate specificity of the NHases.....	26
2.5.7 Functional characterisation and applications of NHases in biocatalysis.....	29
2.5.8 Other aspects of NHase applications.....	31
2.5.9 Application of NHases in bi-phasic solvent systems.....	31
2.6 THERMOSTABLE ENZYMES AND THEIR BIOTECHNOLOGICAL APPLICATION...32	
2.6.1 The novel <i>G. pallidus</i> RAPc8 nitrile hydratase.....	33
2.6.2 Cloning, sequencing and expression of genes from <i>G. pallidus</i> RAPc8.....	34
2.6.3 The crystal structure of the <i>G. pallidus</i> RAPc8 NHase.....	35
2.6.4 Protein engineering of the <i>G. pallidus</i> RAPc8 NHase.....	36
2.7 CONCLUSIONS.....	36

CHAPTER THREE: PRODUCTION, PURIFICATIONS AND CHARACTERISATION OF *G. pallidus* RAPc8 NHase

3.1 INTRODUCTION.....	38
3.1.1 Model reaction for <i>G. pallidus</i> RAPc8 NHase in production of nicotinamide.....	41
3.2 MATERIALS AND METHODS.....	42
3.2.1 Materials.....	42
3.2.1.1 Chemicals and Reagents.....	42
3.2.1.2 Microorganisms.....	43
3.2.1.3 Media.....	43
3.2.1.3.1 Agar Luria Bertani (LB) media.....	43
3.2.1.3.2 Seed and cultivation medium for <i>E. coli</i> BL21 (DE3) pLysS...43	
3.2.2 Methods.....	44

3.2.2.1 Growth and induction of <i>E. coli</i> BL21 (DE3) cells.....	44
3.2.2.1.1 Plate culture production.....	44
3.2.2.1.2 Growth of seed culture.....	44
3.2.2.1.3 Expression of <i>G. pallidus</i> RAPc8 NHase in shake flasks.....	44
3.2.2.1.4 Expression of <i>G. pallidus</i> RAPc8 NHase in a 5 L BioFlo fermentor.....	44
3.2.2.2 Harvesting of the <i>E. coli</i> BL21 (DE3) cells.....	45
3.2.2.3 Cell disruption by sonication.....	45
3.2.2.4 Purification of <i>G. pallidus</i> RAPc8 NHase extracts.....	45
3.2.2.4.1 Heat purification of crude enzyme extracts.....	46
3.2.2.4.2 Ammonium sulfate precipitation purification method.....	46
3.2.2.4.3 Hydrophobic interaction chromatography (HIC).....	46
3.2.2.4.4 Ion exchange chromatography (IEX).....	47
3.2.2.5 SDS-PAGE electrophoresis analysis of the purified <i>G. pallidus</i> RAPc8 NHase	47
3.2.2.6 Standard Biorad assay procedure for Protein concentration determination.....	47
3.2.2.7 Nitrile hydratase activity assay.....	49
3.2.2.8 HPLC quantification of unreacted substrates and reaction products.....	50
3.2.2.9 Investigation of reaction conditions for <i>G. pallidus</i> RAPc8 NHase biocatalytic reactions.....	53
3.2.2.9.1 Determining the amount of enzyme needed to obtain satisfactory substrate conversion for characterization of the NHase.....	53
3.2.2.9.2 Profile of product formation with respect to reaction time in NHase reactions	54
3.2.2.9.3 Determination of substrate concentration on the NHase activity in biocatalytic reactions.....	54
3.2.2.9.4 Determination of the pH optimal of NHase in the biocatalytic reaction.....	55
3.2.2.9.5 Determination of the temperature optimal for the NHase in the biocatalytic reaction.....	55

3.2.2.9.6 Evaluation of the thermostability of NHase at 40 to 70°C over 3 hours.....	56
3.2.2.9.7 Effect of addition of metal ions to the reaction medium on the NHase-hydration activity.....	56
3.2.2.9.8 Effect of organic-aqueous co-solvents on the activity of NHase.....	56
3.2.2.9.9 Analysis of the substrate specificity and kinetic parameters of the <i>G. pallidus</i> RAPc8 NHase.....	57
3.3 RESULTS AND DISCUSSION.....	57
3.3.1 Comparison of the growth curve and biomass yield of <i>E. coli</i> (DE3) in shake flasks and BioFlo fermenter.....	58
3.3.2 Purification of <i>G. pallidus</i> RAPc8 NHase.....	59
3.3.2.1 NHase extract purification by heat treatment strategy.....	60
3.3.2.2 NHase purification by ammonium sulfate precipitation.....	60
3.3.2.3 NHase purification by hydrophobic interaction chromatography (HIC)....	60
3.3.2.4 NHase purification by ion exchange chromatography (IEX).....	61
3.3.2.5 Purification table for the <i>G. pallidus</i> RAPc8 NHase.....	63
3.3.3 SDS-polyacrylamide electrophoresis analysis of <i>G. pallidus</i> RAPc8 NHase.....	63
3.3.4 HPLC analysis of products and unreacted substrates from a <i>G. pallidus</i> RAPc8-catalyzed reaction.....	65
3.3.5 Optimization of conditions for hydration of nitriles by <i>G. pallidus</i> RAPc8 NHase.....	66
3.3.5.1 Determination of NHase-to-substrate ratio for optimal percent substrate conversion.....	67
3.3.5.2 Determination of the effect of increasing substrate concentration on NHase activity.....	68
3.3.5.3 Evaluation of reaction time on substrate conversion using <i>G. pallidus</i> RAPc8 NHase.....	70
3.3.5.4 Determination of the temperature optimum for the <i>G. pallidus</i> RAPc8 NHase biocatalytic reaction.....	71

3.3.5.5 Determination of pH optimum for the <i>G. pallidus</i> RAPc8 NHase biocatalytic reaction.....	73
3.3.5.6 Evaluation of the thermal stability of NHase at 40 to 70°C over 80 min..	74
3.3.5.7 Effect of cosolvent organic/aqueous systems on the catalytic activity of <i>G. pallidus</i> RAPc8 NHase.....	76
3.3.5.7.1 Effect of miscible organic/aqueous cosolvent systems on NHase activity.....	77
3.3.5.7.2 Effect of immiscible organic/aqueous cosolvent system on NHase activity.....	77
3.3.5.7.3 Effect of <i>log P</i> values of solvents on the NHase activity.....	78
3.3.5.8 Effect of metal ions on the activity of <i>G. pallidus</i> RAPc8 NHase.....	79
3.3.5.9 Determination of kinetic parameters and substrate specificity for <i>G. pallidus</i> RAPc8 NHase.....	82
3.3.5.9.1 Measurement of reaction rates for nicotinamide production.....	82
3.3.5.9.2 Use of the Hanes-Woolf and Eadie-Scatchard plots to determine the kinetic parameters of the <i>G. pallidus</i> RAPc8 NHase.....	83
3.3.5.9.3 Determination of V_{\max} , K_m and k_{cat} values for <i>G. pallidus</i> RAPc8 NHase.....	85
3.3.5.9.4 Comparison of 2-cyano-, 3-cyano and 4-cyanopyridine, as substrates for <i>G. pallidus</i> RAPc8 NHase.....	87
3.4 CONCLUSION.....	88

CHAPTER FOUR: DEVELOPMENT OF AN IMMOBILIZED BIOCATALYST USING A RECOMBINANT NHase FROM *Geobacillus pallidus* RAPc8

4.1 INTRODUCTION- Stabilization of the <i>G. pallidus</i> RAPc8 NHase by immobilization.....	91
4.1.1 Old and new methods for immobilization of enzymes.....	92
4.1.1.1 Adsorption and ionic binding as immobilization methods.....	92
4.1.1.2 Cross-linking of enzymes as immobilization technique.....	93
4.1.1.3 Covalent binding of the enzymes as an immobilization technique.....	94

4.1.1.4	Entrapment of enzymes as an immobilization technique.....	96
4.1.1.5	Metal-chelating of enzyme as an immobilization method.....	97
4.1.2	The estimation of deactivation kinetics for the <i>G. pallidus</i> RAPc8 NHase.....	98
4.1.2.1	Half-life of the <i>G. pallidus</i> RAPc8 NHase.....	99
4.1.2.2	Activation energy (E_a) determination for deactivation of <i>G. pallidus</i> RAPc8 NHase.....	99
4.2	MATERIALS AND METHODS.....	100
4.2.1	Materials.....	100
4.2.2	Experimental Methods.....	100
4.2.2.1	Immobilization of NHase by entrapment in Ca-alginate beads.....	100
4.2.2.2	Immobilization of NHase by covalent binding of Eupergit [®] Cand CM...101	101
4.2.2.3	Covalent immobilization on Eupergit [®] C followed by cross-linking with glutaraldehyde and EDAC.....	101
4.2.2.4	Immobilization of NHase on EDA-activated Amberlite XAD-4.....	101
4.2.2.5	Immobilization of NHase on GA-activated Amberlite XAD-4.....	102
4.2.2.6	Immobilization of NHase on Sepabeads EC-series.....	102
4.2.2.6.1	Immobilization of NHase on epoxy Sepabeads (EC-EP) support.....	102
4.2.2.6.2	Immobilization of NHase on amino-epoxy Sepabeads (EC-HFA).....	102
4.2.2.6.3	Immobilization of NHase on ethylendiamino-Sepabeads (EC-EA).....	103
4.2.2.6.4	Immobilization of NHase on hexamethyldiamino-Sepabeads (EC-HA) support.....	103
4.2.2.6.5	Immobilization of NHase onto iminodiacetic-Sepabeads (EC-IDA).....	104
4.2.2.7	Immobilization of NHase on anionic exchanger resins Dowex [®] and DEAE-Sephadex.....	104
4.2.2.8	Immobilization of NHase on cationic exchanger resins Super-Q-Toyopearl and SE-Sephadex	105
4.2.2.9	Immobilization of NHase by adsorption on glass and bio-beads.....	105

4.2.2.10 Determination of immobilized NHase activity.....	105
4.2.2.11 Characterisation of the immobilized NHase biocatalyst.....	106
4.2.2.11.1 Estimation of the loading and immobilization efficiencies of immobilized NHase.....	106
4.2.2.11.2 Comparison of the effect of pH optimal pH of soluble and immobilized NHase.....	107
4.2.2.11.3 Comparison of the effect of temperature on soluble and immobilized NHase.....	107
4.2.2.11.4 Comparison of the effect of water-miscible and immiscible organic cosolvents on NHase activity.....	108
4.2.2.11.5 Investigation of the thermostability of the Eupergit [®] -immobilized NHase.....	108
4.2.2.11.6 Investigation of reusability and recycled use of the immobilized NHase.....	108
4.2.2.11.7 Determination of the effect of substrate concentration on Eupergit [®] -immobilized NHase.....	109
4.2.2.11.8 Kinetic analysis of immobilized <i>G. pallidus</i> RAPc8 NHase using 3-cyanopyridine as substrate.....	109
4.2.2.11.9 Estimation of deactivation rate constant (k_d) and half-life time ($t_{1/2}$) for <i>G. pallidus</i> RAPc8 NHase.....	109
4.3 RESULTS AND DISCUSSION.....	110
4.3.1 Immobilization by covalent binding of NHase.....	110
4.3.2 Immobilization by ionic binding of NHase.....	113
4.3.3 Immobilization by metal chelation of NHase.....	115
4.3.4 Alginate entrapment of the <i>G. pallidus</i> RAPc8 NHase.....	118
4.3.5 Optimization of conditions for biocatalytic hydration of 3-cyanopyridine immobilized <i>G. pallidus</i> RAPc8 NHase.....	121
4.3.5.1 Comparison of effects pH on the activity of the soluble and immobilized NHase.....	121
4.3.5.2 Comparison of the effect of temperature on activity of the soluble and immobilized NHase.....	123

4.3.5.3 Effect of 10 % (v/v) organic co-solvent systems on immobilized <i>G. pallidus</i> RAPc8 NHase activity.....	124
4.3.5.3.1 Comparison of the soluble and immobilized NHase activity in presence of miscible and immiscible co-solvents	125
4.3.5.3.2 Effect of <i>log P</i> values of solvents on the NHase activity.....	127
4.3.5.4 Evaluation of the thermal stability of the immobilized <i>G. pallidus</i> RAPc8 NHase.....	129
4.3.5.5 Investigation of the reusability or recycled use of the Eupergit®C-immobilized NHase.....	130
4.3.5.6 Investigation of the effects of substrate concentration on the Eupergit®C-immobilized NHase activity.....	132
4.3.5.6.1 Evaluation and comparison of the substrate inhibition constant K_i for the EupergitC-immobilized and soluble NHase using Haldane's model.....	133
4.3.5.7 Measurement of kinetic parameters of immobilized <i>G. pallidus</i> RAPc8 NHase.....	134
4.3.5.8 Determination of the deactivation parameters for the Eupergit®C-immobilized <i>G. pallidus</i> RAPc8 NHase.....	137
4.3.5.8.1 Estimation of deactivation constant k_d and half-life $t_{1/2}$	137
4.3.5.8.2 Determination of the activation energy E_a for <i>G. pallidus</i> RAPc8 NHase.....	138
4.4 CONCLUSION.....	139

CHAPTER FIVE: DESIGN, PERFORMANCE AND ANALYSIS OF A PACKED BED REACTOR CONTAINING EUPERGIT®C –IMMOBILIZED *G. pallidus* RAPc8 NHase

5.1 INTRODUCTION.....	142
5.1.1 Theory and model for packed bed reactor design and operation.....	143
5.2 MATERIALS AND METHODS.....	145
5.2.1 Materials.....	145
5.2.2 Equipment and Methods.....	146
5.2.2.1 Packed bed reactor (PBR).....	146

5.2.2.1.1 Investigation of the effects of flow rate on packed bed fluidization.....	147
5.2.2.1.2 Estimation of void fraction (ϵ) for the packed bed reactor.....	148
5.2.2.1.3 Steady-state determination in a packed bed reactor.....	148
5.2.3.1.4 Determination of the performance of Eupergit®C-immobilized NHase the PBR.....	148
5.2.2.2 Investigation of the operational stability of the Eupergit®C-immobilized NHase in a continuous stirred tank reactor.....	149
5.2.3.3 Analytical methods.....	150
5.3 RESULTS AND DISCUSSION.....	150
5.3.1 Investigation of the effect of flow rate on bed fluidization.....	150
5.3.2 Investigation of the performance of Eupergit®C-immobilized <i>G. pallidus</i> RAPc8 NHase in the packed bed reactor.....	151
5.3.2.1 The effect of substrate concentration on substrate conversion and volumetric productivity.....	152
5.3.2.2 The effect of flow rate on substrate conversion and volumetric productivity.....	154
5.3.2.3 The effect bed height on volumetric productivity of the PBR.....	157
5.3.2.4 Investigation of effect of temperature on the volumetric productivity of the PBR.....	159
5.3.2.5 Comparison of operational stability of immobilized NHase in PBR and CSTR.....	161
5.3.2.6 Determination of the deactivation constant <i>G. pallidus</i> RAPc8 NHase in the packed bed reactor.....	162
5.4 CONCLUSION.....	164
CHAPTER SIX: GENERAL DISCUSSION AND CONCLUSION.....	166
FUTURE WORK.....	173
APPENDICES.....	179
REFERENCES.....	190

List of Figures

	PAGE
Fig. 2.1: Schematic diagram of a biocatalysis cycle in enzymatic process development....	11
Fig. 2.2: Schematic diagrams of main reactors employing immobilized enzymes.....	16
Fig. 2.3: Cyanoglycosides most abundant in plants.....	18
Fig. 2.4: Enzyme pathways of nitrile degradation established in microbial systems.....	20
Fig. 2.5: Representation of the $\alpha_2\beta_2$ heterotetramer. The interface between subunits contains the active site metal ion.....	23
Fig. 2.6: Essential commodity amides produced using NHase biocatalysts.....	30
Fig. 3.1: Synthesis of nicotinamide from the hydration of 3-cyanopyridine (3-CNP) by NHase.....	42
Fig. 3.2: Standard curve for protein determination using Bradford's reagent the absorbance was read at 595 nm. $R^2=0.997$	48
Fig. 3.3: Chromatogram of 3-cyanopyridine: Column C18 (4.6 by 150 mm), mobile phase: acetonitrile/10mM $\text{KH}_2\text{PO}_4\text{-H}_3\text{PO}_4$ buffer (1:4), pH 2.8, Abs 235, Flow 1 mL/min.....	51
Fig. 3.4: Standard curve for the 3-cyanopyridine concentration using peak areas obtained from HPLC. Detection at A_{235} , Flow rate 1mL/min and mobile phase 10 mM $\text{K}_2\text{HPO}_4/\text{KH}_2\text{PO}_4\text{-H}_3\text{PO}_4$ buffer (1:4 v/v), pH 2.8, $R^2=0.993$	51

Fig. 3.5:	Chromatogram of nicotinamide: Column C18 (4.6 by 150 mm), mobile phase: acetonitrile/10mM $\text{KH}_2\text{PO}_4\text{-H}_3\text{PO}_4$ buffer (1:4), pH 2.8, Abs 235, Flow 1 mL/min.....	52
Fig. 3.6:	Standard curve for the nicotinamide concentration using peak areas obtained from HPLC. Detection at A_{235} , Flow rate 1mL/min and mobile phase 10 mM $\text{K}_2\text{HPO}_4/\text{KH}_2\text{PO}_4\text{-H}_3\text{PO}_4$ buffer (1:4 v/v), pH 2.8, $R^2=0.992$	53
Fig. 3.7:	Change in the biomass concentration of the <i>E. coli</i> BL21 (DE3) pLysS in LB media shown as cell density (OD_{600}). Cultivation was conducted in shake flask (1L) and BioFlo fermenter (5L), induced by addition of 4 mL of 100 mM IPTG after 2h30min of growth.....	59
Fig. 3.8:	Hydrophobic interaction chromatography (HIC) of the NHase extracts from $(\text{NH}_4)_2\text{SO}_4$ fractionation purification stage, on Hiloal 16/10 Phenyl-Sepharose HP. Protein solution (25 mL) was applied to the column. Eluent A: 1M ammonium sulfate in 50mM potassium phosphate buffer (pH 7.2). Eluent B: 50 mM potassium phosphate buffer (pH 7.2). Fractions (2mL) were collected at a flow rate of 3 mL/min. Fractions 13 to 23 were collected during gradient elution buffer B (0 – 100%).	61
Fig. 3.9:	Ion exchange chromatography (IEX) of NHase extract from the HIC purification stage on Hiprep 16/10 Q-Sepharose. Protein solution (25 mL) was applied to the column. Eluent A: 25 mM potassium phosphate buffer (pH 7.2). Eluent B: 0.5 M sodium chloride in 25 mM potassium phosphate buffer (pH 7.2). Fractions (2 mL) were collected at a flow rate of 3 mL/min. Fractions 35 to 45 were collected during gradient elution buffer B (0 – 100%).....	62

Fig. 3.10:	Sodium dodecyl sulfate/polyacrylamide gel electrophoresis of NHase purification. Lane M, molecular-weight marker; Lane 1, crude NHase extract; Lane 2, (NH ₄) ₂ SO ₄ extract; Lane 3, Heat-treated supernatant; Lane 4, pooled fractions from Q-Sepharose ion-exchange chromatography.....	64
Fig. 3.11:	HPLC chromatogram from 3-cyanopyridine hydration reaction mixture analyzed by LabChrom HPLC using a C 18 (4.6 x 150 mm), mobile phase: acetonitrile-10 mM K ₂ HPO ₄ /KH ₂ PO ₄ buffer (pH 2.8) 1:4 (v/v), flow rate: 1 mL/min at 235 nm.....	66
Fig. 3.12:	Effect of NHase-to-Substrate ratio on conversion of 3-cyanopyridine reaction carried out at 50°C in 50 mM of 3-cyanopyridine in 50mM potassium phosphate buffer, pH 7.2.....	68
Fig. 3.13:	Effect of substrate concentration on <i>G. pallidus</i> RAPc8 NHase activity. The enzyme was incubated in different concentration of 3-cyanopyridine (5 to 500mM) at 50°C in 50 mM potassium phosphate buffer, pH 7.2. Relative activity is expressed as percentage of the highest activity at 100 mM substrate concentration.....	70
Fig. 3.14:	Effect of reaction time on percent substrate substrate conversion. The NHase was incubated at 50 mM of 3-cyanopyridine in 50 mM potassium phosphate buffer (pH 7.2) at 50°C. At the indicated times, aliquots were withdrawn and the product and unreacted substrate analyzed by HPLC.....	71
Fig. 3.15:	Determination of the effect of temperature on <i>G. pallidus</i> RAPc8 NHase activity. Reaction mixture included 50mM of 3-cyanopyridine in 50 mM potassium phosphate buffer (pH 7.2) at different temperature (20 to 70°C). Relative activity is expressed as percentage of the highest activity, measured at 50°C.....	73

- Fig. 3.16:** Effect of pH on the activity of *G. pallidus* RAPc8 NHase activity was measured in a reaction mixture included 50 mM of 3-cyanopyridine in 50 mM of different pHs at 50°C. Relative activity is expressed as percentage of the highest activity, measured at pH 7.....74
- Fig. 3.17:** The measurement of thermostability of *G. pallidus* RAPc8 NHase. The NHase was incubated at different temperatures (40, 50, 60 and 70°C) for 80 min in 50 mM potassium phosphate buffer (pH 7.2). At the indicated time, aliquots were withdrawn and residual activity was measured at 50°C under the standard assay conditions and expressed as percentage activity of zero time (activity of NHase prior to incubation) taken as 100 %.....76
- Fig. 3.18:** Effect of monophasic and biphasic organic-aqueous cosolvent (with varying log P) on the activity of *G. pallidus* RAPc8 NHase. The organic-aqueous solvent system contained 10% organic solvent in 90% of 50 mM potassium phosphate buffer, pH 7.2. The NHase activity is expressed in relative activity (%) taking the reaction in potassium phosphate buffer as 100 %.....79
- Fig. 3.19:** Effect of metal ions on the activity of *G. pallidus* RAPc8 NHase. NHase was incubated for 5 min at 50°C in 3 mL reaction mixture containing 50 mM KH₂PO₄-K₂HPO₄ buffer (pH 7.2), 50 mM 3-cyanopyridine and different concentrations of metal ions.....81
- Fig. 3.20:** Effect of reaction time on nicotinamide produced using different concentrations of 3-cyanopyridine. NHase was incubated for 5 min at 50°C in 3 mL of reaction mixtures containing 50 mM KH₂PO₄-K₂HPO₄ buffer (pH 7.2) and final amount of the enzyme (0.14 mg). All experiments were conducted in duplicate.....83

Fig. 3.21:	The Hanes-Woolf plot for the <i>G. pallidus</i> RAPc8 NHase hydration of 3-cyanopyridine. NHase was incubated for 5 min at 50°C in 15 mL reaction mixture containing 50 mM K ₂ HPO ₄ -KH ₂ PO ₄ buffer (pH 7.2). Different concentrations of 3-cyanopyridine and 0.14 mg final concentration of NHase was used.....	84
Fig. 3. 22:	The Eadie-Scatchard plot for the <i>G. pallidus</i> RAPc8 NHase hydration of 3-cyanopyridine. NHase was incubated for 5 min at 50°C in 15 mL reaction mixture containing 50 mM K ₂ HPO ₄ -KH ₂ PO ₄ buffer (pH 7.2). Different concentrations of 3-cyanopyridine and 0.14 mg of NHase was used.....	85
Fig. 3.23:	Intermediates generated from <i>meta</i> directing effect of the electron-withdrawing cyano functional group.....	87
Fig. 4.1:	Structural representation of Eupergit® C.....	95
Fig. 4.2:	Calcium alginate: chemical and macroscopical structure.....	96
Fig. 4.3:	Iminodiacetic acid activated bead.....	97
Fig. 4.4:	Evaluation of loading efficiency of NHase protein on support carriers. Loading conditions: 20 mL NHase solution (10 mg protein), 5 g support-carrier, room temperature for 72 – 96 h.....	111
Fig. 4.5:	Evaluation of immobilization efficiency of the NHase on support carriers. Immobilization conditions: 20 mL NHase solution (containing 10 mg protein), 5 g support material, room temperature for 72 – 96 h.	113
Fig. 4.6:	Evaluation of loading efficiency of protein on support material. Loading conditions: 20 mL NHase solution (10 mg protein), 5 g support-carrier, room temperature for 72 – 96 h.....	114

Fig. 4.7:	Evaluation of immobilization efficiency of the NHase on ionic carriers. Immobilization conditions: 20 mL NHase solution (containing 10 mg protein), 5 g support material, room temperature for 48 h.....	115
Fig. 4.8:	Evaluation of loading efficiency of protein on metal chelating material. Loading conditions: 20 mL NHase solution (10 mg protein), 5 g support-carrier, room temperature for 72 – 96 h.....	116
Fig. 4.9:	Evaluation of immobilization efficiency of the NHase on metal chelating carriers. Immobilization conditions: 20 mL NHase solution (containing 10 mg protein), 5 g support material, room temperature for 72 – 96 h.....	117
Fig. 4.10:	Evaluation of loading efficiency of protein in Ca-alginate. Loading conditions: 20 mL NHase solution (10 mg protein), 5 g support-carrier, room temperature for 3 - 6 h.....	118
Fig. 4.11:	Comparison of the dependence of the hydrolytic activity of the soluble and immobilized NHase on pH. Acetic acid sodium acetate buffer (pH 4 to 6), potassium phosphate buffer (pH 6 to 8), Tris-HCl (pH 8 to 10), sodium hydrogen phosphate (pH 10 to 12).....	122
Fig. 4.12:	Comparison of the temperature dependence of the hydrolytic activity of the soluble and immobilized NHase at pH 7.2. Reaction carried out at different temperature in 50 mM potassium phosphate buffer, for 5 min. Relative activity was calculated based on the temperature at which the enzyme showed highest activity, taken as 100%.....	124
Fig. 4.13	Comparison of <i>log P</i> values for organic solvents with relative activities of the soluble and immobilized NHase. Relative activities for the reaction without organic solvent (with potassium phosphate only) was taken as 100%.....	128

- Fig. 4.14:** Evaluation of thermal stability of Eupergit[®]C-immobilized NHase. The enzyme was assayed at temperature 40 to 70°C in 50 mM potassium phosphate buffer, pH 7.2 for 80 min. At time intervals of 10 min, aliquots were withdrawn and NHase activity assayed. Relative activity was calculated taking initial activity (at time = 0) as 100 %.....130
- Fig. 4.15:** Effect of repeated use of the Eupergit[®]C-immobilized NHase for hydration of 50 mM 3-cyanopyridine solution. Biotransformation batch runs (5 min) were performed at 50°C in 50 mM potassium phosphate buffer (pH 7.2). Relative activity was calculated taking the initial enzyme activity (cycle 1) as 100%.....131
- Fig. 4.16:** Comparison of the effects of different substrate concentration on the soluble and immobilized NHase activity. The enzyme activity was measured in 50 mM potassium phosphate buffer (pH 7.2). Experiments were conducted at 50°C, with incubation for 5 min with enzyme amount (0.14 mg). Relative activity was calculated at the substrate concentration which gave the highest enzyme activity, taken as 100%.....133
- Fig. 4.17** A non-linear regression Haldene's Model was fitted to substrate inhibition data of soluble (a) and Eupergit[®]C-immobilized *G. pallidus* RAPc8 NHase (b) using Graphpad Prism 5 Software (Hearnes Corporation), K_i (soluble NHase) = 101.1 mM, $R^2=0.857$ and Sy. x =1 2.8 and K_i (immobilized NHase) = 194.7 mM, $R^2=0.9504$ and Sy. x = 2.85.....134
- Fig. 4.18:** Effect of incubation time on nicotinamide production using different substrate concentration. Immobilized NHase is incubated for 5 min at 50°C in 3 mL of activity assay system containing 50 mM K₂HPO₄-KH₂PO₄ buffer (pH 7.2) and final amount of the enzyme (0.14 mg).....135

Fig. 4.19:	Determination of kinetic constants by Hanes-Woolf graph method. Substrate concentration ranges (5 to 100 mM) were used and initial velocities were measured using linear equations described in Fig. 4.18.....	136
Fig. 4.20:	Determination of energy of activation E_a and pre-exponential constants A_d for the <i>G. pallidus</i> RAPc8 NHase.....	139
Fig. 5.1:	A schematic representation of the equipment used for continuous hydration of 3-cyanopyridine to nicotinamide. Bed diameter: 20 mm, substrate : 3-cyanopyridine, 50 mM potassium phosphate buffer, pH 7.2, Bed density 0.6, total biocatalysts weight 5 g, total biocatalyst, porosity: 0.35, Flow rate: 3 mL/min.....	146
Fig. 5.2:	Schematic representation for continuous hydration of 3-cyanopyridine by immobilized <i>G. pallidus</i> RAPc8 NHase at 50°C with stirring speed of 150 rpm. Bed diameter: 20 mm, substrate : 3-cyanopyridine, 50 mM potassium phosphate buffer, pH 7.2, Bed density 0.6, total biocatalysts weight 5 g total biocatalyst, porosity: 0.35, Flow rate: 3 mL/min.....	149
Fig. 5.3:	Investigation of the effects of flow rate on bed fluidization by determining variations in bed heights with a constant flow rate	151
Fig. 5.4:	Relationship between the concentrations of substrate in the feed stream with substrate conversion (%) at a flow rate of 3 mL/min.....	153
Fig. 5.5:	Relationship between the concentrations of substrate in the feed stream and volumetric productivity (g/L/h).....	154
Fig. 5.6:	Effect of flow rate of the feed on the substrate conversion (%) in packed bed reactor at 50°C at constant reactor volume.....	155

Fig. 5.7:	Effect of flow rate on the volumetric productivity in packed bed reactor at different substrate concentrations (0.52, 5.2, 10.4 and 15.6 g/L).....	156
Fig. 5.8:	Volumetric productivities at various bed heights. A maximum volumetric productivity of 45 g/L/h was obtained at a height of 2.4 cm (containing 5 g of biocatalyst, while the productivity declined with the increase in amount of biocatalyst added to the column.....	159
Fig. 5.9	The effect of temperature on the activity of the Eupergit®C-immobilized <i>G. pallidus</i> RAPc8 NHase in a packed bed reactor.....	160
Fig. 5.10:	Comparison in operational performance between the PBR and CSTR in production of nicotinamide at 50°C by immobilized <i>G. pallidus</i> RAPc8 NHase. Substrate concentration of 0.56 g/L, bed height of 2.4 cm, and flow rate of the feed solution at 3 mL/min.....	162
Fig. 5.11:	Semi log plot of ln (relative activity) against time for the optimal conditions from reactor performance analysis.....	163

List of Tables

	PAGE
Table 2.1: Summary of substrate selectivity of various NHases.....	28
Table 2.2: Operating conditions for amide production for three industrial NHases (Nagasawa <i>et al.</i> , 1995).....	30
Table 3.1: Bradford protein assay standard preparation.....	48
Table 3.2: Preparation of 3-cyanopyridine solution standards for HPLC analysis.....	50
Table 3.3: Preparation of nicotinamide solution standards for HPLC analysis.....	52
Table 3.4: Purification table for the <i>G. pallidus</i> RAPc8 NHase.....	63
Table 3.5: A summary of kinetic parameters for <i>G. pallidus</i> RAPc8 NHase.....	86
Table 4.1: A summary of loading and immobilization efficiencies of <i>G. pallidus</i> RAPc8 NHase.....	120
Table 4.2: Comparison of the influence of 10 % (v/v) organic solvent on the soluble NHase and Eupergit® C-immobilized NHase activity. The NHase activity is expressed in relative activity (%) taking the activity in potassium phosphate buffer as 100 %.....	127
Table 4.3: Summary of kinetic parameters for Eupergit® C-immobilized <i>G. pallidus</i> RAPc8 NHase.....	137
Table 4.4: A comparison of the deactivation coefficient (k_d) and half-life ($t_{1/2}$) values for immobilized <i>G. pallidus</i> RAPc8 NHase.....	138

Table 5.1: Properties of the Eupergit®C-immobilized NHase used in the experiments.....145

Table 5.2: Summary of effects of substrate concentration and flow rate (mean residence time) on substrate conversion and volumetric productivity in the packed bed reactor..157

University of Cape Town

List of Schemes

	PAGE
Scheme 2.1: Biochemical pathway for nitrile hydration (Kato <i>et al.</i> , 2000).....	21
Scheme 2.2: Proposed mechanism for NHase catalysis (Huang <i>et al.</i> , 1997; Mascharak <i>et al.</i> , 2001).....	25
Scheme 2.3: Proposed mechanism for NHase catalysis (Huang <i>et al.</i> , 1997; Yano <i>et al.</i> , 2008).....	25
Scheme 2.4: Proposed mechanism for NHase catalysis (Huang <i>et al.</i> , 1997; Mascharak <i>et al.</i> , 2004; Yano <i>et al.</i> , 2008).....	26
Scheme 4.1: Preparation of Schiff base cross-link between an enzyme and glutaraldehyde.....	93

Abbreviations

A	surface area of a packed bed reactor
<i>A</i>	absorbance
BSA	bovine serum albumin
3-CNP	3-cyanopyridine
C_i	initial substrate concentration
C_f	final substrate concentration
C_p	bulk product concentration
Da	Dalton
DO	dissolved oxygen
<i>E. coli</i>	<i>Escherichia coli</i>
EDAC	1-ethyl-3-(dimethylamino-propyl) carbodiimide, hydrochloride
EDA	ethylene diamine
FPLC	fast protein liquid chromatography
GA	glutaraldehyde
g	gram
GC	gas chromatography
HPLC	high performance liquid chromatography
h	hour
HIC	hydrophobic interaction chromatography
HPLC	high performance liquid chromatography
IEX	ionic interaction chromatography
IPTG	isopropyl- β -D-thiogalactopyranoside
k_{cat}	turnover number (s^{-1})
K_i	inhibition constant (mM)
K_m	Michaelis-Menten constant (mM)
k	kilo (10^3)
LB	Luria Bertani
L	liter
m	milli (10^{-3})
M	molar

min	minute
mL	millilitre
M _w	relative molecular weight
NA	nicotinamide
NHase	nitrile hydratase
nm	nanometer
OD	optical density
P	product
PAGE	polyacrylamide gel electrophoresis
pH _{opt}	pH optimum
Q	volumetric productivity
rpm	revolutions per minute
S	substrate
SDS-PAGE	sodium dodecyl sulfate polyacrylamide gel electrophoresis
T _{opt}	temperature optimum
U	μmol/mL.min
UV	ultraviolet
V_i	initial volume
V_f	final volume
V_{\max}	maximum reaction rate (μmol/min mg)
v/v	volume per volume
vvm	volume gas/(volume liquid/min)
w/v	weight per volume
δ	substrate fractional conversion
Z	axial coordinate
ε	void fraction
τ	mean residence time (sec)
°C	degrees Celsius
μ	micro (10 ⁻⁶)

Acknowledgements

I would like to thank and express my gratitude to my supervisor, Prof. Stephanie G. Burton for her involvement in this project, guidance and enthusiasm. Thank you for devoting your life to this pursuit.

I gratefully acknowledge Prof. Don A. Cowan of IMBM who provided valuable assistance in various aspects of microbiology and for providing the recombinant *E. coli* BL21 (DE3) strain I used in the project: without his help, this work would have been difficult to start. The technical assistance and academic insight provided by Dr Tsepo Tsekoa and Prof Trevor Sewell over the past few years are also greatly appreciated.

To my colleagues in Biocatalysis and Technical Biology Group (BTB) in the Department of Chemical Engineering, Refiloe Zwane, Chipso Mupure, Natasha Davids, James Sehata, Anne Gabathuse and Sean Gotoro, for their ideas and support in this project. Special thanks to Dr Marilize Le Roes-Hill.

I thank God, my parents, my family, and friends for the endless love and support throughout my academic career, without them this could not be possible.

Further thanks to all the people who assisted in maintaining the laboratory and ordering of chemicals and equipment, Simisha Pather-Elias and Kerry Horne. Not forgetting Frances Pocock for her efforts to keep the laboratory clean and orderly.

My gratitude is also extended to the National Research Foundation, Department of Chemical Engineering (University of Cape Town) and BTB group for the financial support.

Declaration

I declare that Development of biocatalytic application of the thermostable nitrile hydratase from the thermophilic strain *Geobacillus pallidus* RAPc8 is my own work, that it has not been submitted before for any degree or examination in any University, and that the sources I have used or quoted have been indicated and acknowledged as complete reference.

Idan Chiyanzu

December 2008

Signed:.....

Outputs

Manuscripts in preparation

Idan Chiyanzu, Don Cowan and Stephanie G. Burton. Immobilization of a nitrile hydratase (NHase) from *Geobacillus pallidus* RAPc8 nitrile hydratase: a way to overcome substrate inhibition and enhance stability (In progress).

Idan Chiyanzu, Don Cowan and Stephanie G. Burton. Continuous production of nicotinamide using a packed-bed reactor system with immobilized *Geobacillus pallidus* RAPc8 (NHase) (In progress).

Papers presented

Immobilization and functional characterisation of nitrile hydratase (NHase).’ I. Chiyanzu, D. Cowan, and S. G. Burton. Fifth national conference on biotechnology in Durban, 16th June, 2006.

Continuous production of nicotinamide using a packed-bed reactor system with immobilized *Geobacillus pallidus* RAPc8 (NHase).’ Authors: **I. Chiyanzu**, D. Cowan, and S. G. Burton. South Africa Institution of Chemical Engineers (Western Cape Branch). Research and Development Day Conference 2007, 26th June, 2007, Cape Town.

Immobilization and properties of a thermostable nitrile hydratase (NHase) from *Geobacillus pallidus* RAPc8.’ Authors: **I. Chiyanzu**, D. Cowan, and S. G. Burton. 13th European Congress on Biotechnology, Barcelona, Spain, 16-19 September 2007.

CHAPTER ONE

INTRODUCTION

1.1 Introduction and problem statement

One of the greatest challenges for the chemical industry today is its ability to achieve sustainable technologies that are environmentally benign. With the pressure to reduce rapidly growing industrial pollution and to enhance efficiency in industrial chemistry, biocatalysis is becoming an attractive alternative to conventional chemical processing. Biocatalysis is the application of whole cells or enzymes to carry out chemical transformations. Biocatalytic reactions can be carried out in aqueous media at ambient temperature and pH as compared with the harsh conditions common to conventional chemical processes. Moreover, highly chemo-, regio-, and stereoselective biotransformations can be performed simply, and this makes them economically attractive as well as environmentally acceptable. In some instances, chemo-enzymatic systems are being developed which combine conventional chemical catalysts and the attractive features of enzymes (specificity and selectivity). Examples of commercial commodity chemicals made by biocatalysis include fructose, insulin, amino acids, antibiotics, and acrylamide.

Industrial transformation of nitriles (cyano-compounds) to their corresponding amide derivatives has long been recognized as an important chemical process, but over the past two decades there has been a shift from a conventional copper-catalysed process, to newer processes where biocatalysts are widely employed (discussed in more detail below). Many of these commercialized biologically-based processes use whole cell catalysts in the synthesis of valuable chemical amide products. Compared with isolated enzymes, whole cell catalysts are assumed to be more readily available, inexpensively prepared and the enzymes in cells are protected from the external environment, making them more stable for long term use (Ishige *et al.*, 2005). However, their potential in bio-based processes, particularly for production of nicotinamide and acrylamide, has not been fully realized to date. This is attributed to a number of factors: firstly, instability at elevated temperatures of mesophile-derived biocatalysts results in low reactor performance and the necessity for cooling (Yamada & Kobayashi 1996; Kobayashi & Shimizu 1998). Secondly, whole cell systems suffer unpredictable side reactions such as formation of carboxylic acid by-

products, due to the presence of amidase activity in whole cell biocatalysts, which is a major concern. Thirdly, problems due to permeability and transport of substrates and products across the cell membranes are widespread. Further, the biocatalysts currently used have narrow substrate specificities generally limited to conversion of water-soluble substrates, and they suffer substrate and product inhibition (Eyal *et al.*, 1990). Therefore, the study of thermophile-derived biocatalysts provides opportunities for improved efficiencies in bioconversion of nitriles.

Nitrile hydratase (NHase; EC4.2.1.84) is a metalloenzyme belonging to the hydrolase enzyme class. NHases are classified into two groups with respect to the type of metal ions in their active site, namely the Fe-type having a non-heme iron atom (Sugiura *et al.*, 1987; Brennam *et al.*, 1996) and the Co-type having a non-corrinoid cobalt atom at the catalytic centre (Kobayashi & Shimizu, 1999). NHases catalyse the hydration of nitriles to their corresponding amides. Their occurrence is very diverse, in archaea and bacteria, many fungi and plants, and in intracellular and extracellular forms. Nitrile hydratases from bacteria are widely used in biocatalytic hydration of nitriles (Kato *et al.*, 2000), and have been shown to provide some potential applications in industrial production of amides (Nagasawa and Yamada, 1989; Kobayashi *et al.*, 1992; Cowan *et al.*, 1998; Thomas *et al.*, 2002).

The most successful example of a NHase application is the production of acrylamide from acrylonitrile (Nagasawa *et al.*, 1993). The industrial bioconversion of acrylonitrile to acrylamide, which started in 1985, by using the Fe-type NHase from *Rhodococcus* sp. N-774, was followed by use of another Fe-type NHase from *P. chlororaphis* B23 in 1988, but currently utilizes a Co-type NHase from *Rhodococcus rhodochrous* J1 strain (Nagasawa & Yamada, 1995). Presently, 20 000 metric tons per year of acrylamide are produced (at ~99.99% yield) (Ran *et al.*, 2007), using a series of fixed-bed reactors containing the immobilized *R. rhodochrous* J1 cells.

In 1999, Lonza Guangzhou Fine Chemicals (China) began production of nicotinamide (niancinamide, vitamin B₃) in a process developed by Lonza (Switzerland) (Thomas *et al.*, 2002). The process involves a four-stage chemo-enzymatic synthesis, in which the starting material, 3-methyl-1, 5-diaminopentane (a nylon 6, 6 by-product), is catalytically converted into 3-picoline

which is ammoxidated into 3-cyanopyridine, then finally biocatalytically hydrolyzed to nicotinamide using immobilized *R. rhodochrous* J1 cells.

The nitrile-converting roles of NHases are also used in decontamination of waste streams (Kobayashi & Shimizu, 1998). Effective bioremediation and biodegradation of nitrile-burdened soils and industrial effluents using NHases has been reported (Thompson *et al.*, 1988; Wyatt & Knowles, 1995; Kobayashi & Shimizu, 1998).

Because the mesophilic-derived NHases are unstable under reaction conditions, especially when the enzyme is used in its isolated form, they have been difficult to immobilize. However, with the discovery of thermophilic-derived NHases (Cramp *et al.*, 1997; Cowan *et al.*, 1998; Padmakumar *et al.*, 1999), it is anticipated that with the high thermostability of these enzymes it would be possible to isolate them from whole cells and immobilize them; the immobilization techniques would facilitate the development of continuous large-scale commercial processes, and since the biocatalyst would be reused, products can be easily separated from reaction mixtures, and immobilization can result in further enhanced enzyme stability activity. This immobilization approach has been used successfully to stabilize many enzymes, where increasing the rigidity of the enzyme structure reduces the propensity for inactivation via conformational changes (Blanco *et al.*, 1989; Guisan *et al.*, 1991; Fernandez-Lafuente *et al.*, 1995) and chemical inactivation (Fernandez-Lafuente *et al.*, 1992; Fernandez-Lafuente *et al.*, 1995; Fernandez-Lafuente *et al.*, 1999).

The numerous methods available for achieving the immobilization of enzymes can be subdivided into two broad categories, namely, chemical (where covalent bonds are formed between the enzyme and support), and physical methods (where weaker interactions between the enzyme and support lead to containment of enzyme is utilized). The various configurations of reactors in which immobilized biocatalysts (cells or enzymes) are used have been widely reviewed (Balcão *et al.*, 1996), including batch reactors, fed-batch, continuous stirred tank reactors (CSTRs), packed-bed reactors (PBRs), fluidized bed reactors (FBRs), and membrane reactors (IMERs). However, only a few have been described for nitrile hydration reactions. Batch stirred tank reactors have been reported most commonly in past studies nitrile bioconversions (Nagasawa *et*

al., 1988; Hwang *et al.*, 1989; Hann *et al.*, 1999), probably because they offered simple, low cost operation (Thomas *et al.*, 2002). Other commonly studied reactors involving nitrile-converting enzymes include immobilized-enzyme membrane reactors (Cantarella *et al.*, 1998). For this project, a packed-bed column reactor (PBR) was chosen as a simple and suitable system for application of an immobilized NHase. Once the properties of the immobilized NHase, particularly activity, stability and productivity, were investigated, its biocatalytic performance in a PBR was compared to that in a continuous stirred tank reactor (CSTR).

1.2 Motivation

The rationale behind this project arose out of work previously published by our collaborators on the isolation, cloning and expression of *Geobacillus pallidus* RAPc8 NHase (Pereira *et al.*, 1998; Cameron & Cowan, 2005). The thermostable *G. pallidus* RAPc8 NHase was originally isolated from a moderate thermophilic *G. pallidus* species of bacterium found in a New Zealand thermal environment, in the course of a program to find enzymes for industrial application (Pereira *et al.*, 1998). Preliminary characterisation studies of the recombinant enzyme indicated interesting properties; the *G. pallidus* RAPc8 NHase has an optimum reaction temperature of 50 °C and was found to be highly active over a wide pH range (pH 5.1-8.7). The specificity of *G. pallidus* RAPc8 NHase is relatively wide, most notably with respect to aliphatic nitriles, branched nitriles, and cyclic nitriles (Pereira *et al.*, 1998). Furthermore, *G. pallidus* RAPc8 NHase is unusual in its high catalytic activity in conversion of hetero-aromatic nitriles.

Cloning of *G. pallidus* RAPc8 NHase genes in *E.coli* (BL 21) λ DE3 pLysS has allowed production of higher quantities than the quantities obtainable using native cells. High levels of *G. pallidus* RAPc8 NHase can be achieved by expression in *E.coli* (BL21) λ DE3 pLysS using LB medium at 37 °C upon induction with 0.4 mM IPTG and supplementation with 0.1 mM Co^{2+} ions (Cameron & Cowan, 2005). A maximum level of specific activity (with acetonitrile as substrate) of 49 ± 4 U/mg and an enzyme purity of up to 95 % have previously been achieved (Pereira *et al.*, 1998).

The present study has involved functional characterisation of the enzyme, development of an immobilized NHase biocatalyst and development of a small-scale process system suitable for its biocatalytic application.

1.3 Hypotheses

The central hypothesis of the study is: Efficient and continuous production of commodity amides, such as nicotinamide, can be achieved using immobilized thermostable *Geobacillus pallidus* RAPc8 NHase in an appropriate bioreactor.

This hypothesis can be considered in the following stages:

- 1) Due to the thermostable nature of the *G. pallidus* RAPc8 NHase, high reaction rates for nitrile hydration can be achieved at higher temperatures.
- 2) The operational stability of the NHase biocatalyst can be increased further through immobilization and high biocatalyst stability will lead to reusability of the immobilized biocatalyst in repeated process cycles.
- 3) The high stability of *G. pallidus* RAPc8 NHase will allow the development of a wider range of applications of the biocatalyst including in organic media, extreme pH and temperature.

1.4 Objectives

The primary aim of the research was to demonstrate the application of the thermostable *G. pallidus* RAPc8 NHase, as an isolated immobilized enzyme, in the production of nicotinamide as a model product.

A second aim was to explore the substrate specificity of *G. pallidus* RAPc8 NHase with respect to conversion of hetero-aromatic nitriles to widen the scope of the process for production of a range of useful and chemical compounds.

Specific objectives related to these aims:

- 1) Characterisation of the enzyme kinetics of the thermostable *G. pallidus* RAPc8 NHase to determine the optimal conditions for biocatalytic application.
- 2) Investigation of the reaction with a range of substrates to define the substrate range of the enzyme and to develop further understanding of the active site mechanism.
- 3) Investigation into the application of the *G. pallidus* RAPc8 NHase in organic solvent media.
- 4) Development of an immobilized biocatalyst with the objective of enhanced stability and reusability.
- 5) Application in a continuous reactor based on the application of the immobilized biocatalyst under optimal conditions.
- 6) Generation of data required for mathematical modelling of the nicotinamide production reactions to enable preliminary scale-up of the bioreactor process.

1.5 Experimental methodology

The structure, scope and methodology of this study are interdisciplinary. The approach was based on the understanding that for a process to be industrially viable requires input from different areas ranging from microbiology to chemical engineering. The project involved batch soluble, batch immobilized, and continuous biocatalysis experiments and kinetic modeling.

1.6 Organization of the thesis

Chapter 2 is a review of the literature relevant to the project. This chapter presents a critical review of relevant literature involving general biocatalysis and current development of biocatalysis. Enzymology of nitrile hydratases, including new thermostable NHases, is reviewed in detail. Genetic modification of *G. pallidus* RAPc8, and structural and functional characterisation of the NHase is addressed and the possible types of bioreactors in which the enzyme might be applied are considered. Reactors are reviewed to give a comprehensive background to the work to be conducted in this study.

In **Chapter 3**, production, purification and functional characterisation of *G. pallidus* RAPc8 NHase are described in detail. Particular attention is given to the biochemical properties of the soluble enzyme, and investigation into the kinetics of the hydrolysis reaction, using the soluble enzyme, is reported. By studying different parameters, an optimal approach to hydrolysis of nitriles can be developed.

In work described in **Chapter 4**, immobilization of cell-free NHase on various supports was investigated with the aim of enhancing the operational stability and activity of the enzyme. Comparative studies of the soluble and immobilized enzyme were carried out. The kinetics of the hydrolysis of 3-cyanopyridine using immobilized *G. pallidus* RAPc8 NHase were investigated.

Chapter 5 describes the application of the immobilized NHase in a packed-bed column reactor in the hydrolysis of 3-cyanopyridine to nicotinamide. Attention was given to the performance of the immobilized enzyme in the PBR, evaluated in terms of volumetric productivity and percentage conversion, as well as to the effects of flow rate, mean residence time, bed-height and substrate concentration on productivity. This chapter also presents an investigation into using the immobilized NHase in a continuous stirred tank reactor, as a comparison. The enzymatic performance was analysed based on operational stability.

In **Chapter 6**, major results are discussed, and potential further research work is proposed.

CHAPTER TWO

LITERATURE REVIEW

2.1 Introduction

The chemical industry plays a fundamental role in many economic and manufacturing sectors worldwide, and chemical products are being used in all societal areas that impact upon the quality of life, including housing, agriculture, pharmaceutical and telecommunication (Thomas *et al.*, 2002). The demand for chemical products has expanded into new market segments, such as their use in analytical systems and as intermediates in synthetic applications (Schmid *et al.*, 2002). For example, in the USA alone, the chemical industry converts up to US\$27 billion worth of raw materials into US\$419 billion worth of useful products annually, and worldwide chemical industry revenues had reached 1.5 trillion dollars by year 2000 (Thomas *et al.*, 2002). Chemical production processes are the leading economic factor associated with contributions to a positive balance of trade (<http://www.atp.nist.gov/atp/97wp-cat.htm>).

There is, currently, much attention being focused on biologically-based (bio-based) processes in production of high-value materials in the chemical industry. The efforts made by various stakeholders in the chemical industry are seen no longer to be desirable trends, but as necessities. The global demands to use renewable feedstocks to reduce waste, reduce energy utilization and practice chemistry which is friendly to the environment is causing a shift from chemical-based to biochemical production processes (Bozell, 2008). To date, there are estimated to be 150 implemented biocatalytic processes in industry, with the majority of these being in the pharmaceutical sector (Panke *et al.*, 2005). The most important innovations that bio-based industries have provided include the use of renewable feedstocks (lower cost, biodegradable and biocompatible raw materials), biocatalysts (application of enzymes as catalysts) and/or use of chemoenzymatic processes (steps that involve both traditional chemistry and a biocatalyst to conduct a single reaction). The focus has been on biocatalysts (enzymes and whole cells) as primary tools for achieving 'green' and sustainable technology (Thomas & Raja, 2005).

Biochemical processes, in themselves, have unique potential to produce existing chemicals at lower cost; the processes can also lead to new products, new manufacturing methods and

improved economics. Further benefits are seen in their capacity to significantly increase productivity, purity and yields by using novel biocatalysts coupled with innovative processes. Further, the ability to tailor-make biocatalysts (by protein engineering, site-directed mutagenesis or immobilization), is promising and may lead to processes that are robust with a wide range of applications.

2.2 Biocatalysis

During the past 20 years, biocatalysis has been of increasing interest in organic synthesis. Biocatalysis aims to emulate nature's metabolic pathways by developing enzymatic processes, either *de novo* or by improving existing metabolic pathways. Enzymes are catalysts in cell metabolism, and biocatalysts include any biological entity capable of catalyzing the conversion of a substrate into a product. They exhibit chemo-, regio-, and stereo-selectivity, have high reactivity under ambient conditions, and are readily degradable. In the past, work in biocatalysis has focused on exploiting enzymatic chemistry to offer reactions which are highly selective, efficient under mild conditions, and environmental friendly, to produce substrates of pharmaceutical and agrochemical interest which are in growing demand by industries and consumers (Turner *et al.*, 2000).

More recently, there has been a shift in emphasis to the discovery of new biocatalysts and to redesigning them in order to tailor their properties (Adamczak & Krishna, 2004). New tools such as screening methods (genomic, proteomics and bioinformatics) are becoming widely available and have led to rapid identification and cloning of target genes; expression of novel genes is becoming an important factor in the discovery of new enzyme activities (Bommarius, 2004). The search for genes from organisms that inhabit unusual environments (thermophiles, psychrophiles, and halophiles) has been expected to generate genes that will produce enzymes with novel reaction selectivities (Sellek and Chandhuri, 1999). Further, these new enzymes may have increased stability towards heat, organic solvents, pH and conditions of high ionic strengths.

An increased interest in the use of isolated enzymes in the industrial, analytical and medical procedures has been acknowledged (Kirk *et al.*, 2002). Although purified soluble enzymes seem

to have an additional cost of isolating and relatively poor stability, they also have advantages over the use of whole cells biocatalysts, as soluble enzymes are associated with greater efficiencies of substrate conversion, higher yields, and good product uniformity. Moreover, recent developments in biotechnology, such as recombinant DNA technology, have led to large-scale production of isolated enzymes and new procedures for their stabilization.

This chapter will give an introduction to the development of biocatalytic processes and the challenges that exist in taking biocatalysis to valuable application, from the industrial view point. An account of nitriles and the occurrence of nitrile-converting enzymes and enzymology of the NHase will be given. Industry applications of nitrile-converting enzymes will be introduced and their modes of operation will be explained. The most recent parallel studies (*i.e.* the cloning of gene encoding the NHase enzyme, its expression, structure and genetic engineering) on the *G. pallidus* RAPc8 NHase will be briefly reviewed.

2.3 Development of a biocatalytic process

General principles for the development of efficient biocatalytic processes involving several distinct stages including biocatalyst selection, biocatalyst production, biocatalyst characterisation, biocatalyst immobilization, application in a reactor and product isolation have been recognised. The work on these general principles has been reviewed in a number of publications (Leuenberger, 1990; Burton *et al.*, 2001; Schmid *et al.*, 2001; Beilen & Li, 2002 Kaul *et al.*, 2004).

2.3.1 Biocatalytic development cycle

Typically, development of a biocatalytic process involves interdisciplinary aspects including molecular biology, biotechnology, chemistry and chemical engineering, and each activity is needed for the successful establishment of a process (Beilen & Li, 2002). Fig. 2.1 shows a typical biocatalysis cycle in enzymatic process development. This highlights the issues that play important roles at each stage of a biocatalytic process development. Each is discussed further in details in the following section.

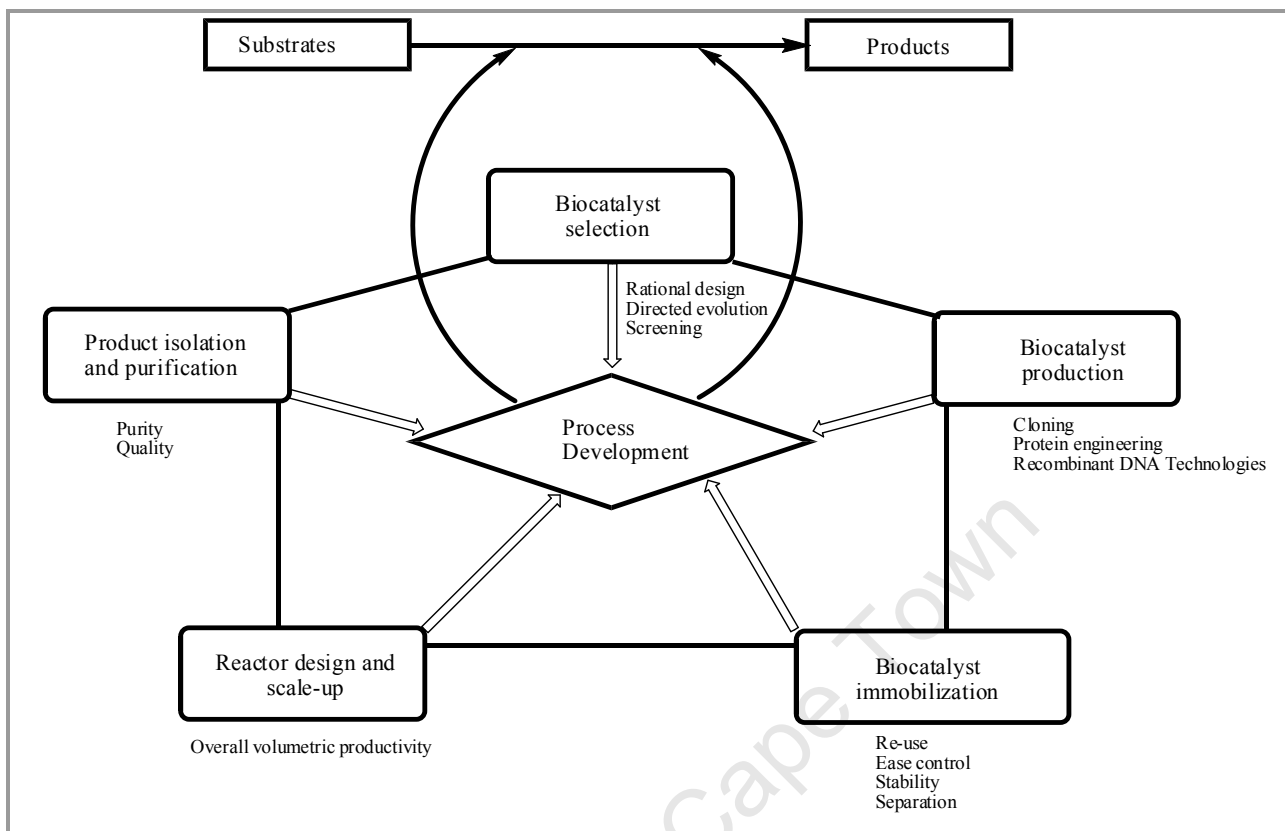


Figure 2. 1: The schematic diagram of a biocatalysis cycle in enzymatic process development. The cycle illustrates sequential biocatalytic development stages and displays major activities of each stage of development (Adapted from Zhao *et al.*, 2002).

2.3.2 Biocatalyst selection for a chemical synthesis

Traditionally, biocatalysis cycles have started by identification of a product, which can perhaps be produced by several possible enzymes or microorganisms converting a suitable substrate to the desired product (Schmid *et al.*, 2001). One or more biocatalysts must then be identified or developed and a process set up for bioconversions. Several strategies can be pursued to obtain the biocatalyst for the relevant biotransformation: (i) use of existing commercial biocatalysts; (ii) genetic modification of existing biocatalysts; (iii) where suitable commercial biocatalysts are not available, novel enzymes displaying catalytic activity for the desired conversion can be sought and isolated through microbial or metagenomic screening (Leuenberger, 1990; Burton *et al.*, 2002). The most common approach is screening. Thus, screening for an enzyme that catalyses a particular process of interest, isolation of the organisms producing it, and optimising production

of the enzyme in cells can result in a biocatalyst which is highly competitive with a traditional chemical catalyst.

2.3.3 Biocatalyst production by fermentation in a suitable expression systems

Production of enzymes in large quantities is necessary both for research (structural and functional studies) and as a determinant of the success of industrial applications, and hence enzyme production must be optimized. Advances in protein engineering and heterologous protein expression (*i.e.* when recombinant DNA techniques are used to express certain genes outside their natural expression organism) coupled with up-to-date fermentation and bio-processing technologies provide means of obtaining large quantities of enzymes. Depending on the target protein, prokaryotic or eukaryotic hosts can be used for the expression. Since the introduction of the protein engineering technology, the bacterial strain *Escherichia coli* has been extensively studied for the purpose of heterologous protein expression (Hanning & Marides, 1998). The advantage of using *E. coli* as host is attributed to many factors including: (i) it is very well characterised, (ii) its genome sequence is known, (iii) many of its biological processes and metabolic pathways are understood and (iv) there are many genetic tools readily available for its manipulation (Kobayashi *et al.*, 1991; Nishiyama *et al.*, 1991; Kim & Oriel, 2000; Cameron & Cowan, 2005).

2.3.4 Biocatalyst characterisation for optimal reaction

The potential application of biocatalysts in industry can best be achieved when operating conditions are optimal for enzyme function. A biocatalytic process needs to achieve adequate conversion (which is determined by the enzyme and the environmental conditions), and high efficiency (defined as the amount of substrate converted per unit of enzyme consumed during the reaction). Several parameters affect the performance of an enzyme in a process. Of particular importance are (i) the overall enzyme kinetics in terms of V_{max} (expressed in $\mu\text{mol.mL}^{-1}.\text{min}^{-1}$), K_m (expressed in mM) and k_{cat} (expressed in s^{-1}), (ii) stability of the enzyme (Burton *et al.*, 2002), (iii) the level of substrate and product inhibition may be important to determine, and (iv) substrate specificity for a given enzyme is an important parameter when the development of

biocatalysts for a wide ranges of products. Moreover, it is now well known that enzymes can function in organic solvents in the near absence of water (Serdakowski & Dordick, 2008), and application of enzymes in non-aqueous media has several advantages including higher substrate solubility, reversal of hydrolytic reactions, and modified enzyme specificity. Other promising approaches are the use of bi-phasic organic/aqueous media and biocatalysis in emulsions, which allow easy product separation from reaction mixture (Ratledge, 2006).

Operating conditions such as temperature and pH are among the most significant operational parameters affecting biocatalytic processes. Increasing temperature could favour the reaction rate, but it may also increase enzyme deactivation effects by unfolding of its three-dimensional structure which lead to decrease of enzyme activity. Operational pH must be controlled at values near the optimal values for enzymatic activity. In many instances, lower or higher pH values may not only alter the stability of enzymes, but may also change the charge properties (by altering the ionization state of the amino acid side chain) of essential amino acid residues in the catalytic centre, thus altering the capacity of the enzyme to catalyse the desired reaction.

2.3.5 Immobilization of enzymes and performance of immobilized biocatalysts.

Most biocatalysts (whole cell and enzymes) are used in immobilized form, as heterogeneous catalysts that can be recovered and reused (Klibanov, 1983). Immobilization can be defined as the association of a biocatalyst with an insoluble matrix (surface attachment) so that it can be retained inside a reactor system, with retention for continuous flow-through reactions where applicable, reducing costs associated with separation processes. Immobilization allows the repetitive use of the biocatalyst and often enhances stability, reducing the process costs (Burton *et al.*, 2002). However, immobilization becomes economically feasible only when the reaction velocity of the resulting biocatalyst is high. Several approaches are currently used to design robust industrial biocatalysts by immobilization, including adsorption and chemical immobilization, where enzymes can be covalently bound to organic or inorganic supports *via* a range of functional groups (Gerbsch & Buchholz, 1995). The second option for immobilization of soluble enzymes is retention by means of ultrafiltration membranes coupled to a reactor (Rios *et al.*, 2004). The main advantages of this design include operation with soluble enzymes,

avoiding limitations of mass transfer and allowing simple operation. However, the approach may be limited to substrates with small molecular weights. Nonetheless, processes based on suspended whole cells or enzymes are in use in the industry. Inexpensive enzymes are often applied in the manner that permits single use, without recovery or reuse.

In the investigation of appropriate immobilization systems, one must include the characterisation of the immobilized biocatalysts. In a typical immobilization investigation the following parameters are measured:

- Loading efficiency % (based on amount of protein in the support carrier),
- Immobilization yield % (based on measurement of total activity and subtraction of the activity in the wash solutions),
- Activity yield % (activity of enzyme remaining in the biocatalyst after immobilization).

These properties of the immobilized enzyme not only help determine the most suitable support, but greatly influence the catalytic performance of the biocatalyst in selected reactor. (Enzyme immobilization is discussed in more detail in Chapter 4).

2.3.6 Immobilized enzyme reactors

A reactor is any equipment that serves as a vessel in which a chemical reaction is conducted. The reactor is often connected to equipment placed upstream and downstream, designed for physical treatment of the raw materials and products (Trambouze *et al.*, 1988). Although reactors perform a common function, namely to carry out a desired chemical transformation, they are designed in a variety of shapes and dimensions, including tanks, columns, drums, mixers, and simple tubes, and the principal characteristics of the target chemical reaction define the criteria used in the reactor design. In bioreactors, the correct environment for optimal activity of the biocatalyst is an important consideration. Four basic reactor configurations are generally employed for application of immobilized enzymes: batch stirred tank reactor, continuous stirred tank reactor, fluidized bed reactor and packed-bed reactor. Reactor classification is based on two major factors, namely: the mode of operation and the flow characteristics of substrate and products. The configurations of different reactor types are shown below (Fig. 2.2).

The numerous reactors (Fig. 2.2) used in the industry today are simple in design and can be operated in continuous-flow; however, alternative reactors such as microchannel enzyme, monolith and multi-stage reactor systems, which might involve relatively little added complication, can afford considerably improved performances. The micro-enzyme reactors, for example, have been developed to allow shorter reaction time and the minimal amount of reagent (Miyazaki and Maeda, 2006). Thus, the microchannel reaction systems have afforded large surface and interface areas, which are advantageous for many catalytic type of reactions. On the other hand, organic polymer and silica-based monolith reactors have as well become attractive alternatives to the conventional reactors (Krenkova and Svec, 2009). Monolith-based reactor have several advantages including better accessibility of the enzyme active for substrate, very low back pressure, stability in most solvents, and ease of preparation in any size and shape (Krenkova and Svec, 2009). One of the most significant advantages of the monolithic-derived enzyme reactors is its excellent mass transfer characteristics, which allows accelerated enzyme-catalysed reactions (Svec, 2003). While multi-stage enzyme reactors (with either plug-flow or continuous stirred tank reactors simultaneously connected) have been reported (Dort 2004); the repeated exposure of substrates to this series of reactors enables increased substrate conversion that subsequently results in higher reactor productivity compared to a single-stage reactor with a similar amount of enzyme loaded.

Although reactor engineering in the last decade has seen a significant increase in the number of immobilized enzyme reactors, the plug-flow and continuous stirred-tank reactors (CSTR) remain the most popular for commercial purposes. In part, this has been due the fact that classic model of Michaelis-Menten that describes most enzyme-catalysed reaction is better represented in PFR and to a lesser extent by CSTRs (Hawaldt *et al.*, 1986). For the purpose of this thesis, the PFR model was taken into account when describing the immobilized NHase in its reactor application details in Chapter 5.

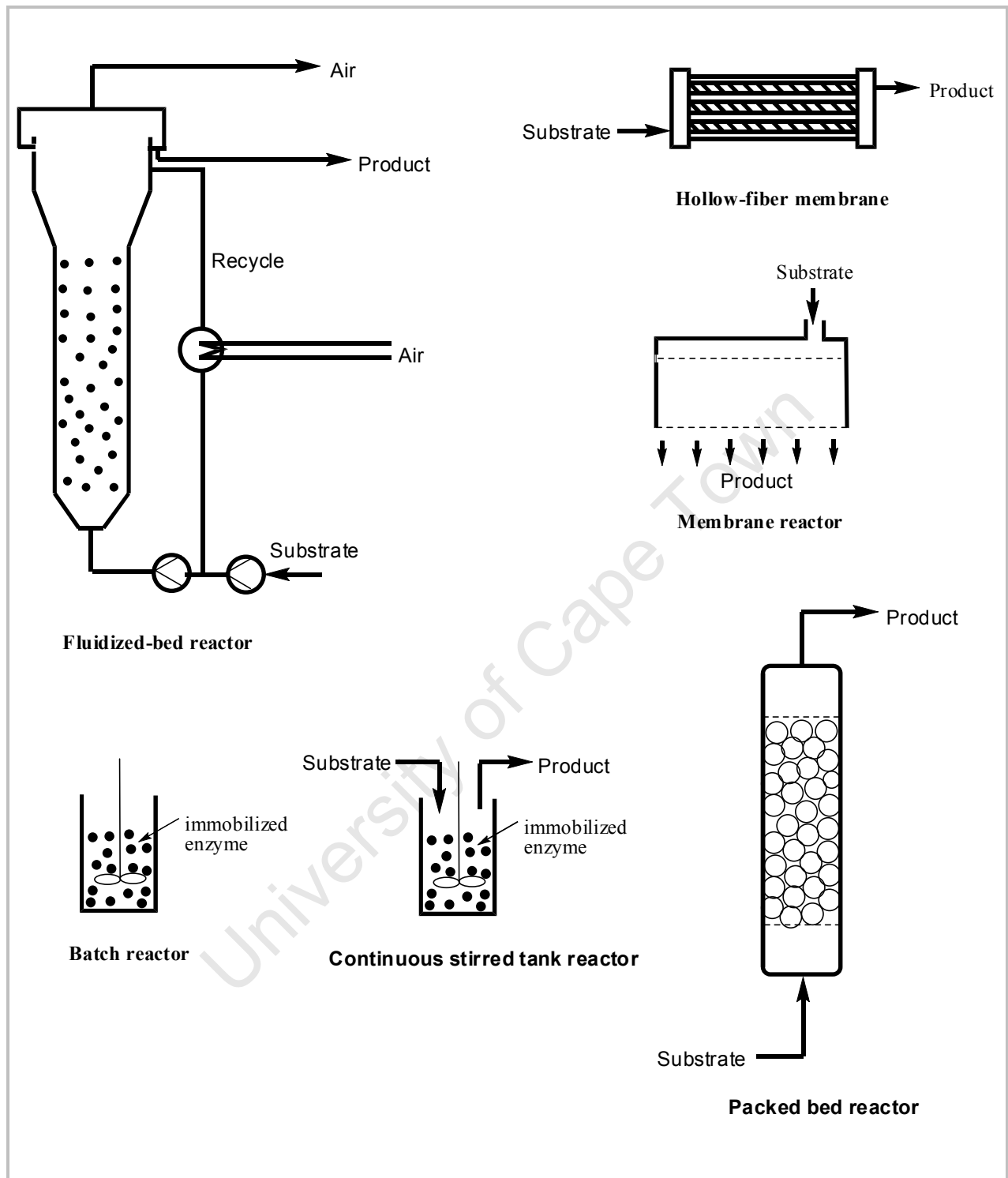


Figure 2. 2: Schematic diagrams of reactors employing immobilized enzymes (Ratlidge, 2006).

2.3.7 Downstream processing of synthesized products in biocatalytic processes

For most of the biocatalytic processes that operate in aqueous media, product extraction procedures need to be developed. Generally, techniques such as precipitation, centrifugation and filtration of products are applied. For example, in the process for acrylamide production from acrylonitrile, insoluble acrylamide is precipitated out of the reaction mixture at the end of a batch operation. *In situ* product recovery processes, in which the product is separated from the reaction mixture during the biotransformation, have numerous advantages and are common (Lye *et al.*, 1999). These *in situ* product-recovery techniques are facilitated by variations in the chemical and physical parameters of the reactants and products, which afford separation through crystallization or distillation. In the case of biocatalysis in bi-phasic organic/aqueous solvents systems, the phases are separated after the biocatalytic step, and then adequate product extraction from the organic phase is achieved (Hill, 2007).

2.4 Nitriles or cyano-containing compounds

Nitriles (cyano-compounds) are widespread in the natural environment; nitrile-containing compounds are important components in the metabolic cycle of plants and many soil organisms including algal and fungi (Kobayashi & Shimizu, 2000). They are used in the synthesis of a wide variety of compounds such as amines, amides, amidines, carboxylic acids, esters, aldehydes, ketones, and heterocyclic compounds, some of which are utilized by plants as chemical defense systems against herbivores (DeVito, 2007). The largest group of nitrilated compounds produced by plants is the cyanogenic glycosides. These are found in seed, roots and the epidermal layers of the leaves, and are hydrolysed by β -glucosidase to give rise to cyanide (HCN) (Harborne *et al.*, 1993). Meanwhile, indole-3-acetonitriles serve as growth hormones during seed germination (Mascharak, 2002). Further, cyanolipids, ricinines, β -cyano-L-alanine and phenylacetonitriles all contain a nitrile functional group and are formed in a wide range of plants (Fig.2.3).

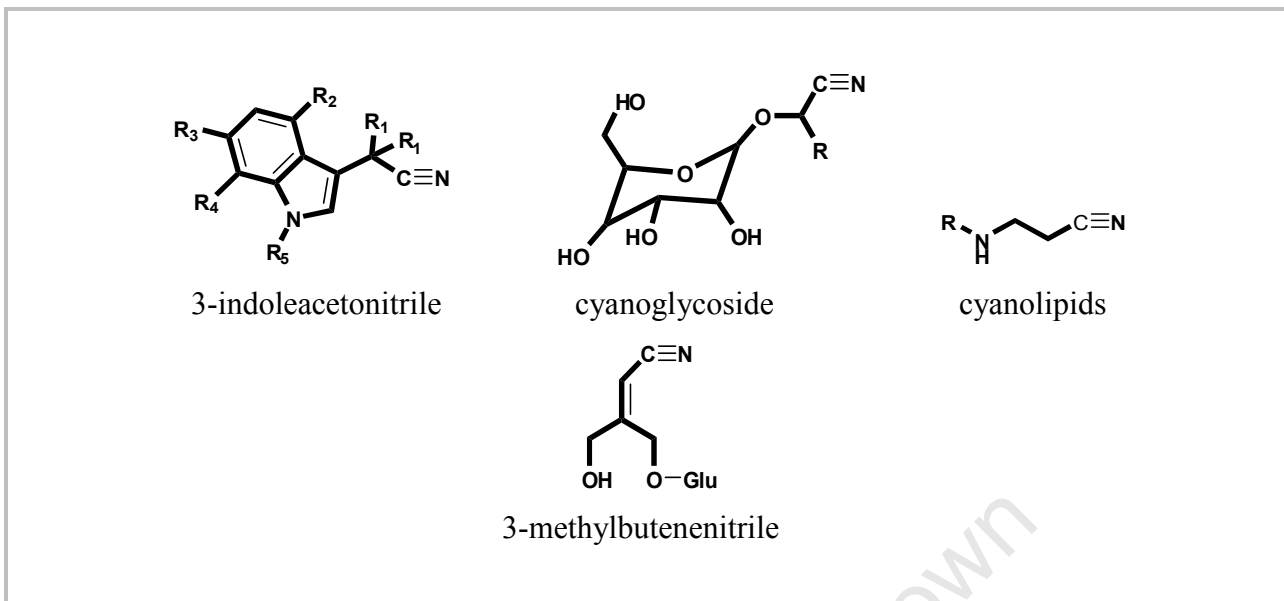


Figure 2. 3: Cyanoglycosides most abundant in plants (Mascharak, 2002).

Nitrile-containing compounds are also widely manufactured and extensively used by chemical industries. Examples of the more important commercial nitriles include: acetonitrile used as a solvent, adiponitrile as a precursor in nylon-6, 6 synthesis, acrylonitrile as a precursor of acrylic fibers and plastic synthesis. Dichlobenil (2, 6-dichlorobenzonitrile), ioxynil (3, 5-diiodo-4-hydrobenzonitrile), and buctril 4-(octanoyloxy)-3, 5-dibromobenzonitrile are widely used in agriculture and, consequently, these compounds have become widely distributed in the environment, in industrial waste water and agricultural residues (Banerjee *et al.*, 2002).

While the commercial interest in selected nitriles has grown, their full potential is limited, in some cases, by the presence of functional groups which are sensitive to harsh chemical methods (Cameron, 2002). The industry has thus preferred microbial biotransformations (using nitrile-converting enzymes) for the conversion of such nitriles into commodity chemicals and intermediates for the pharmaceutical industry.

2.4.1 Occurrence and roles of nitrile-converting enzymes

The existence of nitrile-degrading enzymes in 21 plant families, fungal genera and a number of bacterial species has been reported (Banerjee *et al.*, 2002). While the role of these enzymes is yet

to be established in microbial systems, it is noted that they are responsible for the formation of precursors which undergo further hydrolysis, oxidation, and reduction (Fig. 2.4). For example, nitrogenase enzymes are known to be versatile catalysts which are able to catalyse conversion of many different nitrogen containing compounds such as alkynes, cyanides, azides and nitrogen (Tamagnini *et al.*, 2002). Nitrogenase conversions of nitriles transform the cyano group to a methyl group yielding a hydrocarbon and ammonia (Fig. 2.1, reaction i) (Jallageas *et al.*, 1980). Microbial and plant oxygenases readily oxidize nitriles to cyanohydrins (Fig. 2, reaction ii), which are further degraded to aldehydes and cyanides by oxynitrilase (Fig. 2.1, reaction iii) (Johnson *et al.*, 2000). The cyanides from oxynitrilase (Fig. 2.1, reaction iv) and various metal cyanides (Fig. 2.1, reaction v) are subsequently converted to acids and NH_3 by cyanide dihydratase (Fig. 2.1, reaction vi), CO_2 and NH_3 by cyanase (Fig. 2.1, reaction vii) and HCONH_2 by cyanide hydratase (Fig. 2.1, reaction viii).

Many microorganisms are known to use nitriles as a source of carbon and/or nitrogen for growth (Kato *et al.*, 2000). The enzymatic hydrolysis of nitriles is possibly a most useful pathway for the microbes because the products can then be used in the central metabolism. In this pathway, biotransformation of nitriles takes place by two well-established mechanisms: nitriles are converted directly to carboxylic acid and ammonia by a one-step process using nitrilase enzyme (Fig. 2.1, reaction ix); or they are converted *via* a two step process involving two enzymes. In the first step of the two-step process, nitrile hydratase converts the nitriles to corresponding amide (Fig. 2.1, reaction x) and in the second step amidase enzyme converts the amide to its carboxylic acid and ammonia (Fig. 2.1, reaction xi). It has been recently been suggested that the hydrolytic pathways exist in both eucaryotic and prokaryotic domains, with the majority being in bacteria where they play a crucial role in the microbial metabolism (Kimani *et al.*, 2007).

In the past two decades, the enzymatic hydrolysis of nitriles has been recognized as a potential method for production of a broad spectrum of useful amides and carboxylic acids. The development of these biotransformations was driven by the attempt to find alternatives to the conventional acid- or base-catalysed nitrile hydrolysis and consequently, nitrilases, nitrile hydratases and amidases have become the catalysts of choice in several processes (Nagasawa *et*

al., 1988; Nagasawa & Yamada, 1989; Hann *et al.*, 1999; Kobayashi & Shimizu, 2000; Thomas *et al.*, 2002; Mylerová & Martinkova, 2003).

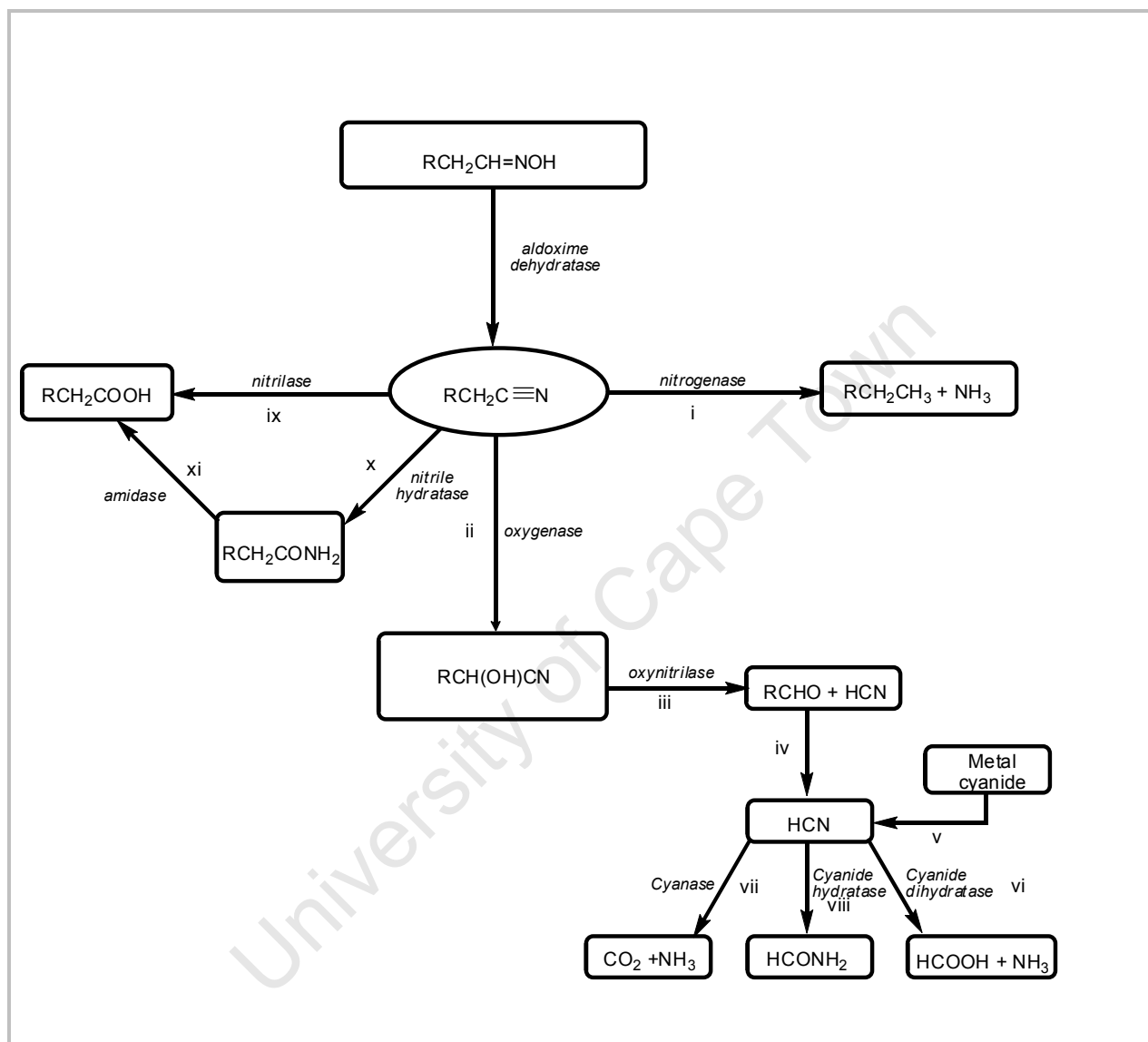
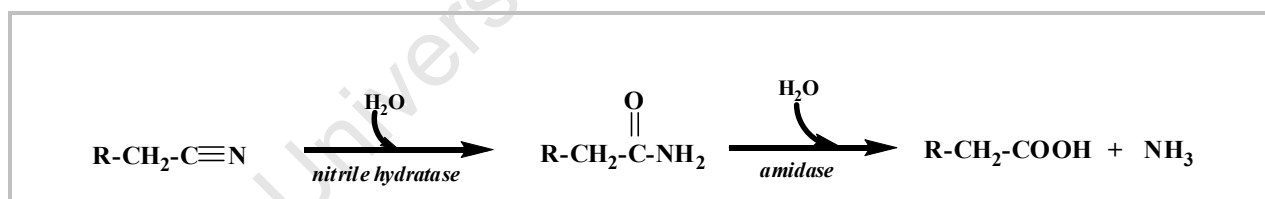


Figure 2. 4: Enzyme pathways of nitrile degradation established in microbial systems (Banerjee *et al.*, 2002).

2.5 Enzymology of nitrile hydratase (NHase)

Nitrile hydratases (NHases) are soluble metalloenzymes known to hydrolyze aliphatic and aromatic nitriles to the corresponding amides (Scheme 2.1). To date, NHases have been identified in a number of bacterial species from different genera, from a diversity of ecosystems such as thermal lake sediments, deep sea trenches and nitrile-containing soils. The majority of NHases which have been isolated and characterized are from mesophilic microbial sources such as *Pseudomonas*, *Agrobacterium*, *Rhodococcus*, *Arthrobacter* and *Corynebacterium* (Endo & Watanabe, 1989; Duran *et al.*, 1992; Bauer *et al.*, 1994; Komeda *et al.*, 1996; Payne & Oriel, 1997), *Bacillus* species (Kim *et al.*, 2000). Recently, a widespread distribution of nitrile-hydrolysing activity has been reported in actinomycetes (Brandão *et al.*, 2002).

Although most previously reported NHase studies have concerned mesophilic-derived NHases, some thermophilic NHases have been discovered and characterized. To date, four thermostable NHases have been reported in literature; from *Geobacillus pallidus* Dac521 (Cramp *et al.*, 1997), *Geobacillus* spp. RAPc8 (Pereira *et al.*, 1998), *B. smithii* (Takashima *et al.*, 1998) and *Pseudonocardia thermophila* (Yamaki *et al.*, 1997). The bacteria having thermostable NHases have mostly been recovered from geothermal habitats (Yamaki *et al.*, 1997; Pereira *et al.*, 1998).



Scheme 2. 1: Biochemical pathway for nitrile hydration (Kato *et al.*, 2000).

2.5.1 Molecular size of the NHases

NHases consist of two subunits (α and β) having molecular weights ranging from 22 to 29 kDa, and not related in amino acid sequence. Although the NHases are known to have minimal functional unit of $\alpha\beta$ dimer, they usually exist in heterotetrameric $(\alpha\beta)_2$ or heterodimeric $(\alpha_2\beta_2)$ forms depending on the species of origin (Huang *et al.*, 1997). The NHase from *R. rhodochrous* J1 produces H-NHase with Mw = 505 kDa (Komeda, 1996), *R. rhodochrous* K22 has Mw = 650 kDa (Kobayashi, 1992), *G. pallidus* DAC521 has Mw = 165 (Cowan, 1998), and *G. pallidus* RAPc8 has MW = 110 kDa (Pereira *et al.*, 1998). In another case, the molecular weight of *Rhodococcus* sp. N-771 in solution, the NHase has been found to isomerise between dimer and tetramer forms, with the latter being predominant (Nakasako *et al.*, 1999).

2.5.2 Cofactors for the NHases

Using a combination of several spectroscopic studies Huang and co-workers found that the NHases contain either a low-spin non-heme Fe (III) ion per $\alpha\beta$ dimer, or a non-corrinoid Co (III) ion per $\alpha\beta$ dimer (Huang *et al.*, 1997; Miyanaga *et al.*, 2001). Thus, based on the metal ion in the active site, the NHases are subcategorised into groups: (i) the Fe-type NHases and (ii) Co-type NHase. The role of the metal ion in the active site and the critical role the metal centre plays in respective catalytic mechanism are discussed in detail later in Section 2.5.5. However, the mechanism by which the iron and cobalt are transported to NHase without toxicity is unclear, although a permease has been identified which transports the metal ions across the cell membrane. Although earlier studies implicated pyrroloquinoline quinone (PQQ) as a cofactor for the NHase from *Rhodococcus* sp. R312 (Nagasawa and Yamada, 1987), this was disapproved when the structure of the NHase was resolved by Huang and coworkers (1997).

2.5.3 Structure of the NHase

Various spectroscopic studies have been carried out to clarify the detailed structures of a number of NHases. To date, the structural characterisation of NHases has been chiefly focused on the Fe-type NHases from *Rhodococcus* sp. R312 (Huang *et al.*, 1997), while other Fe-type NHases reported include *Rhodococcus* sp. N-771 (Nakajima *et al.*, 1987). The structures of the two

NHases are found to be very similar both in their active and inactive form (Nagashima *et al.*, 1998). For example, each structure is made up of two heterodimers ($\alpha\beta$)₂, with the α subunit was found to consist of a long extended N-terminal ‘arm’ with 10 to 52 residues, containing two α -helices (Fig. 2.5). On the other hand, the C-terminal domain (C^B) exhibits an unusual four layered α - β - β - α structure. The β subunit consists of a long (30 residues) N-terminal loop that wraps around the α subunit, a helical domain with 30 to 112 residues which packs with N-terminal domain of the α subunit, and a C-terminal domain (C^A) consisting of a β -roll and one short helix (Huang *et al.*, 1997).

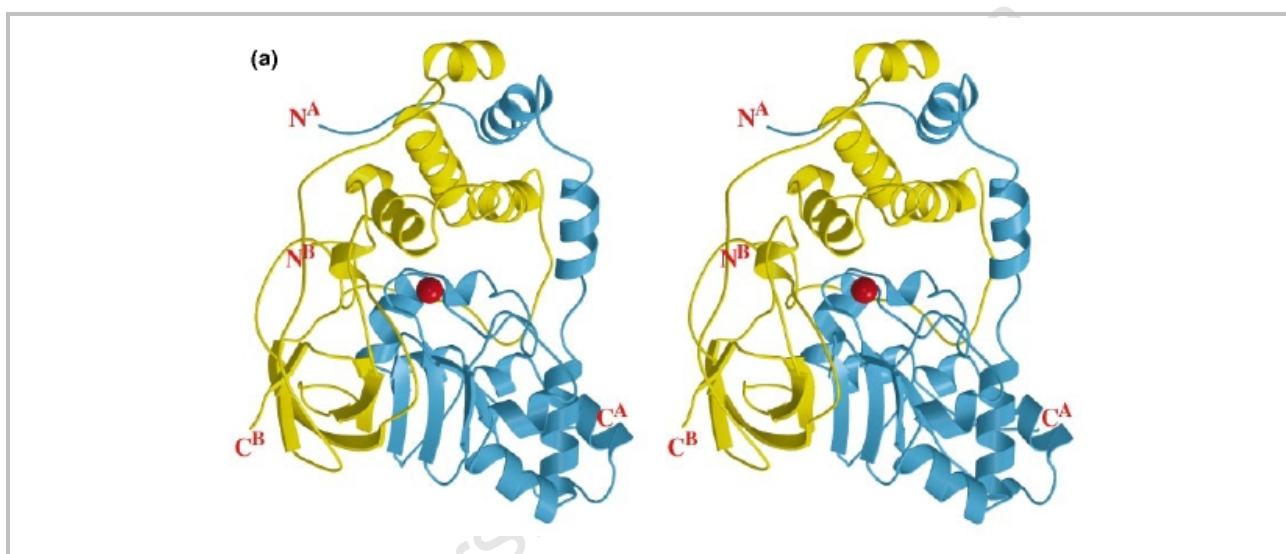


Figure 2. 5: Representation of the $\alpha_2\beta_2$ heterotetramer structure of the NHase from *R. rhodochrous* J1. The interface between subunits contains the active centre metal ion (With permission from Huang *et al.*, 1997).

2.5.4 Structure of the active centre in the NHases

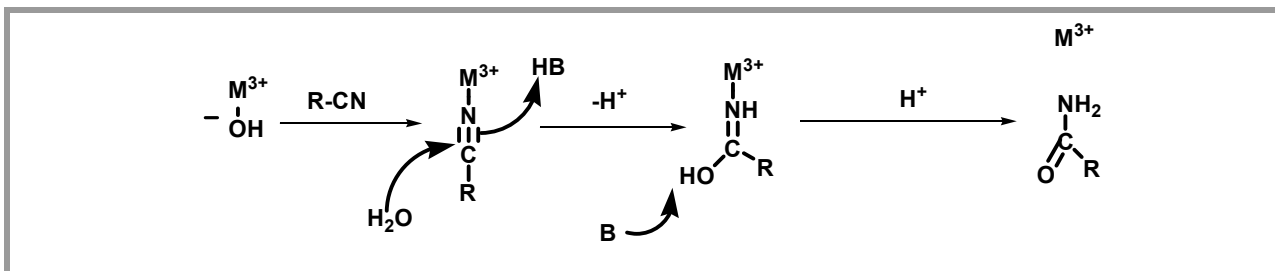
The active center of the NHases, which is located at interface of the α and β -subunit, contains a metal ion, a low-spin non-heme iron (Fe^{III}) chelating to the α -subunit through ligands. The protein ligands to the iron are the sidechains of the three cysteine residues (α Cys 110, α Cys 113, α Cys 115) and two main-chain amide nitrogen atoms (α Cys 115 and α Ser 114) (Huang *et al.*, 1997). In all known NHases, the α -subunit has a highly conserved amino acid sequence (C-X-Y-C-S-C-X) that forms the metal binding site (Huang *et al.*, 1997). The ligands co-ordinated to the iron form an octahedral orientation with the ligands at the five vertices of the octahedron, while

the sixth is occupied by either a water or hydroxide molecule when the enzyme is active and nitric oxide when inactive (Scarow *et al.*, 1996).

The crystal structure of a cobalt-containing NHase from *Pseudonocardia thermophila* JCM 3095 at 1.8 Å resolution revealed that the catalytic centre of the enzyme has the same motif (claw-setting motif) as in Fe-type and is highly conserved in all known NHases (Huang *et al.*, 1997; Endo *et al.*, 2001). The ligands to the cobalt ion include α Cys 108, α Cys 111, α Cys 113 and main chain amide nitrogen atoms of α Cys 113 and α Ser 112. Of the protein ligands, α Cys 111 and α Cys113 are post translationally modified to cysteine-sulfinic acid and cysteine-sulfenic acid, respectively. Research has revealed that three residues, namely β Leu51, β Phe51 and β Trp72 in the *P. thermophila* NHase participate in the recognition of a substrate. The above-mentioned residues form a hydrophobic pocket initially meant to accommodate both the alkyl chain and aromatic ring of a nitrile substrate. As evident for all Co-type NHases such as β Trp72 in *P. thermophila*, in close proximity of the active is tyrosine residue which allows for binding much larger substrates than that in the Fe-type NHase (Miyanaaga *et al.*, 2001).

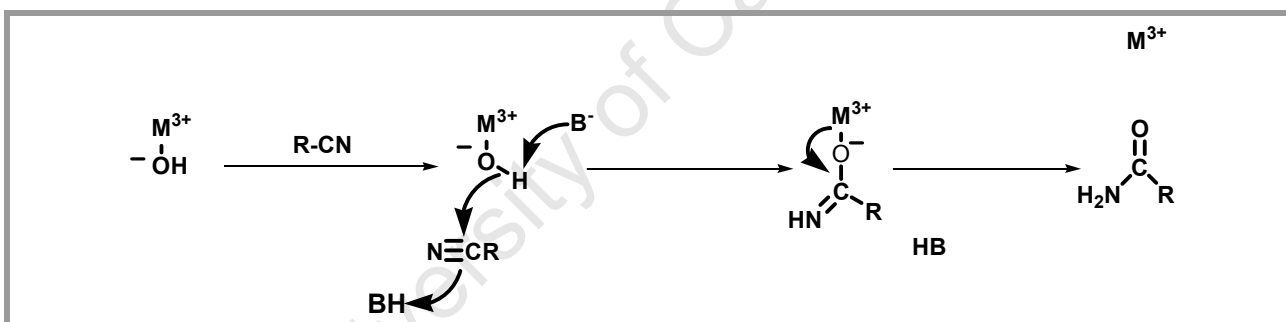
2.5.5 Mechanism of action for the NHases

On the basis of structural studies, three possible catalytic mechanisms have been proposed (Huang *et al.*, 1997). All members of the NHase share a general mechanism for the hydrolysis of nitriles in which the involvement of a metal ion, acting as a Lewis acid, is proposed. The mechanism, based on the effects of addition of substrate or competitive inhibitor on the EPR and Resonance Raman Spectra, involves either direct or indirect activation the nitrile before hydrolysis (Nagasawa *et al.*, 1986; Huang *et al.*, 1997). In the first mechanism postulated, the nitrile substrate is thought to displace a hydroxide ligand from the coordination sphere of the metal center and the metal-bound nitrile undergoes hydrolysis by a water molecule (Scheme 2.2). The metal generates a metal-bound intermediate that rearranges to the amide product and the amide is released. This mechanism is known as the inner-sphere mechanism due to the close proximity of nitrile substrate to the metal ion during the hydrolysis (Mascharak, 2002).



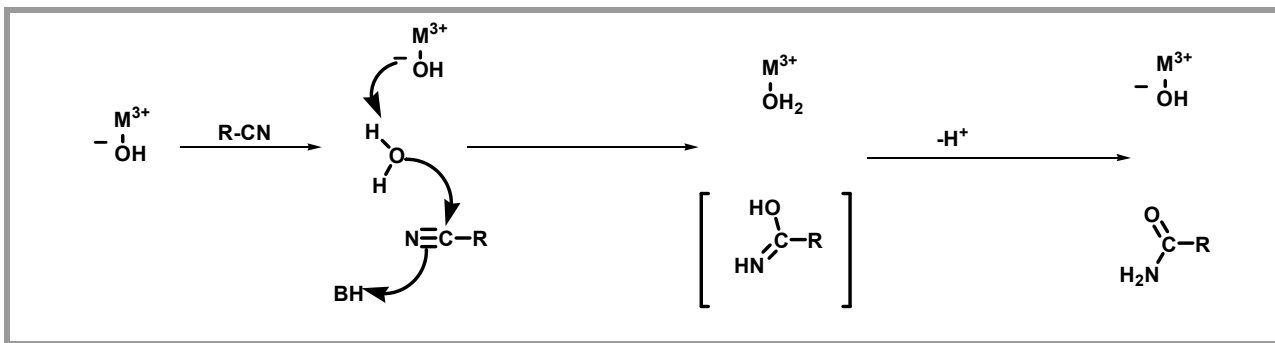
Scheme 2. 2: Proposed inner sphere reaction mechanism for NHase biocatalysis of nitrile compounds *via* nucleophilic attack by a water molecule on the alkyne carbon (Huang *et al.*, 1997; Mascharak *et al.*, 2001).

The second mechanism postulated, referred to as the outer-sphere mechanism, and involves a nucleophilic attack of the metal-bound hydroxide on the nitrile substrate at the active-site pocket (Scheme 2.3). The intermediate generated is an iminolate species that is *O*-bonded to the metal. Rearrangement of the intermediate releases the amide as product and dissociation of them metal ion.



Scheme 2. 3: Proposed outer sphere reaction mechanism for NHase biocatalysis of nitrile compounds *via* nucleophilic attack by a metal-bound hydroxide on the alkyne carbon (Huang *et al.*, 1997; Yano *et al.*, 2008).

The third mechanism, favoured by Huang *et al.*, (1997), known as the outer-sphere mechanism, involves the metal-bound hydroxide causing deprotonation of a free water molecule near the active site. A nucleophilic attack of the hydroxide ion on the nitrile substrate generates an amide (Huang *et al.*, 1997). The schematic representation of the mechanism is outlined below (Scheme 2.4).



Scheme 2. 4: Proposed outer sphere reaction mechanism for NHase biocatalysis *via* nucleophilic attack by a hydroxide ion on the alkyne carbon (Huang *et al.*, 1997; Maschark *et al.*, 2004; Yano *et al.*, 2008).

Due to the slow rates of ligand exchange exhibited by trivalent metals, it has been argued that the third mechanism (Scheme 2.4) is the most likely since this does not involve ligand exchange, unlike the first and second mechanisms (Huang *et al.*, 1997). Secondly, the observation that the rates of hydration of certain nitriles are very similar between Co-type and Fe-type NHases, whilst the exchange kinetics of the two-spin Fe^{III} and Co^{III} are very different, has also been interpreted as an indication that the third mechanism is most likely (Mascharak *et al.*, 2004). Lastly, a Co-chelate complexes have shown to bind the nitrile reagent, leading to the confirmation of that the direct association model (Scheme 2.4) is the favoured mechanism (Nakasako, 1999).

2.5.6 Substrate specificity of the NHases

The substrate specificity of NHases has been studied in detail and there appear to be clear differences between the specificities of NHases from various organisms (Table. 2.1). Although most NHases are known to hydrolyse aliphatic nitriles exclusively, some can also convert aromatic nitriles. Aliphatic and aromatic nitrile hydrolyzing NHases have been isolated and characterized from *Corynebacterium* sp. C5 (Yamamoto *et al.*, 1992), *R. erythropolis* (Duran *et al.*, 1993) and *R. rhodochrous* J1. The *R. rhodochrous* J1 NHase exhibited broad substrate specificity with particularly high specific activities on acetonitrile, chloroacetonitrile, acrylonitrile, propionitrile, n-butyronitrile, and a wide range of aromatic nitriles (Nagasawa *et al.*, 1991).

Several reports detail the substrate specificity of the five known moderate thermophilic NHases including *Geobacillus pallidus* Dac521 which has a preference for aliphatic nitriles (Cowan *et al.*,

1998), *Geobacillus* sp. RAPc8 with a very wide range of substrates such as cyclic, dinitrile, aliphatic and branched nitriles (Pereira *et al.*, 1998; Cameron, 2002), and *Bacillus smithii* SC-J05-1 with a relatively wide range of substrates such as linear, branched and aliphatic nitriles (Takashima *et al.*, 1998). The NHase from *Pseudonocardia thermophila* has preference for aliphatic nitriles, although only a few nitrile substrates were reported for this strain (Miyanaaga *et al.*, 2004). The reason for variation in substrate preference could be either (i) electronic differences between cobalt and iron in the active site/catalytic centre, (ii) bulky substrates such aromatics being too large to fit the active site of the Fe-type NHase, or (iii) the entrance to the active site being responsible for the substrate selectivity observed in Fe-type NHases (Desai & Zimmer, 2004). NHases showing enantioselectivity toward nitrile substrates in aqueous and organic solvents are becoming common and have been described previously. For example, NHases from gram-negative microorganisms such as NHase from *Pseudomonas putida* NRRL-18668 hydrolyse S-isomers 50-fold faster than R-isomers (Payne *et al.*, 1997); the NHase from *Agrobacterium tumefaciens* d3 has been reported to hydrolyse racemic (R,S)-phenylpropionitrile with high enantioselectivity to (S)-2-phenylpropionic acid *via* the (S)-2-phenylpropionamide (Bauer *et al.*, 1998), and NHase from *Rhodococcus equi* A4 exhibited preference for S-isomers (Martinková *et al.*, 1996).

Table 2.1: Summary of substrate selectivity of various nitrile hydratases.

Microorganism	Substrate preference	Reference
<i>A. tumefaciens</i>	Aromatic, cyclic, enantioselective	Bauer <i>et al.</i> ,1994
<i>G. pallidus</i> BR449	*nd	Kim & Oriel, 2000
<i>G. pallidus</i> RAPc8	Aliphatic, cyclic,dinitriles	Pereira <i>et al.</i> , 1998
<i>G. pallidus</i> DAC 521	Aliphatic	Cramp & Cowan, 1999
<i>B. smithii</i>	aliphatic	Takashima <i>et al.</i> ,1998
<i>Ps. thermophila</i>	Nd	Yamaki <i>et al.</i> , 1997
<i>P. putida</i>	Aliphatic,dinitrile, enantioselective	Payne <i>et al.</i> , 1997
<i>Rhodococcus</i> sp.YH3-3	Aliphatic, aromatic	Kato <i>et al.</i> , 2000
<i>R. rhodochrous</i> J1 H-NHase	Aliphatic, aromatic	Komeda <i>et al.</i> , 1996
<i>R. rhodochrous</i> J1 L-NHase	Aliphatic, aromatic	Komeda <i>et al.</i> , 1996
<i>R. erythropolis</i>	Aliphatic, aromatic	Duran <i>et al.</i> , 1992
<i>Rhodococcus</i> sp. R312	Aliphatic, cyclic	Nagasawa <i>et al.</i> , 1986
<i>P. chlororaphis</i>	Aliphatic	Nagasawa <i>et al.</i> , 1987
<i>Rhodococcus</i> sp. N-774	Aliphatic	Endo & Watanabe,1989
<i>Rhodococcus</i> sp. N-771	Aliphatic	Yamada & Kobayashi,1996

* Not determined

2.5.7 Functional characterisation and applications of NHases in biocatalysis

In the field of biotechnology, nitrile biotransformations using NHases are already well-established. Probably, the major driving force behind applications of nitrile hydratases comes from the potential capacity of these enzymes to perform valuable biotransformations under very mild conditions (neutral to mildly alkaline pH, ambient temperatures), their ability to exhibit chemo-, region- and stereo-selectivity and achieve valuable products (Fig. 2.6).

The first industrial application of nitrile hydratases was reported by Nagasawa & Yamada (1989) at Nitto Chemical Industries, Ltd in Japan, who developed columns of immobilized *Rhodococcus* sp. N774 cells for the hydrolysis of acrylonitrile into its corresponding acrylamide (Endo & Watanabe, 1989). In the late 1980s and early 1990s, two other microorganisms with nitrile hydratase activity were applied on an industrial scale, namely *Pseudomonas chlororaphis* B23, and *Rhodococcus rhodochrous* J1 for acrylamide production (Fig. 2.6a) (Nagasawa *et al.*, 1987, Nagasawa *et al.*, 1993). Lonza Guangzhou Fine Chemicals manufactures nicotinamide (Fig. 2-11b) and isonicotinamide (Fig. 2.6c) from 3-cyanopyridine and 4-cyanopyridine respectively, using immobilized *Rhodococcus rhodochrous* J1 cells. *Pseudomonas chlororaphis* B23 cells have been used, on the other hand, as a regioselective biocatalyst for the commercial production of 5-cyanovaleramide (5-CVAM) (Fig. 2.6d) from adiponitrile (Hann *et al.*, 1999) and *S*-mandelamide (Fig. 2.6e) is produced employing *Pseudomonas putida* (McLeish *et al.*, 2003). Continuous production of commodity amide compounds has been afforded using immobilized cells with NHase activity. The commercial-scale production of a range of chemical commodities using NHases under mildly acidic/neutral to slight alkaline pH and ambient temperature is summarized in Table 2.2, which summarizes and compares the principal industrial parameters employed in amide production based on the different NHases.

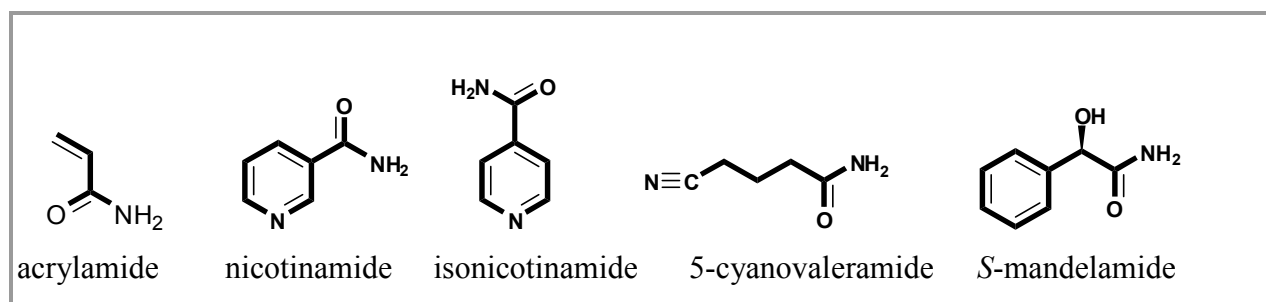


Figure 2. 6: Essential commodity amides produced using NHase biocatalysis

Table 2. 2: Operating conditions for amide production for three industrial NHases (Nagasawa & Yamada, 1995)

Parameters	<i>Rhodococcus</i> sp. N-774	<i>P. chlororaphis</i> B23	<i>R. rhodochrous</i> J1
Cofactor	Fe ^{III}	Fe ^{III}	Co ^{III}
pH stability	7.0-8.5	6.0-7.5	6.0-8.5
Temp. stability (°C)	35	20	40
Reaction temp. (°C)	5-10	5-10	5-10
Immobilization support	Polyacrylamide	Ca-alginate	Polyacrylamide
Half-lives (min)	30 min at 35°C	11min at 30 °C	58 min at 60 °C
Product	Acrylamide	Acrylamide&5-CVAM	Acrylamide&nicotinamide
Substrate concentration	27 g/L	40 g/L	50g/L
Product concentration	20 g/L	27 g/L	35-40 g/L
Cultivation time (h)	48	45	72
Production scale (T)	4000	6000	>30 000
First year of production	1985	1988	1991
Company	Nitto Chemical Industries	Nitto Chemicals Industries	Lonza Guangzhou Fine Chemicals

2.5.8 Other aspects of NHase applications

The production of nitrile-containing industrial effluents has prompted further application-oriented studies of NHases, and the value of NHase in the treatment of wastewaters is being increasingly documented (Wyatt & Knowles, 1995). This concept is receiving increasing attention and is deemed a low-cost technique compared to the conventional chemical approaches (Kobayashi & Shimizu, 1998). Two approaches to the decontamination of the waste-streams previously reported include (i) the enzymatic degradation of acrylonitrile in aqueous polymer emulsions used in raw rubber and plastic manufacture, (Battisel *et al.*, 1997) and (ii) development of a stable activated sludge system with a consortium of microbial isolates for the treatment of the toxic waste streams produced from the large-scale manufacture of acrylonitrile (Thompson *et al.*, 1988).

Nitrile hydratase has also been used to efficiently degrade nitrile-containing herbicides such as dichlobenil (2, 6-dichlorobenzonitrile) and bromoxynil (3, 5-dibromo-4-hydroxybenzonitrile). *Agrobacterium radiobacter* is used for the degradation of the herbicides under non-sterile conditions in batch and continuous processes (Banerjee *et al.*, 2002). Results obtained from the degradation processes have shown that up to 65% of bromoxynil herbicide concentrates were degraded in 5 days.

2.5.9 Application of NHases in bi-phasic solvent systems

Two-phase (biphasic) solvent systems are reaction media in which both organic and aqueous phases are present. Practically, these systems offer an opportunity to biotransform poorly aqueous-soluble (lipophilic) substrates whose reactions are limited by their solubility in the aqueous reaction medium (Leuenberger, 1990). The organic phase in any biphasic system enables solubilization the substrate and product, while biocatalysts remain in the aqueous phase with their catalytic activity retained. Several examples of organic solvents which have been used successfully for such co-solvent systems in a number of biocatalytic reactions, including: n-alkanes, cyclohexane, toluene, benzene, chloroform, carbon tetrachloride, methylene dichloride, ethyl or butyl acetate and diethyl ether (Gupta, 1992).

In particular, NHases are found to be functional in *n*-alkane (C-8 or C-16)/aqueous biphasic mixtures and monophasic water-saturated C-6 to C-11 *n*-alkanols (Layh & Willets, 1998). For example, the NHase from *Rhodococcus equi* was found to function in the presence of high concentration of hydrocarbons [90% (v/v) of isooctane] while methanol or ethanol were suitable only at 20% v/v (Přepechalová *et al.*, 2001). Nagasawa and coworkers have shown that the NHase retains 89 – 100% of its original activity in the presence of 50% (v/v) of acetone, 1, 4-dioxane, *N*, *N*-dimethylformamide, tetrahydrofuran, dimethyl sulfoxide and ethylene glycol (Nagasawa *et al.*, 1993). Further, application of the NHase from *Rhodococcus equi* showed that the enantiomeric ratio value (*E*) increased from 15 to 41 when a biphasic system composed of aqueous phosphate buffer and hexane (50%) was used in the reaction (Přepechalová *et al.*, 2001). Due to the hydrophobic nature of most nitriles, introduction of an organic co-solvent in their reaction media will be advantageous from an industrial perspective, and tolerance of NHase to organic solvents contributes to the view that the enzyme could, in the future, be successfully applied in numerous processes.

2.6 Thermostable enzymes and their biotechnological application

Thermostable enzymes are generally obtained from microorganisms that originate from extreme hot environments, and they are in increasing industrial demand due to their ability to tolerate harsh industrial process conditions (Haki & Rakshit, 2003). Considerable efforts have been devoted to the search for such enzymes and possible commercial applications because of their overall inherent stability (Demirijan *et al.*, 2001). There are several advantages to exploiting enzymes that are stable and active at elevated temperature; allowing a higher operation temperature has a significant influence on the bioavailability and solubility of many reaction components, as well as allowing for higher reaction rates, and reducing the risk of contamination that leads to undesired complications (Becker, 1997). However, although use of thermostable enzymes at higher temperatures seems to be a powerful tool to enhance biocatalytic performance, the main drawback would be its higher energy requirements leading to higher operational costs when compared to processes at ambient temperatures.

To date, only a few thermophilic nitrile-metabolizing enzymes have been isolated, exemplified by the nitrile hydratases from a moderately thermophilic *Geobacillus* sp. (Cramp *et al.*, 1997;

Pereira *et al.*, 1998; Takashima *et al.*, 1998), and from *Pseudonocardia thermophila* (Yamaki *et al.*, 1997).

2.6.1 The novel *G. pallidus* RAPc8 nitrile hydratase

A new moderately thermostable cobalt-containing NHase enzyme was isolated from a thermophilic *Geobacillus* species, in the course of a program to find enzymes with novel properties and activities for industrial application (Pereira *et al.*, 1998). The discovery of this NHase was a result of screening a number of microbial isolates from sediment samples, taken from several New Zealand thermal environments, for nitrile-degrading activity. The native bacterial strain has been characterized on the basis of 16S ribosomal DNA sequencing studies indicating that the organism was a *Bacillus* species, being 99.9% identical to *Bacillus* (starch positive) (DSM 2349). The isolate was hence designated *Bacillus* sp. RAPc8, now known as *Geobacillus pallidus* RAPc8 (Pereira *et al.*, 1998).

Culture studies of the *G. pallidus* RAPc8 NHase were used to determine a maximum specific growth temperature of 65°C, and no growth was observed at either lower (37°C) or higher temperatures (70°C). The optimum temperature for production of nitrile-degrading activity was observed to be 60°C and the strain was found to constitutively produce the nitrile-degrading activity. Chemical inducers such as cobalt, urea, acetamide, valeramide, and benzamide did not increase activity. A preliminary study of substrate specificity of the NHase enzyme from *G. pallidus* RAPc8 was conducted; a broad substrate specificity range on aliphatic nitriles, with particular preference for the branched and cyclic aliphatic nitriles, was observed. For example, the enzyme exhibited turnover rates for propionitrile and acetonitrile under optimum reaction conditions of 436 sec⁻¹ and 765 sec⁻¹, respectively (Pereira *et al.*, 1998). Within the substrate specificity of the enzyme, no reaction with the aromatic substrates benzonitrile or benzylocyanide was observed, but the NHase did react with heteroaromatic nitriles (Cowan *et al.*, 1998). Based on these findings, work on the protein engineering of *G. pallidus* RAPc8, aimed at improving its substrate specificity on aromatic substrates was conducted and is described in Section 2.6.3.

2.6.2 Cloning, sequencing and expression of genes from *G. pallidus* RAPc8 (Cameron & Cowan, 2005)

The gene encoding nitrile hydratase from *G. pallidus* RAPc8 was cloned into *E. coli* and sequenced. Heterologous expression has been shown to offer a number of advantages including the opportunity to obtain large amounts of enzymes for characterisation and it also allows the use of modern molecular biology techniques (directed evolution and site directed mutagenesis) to improve enzyme properties that may be important for biotechnological application.

A sequence analysis of the cloned DNA responsible for the NHase gene revealed an open reading frame of 5.9 kb coding for a protein of 122-amino acids. A comparison of the deduced amino acid sequence with sequences in relevant databases indicated no significant homology with previously identified gene sequence. The NHase gene was then overexpressed in *E. coli* cells under the control of the T7 promoter. The recombinant clone of *E. coli* BL21 (DE3) produced significant levels of NHase activity, with a specific activity of 49 U/mg of soluble enzyme per liter of medium. This reflected a many-fold increase in the specific yield compared to the yields from the native microorganism (Pereira *et al.*, 1998). The overexpression of the NHase in *E. coli* also established that for maximal enzyme activity, a protein (P14K) was required to be co-expressed. Co-expression of NHase with various activators has been shown to improve specific activity of the recombinant enzyme (Wu *et al.*, 1997) and to assist in the folding of the NHase α subunit prior to α - β association, and subsequently formation of $\alpha_2\beta_2$ heterotetrameric structure (Cameron & Cowan, 2005).

The recombinant NHase was purified to apparent homogeneity on the basis of heat treatment, ammonium sulphate precipitation and two chromatographic steps. The purified recombinant enzyme showed two bands with an estimated molecular weight of 28 kDa and 29 kDa in a sodium dodecyl sulfate-polyacrylamide gel representing the α - and β subunits, respectively. The general enzymatic properties of the purified recombinant *G. pallidus* RAPc8 NHase protein were the same as those of the native one, with the optimal activity measured at 60°C within a broad pH range from 5.1 to 8.7, and an optimum at pH 7.2.

2.6.3 The crystal structure of *G. pallidus* RAPc8 NHase

Crystal structures of several NHases homologous to the *G. pallidus* RAPc8 NHase have been resolved. For example, the crystal structure of the cobalt-containing NHase from *Pseudonocardia thermophila* JCM 3095 (Miyanaga *et al.*, 2001), the iron-containing nitrile hydratase from *Rhodococcus* sp. N-771 and the cobalt-containing nitrile hydratase from *Bacillus smithii* (Komeda *et al.*, 1996) have been elucidated, showing significant structural similarities. Recently, the *G. pallidus* RAPc8 structure was described (Tsekoa *et al.*, 2004), and was found to closely resemble that of the NHase from *P. thermophila* JCM 3095 (Tsekoa, 2005).

The main features of the *G. pallidus* RAPc8 NHase crystal structure included a complex interaction between the α and β subunits with regard to dimer formation, which appeared as a dynamic process rather than the docking process previously reported in similar NHases (Nagashima *et al.*, 1998). The cobalt-containing active site shared a typical claw-setting motif unique to NHases (Huang *et al.*, 1997), and co-ordination to the cobalt was shown to be octahedral with amino acids α Cys119, α Ser120, α Cys121 providing ligands to the metal centre on the vertices of the octahedron. Further, the electron density in this region demonstrated that the α Cys119 and α Cys121 are oxidized to cysteine sulfinic and cysteine sulfenic acid, respectively (Tsekoa, 2005).

Analysis of the NHase crystal structure showed accessible channels located at the interface between the α and β subunits. These channels are open to bulk solvents from either side of the molecule and are possible candidates for the entrance of substrates to the metal centre. Structural analysis of the channels showed that the modified cysteine residues (that form the cobalt-binding claw-setting motif at the active site) were among the residues identified as part of the channel. Differences in the substrate specificity have, in the past, been reported to be related to the passage of substrates to the catalytic centre through the channel (Nagasawa *et al.*, 1998). A hypothesis was proposed that the spatial arrangement of residue β W76 is responsible for the difference in substrate preferences between the Co-type and Fe-type NHase (Cowan *et al.*, 2003).

The most prominent feature observed in the *G. pallidus* RAPc8 NHase was the presence of an additional α -helix comprising amino acid 116 – 126 on the β subunit (Tsekoa, 2005). The additional helical content in the NHase was suggested to contribute to an increase in thermostability observed in the enzyme. Increased helix structures in protein are known to be involved in additional interaction between dimers and this interaction further contributes to thermostability (Kumar *et al.*, 2000).

2.6.4 Protein engineering of *G. pallidus* RAPc8 NHase

Mutation of the *G. pallidus* RAPc8 NHase was conducted to improve the physiochemical and catalytic characteristics. The importance of mutation of the aromatic specificity of *G. pallidus* RAPc8 NHase was due to the great potential of aromatic products of NHase biotransformations as pharmaceutical products and the ability for the *G. pallidus* RAPc8 to produce these compounds would be highly desirable.

The active site and substrate specificity of *G. pallidus* RAPc8 NHase, which preferentially catalyses heteroaromatic nitriles (e.g. 3-cyanopyridine) but not homoaromatic nitriles (benzonitrile), was investigated. Amino acid residues selected as targets for site-directed mutagenesis were located in the conserved region designated as the substrate-binding/active site. Aromatic side chains (assumed to contribute to aromatic-aromatic trapping through pi-cloud-pi-cloud association), were replaced with glycine. Mutation of this tryptophan to glycine did not result in detectable levels of activity. However, it resulted in decreased inhibition by benzonitrile (Tsekoa, 2005).

2.7 CONCLUSIONS

This review has shown that biocatalytic processes have broad applications in organic synthesis, particularly in the synthesis of pure drug intermediates, specialty chemicals, and even commodity chemicals in the pharmaceutical, chemical and food industries. Their ability to function with a broad chemo-, regio- and stereo-selectivity offers several advantages compared to conventional chemical approaches. Coupled with high-throughput screening, cloning, and protein engineering techniques, which allow creation of enzymes with new properties, this makes biocatalysts

eminently suitable for industrial applications. In the past two decades, NHases have been shown to have industrial potential in commercial processes for production of chemical commodities including acrylamide, nicotinamide, 5-cyanovaleramide and *S*-mandelamide.

Through the search for novel enzymes, a thermostable NHase was found in the strain *G. pallidus* RAPc8. The *G. pallidus* RAPc8 NHase was isolated, cloned in *E. coli* BL21 (DE3) and partially characterized. The NHase exhibits broad substrate selectivity and can be used at high temperatures, in which higher reaction rates can potentially be achieved. Since many of the commercial applications of NHase were based on mesophilic-derived biocatalysts we expect that their synthetic utility will be extended even further in the use of thermophilic-derived NHases.

The following chapters of the thesis will describe a detailed experimental approach to the production of NHase from *E. coli* BL21 (DE3), functional characterisation of the thermostable NHase in its soluble state will be conducted in terms of pH, temperature, stability profiles, substrate concentration, co-organic solvents, metal ions, kinetic studies, and the investigation leading to successful immobilization of the NHase. Potential for the development of a continuous process in production of nicotinamide in packed-bed reactor is described in detail.

CHAPTER THREE

PRODUCTION, PURIFICATION AND CHARACTERISATION OF *Geobacillus pallidus* RAPc8 NHase

3.1 INTRODUCTION

In order to establish the novelty of the biocatalyst developed from *G. pallidus* RAPc8 NHase, experiments were conducted into its selectivity, activity and stability under biocatalytic reaction conditions. Prior to the initial NHase characterisation, production of the NHase in large quantities was carried out, together with purification. Throughout most of this study, NHase was routinely produced and purified using protocols previously reported by Pereira *et al.* (1998) and Cameron (2002). The important criteria for successful industrial application of enzymes are firstly, that the production, isolation and purification of the desired enzyme need to be reproducible and scaleable. Secondly, it is important to recognize that prior knowledge of suitable reaction conditions will help in the design and achievement of an efficient enzymatic process. Although the specific reaction conditions for many NHases have been extensively studied, little was known for the novel *G. pallidus* RAPc8 NHase. Pereira *et al.* (1998) and Cameron (2002) reported structural and partial functional characterisation of the native and recombinant *G. pallidus* RAPc8 NHase, but did not identify the parameters for maximising the rate of hydration of nitrile substrates. In this study, confirmation of conditions for *G. pallidus* RAPc8 NHase production, scalability of production and full functional characterisation are reported, using the hydrolysis of 3-cyanopyridine to nicotinamide as a model reaction (Section 3.1.1).

Enzyme production and purification processes vary a great deal depending on the required quality, quantity, application, and value of the enzyme. Bulk commodity enzymes, for example, have an inherent low value and this necessitates a low cost of manufacture with minimal processing. On the other hand, high tech research, therapeutic and diagnostic enzymes are expected to be of high purity which is associated with high standards of processing. In the past two decades, high standards in enzyme production have been facilitated by the development of

recombinant techniques leading to the availability of various host-vector expression systems. The bacterial strain *Escherichia coli* BL21 is commonly used as a host for overexpression of intra-cellular enzymes, while *Bacillus* and fungal *Aspergillus* strains are very prolific producers of extra-cellular enzymes. *E. coli* is commonly used for intracellular enzymes because it is readily genetically manipulated and cultured, and it tolerates high levels of expressed foreign protein (Rosenberg, 1996).

Batch cultivation is the simplest way to produce recombinant protein in *E. coli* BL 21 (Fan *et al.*, 2005). Luria-Bertani (LB) medium (consisting of bacto-tryptone, yeast extract and sodium chloride) is supplied from the start, and growth is unrestricted. Growth of *E. coli* requires carbon and nitrogen which are conveniently supplied by the bacto-tryptone and yeast-extracts, respectively. However, batch cultivation only yields moderate cell densities, and enzyme yields generally level out due to limitation in nutrients and/or oxygen, and changes in pH (Lee, 1996). Induction is often essential as enzyme synthesis is often repressed and the enzyme is only produced in the presence of the inducer. In order to obtain high levels of foreign protein expression in *E. coli*, inducers are applied prior to the exponential growth phase. The timing of addition of the inducer is very important for the production of maximum enzyme expression. The inducer may be the enzyme substrate, as is often the case for intracellular enzymes. Co-enzymes can act as inducers as well; for example, production of pyruvate decarboxylase is induced by thiamine diphosphate (Tittmann *et al.*, 1998). In laboratory-scale production, isopropyl- β -D-thiogalactopyranoside (IPTG)-inducible promoters, which regulate protein transcription, are widely used (http://www.ambion.com/techlib/spec/sp_9462.pdf), and in some cases, inorganic ions are required in order for the enzyme to be produced in an active form.

Physical conditions of growth such as temperature, pH, and osmotic pressure strongly affect microbial biomass and enzyme production. The temperature affects enzyme activities in microbial metabolic pathways in that when the temperature is low, the metabolic rate is reduced, and when the temperature is very high, the microbial enzymes may be deactivated. Since microbes and enzymes are very sensitive to pH, the selection of optimal pH is essential for their production (McMahon *et al.*, 1999). Most microbial species are maintained at pH ranges (5 to 9), and further increases in pH result in decreased microbial cell biomass production. However,

several alkaline- and acid-tolerant microorganisms have been characterized recently and fermentation conditions for biomass production for such strains would be different (Techapun *et al.*, 2002). Osmotic pressure or salt concentration affects biomass production in that when these exceed the optimal level required by the microbial cytoplasm, dehydration and shrinking follow. On the other hand, if the osmotic pressure is excessively low, cell components swell and organelles may burst, adversely influencing cell density and cell survival.

In production of enzymes, the extraction and purification stages are as important in achieving high yields of very active enzymes as the fermentation stages. The main challenge in the recovery and purification stages is to minimise the losses of activity in the target enzyme. For intracellular enzymes, for example, bacterial cells must be disrupted to release the enzyme. Although techniques such as freeze-drying, simple freezing, and homogenisation serve as convenient methods for disruption and avoid protein degradation, they can be expensive and time consuming. Sonication of bacterial cells is convenient or practical; here, the process of cell breakage requires high-pressure ultrasound to impact on the cell wall and cause breakage of cells. Expression of protein in recombinant *E. coli* cell systems entails the production of endogenous cellular component such as lipids, nucleic acids, sugars, proteases, as well as the target protein. To achieve recovery of the target protein to near homogeneity, it is necessary take this into account and to exploit the physical and biochemical properties of the protein (size, charge, solubility, hydrophobicity, precipitation). In this study, recombinant *G. pallidus* RAPc8 NHase was purified by employing previously reported protocols including heat treatment, ammonium sulphate precipitation, hydrophobic interaction and ion exchange chromatographies (Pereira *et al.*, 1998; Cameron, 2002).

Since part of this research was to establish the biochemical and biocatalytic properties of the *G. pallidus* RAPc8 NHase, it was noted that accurate selection of essential process parameters was necessary, in order to overcome obstacles which could hinder the biocatalytic applications of the NHase. For example, the rates of enzyme-catalysed reactions depend on factors such as the concentration of substrate and product, pH and temperature of the medium, as well as the presence of any chemical inhibitors. The presence of non-conventional media (*e.g.* organic solvents) in reaction mixture may be desirable and the effects of this were evaluated. Organic

solvents can be added to the reaction medium, offering some advantages over the use of pure aqueous media. Improved substrate solubility, reduction of unwanted side reactions, and the ability to shift thermodynamic equilibrium towards synthesis of desired products, would be some such advantages. Further, the metallo-dependence of NHase enzymes has been reported by various researchers. Investigations by several authors have indicated that metal ions (either cobalt, zinc or iron ions) are required as cofactors in the NHase catalytic activity (Nagasawa *et al.*, 1991; Huang *et al.*, 1997; Payne *et al.*, 1997). Cameron (2002) found that the NHase from *G. pallidus* RAPc8 (formerly *B. pallidus* RAPc8) was induced by addition of 5 μ M Co^{2+} ions to the growth medium. This has also been reported by Tsekoa *et al.* (2004) and Pereira *et al.* (1998) who found that the *G. pallidus* RAPc8 NHase required Co^{2+} ions for optimal activity, but a detailed investigation of metal ion dependence had not been carried out. On the other hand, metal ions at elevated concentrations can also have inhibitory effects on enzyme catalytic activity (Medyantseva *et al.*, 1998).

In work described in this chapter, larger than previously reported quantities of *G. pallidus* RAPc8 NHase from recombinant *E. coli* BL 21 (DE3) strain were produced. At the onset, *E. coli* BL21 (DE3) was grown in a small-scale flask cultures, and later, a large-scale 5L BioFlo fermenter was used. The objective was to achieve high levels of production of the NHase enzyme, with high activity that was required for later experimental protocols. The culture method used here was established previously but was adapted (Cameron, 2002). Further, preliminary experiments were conducted in order to establish reaction conditions before optimisation of some biochemical properties of the NHase from *G. pallidus* RAPc8, and its full functional characterisation, was conducted.

3.1.1 Model reaction for *G. pallidus* RAPc8 NHase in the production of nicotinamide

In this study, the model reaction chosen for development of the *G. pallidus* RAPc8 NHase as a biocatalyst was the hydration of 3-cyanopyridine to nicotinamide, also known as 3-pyridinecarboxamide (Fig. 3.1). While it was known that *G. pallidus* RAPc8 NHase reacts with a wide range of nitriles, it was also recognised that the NHase converts 3-cyanopyridine to nicotinamide more readily than other heteroaromatic substrates (Cameron & Cowan, 2005).

Given the industrial importance of nicotinamide, it was of interest to further investigate its effective production.

Nicotinamide is a white crystalline, water-soluble solid and forms part of the vitamin B complex. In cells, nicotinamide is incorporated into nicotinamide adenine dinucleotide (NAD^+) and nicotinamide adenine dinucleotide phosphate (NADP^+), the coenzymes in a wide variety of enzymatic oxidation-reduction reactions (Belenky *et al.*, 2007). Pharmaceuticals utilize nicotinamide widely to enhance and develop consumer care products, while the food and nutritional industries also require supplementation of nicotinamide in most food products. Worldwide, production of nicotinamide is estimated to amount to approximately 15, 000 tonnes per year (Lonza, 2001).

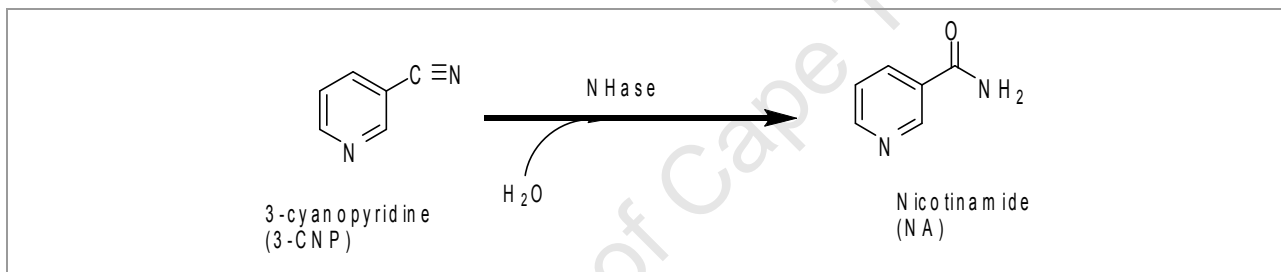


Figure 3. 1: Synthesis of nicotinamide (NA) from the hydration of 3-cyanopyridine (3-CNP) catalysed by NHase.

3.2 MATERIALS AND METHODS

3.2.1 Materials

3.2.1.1 Chemical and reagents

Chemicals and solvents were purchased from Sigma-Aldrich (SA), Merck Chemicals and Fluka Supplies. All chemicals and solvents were of analytical grade.

3.2.1.2 Microorganisms

G. pallidus RAPc8 nitrile hydratase was recombinantly expressed in *E. coli* BL21 (DE3) pLysS, a protease-deficient strain of *E. coli* that expresses T7 lysozyme, according to the methods of Cameron (2002). Cells were transformed with expression vector pNH14K the plasmid carrying the coding sequences for the α and β subunits of nitrile hydratase as well as the coding sequence for P14K under control of the T7 DNA polymerase promoter (Cameron, 2002). Prof. Don Cowan of the Institute for Microbial Biotechnology and Metagenomics (IMBM), University of Western Cape, kindly provided the recombinant *E. coli* BL21 (DE3) pLysS strain. Glycerol stocks of the *E. coli* BL21 (DE3) pLysS strain were kept at -20 °C.

3.2.1.3 Media

All seed and cultivation media for fermentation were prepared to appropriate concentrations for addition of 10 % (v/v) inoculum. Antifoam, up to 0.025 % (v/v), was added separately for cultivation carried out in 1 and 5 L BIOFLO 110 fermenters. All media were sterilized by autoclaving at 120 °C, 1 atm for 20 min.

3.2.1.3.1 Agar Luria Bertani (LB) medium

The medium contained bacto-tryptone (10.0 gL⁻¹), yeast extract (5.0 gL⁻¹), sodium chloride (10.0 gL⁻¹), and agar (1.5 gL⁻¹). Ampicillin was added to a final concentration of 50 µg/mL after autoclaving and cooling to 50 °C. The medium was poured directly into petri dishes and stored at 4 °C until required.

3.2.1.3.2 Seed and cultivation medium for *E. coli* BL21 (DE3) pLysS

The medium contained bacto-tryptone (10.0 gL⁻¹), yeast extract (5.0 g L⁻¹), and sodium chloride (10.0 gL⁻¹), dissolved in 950 mL of deionized H₂O with shaking. The pH was adjusted to 7.0 with 5 N NaOH (approximately 0.2 mL). The total volume of the solution was adjusted to 1 L with deionised H₂O and sterilized by autoclaving for 20 min at 1 atm.

3.2.2 Methods

3.2.2.1 Growth and induction of *E. coli* BL21 cells

3.2.2.1.1 Plate culture production

Frozen stocks of transformed *E. coli* BL21 (DE3) were streaked onto LB agar plates using sterile technique and plates were incubated at 37 °C overnight. The cultures were maintained at 4 °C for two months.

3.2.2.1.2 Growth of seed culture

A colony of *E. coli* BL21 (DE3) from an LB agar plate was inoculated into 250 mL LB broth medium (in a 500 mL Erlenmeyer flask) supplemented with 50 µg of ampicillin per mL. The broth was then incubated at 37 °C with shaking at 220 rpm in a temperature controlled orbital shaker, overnight or until an absorbance (A_{600}) of 1.2 measured at 600 nm was reached.

3.2.2.1.3 Production of *G. pallidus* RAPc8 NHase in shake flasks

Cotton wool-stoppered 2 L Erlenmeyer flasks containing 1 L of cultivation medium with 50 µg of ampicillin per mL were used in the shake flask studies of *G. pallidus* RAPc8 nitrile hydratase production. 25 mL (2.5% of total volume) seed culture was inoculated into the shake flasks and cultures were agitated at 220 rpm in a bench top orbital shaker incubator at 37 °C. At time intervals of 30 min, during the incubation period, 1 mL of culture was transferred to a cuvette and the absorbance A_{600nm} was measured until the $A_{600nm} = 0.3$. The culture was then induced by addition of 5 mL of IPTG to give a final concentration of 0.4 mM. A solution of 800 µL Cobalt chloride (0.1 mM) was added to the culture 15 min before induction. After 4 h of cell growth, when the absorbance A_{600} was found to be 0.8, cells were harvested by means of centrifugation at 7000 x g, at 4 °C for 15 minutes. Sonication of the cells, followed by the centrifugation, yielded enzyme extracts in the supernatant (details in Section 3.3.6).

3.2.2.1.4 Expression of *G. pallidus* RAPc8 NHase in a 5 L BioFlo fermenter

Five litres of cultivation medium was added to a BioFlo 110 Fermenter vessel, sterilized at 120 °C for 20 min and upon cooling, 50 µg/mL of ampicillin (total concentration) was added. The fermenter was equipped with a heat-blanket, a 4-baffled stainless insert agitation impellers and

dissolved oxygen and pH probes. The control system a module comprised primary control unit (PCU), power controller, four pump modules and pH/DO controller. Inoculum was prepared as described in Section 3.3.2. The inoculum was cultivated overnight at 37 °C on a rotary shaker at 220 rpm. Inoculum (250 mL, approx. 5% working volume) was added and set points on the controller were set prior to inoculation: temperature= 37 °C, pH = 7.0, initial dissolved oxygen = 100 %, agitation = 350 rpm and airflow = 2.5 vvm. Increasing cell density from the time of inoculation through to the end of the fermentation was recorded.

3.2.2.2 Harvesting of the *E.coli* BL21 (DE3) cells

After the cells had grown for the appropriate length of time (Section 3.3.3 and 3.3.4), they were harvested by centrifugation for 15 min at 7 500 x g at 4 °C, washed with 25 mL of 50 mM potassium phosphate buffer, pH 7.2. The supernatant was discarded and the pellet resuspended in a minimal volume of 50 mM potassium phosphate buffer to give a total volume of extract of 25 mL. The cells were then stored at – 20 °C for a short-time before being sonicated.

3.2.2.3 Cell disruption by sonication

The cells (3.45g), obtained as described in Section 3.3.5 above, were resuspended in 20 mL of 50 mM potassium phosphate buffer by gently pipetting the cells. The cells were exposed to discontinuous bursts of ultrasound (1 min burst, 30 sec break cycles, at 60 % power for 10 min) while being maintained at 0 °C, using a Soniprep Ultrasonic Instrument. Disrupted cells were then centrifuged at 7 500 x g for 15 min, at 4 °C, and the cell-free supernatant was retained for further purification.

3.2.2.4 Purification of *G. pallidus* RAPc8 NHase

Unless otherwise stated, all purification steps were performed at room temperature. All chromatographic procedures were performed on an ÄKTA fast protein liquid chromatography system (Amersham Biosciences) using recommended flow rates and pressure limits for each of the pre-packed columns utilized. Samples from each stage of purification were analyzed and verified for purity by 12% sodium dodecyl sulfate (SDS)-polyacrylamide gel electrophoresis. NHase activity was measured using the HPLC detection method and protein determinations were

carried out using bovine serum albumin (BSA) standard solution, and the Bradford colourimetric method (Bradford, 1976).

3.2.2.4.1 Heat purification of crude enzyme extracts

Heat treatment was employed as the first step in the protein purification, thereby precipitating undesired heat-sensitive *E. coli* protein. Cell free enzyme extract obtained as described in section 3.2.2.3 (25 mL) was incubated in a water bath at 55°C for 45 minutes. The samples were centrifuged at 7000 x g, for 15 minutes at 4°C. The supernatant was then transferred to a sterile tube.

3.2.2.4.2 Ammonium sulphate precipitation purification method

Precipitation was used in the second step of purification, to remove undesired protein components prior to chromatography steps. 2.68 g of ammonium sulphate was added to a 25 mL of enzyme extract, with gentle stirring, to the protein extract to give a concentration of 20% saturation. After being left on ice for 1 h, the precipitate was removed by centrifugation at 7000 x g for 15 minutes at 4°C. The supernatant was collected and retained for subsequent chromatographic stages.

3.2.2.4.3 Hydrophobic interaction chromatography (HIC)

The supernatant (25 mL) from the ammonium sulphate precipitation step was loaded onto a pre-packed Hiload 16/10 Phenyl-Sepharose column on the FPLC system. The column was equilibrated with 1.0 M ammonium sulphate in 50 mM potassium phosphate buffer, pH 7.2. Elution of bound protein was achieved with a linear gradient of decreasing ammonium sulphate concentration generated by 50 mM potassium phosphate buffer, pH 7.2 at a flow rate of 3.0 mL/min. Protein was monitored by a UV detector measuring absorbance at A_{280} . The eluate was collected in 2 mL fractions, and those containing protein were combined and dialysed overnight against 20 mM potassium phosphate buffer.

3.2.2.4.4 Ion Exchange Chromatography (IEX)

The NHase solution obtained from HIC was loaded on the pre-packed HiPrep 16/10 Q-sepharose FF column on the FPLC system. The column was equilibrated with 25 mM potassium phosphate buffer, pH 7.2 and bound protein was eluted with a linear gradient of increasing sodium chloride (0 to 0.5 M) in 25 mM potassium phosphate buffer. Protein was monitored by a UV detector measuring absorbance at A_{280} . Fractions of 2 mL were collected and those containing protein fractions were concentrated by dialysis against 50 mM potassium phosphate buffer, pH 7.2.

3.2.2.5 Sodium dodecyl sulphate-polyacrylamide electrophoresis (SDS-PAGE) analysis of the purified *G. pallidus* RAPc8 NHase

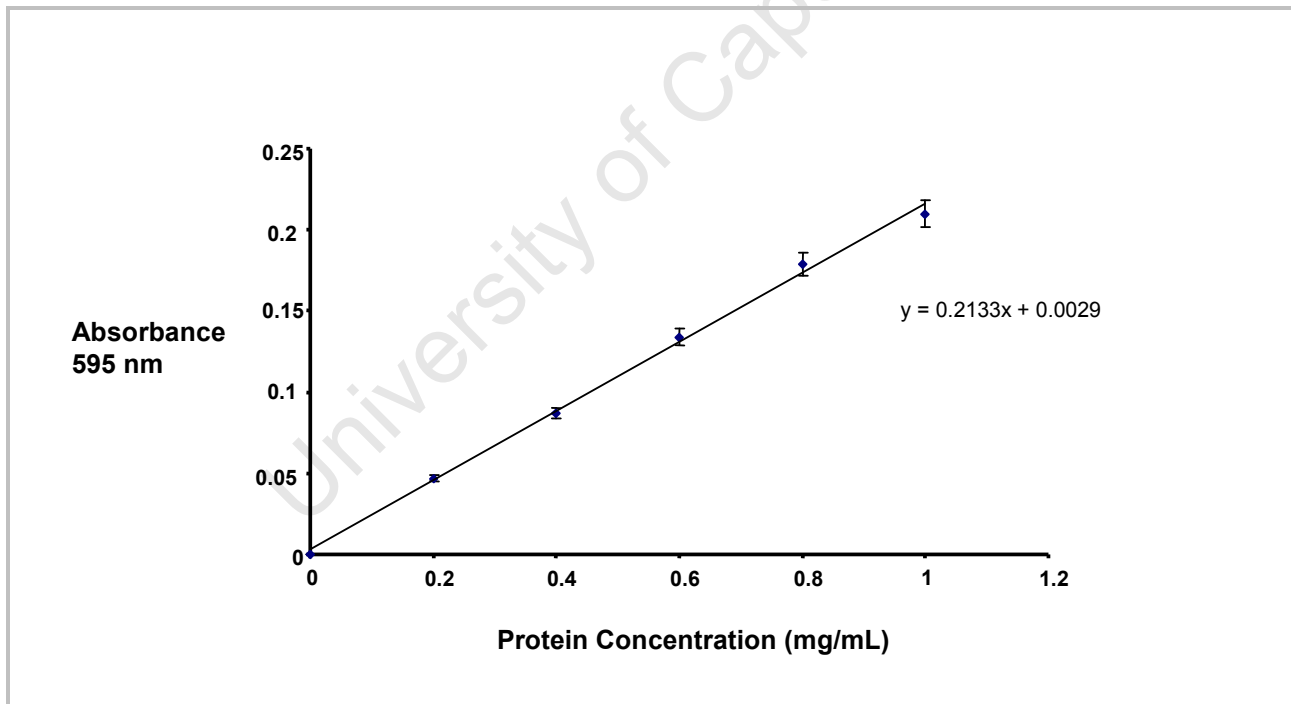
Electrophoresis was carried out in a 12% polyacrylamide gel in the presence of 20% SDS at 50 mA and 150 V using the Laemmli method (Laemmli, 1970). The sample (20 μ L) was incubated for 5 min in boiling water and then loaded on the gel (Appendix C-8 and C-9). The gel was run at 150 volts, 28.0 mA for 1 h. Protein bands were stained with 0.25% solution of Coomassie Blue R-250 (Appendix C-5) for a maximum of three hours, and the excess dye was removed (destained) by soaking gel overnight in destaining solution (detailed procedures in Appendix D.6).

3.2.2.6 Standard Biorad assay procedure for protein concentration determination

Protein concentrations were determined using the Bradford Coomassie Brilliant Blue dye assay (Bradford, 1976). Protein standards were prepared using bovine serum albumin (BSA). The dye reagent was prepared by diluting 1 volume dye reagent concentrate (supplied by Bio Rad) with four volumes deionized water, and the diluted reagent was then kept at 4°C. Six to seven dilutions of the BSA protein standard were prepared (Table 3.1), with concentrations representative of the protein solution to be tested (0 to 1.0 mg/mL). Samples (20 μ L) of each standard were pipetted into test tubes containing 1 mL of diluted dye reagent (dye reagent 1:4 v/v distilled water), the test tubes were vortexed, and samples were incubated at room temperature for 5 min. Protein solutions were normally assayed in duplicate. Absorbances were measured at 595 nm and a typical standard curve is shown in Fig. 3.2.

Table 3. 1: Bradford protein assay standard preparation

10 mg/mL BSA (μ L)	Deionized H ₂ O (μ L)	Standard Conc. (mg/mL)	Absorbance 595 nm
0	1000	0	0.0
20	980	0.2	0.05
40	960	0.4	0.09
60	940	0.6	0.13
80	920	0.8	0.18
100	900	1.0	0.21

**Figure 3. 2: Standard curve for protein determination using Bradford's reagent. The absorbance was read at 595 nm. $R^2=0.997$**

3.2.2.7 NHase activity assay

NHase activity was determined by HPLC, based on the amount of nicotinamide (product) formed, as in a previously described method (Nagasawa *et al.*, 1988). The reaction mixture consisted of 50 mM K₂HPO₄/KH₂PO₄ buffer (pH 7.2), 50 mM of 3-cyanopyridine and an appropriate amount of soluble enzyme (approximately 0.015 to 0.14 mg protein), in a final volume of 3 mL in a 30 mL vial. The mixture was incubated at 50°C with stirring (150 r.p.m) for 5 min, and the reaction was terminated by adding 0.2 mL of 3 M HCl or 0.1 mL of trichloroacetic acid.

One unit of NHase activity was defined as the amount of enzyme that catalysed the production of 1 μmole of product per minute under the standard assay conditions.

Activity of the enzyme was determined by Equation 3.1 (below):

$$\text{Activity} = \frac{C_p (\mu\text{mol})}{\text{mL}} \times V_{\text{total}} (\text{mL}) \times \frac{1}{t} (\text{min}) \quad 3.1$$

C_p Concentration of product from HPLC (μmol/mL)

V_{total} Total volume of reaction (mL)

t Time (min)

The specific activity of the enzyme was determined by Equation 3.2

$$\text{Specific activity} = \frac{\text{Activity (U)}}{\text{Protein concentration (mg)}} \quad 3.2$$

3.2.2.8 HPLC quantification of unreacted substrates and reaction products

Standard solutions of 3-cyanopyridine and nicotinamide were prepared by dissolving appropriate amounts of the two compounds in deionised water to give the desired concentrations (Table 3.2 and Table 3.3), respectively. Typical standard curves are shown in Fig. 3.4 and Fig. 3.5, respectively. The HPLC analysis and quantification were performed with a Lachrom (Hatch) series system equipped with a UV detector and a pre-packed C 18 column (4.6 by 150 mm dimension). Analyses were conducted at a flow rate of 1.0 mL/min, with detection at wavelength of 235 nm at 25°C using mobile phase: acetonitrile: 10mM $\text{KH}_2\text{PO}_4/\text{K}_2\text{HPO}_4\text{-H}_3\text{PO}_4$ buffer (1:4 v/v), pH 2.8 and the resulted in chromatograms with single peaks (Fig. 3.3 and Fig. 3.5) for the 3-cyanopyridine and nicotinamide, respectively. A plot of the peak areas against standard concentrations prepared using 0 to 12 mM 3-cyanopyridine or nicotinamide resulted in typical standard curves shown in Fig. 3.4 and Fig. 3.6.

Table 3. 2: Preparation of 3-cyanopyridine solution standards for HPLC analysis

1 M 3-cyanopyridine (mL)	0.05 M $\text{K}_2\text{HPO}_4/\text{KH}_2\text{PO}_4$ (mL)	Standard Conc. (mM)	Area under peak (mean)
0	1000	0	0
2	998	2	1114721
4	996	4	2286479
6	994	6	3117598
8	992	8	4220841
10	990	10	4888602
12	988	12	5641057

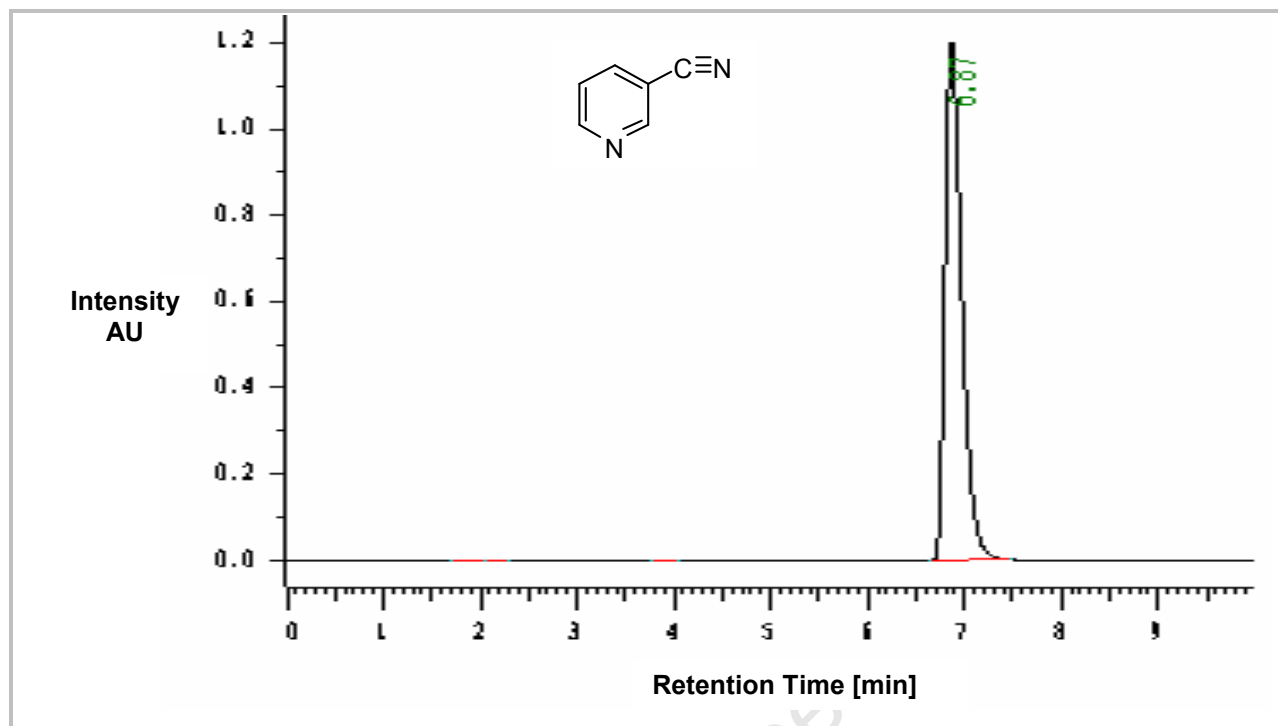


Figure 3. 3: Chromatogram of 3-cyanopyridine: Column C18 (4.6 by 150 mm), mobile phase: acetonitrile: 10mM $\text{KH}_2\text{PO}_4/\text{K}_2\text{HPO}_4\text{-H}_3\text{PO}_4$ buffer (1:4 v/v), pH 2.8, $A_{280\text{nm}}$, Flow: 1 mL/min

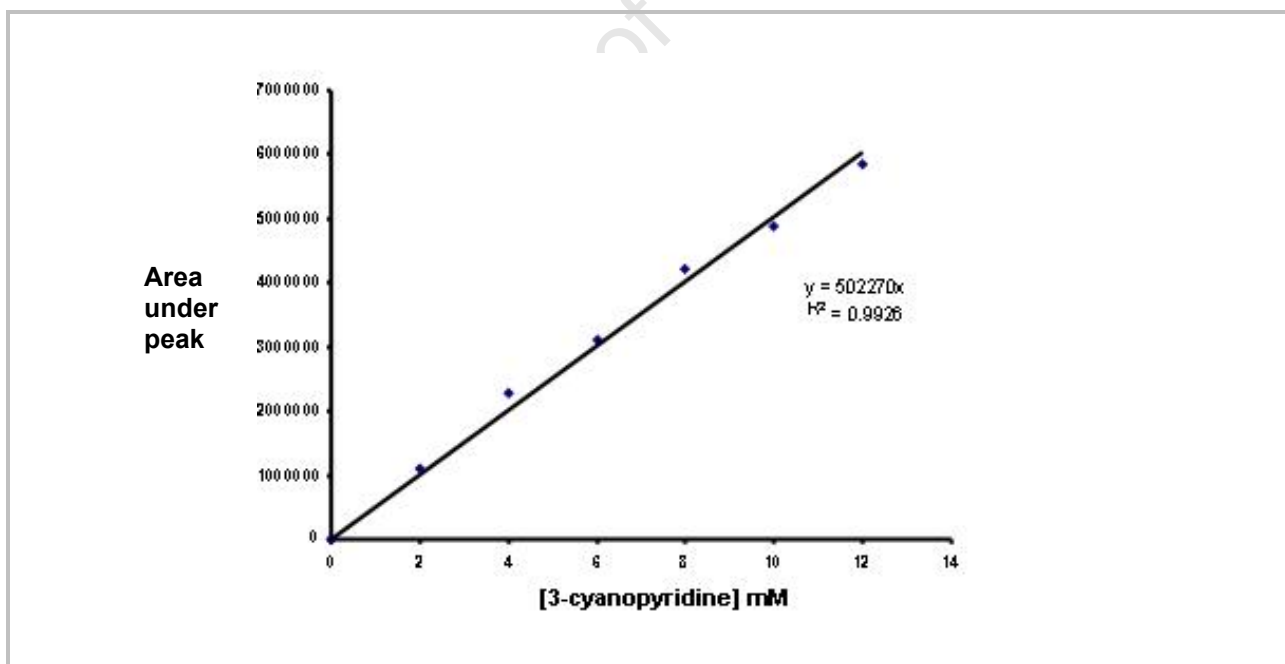
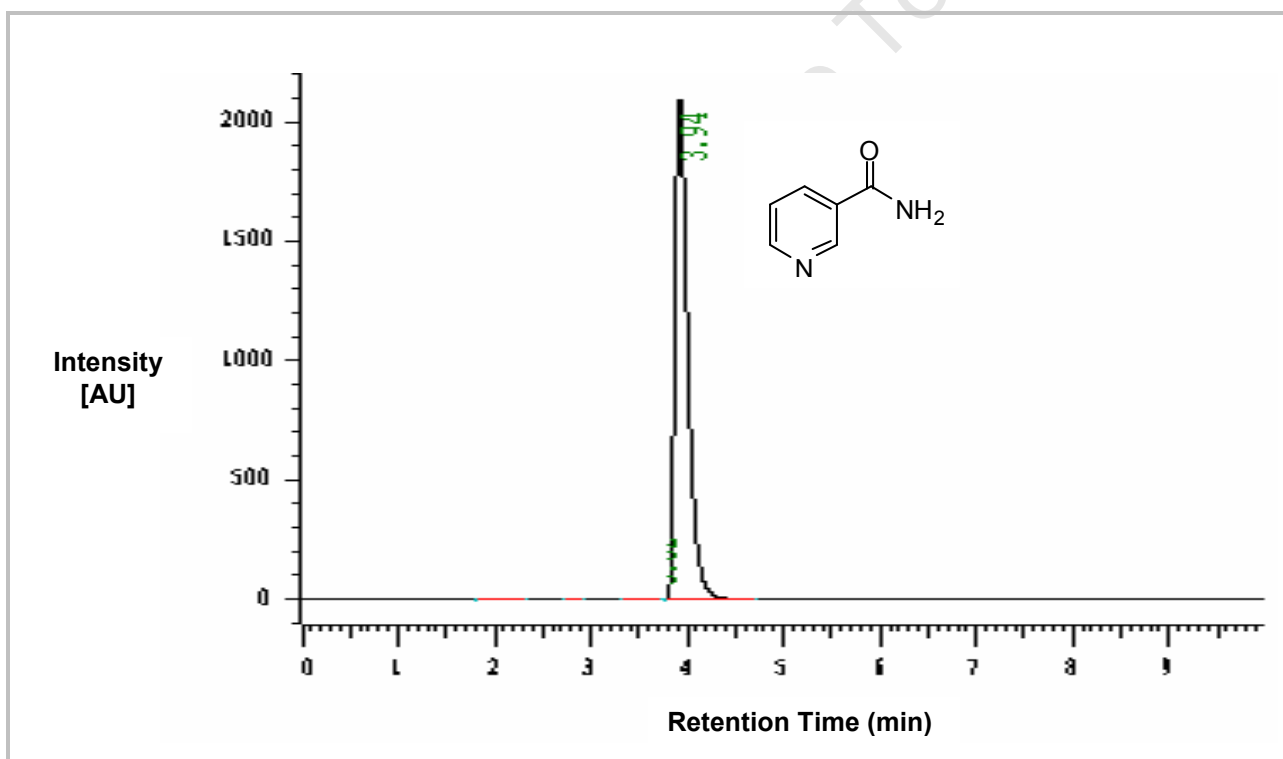


Figure 3. 4: Standard curve for 3-cyanopyridine concentration using peak areas, obtained from HPLC. Detection at A_{235} , flow rate 1 mL/min and mobile phase: 10mM $\text{KH}_2\text{PO}_4/\text{K}_2\text{HPO}_4\text{-H}_3\text{PO}_4$ buffer (1:4 v/v), pH 2.8. $R^2=0.993$.

Table 3. 3: Preparation of nicotinamide solution standards for HPLC analysis

1 M nicotinamide (mL)	0.05 M K ₂ HPO ₄ / KH ₂ PO ₄ (mL)	Standards Conc. (mM)	Area under peak (mean)
0	1000	0	0
2	998	2	1392527
4	996	4	2658530
6	994	6	4044382
8	992	8	5316189
10	990	10	6511898
12	988	12	7188273

**Figure 3. 5: Chromatogram of nicotinamide: Column C18 (4.6 by 150 mm), mobile phase: acetonitrile: 10mM KH₂PO₄-H₃PO₄ buffer (1:4 v/v), pH 2.8, $A_{280\text{nm}}$, Flow: 1 mL/min**

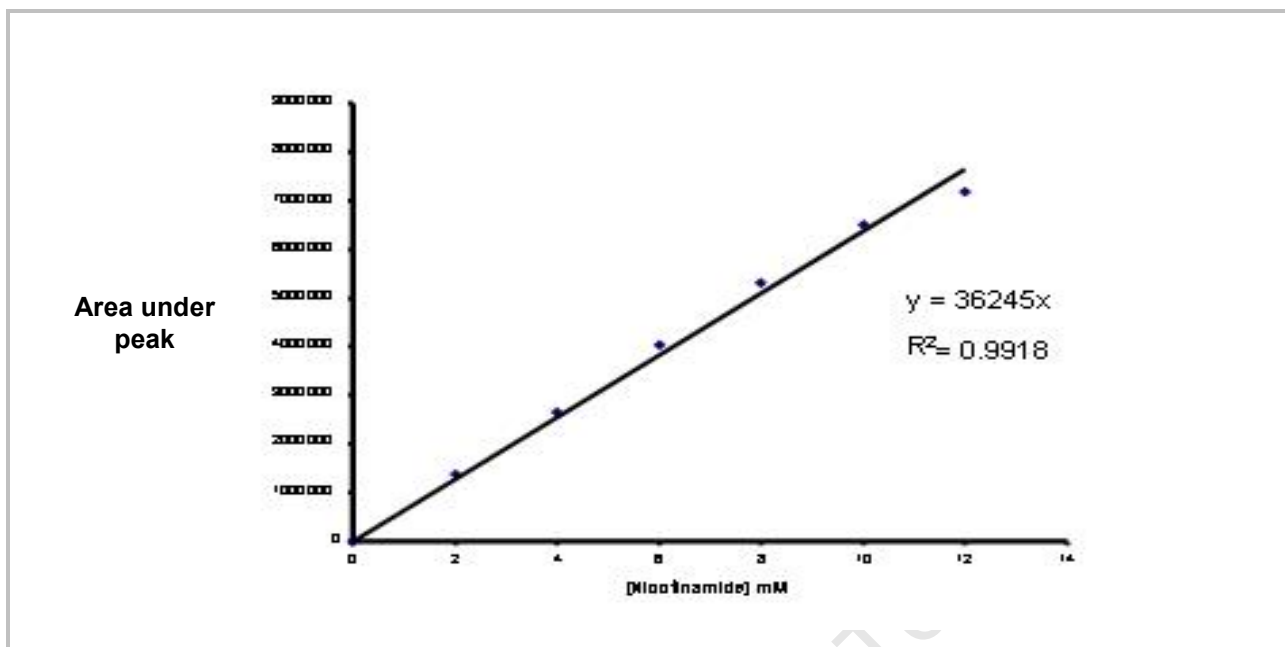


Figure 3. 6: Standard curve for the nicotinamide concentration using peak areas obtained from HPLC.

Detection at A_{235} , flow rate 1 mL/min and mobile phase: 10mM KH_2PO_4 - H_3PO_4 buffer (1:4 v/v), pH 2.8.

$R^2=0.992$.

3.2.2.9 Investigation of reaction conditions for *G. pallidus* RAPc8 NHase biocatalytic reactions

The primary characterisation of *G. pallidus* RAPc8 NHase was performed to determine the conditions for the biocatalytic reaction of 3-cyanopyridine to nicotinamide.

3.2.2.9.1 Determining the amount of enzyme needed to obtain satisfactory substrate conversion for characterisation of the NHase

The aim of this experiment was to determine the exact amount of enzyme to be used in each reaction during characterisation. To ascertain the best of NHase concentration for standard biocatalytic reactions, various amounts of purified enzyme solution, prepared as described in Section 3.2.2.4, (0.015 to 0.18 mg) were used. The reactions were carried out at 50°C , in a 5 mL vial and the respective amount of enzyme solution was added to 3 mL of 50 mM K_2HPO_4 - KH_2PO_4 buffer, pH 7.2. The mixture was pre-incubated for 1 min. A solution of 3-cyanopyridine (substrate) was then added to give a final concentration of 50mM, and the reaction mixture was further incubated for 5 min. For each reaction, a 1 mL sample was drawn out, 200 μL of 3 M HCl

was added to stop the reaction, and the HPLC method (Section 3.2.2.8) was used to determine the amount of product formed. Experiments were conducted in duplicate. The NHase concentration selected on the basis of this experiment was used in subsequent experiments (See Section 3.2.2.9.2 to 3.2.2.9.9).

3.2.2.9.2 Profile of product formation with respect to reaction time in NHase reaction

This experiment was conducted to determine the best time period to use for the biocatalytic reactions of NHase. To determine most suitable reaction time for biocatalytic reactions, the enzyme substrate reaction mixture was incubated for different incubation periods from 0 to 30 min. Purified NHase solution prepared as described in Section 3.2.2.4 (100 μL , approximately 5.6×10^{-2} U) was mixed with 2.75 mL of 50 mM $\text{K}_2\text{HPO}_4\text{-KH}_2\text{PO}_4$ buffer, pH 7.2, and pre-incubated for 1 min at 50°C. A solution of 3-cyanopyridine (substrate) was then added to give a final concentration of 50mM, and the reaction mixtures (in separate bottles) were further incubated for various time intervals from 1 to 30 min. At each time interval, a 1 mL sample from a particular reaction bottle was withdrawn, 200 μL of 3 M HCl was added to stop the reaction, and the amount of product formed was analyzed HPLC.

3.2.2.9.3 Determination of substrate concentration on the NHase activity in biocatalytic reactions

As the present study was aimed at developing a reaction for a potentially commercial viable process, the effects of process scale-up of the biocatalytic reaction are vital and had to be considered. Thus, higher substrate concentrations were investigated for possible inhibition effects under reaction conditions.

The effect of substrate concentration on NHase activity was measured with different concentrations of 3-cyanopyridine in the reaction mixture (5 to 500 mM). Purified NHase solution (100 μL , approximately 5.6×10^{-2} U) was mixed with 3.0 mL of 50 mM $\text{K}_2\text{HPO}_4\text{-KH}_2\text{PO}_4$ buffer, pH 7.2, and pre-incubated for 1 min at 50°C. Varying volumes of 3-cyanopyridine were added to different the reaction tubes to achieve final concentrations ranging

from 0 to 500 mM of substrate, and reaction mixtures were further incubated for 5 min at 50°C. The product formed was determined by HPLC as described previously (Section 3.2.2.8) and activity was calculated as described in Section 3.2.2.7. Relative activity was expressed as a percentage of the highest specific activity, measured using 100 mM substrate concentration.

3.2.2.9.4 Determination of the pH optimal of NHase in the biocatalytic reaction

The effect of pH on the production of nicotinamide by purified NHase was determined using reaction mixtures adjusted to specified pH values as follows: pH 4.0, 5.0 and 6.0 (0.05 M CH₃COOH-CH₃COONa buffer); pH 6.0, 7.0 and 8.0, (0.05 M KH₂PO₄-K₂HPO₄ buffer); pH 8.0, 9.0 and 10 (0.05 M Tris hydrochloric acid buffer), and 10, 11 and 12 [0.05 M NaHPO₄/NaOH buffer]. 50 mM of the specified buffer were used and to each, purified NHase (100 µL, approximately 5.6×10^{-2} U) was added to give a total reaction volume of 3 mL. The mixture was pre-incubated at 50°C for 5 min. A solution of 3-cyanopyridine was added to give a final concentration of 50 mM, and the reaction mixture was incubated for a further 5 min at 50°C. The reaction was stopped by addition of 200 µL of 3 M HCl, the product formed was determined by HPLC as described previously (Section 3.2.2.8), and the activity was calculated as described above (Section 3.2.2.7). Relative activity was expressed as a percentage of the highest activity, measured at pH 7.

3.2.2.9.5 Determination of the temperature optimal for the NHase in the biocatalytic reaction

Assays of NHase at specified temperatures (20 to 70°C) were performed as follows: In a 5 mL vial, purified NHase (100 µL, approximately 5.6×10^{-2} U) was added to 50 mM KH₂PO₄-K₂HPO₄ buffer, pH 7.2, to give a final volume of 3 mL reaction solution. The reaction mixture was pre-incubated for 1 min at the desired temperature. A solution of 3-cyanopyridine was added to give a final concentration of 50 mM and the reaction mixture was further incubated for 5 min at the desired temperature. The reaction was stopped by addition of 200 µL of 3 M HCl and product formed was determined by HPLC as described previously (Section 3.2.2.8) and activity was calculated as described above (Section 3.2.2.7). Relative activity was expressed as a percentage of the highest activity, measured at 50°C.

3.2.2.9.6 Evaluation of the thermostability of NHase at 40 to 70°C over 80 min

To study the effect of temperature on soluble NHase stability, aliquots of the enzyme were incubated at different temperatures between 20 to 70°C for 3h in 50 mM potassium phosphate buffer, pH 7.2. Purified enzyme solution (100 μ L, approximately 5.6×10^{-2} U) was withdrawn every 30 min and assayed for residual activity. The samples were added to 3 mL of 50 mM KH_2PO_4 - K_2HPO_4 buffer, pH 7.2, and pre-incubated for 1 min at 50°C. A solution of 3-cyanopyridine was added to give a final concentration of 50 mM and the reaction mixture was further incubated at 50°C for 5 min. A solution of 200 μ L of 3 M HCl was added to stop the reaction, product formed determined by HPLC (Section 3.2.2.8), and the activity was calculated as described (Section 3.2.2.7). NHase activity in the sample without incubation (incubated at 4°C) was taken as 100 %.

3.2.2.9.7 Effect of addition of metal ions to the reaction medium on the NHase-hydration activity

The influence of metal ions (added as BaCl_2 , CoCl_2 , CuCl_2 , FeCl_3 , MgCl_2 , MnCl_2 , KCl , and ZnCl_2) on NHase activity was investigated. Reaction mixtures consisting of varying concentrations of metal ions (0, 2, 4, 6, 8, 10, and 12 mM) in potassium phosphate buffer with NHase solution (100 μ L, approximately 5.6×10^{-2} U) were preincubated at 50°C for 1 min. A solution of 3-cyanopyridine was added to give a final concentration of 50 mM and the reaction mixture was incubated for a further 5 min at 50°C with stirring at 150 r.p.m. A solution 200 μ L of 3 M HCl was added to stop the reaction, the product formed was analyzed by HPLC, and the activity calculated as described previously (Section 3.2.2.8), and the activity was calculated as described (Section 3.2.2.7). The activity in the sample without any additive (only potassium phosphate buffer) was taken as 100 %.

3.2.2.9.8 Effect of organic-aqueous co-solvent systems on the activity of NHase

Bi-phasic or mixed solvent systems consisting of 10 % (v/v) organic solvents (in order of increase *log* P values): formaldehyde, methanol, 1,4-dioxane, ethanol, acetone, propanol, tetrahydrofuran, ethyl acetate, dichloromethane, chloroform, benzene, toluene, cyclohexane, and

n-hexane in 50 mM potassium phosphate buffer, pH 7.2 were prepared. Purified NHase solution (100 μ L, approximately 5.6×10^{-2} U) was added to each cosolvent system and reaction mixture was pre-incubated for 1 min at 50°C. Exactly 150 μ L of 3-cyanopyridine was then added to give a final concentration of 50mM and the mixture was incubated for 5 min, then 200 μ L of 3 M HCl was added to stop the reaction, product formed determined by HPLC (Section 3.2.2.8.1), NHase activity calculated as described (Section 3.2.2.7). Relative activity was expressed as a percentage of NHase activity in potassium phosphate buffer (100 %).

3.2.2.9.9 Analysis of the substrate specificity and kinetic parameters of G. pallidus RAPc8 NHase

The initial reaction rates for NHase conversion of 2-cyano, 3-cyano and 4-cyanopyridine as substrates were determined (separately). The reaction mixture consisted of 50 mM potassium phosphate buffer (pH 7.2), 150 μ L of respective substrate (final concentration of 50 mM) and purified NHase solution (100 μ L, approximately 5.6×10^{-2} U). The assays were performed in duplicate. Kinetic parameters of the purified enzyme were estimated for all substrates by using concentrations ranging from 0 to 100 mM. Initial rates were determined by a plot of product concentration against time and kinetic parameters were calculated from Hanes-Woolf and Eadie-Scatchard plots analyzed using Microsoft Excel. Experiments were conducted in duplicate and the difference between the two measurements was divided by the mean to calculate the error percentage and assuming that the measurements errors are even distributed, the size of error bar determined.

3.3 RESULTS AND DISCUSSION

In primary characterisation of the *G. pallidus* RAPc8 NHase, three separate experiments were conducted. The first experiments involved production and purification of the *G. pallidus* RAPc8 NHase. In the second set of experiments, a set of preliminary investigations were conducted to establish the exact amount of enzymes, reaction time and substrate concentration. It was necessary to conduct this preliminary investigations because the three selected variable were used as guidelines up on the rest of investigations that were conducted. In the third experiments,

optimization of the biocatalyst reaction conditions was investigated. Details of the results are reported below.

3.3.1 Comparison of the growth curve and biomass yield of *E. coli* BL21 (DE3) in shake flasks and BioFlo fermenter

In order to obtain *G. pallidus* RAPc8 NHase to use as a biocatalyst in various experiments, 1L shake flasks and a 5 L BioFlo fermenter were used for the expression of the NHase from the recombinant *E. coli* BL21 (DE3) strain harbouring the NHase genes. It had been found previously that production of the *G. pallidus* RAPc8 NHase was achievable by addition of inducer, namely isopropyl- β -D-thiogalactopyranoside (IPTG) (Cameron & Cowan, 2005). The inducer was added at the beginning of the exponential growth phase, which was attained after approximately 150 min after incubation with a 5% (v/v) inoculum, in this study (Fig. 3.7). Prior to induction, it was necessary to add cobalt chloride to give a final concentration of 0.1 mM. This quantity of cobalt ions required in the culture medium for expression and is essential for nitrile hydratase activity (Komeda *et al.*, 1996; Kobayashi *et al.*, 1991; Kim & Oriel, 2000). Previous authors used flasks and not automated fermenters in the production of *G. pallidus* RAPc8 NHase. Differences between the cell growth profiles of the shake flask and BioFlo fermenter were quite noticeable (Fig. 3.7). After induction, higher optical density indicated greater biomass in the BioFlo fermenter at each time interval, compared to the 1 L shake flask. This may be explained on the basis that a better microbial growth was achieved in the BioFlo fermenter because the physical parameters were more controlled. For example, the optimal growth pH for the *E. coli* BL21 (DE3) cell was maintained at required value of pH 7.0 throughout the fermentation period by the automated addition of either hydrochloric acid or sodium hydroxide, whereas in the shake flask, this did not happen. However, the growth of recombinant *E. coli* BL21 (DE3) strain in both experiments in this study required 4 h to reach stationary phase, comparable to time reported previously by Cameron (2002) in 1L shake flask. After the 4 h fermentation the biomass quantities from the shake flask (1L) and BioFlo fermenter (5L) experiments were 3.4 g and 16.3 g (wet mass), respectively.

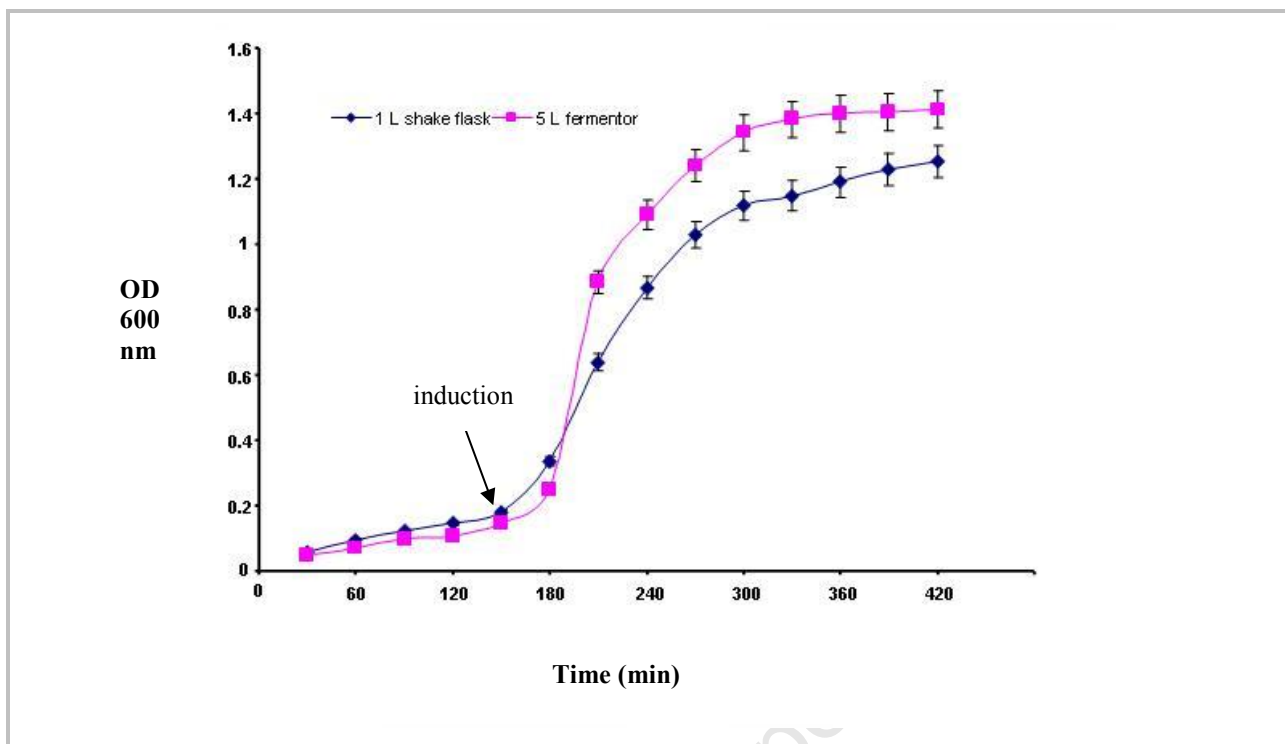


Figure 3. 7: Change in the biomass concentration of *E. coli* BL21 (DE3) (pLysS) in LB media shown as cell density (OD₆₀₀). Cultivation was conducted in shake flask (1L) and BioFlo fermentor (5 L), induced by addition of 5 mL and 25 mL of 100 mM IPTG to the 1L and 5L cultures, respectively, after 2h30min of inoculation.

3.3.2 Purification of *G. pallidus* RAPc8 NHase

The NHase was previously purified from the native bacterial strain *G. pallidus* RAPc8 (formerly *Bacillus* sp. RAPc8) using three consecutive chromatographic techniques including Superdex 200 gel permeation chromatography, Q-Sepharose ion exchange chromatography and chromatofocusing on Mono-P (Pereira *et al.*, 1998). In an alternative approach, heat-treatment was used to achieve partial purification of heterologously expressed recombinant *G. pallidus* RAPc8 NHase (Cameron, 2002). In this study, the combination of methods was used in the purification of recombinantly expressed NHase.

3.3.2.1 NHase extract purification by heat treatment strategy

Heat treatment was applied in the initial stages of purification to liberate the thermostable protein from host-cell proteins, and nucleic acids that are generally heat-labile at 55°C. The NHase had been reported to maintain its activity at 60°C (Cameron, 2002), in contrast to proteins produced by the host *E.coli*, which denature and precipitate at this high temperature. In this approach, the difference in temperature stabilities has been exploited to eliminate undesirable products. Heat treated resulted in a 1.3-fold increase in specific activity with a yield of 88.1% recovered total activity. Heat treatment method has been proven effective in removing undesired protein from NHase extract solution (Cramp & Cowan 1999; Tsekoa 2005). The main drawback of this method is the higher temperature requirements which are used to achieve higher removal efficiency but sometime compromises the enzyme activity (Henley & Sadana, 1986). The low specific activity and fold purification obtained for the *G. pallidus* RAPc8 NHase after heat treatment strategy could be explained in terms of protein denaturation due to heat.

3.3.2.2 NHase purification by ammonium sulphate precipitation

NHase extracts, after heat-treatment, were used in the next purification stage of protein precipitation using $(\text{NH}_4)_2\text{SO}_4$. Because protein solubility is a function of ionic strength and pH, undesired protein can be precipitated by the process of salting out. Thus, separation and purification of many proteins can be effectively achieved by addition of various salts. Of these, ammonium sulphate has been the most widely used, due to its high solubility and relatively low price (Tsekoa, 2005; Hourai *et al.*, 2005). In the purification of the NHase after heat treatment, proteins were precipitated by addition of ammonium sulphate to 20 % saturation of the supernatant (Tsekoa, 2005).

3.3.2.3 NHase purification by Hydrophobic Interaction Chromatography (HIC)

HIC separates components with differences in hydrophobicity. Previous studies achieved purification of a recombinant NHase from *Bacillus* sp. BR449 to near homogeneity cells by use of Phenyl-Sepharose HIC (Kim *et al.*, 2001). Further, Pereira *et al.* (1998) and Cameron (2002) employed a similar technique for purification of native and recombinant *G. pallidus* RAPc8 (formerly *Bacillus* sp. RAPc8) NHase, respectively. In typical procedures, high ionic strength

enzyme solutions (e.g. solutions containing 1 M ammonium sulphate) are used and proteins bind as they are loaded onto a HiLoad 16/10 Phenyl-Sepharose HP column. In this study, the conditions in the column were altered by decreasing the salt concentration, and bound proteins were eluted as a result of the continuously decreasing salt gradient (1 – 0 M). Fig. 3.8 shows two peaks of protein that were eluted in fractions. Fractions under the peaks that exhibited high absorbance (280 nm) were collected and reserved for SDS-PAGE to determine the presence of NHase. The pooled fractions contained a yield of 27% relative to original mixture, but the specific activity had decreased to 0.6-fold.

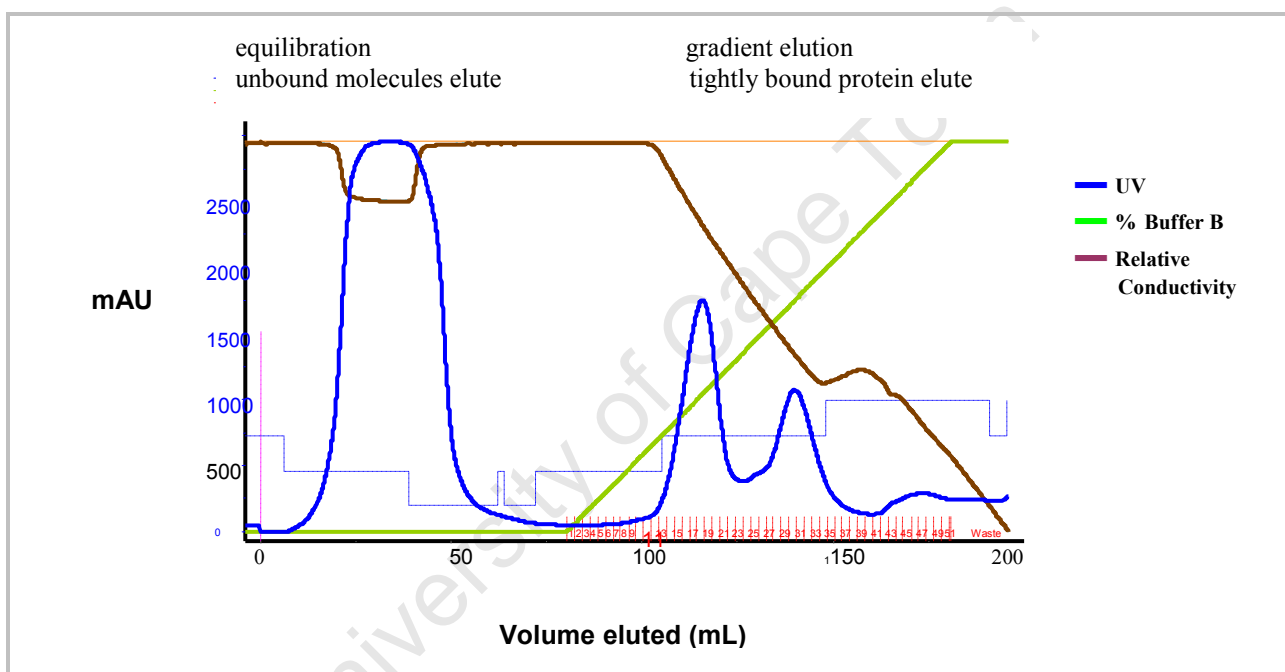


Figure 3. 8: Hydrophobic interaction chromatography (HIC) of the NHase extracts from $(\text{NH}_4)_2\text{SO}_4$ fractionation purification stage, on Hiload 16/10 Phenyl-Sepharose HP. Protein solution (25mL) was applied to the column. Eluent A: 1 M ammonium sulfate in 50 mM potassium phosphate buffer (pH7.2). Eluent B: 50 mM potassium phosphate buffer (pH 7.2). Fractions (2mL) was collected at a flow rate of 3.0 mL/min. Fractions 13 – 23 were collected during gradient elution Buffer B (0 – 100 %).

3.3.2.4 NHase purification by Ion Exchange Chromatography (IEX)

Ion exchange chromatography was employed as a polishing step to achieve final purity (Amersham Bioscience, Handbook).

Previously, Pereira and co-workers (1998) first reported the purification of NHases using a strong anion exchanger (Q-Sepharose) yielding a very high degree of purification. Several other reports on the purification of NHases using anion exchange chromatography include Cameron (2002) and Tsekoa (2005). The NHase extract obtained after HIC was loaded onto a HiPrep 16/10 Q-Sepharose FF column equilibrated with 25 mM potassium phosphate buffer. Bound protein was eluted with a linear gradient of increasing sodium chloride concentration (0 to 0.5 M). The protein collected in fractions 35 to 45 was prepared for SDS-PAGE analysis as described in Section 3.2.2.3. A final yield (ratio of total activity for the pure enzyme to the crude enzyme expressed in percentage) of 66.7 % was achieved with a 5.1-fold enrichment of enzyme per protein. The increase in total activity in this stage of purification indicated that the loss in NHase in Section 3.3.2.3 is reversible. Further structural studies will greatly help in increasing the understanding of the molecular and chemical determinants of inactivation/reactivation of the NHase.

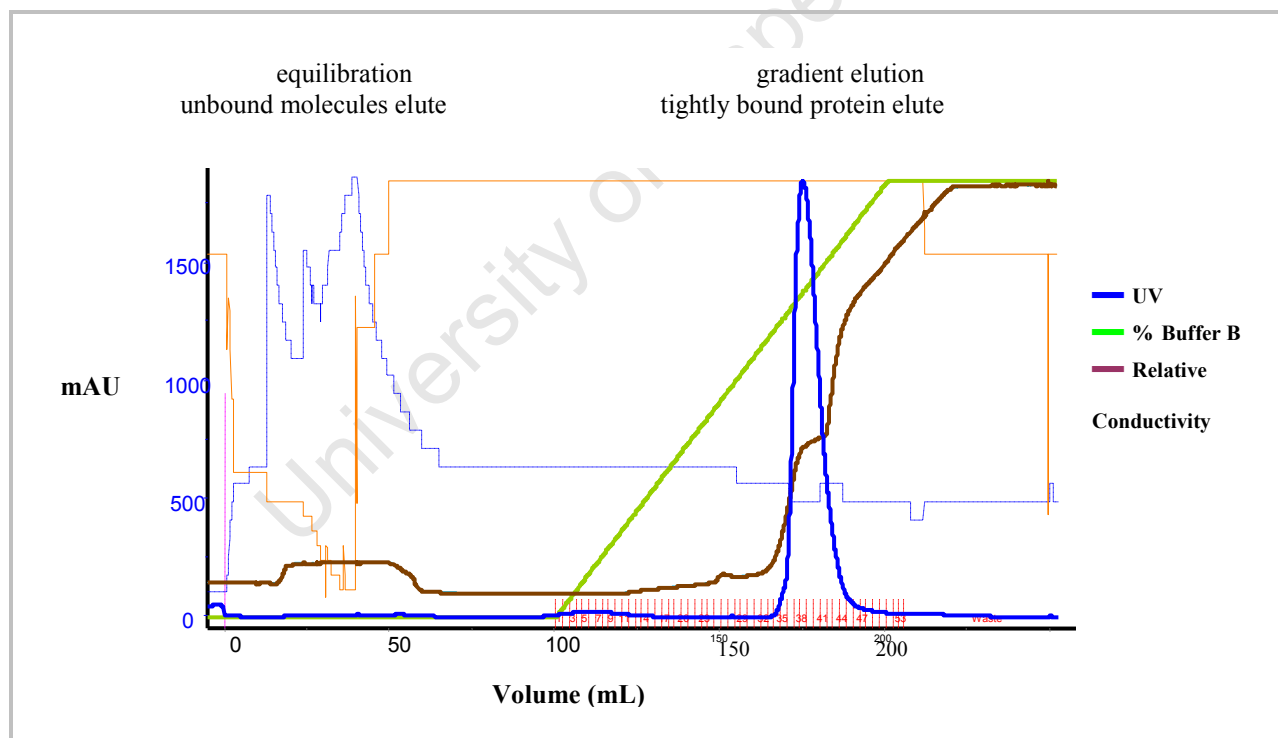


Figure 3. 9: Ion exchange chromatography (IEX) of NHase extract from the HIC purification stage on HiPrep 16/10 Q-Sepharose. Protein solution (25 mL) was applied to the column. Eluent A: 25 mM potassium phosphate buffer (pH7.2). Eluent B: 0.5 M sodium chloride in 25 mM potassium phosphate buffer (pH 7.2). Fractions (2 mL) were collected at a flow rate of 3.0 ml/min. Fractions 35 - 45 were collected during gradient elution with buffer B (0 – 100%).

3.3.2.5 Purification table for the *G. pallidus* RAPc8 NHase.

A summary of all the purification stages with the yield and purification folds are shown in Table 3.2. The present results are consistent with values reported by other authors using different protocols for *G. pallidus* RAPc8 NHase (Tsekoa 2005) and *Bacillus pallidus* Dac521 (Cramp and Cowan, 1999). Consistent with what was found in literature, the heat treatment provided a way to remove of most protein contaminants from the *G. pallidus* RAPc8 NHase extracts in a simple and inexpensive way. In industrial-scale production of large amounts of NHase, partial purification could be performed in a single heating step which is a fast protocol, and inexpensive compared with conventional chromatographic methods.

Table 3.4: Purification table for the *G. pallidus* RAPc8 NHase

Stage	Volume	Total protein	Total activity	Specific activity	Yield	Purification Fold
	mL	mg/mL	$\mu\text{mol/mL.min}$	$(\mu\text{mol/mL.min})/\text{mg}$	%	
Crude	28	199.08	84	0.42	100.0	1.0
HT	25	132.8	74	0.56	88.1	1.3
HIC	25	94	22.7	0.24	27.0	0.6
IEX	25	25.9	56	2.16	66.7	5.1

3.3.3 Sodium dodecyl sulphate-polyacrylamide electrophoresis (SDS-PAGE) gel analysis of *G. pallidus* RAPc8 NHase

At each stage of purification, fractions were collected and stored, and SDS-PAGE analysis of the fractions was then carried out as previously described in Section 3.2.2.5. Figure 3.10 shows results of the SDS-PAGE which indicated that the heat treatment strategy in NHase purification was sufficient to yield more than 80 % homogenous enzyme. However, the chromatographic steps were incorporated to remove any minor contaminants remaining and possible aggregates, and to prepare the target protein for its immediate use in biocatalytic reactions (Davey & Lord, 2003).

The molecular weight of the two subunits of NHase were confirmed by the presence of 28 ± 2 kDa and 29 ± 2 kDa bands corresponding to the α and β -subunits of NHase, which agrees well with the subunit molecular weights of the NHase from native bacterial *G. pallidus* RAPc8 as determined by gel filtration on a Superdex 200 column (Pereira *et al.*, 1998). The results confirm the suggestion that *G. pallidus* RAPc8 NHase is a multimeric enzyme (Pereira *et al.*, 1998). Except for the NHase from *Pseudomonas chlororaphis*, there are considerable structural and size similarities in the subunits for known bacterial NHases, which generally consist of non-identical subunits α and β : (24 – 28 kDa and 25 – 39 kDa respectively), usually with the α subunit smaller than of the β subunit (Cowan *et al.*, 1998; Endo & Watanabe, 1989; Cramp & Cowan, 1999).

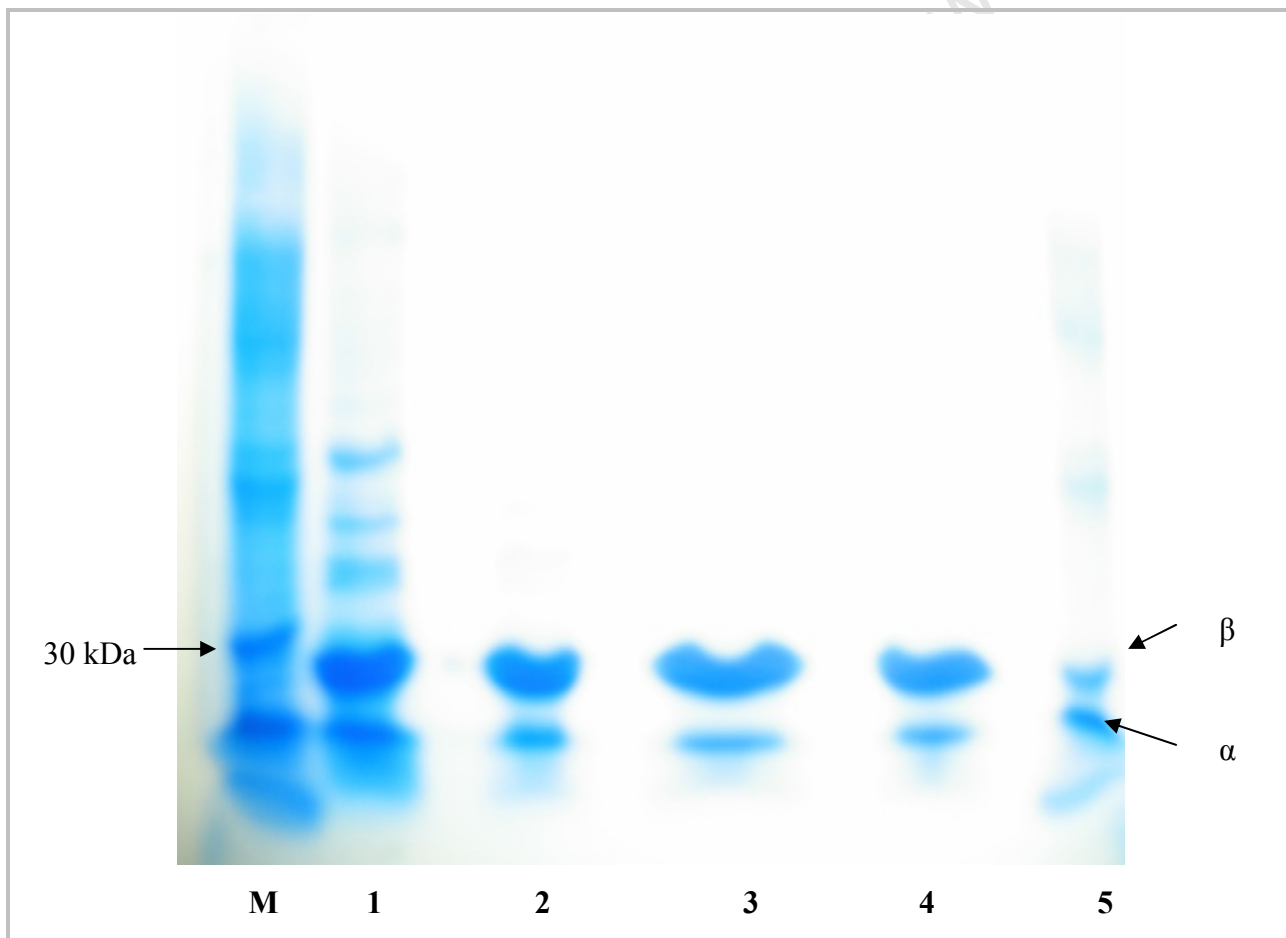


Figure 3. 10: Sodium dodecyl sulfate/polyacrylamide gel electrophoresis of NHase purification. Lane *M*, molecular-weight marker; Lane 1, crude NHase extract; Lane 2, heat-treated extract; Lane 3, $(\text{NH}_4)_2\text{SO}_4$ supernatant; Lane 4, pooled fractions from Phenyl-Sepharose hydrophobic interaction chromatography; and Lane 5, pooled fractions from Q-Sepharose ion-exchange chromatography.

3.3.4 HPLC analysis of product and unreacted substrate from a *G. pallidus* RAPc8-catalyzed reaction

Since the conversion of 3-cyanopyridine to nicotinamide was used as the model reaction for the characterisation of the NHase as a biocatalyst, HPLC analysis was performed in order to identify the reaction products of hydration of 3-cyanopyridine in aqueous medium by the NHase. A preliminary reaction containing 50 mM potassium phosphate buffer, 50 mM of 3-cyanopyridine and purified NHase (100 μ L, approximately 5.6×10^{-2} U), to give a final volume of 3 mL reaction solution, was incubated over 1 min of reaction time to result in approximately 10 % conversion of the 3-cyanopyridine. As both the substrate and product are water-soluble, separation of the components in the reaction mixture, based on the differential solubility in acetonitrile/potassium phosphate buffer mixture in HPLC reverse-phase column, is shown in Figure 3.11 below. The approximate retention times were 3.86 min and 6.38 min for the nicotinamide and 3-cyanopyridine, respectively. The peaks were checked by comparing with authentic commercially available nicotinamide and 3-cyanopyridine. Thus, the single peak at retention time 3.86 min (Fig. 3.11) verified that hydration of 3-cyanopyridine by using purified *G. pallidus* RAPc8 NHase gave a single product. Using this approach, the yields and purity of amide products could be improved, as compared with whole-microbial cell systems widely used to produce amides from nitriles (Martínková & Mylerová, 2003), where carboxylic acids and ammonia are often produced as by-products resolved as separate peaks (Kubáč *et al.*, 2008). Therefore, the purified form of NHase, as was used in this study, might prove to be the biocatalyst of choice for the future synthesis of pure amides from nitriles.

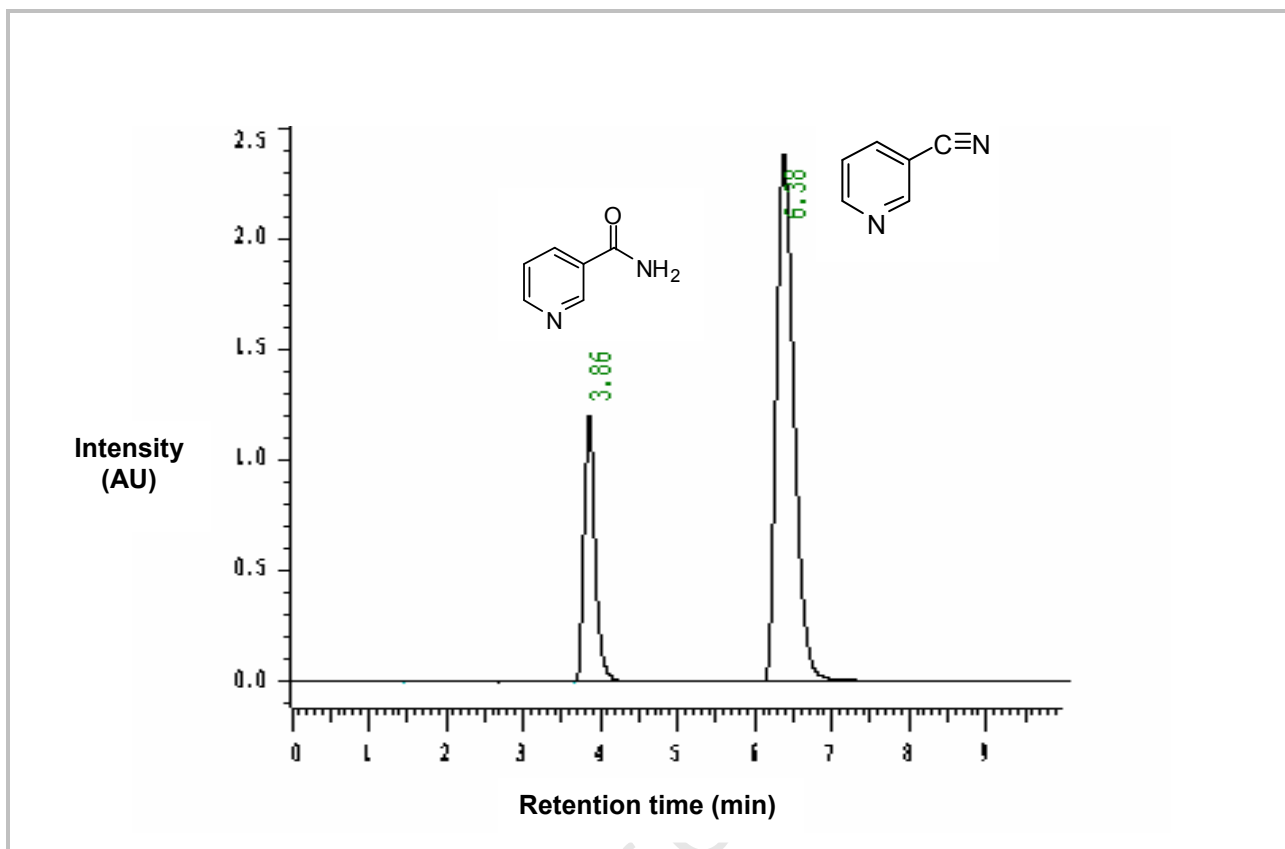


Figure 3. 11: HPLC chromatogram from 3-cyanopyridine hydration reaction mixture analyzed by LabChrom HPLC using a C 18 (4.6 x 150 mm), Buffer: acetonitrile-10 mM KH₂PO₄-H₃PO₄ buffer (pH 2.8) 1:4 (v/v), Flow rate: 1 mL/min at 235 nm.

3.3.5 Optimization of conditions for hydration of nitriles by *G. pallidus* RAPc8 NHase

The study by Pereira *et al.* (1998) and Cameron (2002) on the *G. pallidus* RAPc8 NHase involved its isolation, cloning and structural analysis. Partial functional characterisation of the NHase was carried out later (Cameron & Cowan, 2005). In the present study, for the successful application of this NHase in biocatalytic processes, the enzyme's optimal operating conditions were sought. Hence, a functional characterisation was conducted. Our hypothesis was that establishment of these conditions would give insights toward the development of an efficient bioprocess. Typical biochemical properties were determined using batch reactions and 3-cyanopyridine as the reaction substrate.

3.3.5.1 Determination of NHase-to-substrate ratio for optimal percent substrate conversion

It was necessary to determine the most suitable ratio between enzyme and substrate in the enzymatic reaction, in the initial development stages of a biocatalytic process, to minimize enzyme consumption and ensure measurable amounts of product while avoiding substrate inhibition. Thus, to ascertain the amount of enzyme required to achieve complete substrate conversion for given amounts of substrate, different amounts of NHase were introduced into the reaction mixture and reactions were conducted as described in Section 3.2.2.7. Results are shown in Figure 3.12. As expected, the percentage substrate conversion increased with increasing NHase-to-substrate ratios. The substrate conversion had reached 99.9 % after which it reached a limit, using a NHase-to-substrate mass ratio of 1:5.6 (equivalent of NHase-to-substrate, 1:18 mol ratio), a result which was similar to those obtained by other authors (Nagasawa *et al.*, 1988). Therefore, the ratio (1:5.6) was selected as the suitable conditions under which further experiments would be conducted and further optimization of the reaction conditions was undertaken. It should be noted that the ratio simply provided a working protocol for further investigations, and is not suggested to be the best possible ratio.

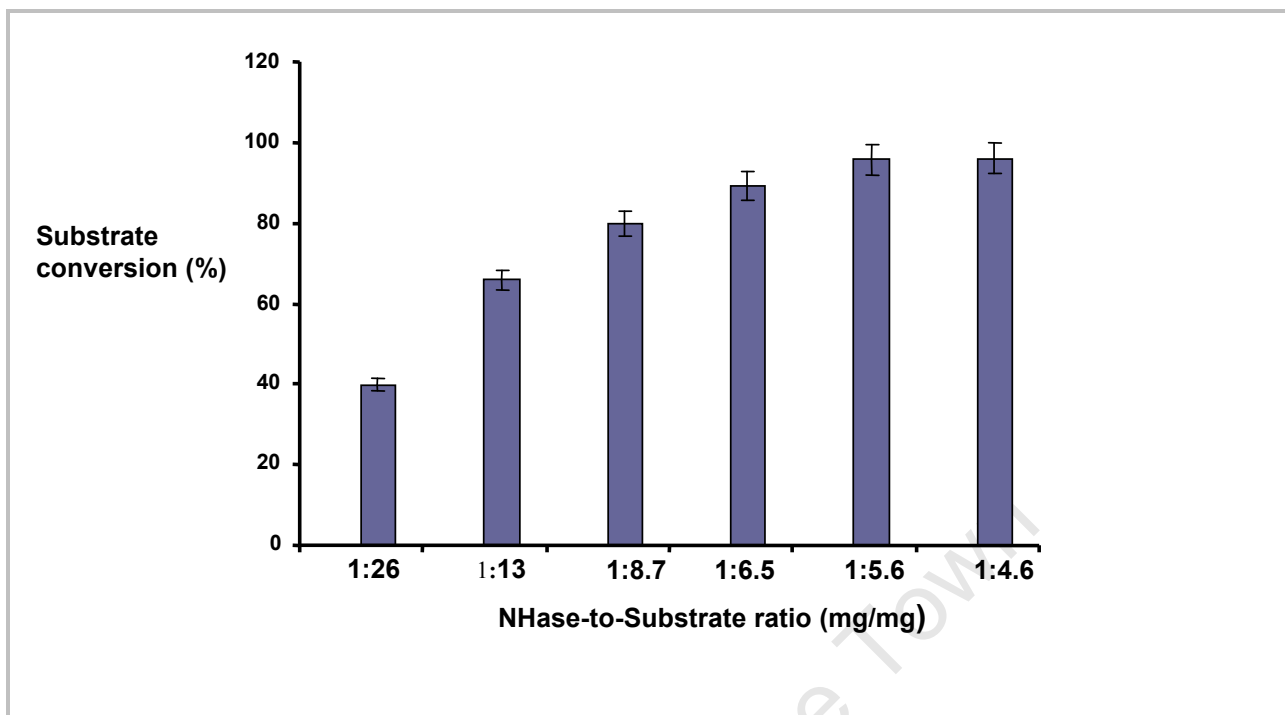


Figure 3.12: Effect of NHase-to-substrate ratio on conversion of 3-cyanopyridine reaction carried out at 50 °C in 50 mM of 3-cyanopyridine using 50 mM potassium phosphate buffer, pH 7.2.

3.3.5.2 Determination of the effect of increasing substrate concentration on the biocatalytic activity of NHase (or investigation of substrate inhibition on the NHase)

From a practical viewpoint, the substrate concentration in a biocatalytic reaction should be as high as possible to obtain high concentration of product. For example, a biocatalytic process can usually only be economically viable if it can achieve product concentrations comparable to chemical processes, of at least 50 – 100 g/L (Pollard *et al.*, 2007). In this study, the effect of substrate concentration on the rate of the NHase reaction was studied by using varying concentrations of 3-cyanopyridine (5 to 500 mM) at 50 °C in potassium phosphate buffer, pH 7.2 for 5 min. A typical profile of substrate inhibition for a single substrate system was obtained and the results are shown Fig. 3.13. As expected, the rate of product formation increased with an increase in substrate concentration, to a maximum threshold observed at 100 mM, assigned a relative activity of 100%. Further increases in substrate concentration beyond this resulted in a decreased rate of reaction. For example, at 200 mM substrate concentration, the relative activity was observed at 93.5 %. Further addition of enzyme at this time (in separate experiments) had no

effect, indicating that this was not due to saturation, but to higher substrate inhibition. This is consistent with findings reported for other NHases which have also exhibited substrate inhibition at high substrate concentration (Nagasawa & Yamada, 1995).

Substrate inhibition is a special case of reversible inhibition which occurs in 20% of all known enzymes (Papežová *et al.*, 2007). It is considered to be caused by binding of more than one substrate molecule to an active site, sometimes resulting in the formation of an inactive enzyme-substrate complex (ESS) thereby preventing the generation of a product molecule (Tan *et al.*, 1996). Moreover, high viscosity due to increased substrate concentration in a reaction could cause diffusional restrictions contributing to the substrate inhibition effect (Miranda *et al.*, 1991). Recent crystallographic studies of the *G. pallidus* RAPc8 NHase (Tsekoa, 2005) indicate the existence of substrate entry channels that lie at the interface between the α and β subunits of the NHase transversing the active site. Further, it has been shown that substrate binding in NHases generally results in conformational changes in channel. This effect was also demonstrated with *P. thermophila* NHase which showed conformational changes occurring upon substrate-binding at the side-chain level, probably within the substrate channel (Miyanaga *et al.*, 2004). It may be suggested that the substrate inhibition observed in *G. pallidus* RAPc8 NHase was due to large conformational changes in substrate channels caused by increasing substrate concentration, and subsequently this affects the catalytic ability of the enzyme. Particularly, changes to the cysteine residues (that form the cobalt-binding claw-setting motif at the active site of the NHase) may lead to lack of activity and, hence substrate inhibition (Cramp & Cowan, 1999).

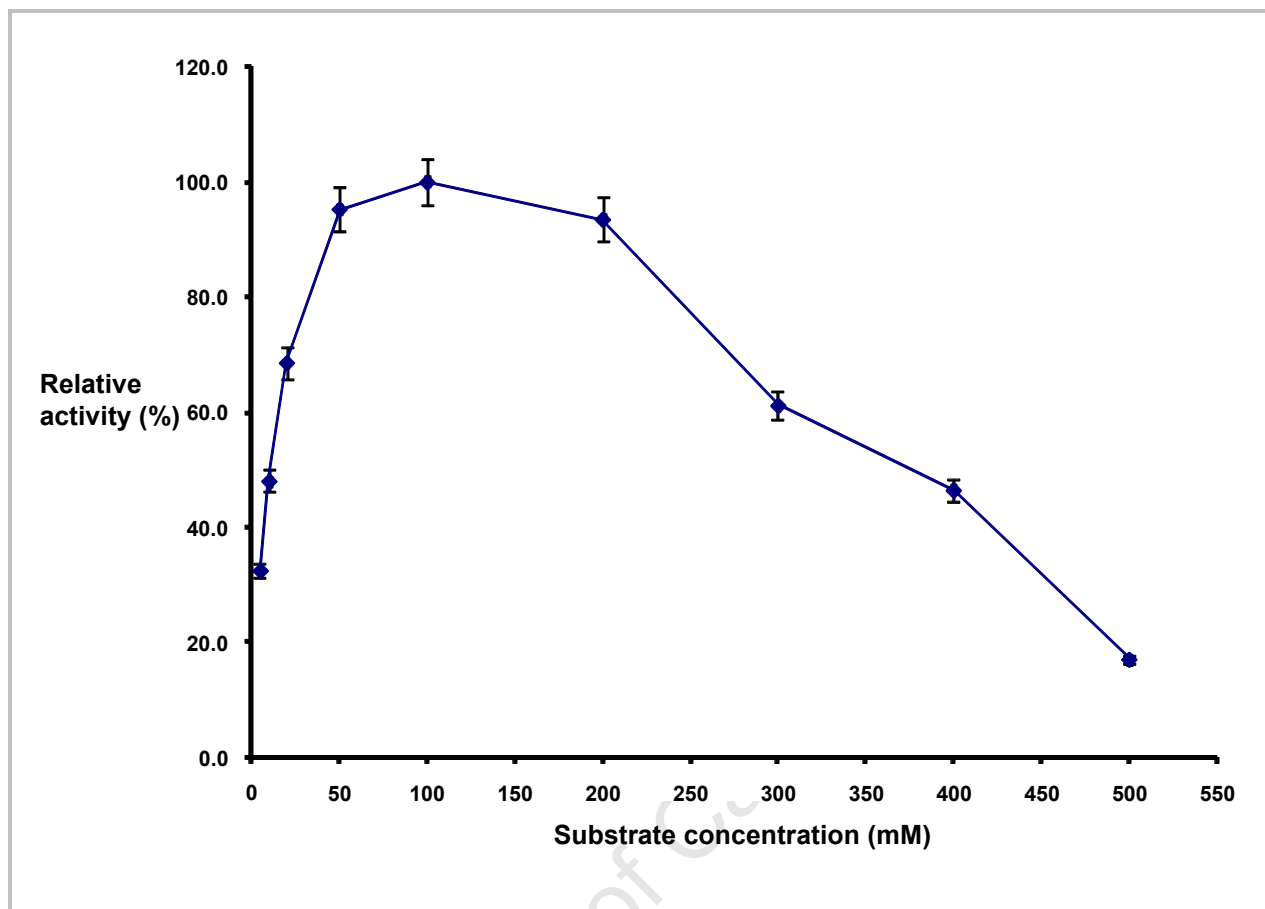


Figure 3. 13: Effect of substrate concentration on *G. pallidus* RAPc8 NHase activity. The enzyme was incubated in different concentration of 3-cyanopyridine (5 to 500 mM) at 50 °C in 50 mM potassium phosphate buffer pH 7.2. Relative activity is expressed as percentage of the highest activity at 100 mM substrate concentration.

3.3.5.3 Evaluation of reaction time on substrate conversion using *G. pallidus* RAPc8 NHase

For the purpose of optimizing the biocatalytic reaction, it was necessary to determine the extent of substrate conversion over time and ascertain whether a longer reaction time than 5 min would give higher conversions in the standard assay method. Fig. 3.14 shows the time course for the hydrolysis of 3-cyanopyridine to nicotinamide at 50°C, in phosphate buffer, pH7.2 using 3-cyanopyridine concentrations (50 mM). Product formation increased with increasing reaction time up to approximately 90% substrate conversion for 5min, after which no further product concentration increase was observed. Based on the results obtained, it was also observed that a 5

min reaction time was sufficient to allow almost complete conversion of substrate to product and therefore was select for further characterization studies on the hydration of 3-cyanopyridine.

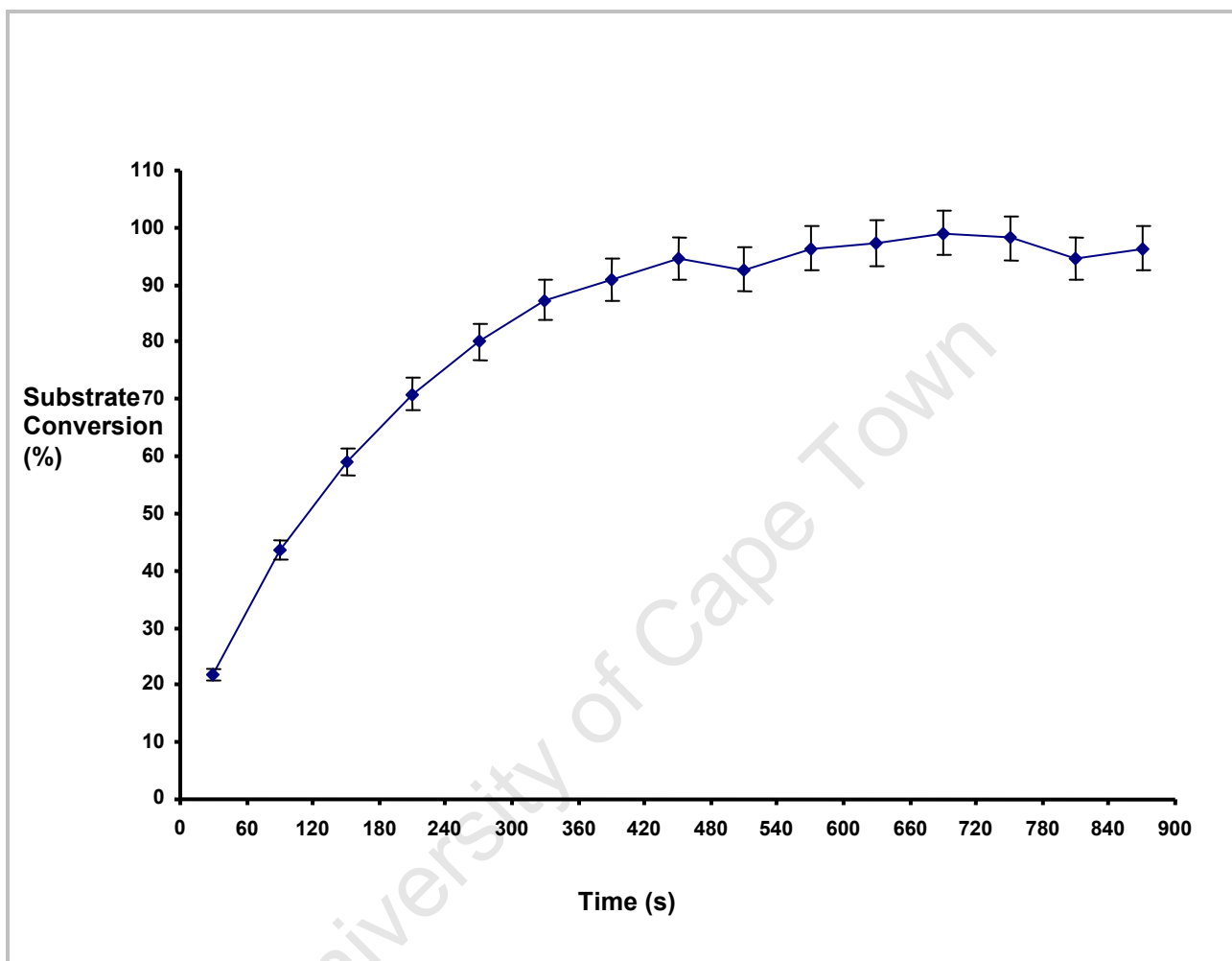


Figure 3. 14: Effect of reaction time on percent substrate conversion. The NHase was incubated at 50 mM of 3-cyanopyridine in 50 mM potassium phosphate buffer (pH 7.2) at 50°C. At the indicated times, aliquots were withdrawn and the product and unreacted substrate analyzed by HPLC.

3.3.5.4 Determination of the temperature optimum for the *G. pallidus* RAPc8 NHase biocatalytic reaction

The effect of varying temperature on *G. pallidus* RAPc8 NHase catalytic activity was investigated by incubating it under standard assay conditions at the following temperatures: 20°C, 30°C, 40°C, 50°C, 60°C, and 70°C. The results are shown in Fig. 3.15. Initially, the specific

activity of NHase increased with increasing temperature from 20°C to 60°C. The maximum relative activity was observed at exactly 60°C which is high compared to the mesophilic-derived NHases which have their maximum activity between 20°C and 40°C. The results clearly demonstrate that *G. pallidus* RAPc8 NHase was more thermostable, in agreement with previous findings reported by Pereira *et al.* (1998) and Cameron & Cowan (2005). This is not surprising as the optimal temperature for activity of purified enzymes is typically fairly consistent with the optimal growth temperature of the native source organism. Since the optimal growth temperature of bacterial *G. pallidus* RAPc8 is 65°C (Pereira *et al.*, 1998), this result was expected.

However, when a further increase in temperature above 70°C, the NHase showed a rapid decline in specific activity presumably due to thermal denaturation of the protein at high temperatures. Pessela and co-workers (2007) proposed that the first step in inactivation of multimeric enzymes normally starts by subunits dissociation and followed by unfolding of the assembly which leads to loss of catalytic activity. Thus, it is possible that *G. pallidus* RAPc8 NHase exhibited the rapid inactivation at 70°C coinciding with the multimeric enzyme dissociation. From this point of view, the development of the general strategies to stabilize the quaternary structure of the heterotetrameric structure may lead to the design of efficient bioprocesses for biotransformation of nitriles.

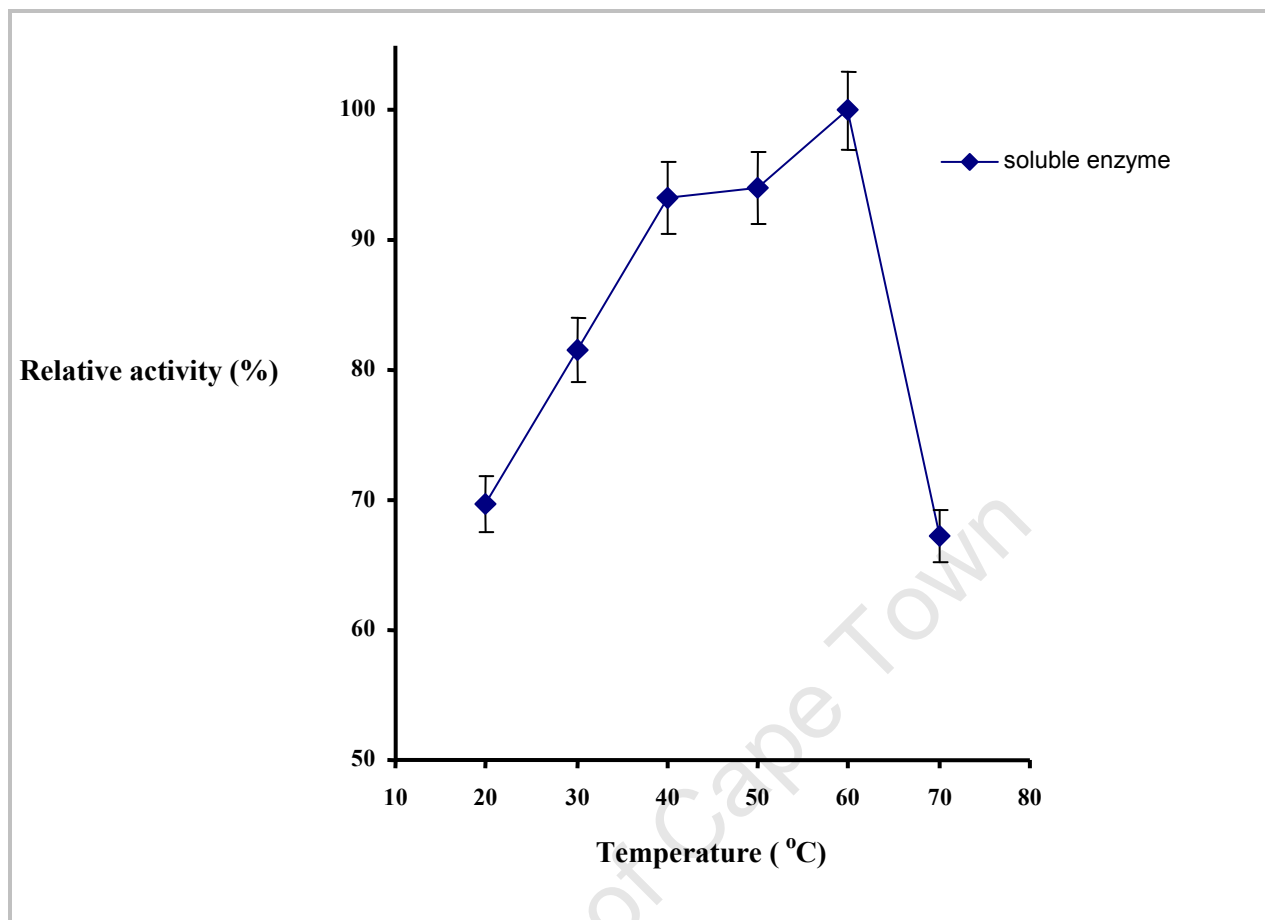


Figure 3.15: Determination of the effect of temperature on *G. pallidus* RAPc8 NHase activity. Reaction mixtures included 50 mM of 3-cyanopyridine in 50 mM potassium phosphate buffer (pH 7.2) at different temperatures. Relative activity was expressed as a percentage of the highest activity which was measured at 60°C.

3.3.5.5 Determination of pH optimum for the *G. pallidus* RAPc8 NHase biocatalytic reaction

The effect of pH on the NHase activity was investigated by exposing the NHase to various buffers at pHs: pH 4.0, 5.0 and 6.0 (0.05 M $\text{CH}_3\text{COOH}-\text{CH}_3\text{COONa}$ buffer); pH 6.0, 7.0 and 8.0, (0.05 M $\text{KH}_2\text{PO}_4-\text{K}_2\text{HPO}_4$ buffer); pH 8.0, 9.0 and 10 (0.05 M Tris hydrochloric acid buffer), and 10, 11 and 12 [0.05 M $\text{NaHPO}_4-\text{NaOH}$ buffer] after 5 minutes of incubation at 50°C (Fig. 3.16). Most reported mesophilic and thermophilic derived NHases operate within the pH range 7.0 to 7.5 (Cowan *et al.*, 2003). The relative activity decreased at pH above and below the optimal. The change in the pH would be expected to affect enzyme-substrate reaction. For example, the enzyme active-site possesses ionizing side-chain residues. In NHases, cysteine residues are

critical for activity, and since thiol side-chains ionise at a pKa value of 4.6 (Cramp & Cowan, 1999), the titration of the thiol side-chain dissociation or denaturation of subunits might result in loss of activity at extreme pHs. It is worthy to note that Tris-HCl buffer in this study further depressed the NHase activity as it was used outside its optimum pH range.

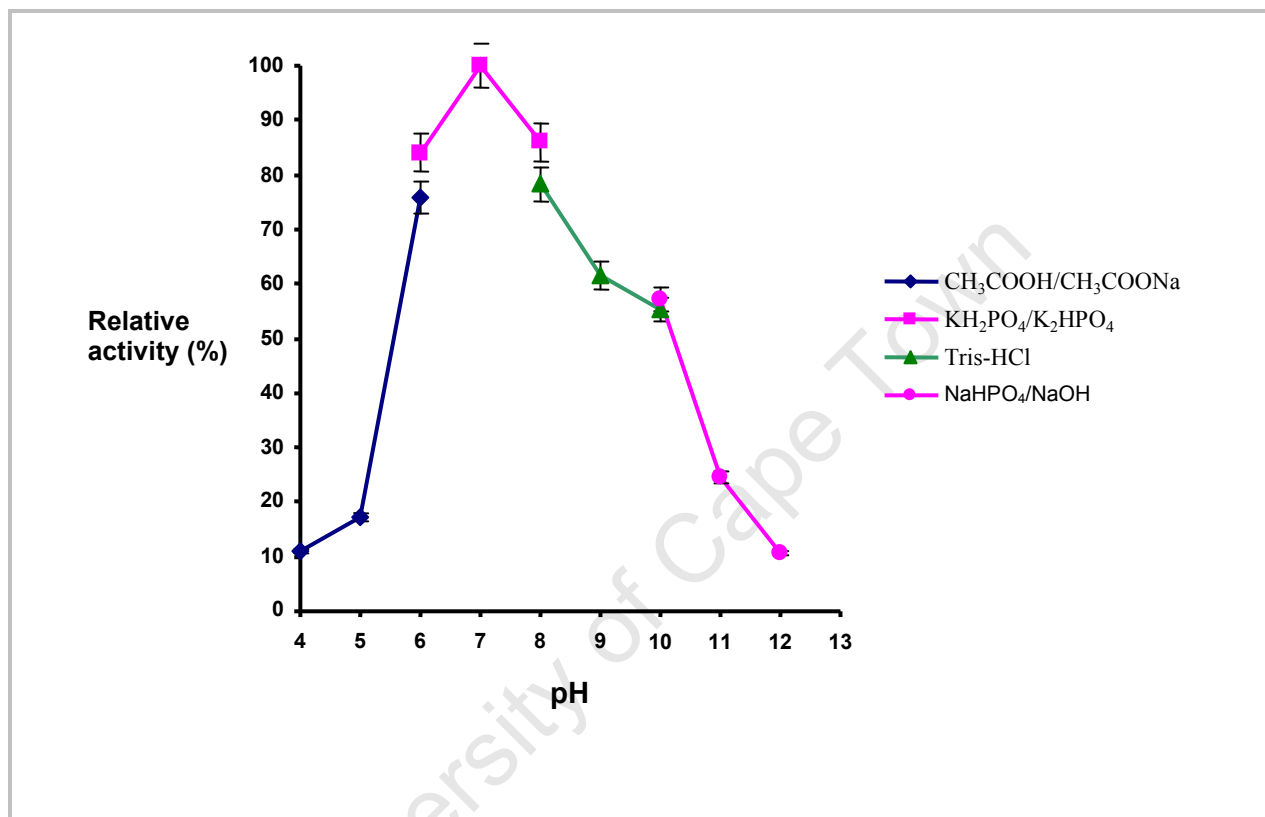


Figure 3.16: Effect of pH on activity of *G. pallidus* RAPc8 NHase activity. Reaction mixture included 50 mM of 3-cyanopyridine in 50 mM of different pHs, at 50 °C. Relative activity is expressed as percentage of the highest activity, at pH 7.0

3.3.5.6 Evaluation of the thermal stability of NHase at 40°C to 70 °C over 80 min

The thermal stability of *G. pallidus* RAPc8 NHase was investigated by incubating the enzyme at different temperatures (40°C to 70°C), and measuring the activity under standard assay conditions. Fig. 3.17 shows the activity of *G. pallidus* RAPc8 NHase against time over a period of 80 min. The enzyme activity was stable at temperatures from 40°C to 50°C. It showed the highest stability at 40 °C and least stability at 70°C over a period of 1 h. The results indicate that

at the lower temperatures (40°C to 50°C), the enzyme molecule was reasonably stable. It is well-known that most reported thermophilic-derived NHases are thermostable compared to the mesophilic NHases (Cowan *et al.*, 2003).

There has been great interest in understanding how proteins from thermophilic microorganisms are stabilized. Among the most prominent suggestions are: greater hydrophobicity (Haney *et al.*, 1997), better packing (Russell *et al.*, 1997), smaller and less numerous cavities, increased area surface buried oligomerization (Salminen *et al.*, 1996), amino acid distribution within and outside the secondary structure (Zuber, 1988; Haney *et al.*, 1997; Russell *et al.*, 1998), increased occurrence of proline residues (Haney *et al.*, 1997; Watanabe *et al.*, 1997; Bogin *et al.*, 1998), increased helical content, increased polar surface area (Haney *et al.*, 1997, Vogt & Argos 1997, Vogt *et al.*, 1997), increased hydrogen bonding (Vogt & Argos, 1997; Vogt *et al.*, 1997) and salt bridges (Yip *et al.*, 1995; Kumar *et al.*, 2000). In a recent study, homologous mesophilic and thermophilic NHases sequences were compared in order to identify structural determinants of thermostability (Tsekoa, 2005). In the study, alignment analysis between the *G. pallidus* RAPc8 NHase and a thermophilic *Bacillus smithii* revealed differences in their loops and termini, where the single most prominent difference was the presence of an additional α helix comprising of 116-126 of the the β subunit of the *G. pallidus* RAPc8 NHase. An increased helical structure in proteins has been linked with an increase in thermostability (Kumar *et al.*, 2000). Presumably, this additional interaction may contribute to the thermostability of the NHase by contributing to maintenance of a heterotetramer resistant to inactivation (Tsekoa, 2005). The results of this investigation indicated that the *G. pallidus* RAPc8 NHase was more thermostable than that of enzymes reported for nitrile hydration in literature (Section 2.5.7, Table 2.2). Thus, further stabilization of the NHase would be essential for the successful development of an industrial biocatalyst and various stabilization strategies a latter described in Chapter 4.

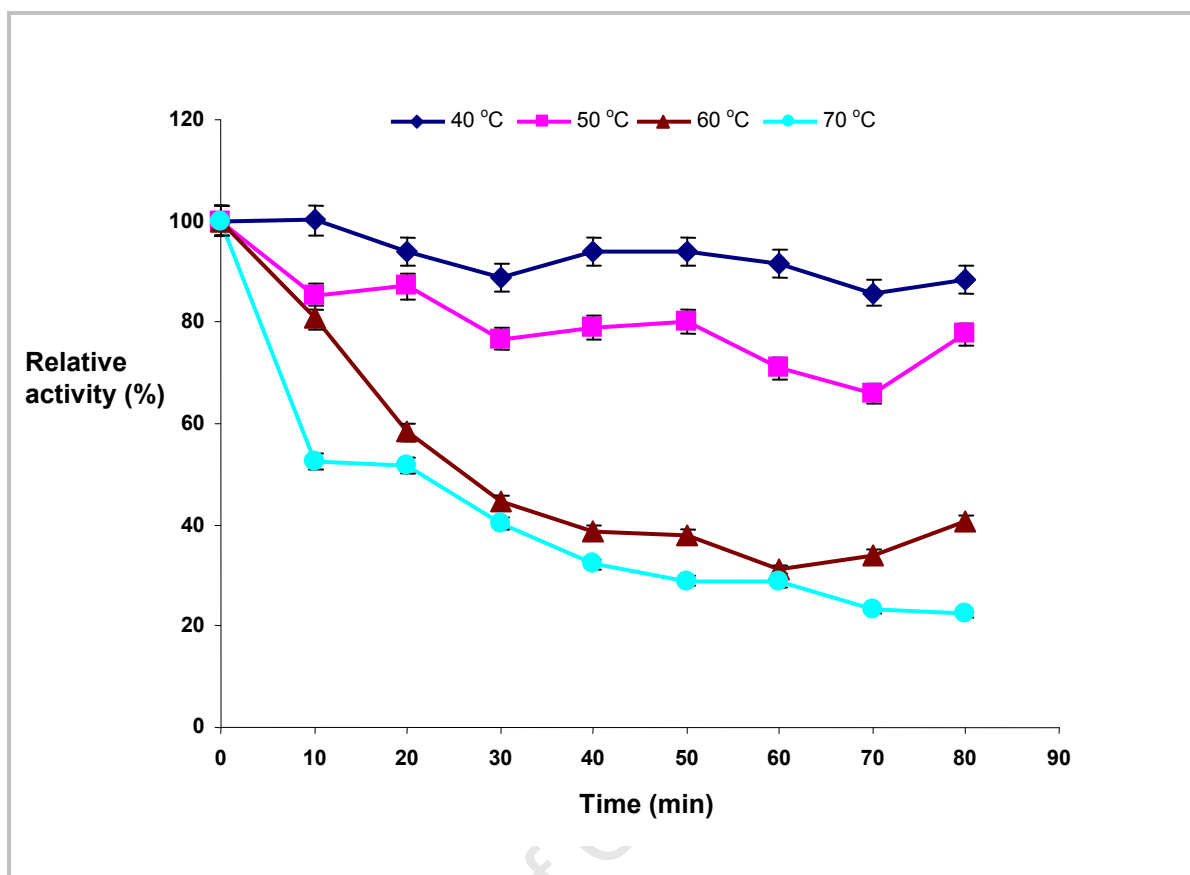


Figure 3. 17: The measurement of thermostability of *G. pallidus* RAPc8 NHase. The NHase was incubated at different temperatures (40, 50, 60, and 70 °C) for 80 min in 50 mM potassium phosphate buffer (pH 7.2). At the indicated times, aliquots were withdrawn and residual activity was measured at 50 °C under the standard assay conditions and expressed as a percentage of activity at zero time (prior to incubation) taken as 100%

3.3.5.7 Effect of cosolvent organic/aqueous systems on the catalytic activity of *G. pallidus* RAPc8 NHase

NHases have been used in mixed aqueous/organic solvent systems at both low (Mylerová & Martinková, 2003) and high (Layh & Willets, 1998) organic solvent concentrations. However, there are large differences between reported tolerances to non-aqueous media among the NHases. For example, *R. rhodochrous* J1 cells containing NHase have been reported to be tolerant in the presence of *n*-propanol and isopropanol (Nagasawa *et al.*, 1993), while *Rhodococcus equi* NHase optimal activity has been reported with application in the presence of high concentration of hydrocarbons up to 90% (v/v) of isooctane but only up to 20% (v/v) in methanol or ethanol (Přepechalová *et al.*, 2001). Since it was difficult to accurately predict the behavior of the *G.*

pallidus RAPc8 NHase in cosolvent systems suitable for their application of the NHase, the best approach was to start with low concentrations of the most common organic solvents. Thus, fourteen organic solvents, with varying *log P* values, were chosen for addition to the *G. pallidus* RAPc8 NHase reaction medium in a ratio (1:9 v/v) of organic solvent to potassium phosphate buffer. The *log P* value for solvents is widely used as a parameter to describe solvent polarity; *P* is the partition coefficient of a given solvent between water and octanol in a two-phase system (Tehrany *et al.*, 2004).

3.3.5.7.1 Effect of miscible organic/aqueous cosolvent systems on NHase activity

When different water-miscible organic solvents were used as cosolvents, the NHase generally exhibited low to modest activities (Fig. 3.18). The relative activities in the presence formaldehyde, acetone, tetrahydrofuran, ethanol, methanol and 1, 4-dioxane were found to 20, 39.9, 46.4, 58.0, 69.9 and 79.35 %, respectively when 10 % (v/v) cosolvent organic/aqueous systems were used. In the presence of propanol, the enzyme activity was relatively well preserved with a relative activity of 93.5 %. In miscible water-organic solvent systems, enzymatic activity is often lost due to replacement of the water essential for catalytic and structural functions in the protein's hydration surface layer by the organic solvent (Gorman *et al.*, 1992). The role of water is considered to be in promotion of flexibility upon binding to the enzyme, and optimal water activity is fundamental to effective enzyme activity. Thus, displacement of bound water molecules by organic cosolvent can result in dramatic change in protein structure, leading to inactivation (Lee *et al.*, 2002). In the *G. pallidus* RAPc8 NHase, seven bridging water molecules have been identified as being involved in maintenance of the geometry required for the α and β dimeric structure essential of catalytic function of the NHase (Tsekoa, 2005). These results suggest the importance of maintaining the water molecules in the hydration shell of the NHase enzyme. In order to investigate the possible application of this enzyme in the presence of other types of organic solvents such as those that are water-immiscible, further experiments were carried out.

3.3.5.7.2 Effect of immiscible organic/aqueous cosolvent system on NHase activity

The activity of NHase was tested in two-phase organic/aqueous systems containing 10 % ethyl acetate, dichloromethane, chloroform, benzene, toluene, cyclohexane and n-hexane. In general, it

was found that in the presence of these water-immiscible cosolvents, the NHase activity was either preserved or increased (Fig. 3.18). For example, presence of ethyl acetate, benzene and toluene gave relative activities of 106.0, 112.8, and 103.3 %, respectively. The presence of n-hexane, cyclohexane, chloroform and dichloromethane resulted in the NHase having relative activities in the range 74 to 94.5 %. Thus, two-phase aqueous/organic solvent systems can offer different advantages in contrast to water-miscible cosolvents, such as higher retention of enzyme activity. The ability of *G. pallidus* RAPc8 NHase to retain catalytic activity in the presence of immiscible organic solvents was presumably because the essential water was not displaced from the enzyme microenvironment. However, the slight loss of NHase activity with chloroform and dichloromethane may be explained by possible role of interfacial surface tension effects (Owusu *et al.*, 1989; Halling *et al.*, 1998). Use of water-immiscible organic cosolvents in NHase-catalysed reactions would be advantageous to this process, since the substrate could be kept in a different phase from the biocatalyst, thus allowing high concentrations of substrate without substrate inhibition (Sellek & Chaudhuri, 1999). The effect of addition of co-solvents to the enzyme in its immobilized form is later investigated further (Chapter 4, section 4.3.5.3).

3.3.5.7.2 Effect of log P value of solvents on NHase activity

There appears to be somewhat imprecise correlation between the activity of NHase and co-solvents especially with log P values in the range of -1.5 to 2. On the other hand, all solvents with log P > 2 showed high percentage relative activity, especially with benzene (113%) with a log P 2.0, followed by toluene (103%) with log P 2.5. However, no conclusion can be drawn directly from these results, and probably, a varied buffer-to-solvent ratios should be investigated in future.

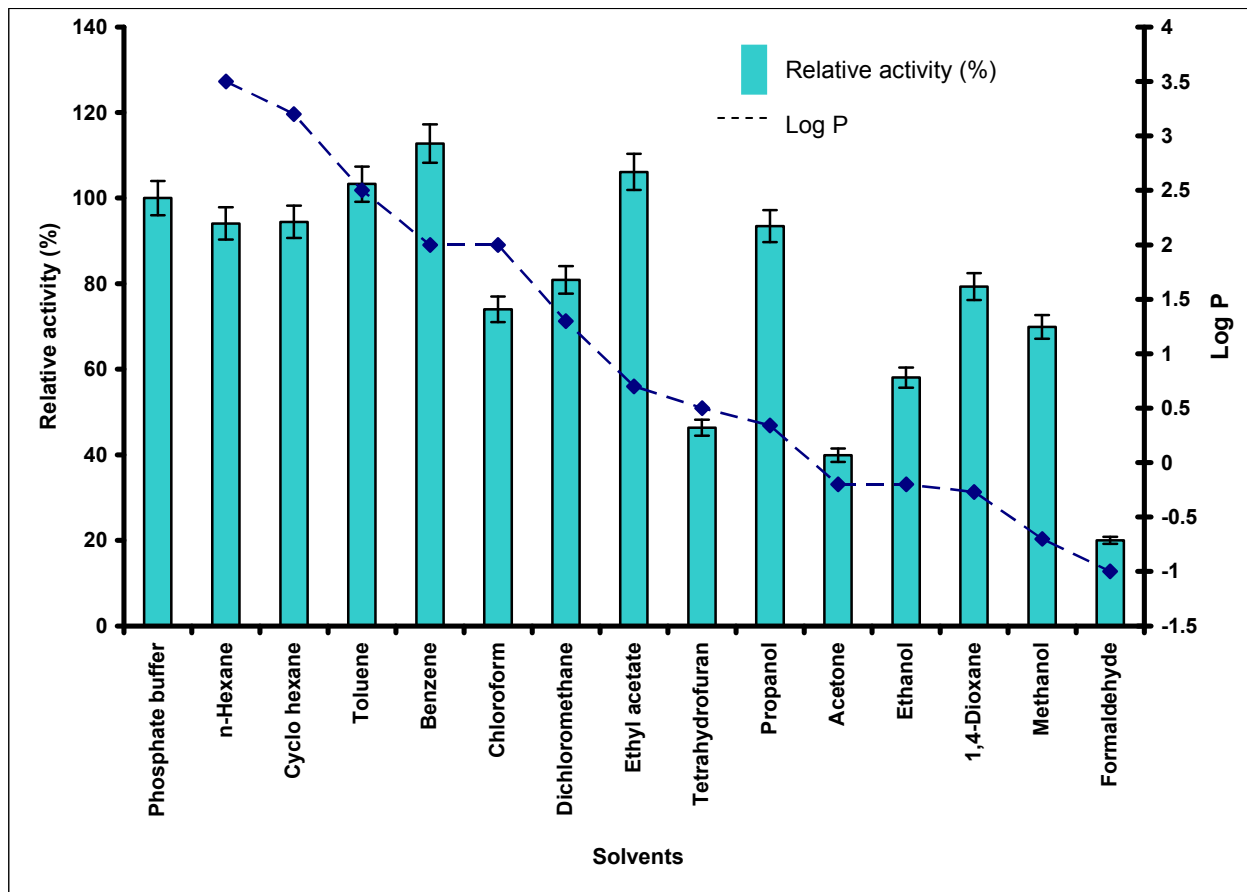


Figure 3. 18: Effect of monophasic and biphasic organic-aqueous solvent systems (or $\log P$) on the activity of *G. pallidus* RAPc8 NHase. The organic-aqueous solvent systems contained 10 % organic solvent and 90 % 50 mM potassium phosphate buffer, pH 7.2. The NHase activity is expressed as relative activity (%) taking the reaction in potassium phosphate buffer as 100 %.

3.3.5.8 Effect of metal ions on the activity of *G. pallidus* RAPc8 NHase

To demonstrate the effect of metal ions on *G. pallidus* RAPc8 NHase catalytic activity, a range of concentrations (0 to 12 mM) of various cations were added to the reaction mixture of NHase, since generally, NHases have been shown to activated by metal ions. The effect of the metal ions on the NHase-hydration activity as shown in Fig. 3.19. Although most of the metal ions activated NHase activity, no direct correlation was found between their degree of solubility of the salts ($\text{ZnCl}_2 > \text{FeCl}_2 > \text{CuCl}_2 > \text{MnCl}_2 > \text{MgCl}_2 > \text{CoCl}_2 > \text{BaCl}_2 > \text{KCl}$) and degree of enzyme activation. In the presence of the positive monovalent alkali metal ion K^+ , the NHase activity was increased

by 1.7-fold at 6 mM metal ion concentration (Fig. 3.19). In fact, K^+ was a stronger activator at all concentrations tested. A possible folding enhancement or stabilisation of subunits in the heterotetrameric structure of the NHase, through the low charge density monovalent cation, has been proposed (Nagasawa *et al.*, 1991), and may explain this effect. Furthermore, K^+ has been reported to play an important role in many enzyme-catalysed reactions by allosteric regulation effect. Research has demonstrated that the low outer electron molecule of K^+ tend to undergo electrostatic bonding with protein ligands which is important for activity in pyridoxal phosphate enzyme catalysis (Page & Di Cera, 2006). Moreover, K^+ concentration was much higher than indicated because of the 50 mM potassium phosphate buffer.

The presence of bivalent metal ions was found to enhance the activity of NHase in a concentration-dependent way. Co^{2+} was a stronger activator than Fe^{2+} , which was in turn stronger than Ba^{2+} and Mg^{2+} . The highest effects were observed at different concentrations: a relative NHase activity of 160 % was observed in the presence of 12 mM Co^{2+} , 130 % in the presence of 8mM Ba^{2+} , 125 % in the presence of 6mM of Fe^{2+} and 120 % in the presence of 12 mM of Mg^{2+} . While Ba^{2+} and Mg^{2+} might also function as stabilizers of the NHase structure, Co^{2+} and Fe^{2+} metal ions are associated with the structural formation and active site chemistry. These latter metal ions are involved in the catalytic core known to initiate the catalytic process in the NHases (Huang *et al.*, 1997; Kobayashi & Shimizu, 1999).

By contrast, other transition metal ions were observed to have deactivating effects on the *G. pallidus* RAPc8 NHase activity. Although Zn^{2+} and Mn^{2+} showed less inhibitory effects on the enzyme activity, Cu^{2+} significantly inhibited the NHase activity. The inhibition of Cu^{2+} was concentration dependent; the relative activity of the NHase dropped sharply with increasing Cu^{2+} concentration to approximately 25 % at 2mM. It is well known that NHases contain cysteine residues in the active site (Huang *et al.*, 1997). While the thiolate group of the cysteine residue in the NHase acts catalytically as a nucleophile, it is also known to be an excellent ligand for metals such Zn^{2+} , Cd^{2+} and Cu^{2+} (Mounaji *et al.*, 2003). Inhibition is observed when metal ions bind directly to the cysteine at the active site, and this unwanted metal binding leads to loss of enzyme activity. Binding of Cu^{2+} to sulfhydryl groups of a NHase from *Bacillus sp.* DAC521 has been reported previously, resulting in a decrease in catalytic activity (Cramp *et al.*, 1997). We

therefore conclude that this could have been the cause of loss of activity in *G. pallidus* RAPc8 NHase in the presence of Cu^{2+} . A second possible mechanism of metal poisoning is the substitution of the catalytic metal by an inhibitory metal, leading to loss of enzyme which activity has been reported in human porphobilinogen synthases (Jaffe *et al.*, 2001). However, to our knowledge, this has not been reported in the NHase enzymes, and further investigations would be needed to test the possibility.

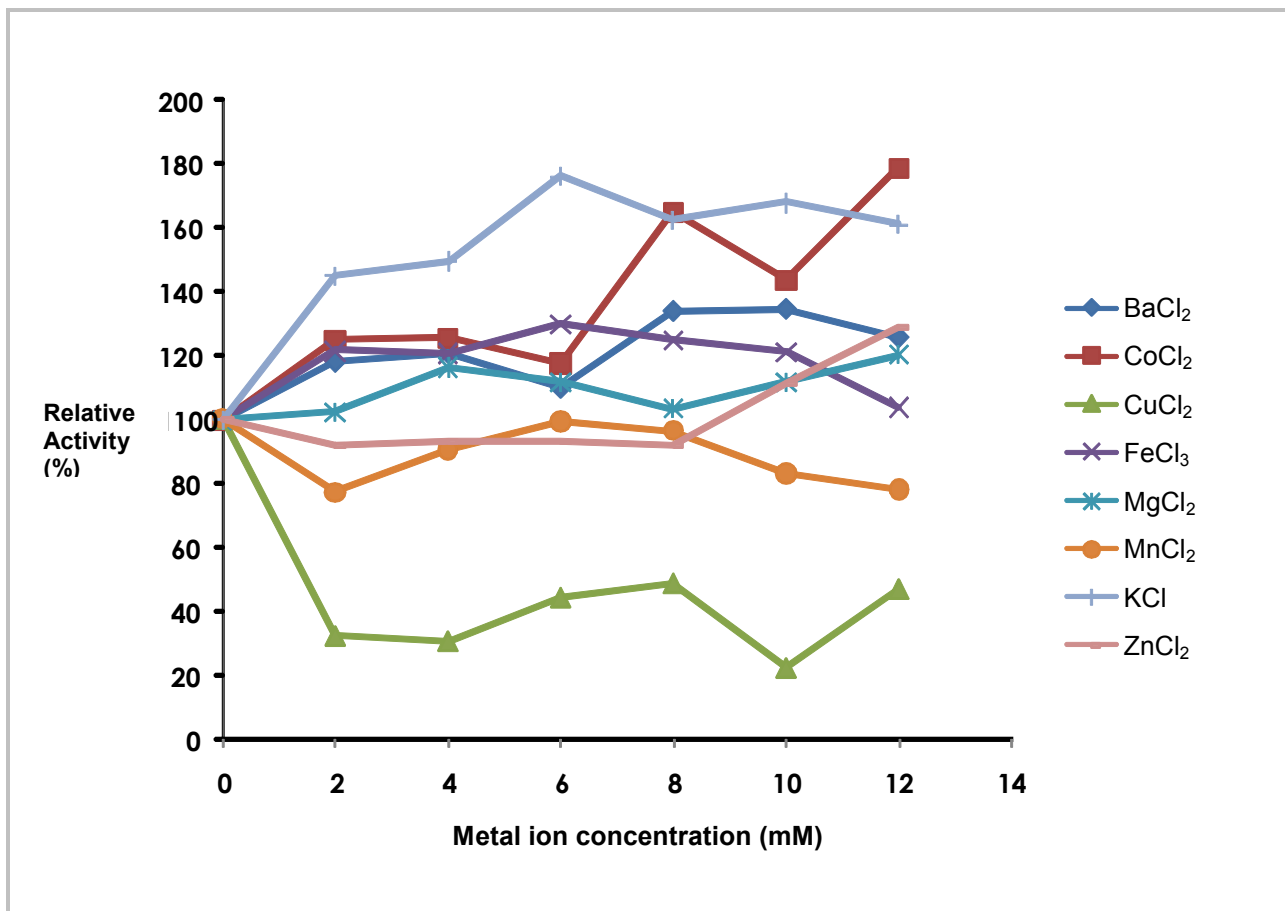


Figure 3.19: Effect of metal ions on the activity of *G. pallidus* RAPc8 NHase. NHase was incubated for 5 min at 50°C in 3 mL reaction mixture containing 50 mM KH_2PO_4 - K_2HPO_4 buffer (pH 7.2), 50 mM 3-cyanopyridine and different concentrations of metal ions. Final concentration of the enzyme was 0.14 mg/mL.

3.3.5.9 Determination of kinetic parameters and substrate specificity for *G. pallidus* RAPc8 NHase

3.3.5.9.1 Measurement of reaction rates for nicotinamide production

Previous studies by Pereira *et al.* (1998) estimated the kinetics of NHase from *G. pallidus* RAPc8 in their preliminary characterisation of the recombinant enzyme, using aliphatic substrates (acetonitrile, valeronitrile, or acrylonitrile) for the determination of the enzyme kinetics, by analysis of ammonia from the conversion of amides to the corresponding acids, using the phenol-hypochlorite ammonia detection method. In the present study, a different approach was taken to determine *G. pallidus* RAPc8 NHase kinetics, using a direct measurement of the conversion of 3-cyanopyridine substrate to nicotinamide, which was then analyzed by HPLC. Using the method of initial rates, the rate was measured at the beginning of the reaction for several different concentrations of substrate. For each of a series of substrate concentrations, a plot of the amount of product against reaction time should be a straight line with a slope equal to the initial rate (Fig. 3.20). These can then be used to evaluate the enzyme kinetic parameters K_m and V_{max} .

The reaction kinetics of soluble *G. pallidus* RAPc8 NHase were determined for three of the most readily converted heteroaromatic substrates: 2-cyanopyridine, 3-cyanopyridine and 4-cyanopyridine, using a discontinuous assay. Reaction mixtures (15mL), in 30-mL stirred tubes containing 50 mM KH_2PO_4 - K_2HPO_4 buffer pH 7.2, varying concentrations of the nitrile substrates, and 0.14 mg of purified *G. pallidus* RAPc8 NHase, were incubated at 50°C for 1.7 min.

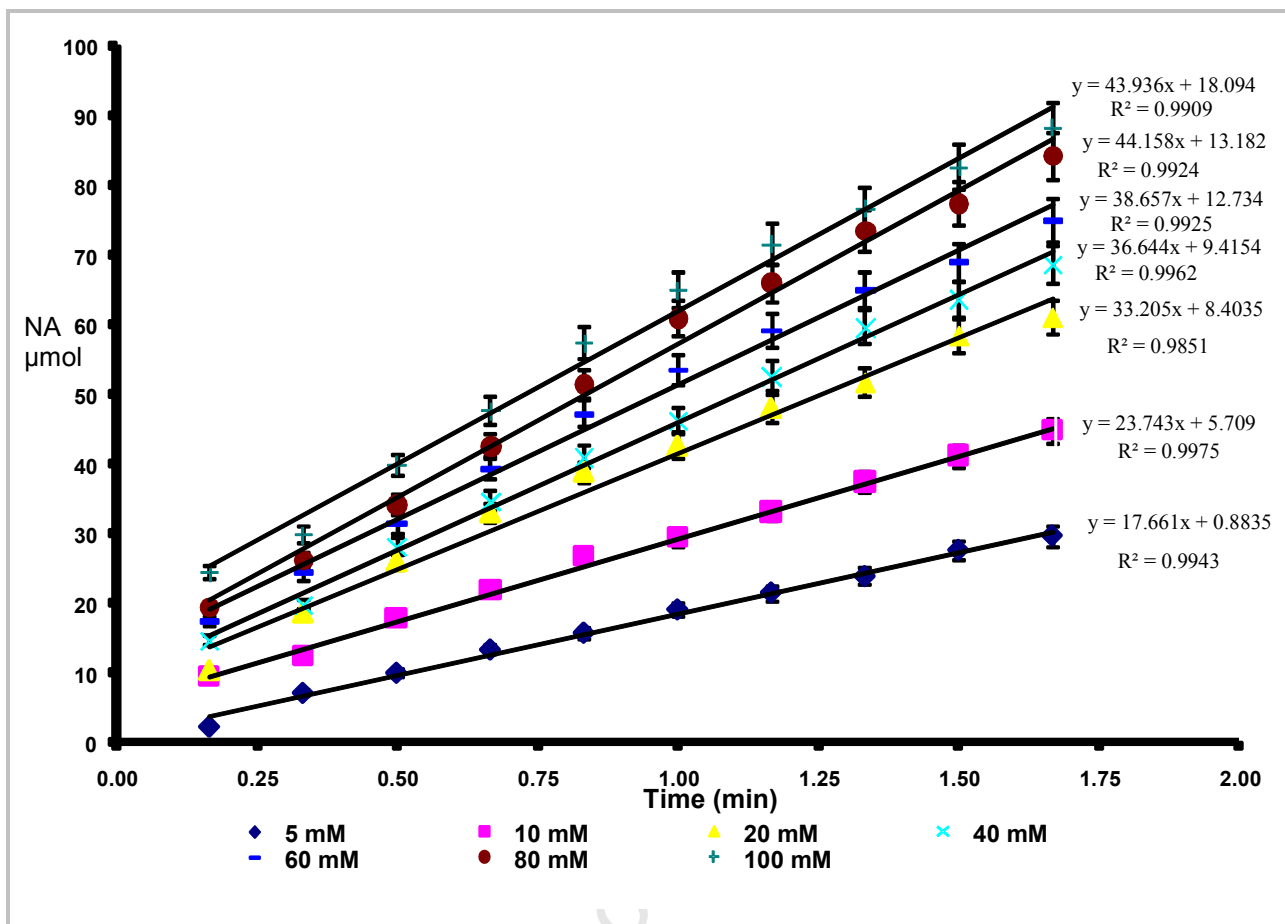


Figure 3. 20: Effect of reaction time on nicotinamide produced using different concentrations of 3-cyanopyridine. NHase was incubated for 1.7 min at 50 °C in 3 mL reaction mixtures containing 50 mM KH₂PO₄-K₂HPO₄ buffer (pH 7.2) and final concentration of the enzyme (0.14 mg). All experiments were conducted in duplicate.

3.3.5.9.2 Use of the Hanes-Woolf and Eadie-Scatchard plots to determine the kinetic parameters the *G. pallidus* RAPc8 NHase

Graphical depiction of the change in substrate concentration as a function of reaction velocity indicating first order kinetics over time (1.7 min) is expressed in their linearised forms of the Michaelis-Menten equation (along with the line of best fit), using Hanes-Woolf plot (Fig. 3.21) and Eadie-Scatchard plot (Fig. 3.22). The summary of V_{\max} and K_m values determined for 2-cyano, 3-cyano and 4-cyanopyridine, by each of the linear transformations can be seen in Table 3.4. Also included are the correlation coefficients (R-square values) for the linear fit of each plot. The Hanes-Woolf plot estimates provided the best approximations, with correlation coefficients

of 0.9951, very close to one. Clearly, the Eadie-Scatchard plot shown here has some defects, as its R-squared value was 0.9583. Variation in the V_{\max} and K_m values for each substrate was observed when different plots were used (Table 3.5). For example, the Hanes-Woolf plot gave higher values especially the V_{\max} and K_m for 2-cyano and 3-cyanopyridine. This could be attributed to the difference in distribution of error and the R-square value (which is an indication of how well the model fits the data) between the two plots.

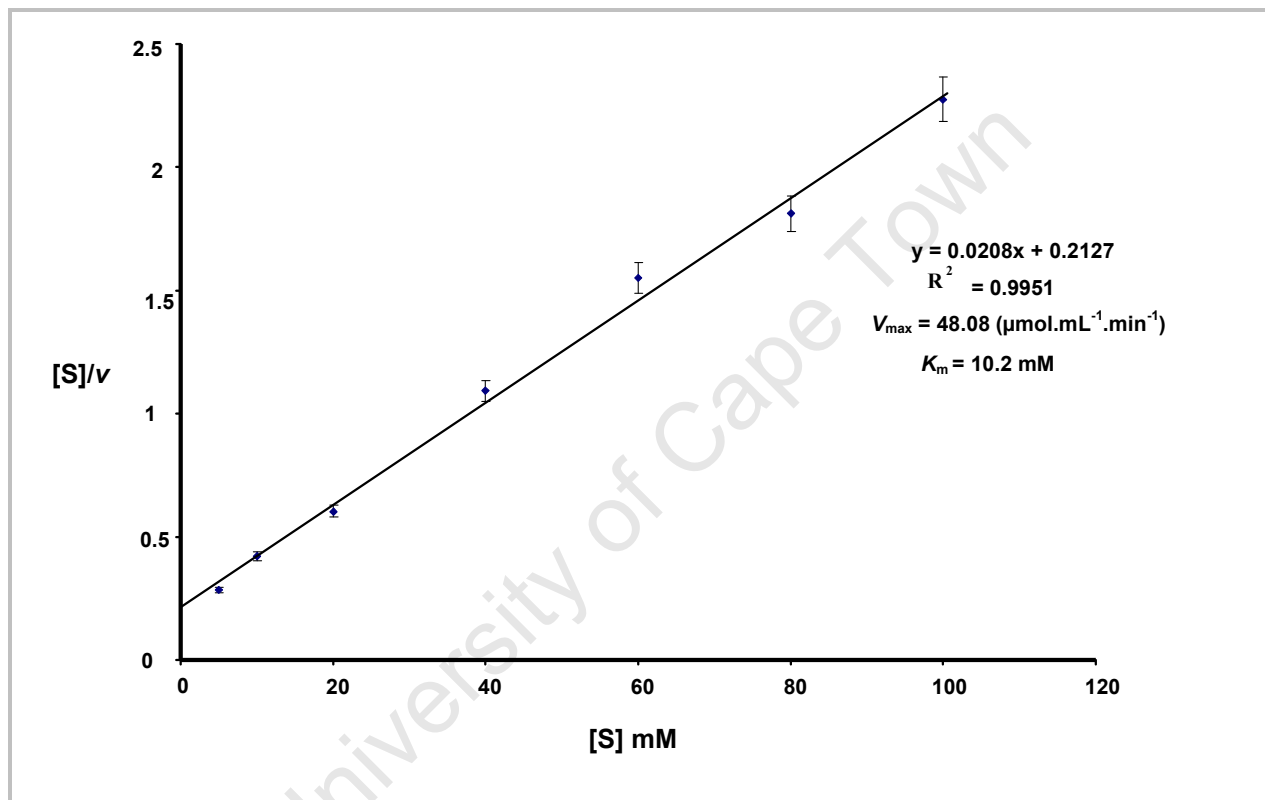


Figure 3. 21 The Hanes-Woolf plot for the *G. pallidus* RAPc8 NHase hydration of 3-cyanopyridine. NHase was incubated for 1.7 min at 50°C in a 15 mL reaction mixture containing 50 mM KH_2PO_4 - K_2HPO_4 buffer (pH 7.2), different concentrations of 3-cyanopyridine and 0.14 mg final concentration of NHase.

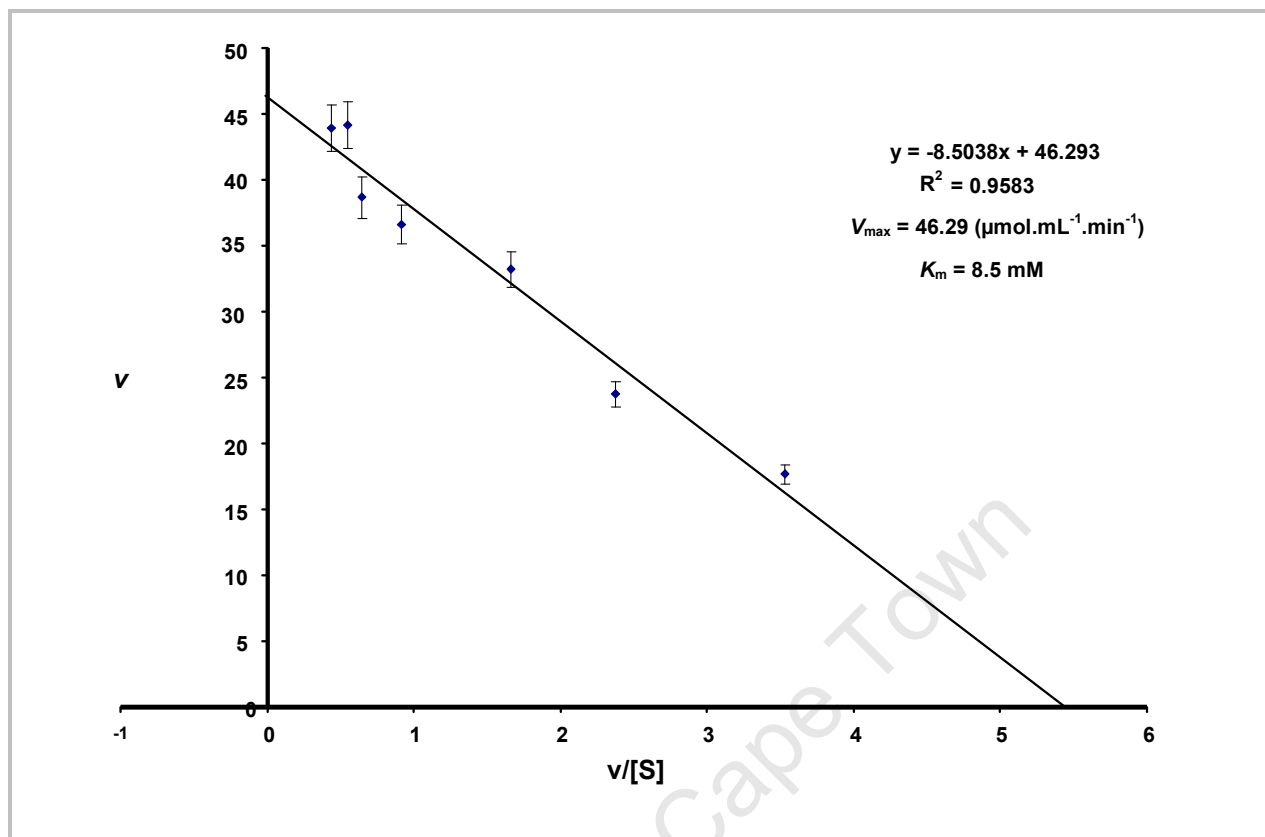


Figure 3. 22: The Eadie-Scatchard plot for the *G. pallidus* RAPc8 NHase hydration of 3-cyanopyridine. NHase was incubated for 1.7 min at 50°C in 15 mL reaction mixture containing 50 mM KH_2PO_4 - K_2HPO_4 buffer (pH 7.2), different concentrations of 3-cyanopyridine and 0.14 mg/mL final concentration of NHase.

3.3.5.9.3 Determination of the V_{max} , K_m and k_{cat} values for *G. pallidus* RAPc8 NHase

The *G. pallidus* RAPc8 NHase displayed the highest reaction velocity (V_{max}) of 48 $\mu\text{mol.mL}^{-1}.\text{min}^{-1}$ with 3-cyanopyridine substrate at 50°C. The enzyme showed relatively lower reaction velocities with substrates 2-cyanopyridine and 4-cyanopyridine, with V_{max} values of 34 $\mu\text{mol.mL}^{-1}.\text{min}^{-1}$ and 15 $\mu\text{mol.mL}^{-1}.\text{min}^{-1}$, respectively. The Michaelis constant K_m values obtained for 2-cyano-, 3-cyano-, and 4-cyanopyridine were 5.3 mM, 10.2 mM and 8.7 mM, respectively. In some of the reports cited in literature, V_{max} and K_m values were found to be 5.8 $\mu\text{mol/min/mg}$ and 28 mM, respectively for a NHase from *Brevibacterium* R-312 strain, using 3-cyanopyridine (Eyal *et al.*, 1990). Most recently, Prasad *et al.* (2007) studied a bench-scale conversion of 3-cyanopyridine to nicotinamide using resting cells of *Rhodococcus rhodochrous* PA-34, and

experiments gave V_{\max} value of 22.2 $\mu\text{mol}/\text{min}/\text{mg}$ and K_m value of 625 mM. However, these were results obtained using whole cells rather than isolated enzyme and are therefore not directly comparable. In this study, the lower K_m values indicate that *G. pallidus* RAPc8 NHase had a higher affinity when 3-cyanopyridine was used. Further, the V_{\max} value for the *G. pallidus* RAPc8 NHase was 2-fold and 8-fold higher than those for the *Rhodococcus rhodocrous* PA-34 and *Brevibacterium* R-312 NHases, respectively. Studies by Eyal *et al.* (1990) demonstrated that a NHase from *Brevibacterium* R-312 had a $K_m = 28$ mM and $V_m = 5.8 \mu\text{mol}.\text{min}^{-1}\text{mg}^{-1}$ protein at 25°C for 3-cyanopyridine substrate. Although data obtained using whole cells is not directly comparable with the current studies, the results shown for *G. pallidus* RAPc8 NHase may be a superior enzyme for the hydration of 3-cyanopyridine over the other NHases. Generally, enzyme preparations which show higher reaction rates and affinity for desired substrates are important in biotransformation, and hence, this work shows that the *G. pallidus* RAPc8 NHase constitutes a promising biocatalyst for the hydration of 3-cyanopyridine, to produce nicotinamide.

Table 3. 5: A summary of kinetic parameters for *G. pallidus* RAPc8 NHase.

Plot	Hanes-Woolf		Eadie-Scatchard		Hanes-Woolf	
Substrate	V_{\max} ($\mu\text{mol}.\text{ml}^{-1}.\text{min}^{-1}$)	K_m (mM)	V_{\max} ($\mu\text{mol}.\text{ml}^{-1}.\text{min}^{-1}$)	K_m (mM)	k_{cat} (s^{-1})	k_{cat}/K_m ($\text{mM}.\text{s}^{-1}$)
2-cyanopyridine	33.8	5.3	31.5	2.5	443.3	177.3
3-cyanopyridine	48.1	10.2	46.3	8.5	629.6	74.1
4-cyanopyridine	15.3	8.7	16.0	2.3	201.3	87.5

3.3.5.9.4 Comparison of 2-cyano, 3-cyano and 4-cyanopyridine, as substrates for *G. pallidus* RAPc8 NHase

The broad substrate specificity of NHase has been studied previously (Cameron, 2002), but whole-microbial cells were used in the study. The author demonstrated that 3-cyanopyridine was preferred over the other heteroaromatic nitriles 2-cyano- and 4-cyanopyridine. In this study, similarities in the NHase preference for 3-cyanopyridine compared to 2- and 4-cyanopyridine were observed using the purified enzyme and we can conclude that the *meta*-substituted pyridine ring is optimal for effective bioconversion of heteroaromatic substrates. The reactivity of 3-cyanopyridine can be accounted for chiefly on the basis of the stability of the intermediate carbocation analogue, in the mechanism for electrophilic substitution reaction (Morrison & Boyd, 2001). The electron-withdrawing effect of the cyano-functional group adjacent to the π system deactivates the heteroaromatic ring by decreasing the electron density. However, resonance only decreases the electron density at the *ortho*- and *para*- positions, and thus these sites will not be preferred for the reaction (Fig. 3.23). It is clear from the structures of intermediates formed that the positive charge is equally distributed over three secondary carbon atoms in the *meta*-substituted ring, making the intermediate more stable. In keeping with this explanation 2-cyano- and 4-cyanopyridine would not give rise to such stable intermediates and thus, they are less favoured for NHase reaction and consequently they have slower reaction rates, compared to 3-cyanopyridine.

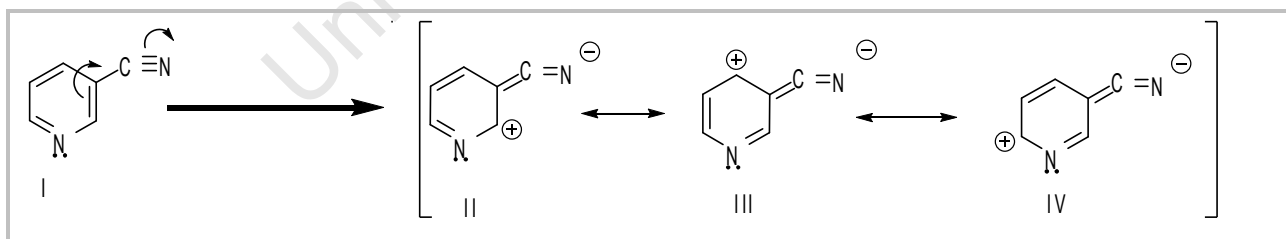


Figure 3.23: Intermediates generated from the *meta* directing effect of the electron-withdrawing cyano-functional group (Morrison & Boyd, 2001).

3.4 CONCLUSION

This chapter first described the commonly used method of bacterial cell culture involving shake flask fermentation for expression of the recombinant *G. pallidus* RAPc8 NHase and confirmed enzyme production protocols described previously (Pereira *et al.*, 1998 and Cameron, 2002). Further investigation, in this study, using a bioreactor-based production system, showed that the use of an automated BioFlo bioreactor of higher bacterial cell biomass yields, did not contribute to production of a higher total enzyme activity. Thus, the shake flask culture total yield was 3.4 g in 1 L, while that in Bioflo bioreactor gave 16.3 g in 5L (wet cell mass basis). These results represent a sound basis from which scale-up of the production of the biomass is achievable. However, this was not a central objective for the present study.

To obtain the desired purity of the *G. pallidus* RAPc8 NHase, cell-free enzyme extracts were exposed to four purification steps; heat treatment, $(\text{NH}_4)_2\text{SO}_4$ precipitation, phenyl-Sepharose (hydrophobic interaction) chromatography and Q-Sepharose (anion exchange) chromatography. Overall, *G. pallidus* RAPc8 NHase was obtained with 66.7% yield on the basis of crude enzyme extract, at a purification factor of 5.1-fold enrichment of the crude extracts of NHase. SDS-PAGE confirmed the purity of the NHase as two bands representing the α and β subunits with molecular weight of approximately 28 kDa and 29 kDa, respectively. This confirmed earlier reports on the NHase being multimeric, with a total molecular weight of 110 kDa (Pereira *et al.*, 1998).

The reaction conditions for the biocatalytic conversion of 3-cyanopyridine (used as a model reaction) were investigated to establish the most suitable operating conditions for characterising the NHase. The experiments were carried out with the broader aim of assessing the viability of developing an industrial process. The optimal temperature for the biocatalytic reactions was found to be 50 °C, and the optimal pH for NHase maximum activity was found to be pH 7.0. This confirmed earlier findings for the native and recombinant *G. pallidus* RAPc8 NHase (Pereira *et al.*, 1998; Cameron & Cowan, 2005) and is consistent with reported temperature and pH optimal for other thermophilic NHases (Cowan *et al.*, 1998).

In the standard assay system, the soluble NHase enzyme was able to convert 3-cyanopyridine (substrate) up to 100 mM concentration only. The system was therefore apparently being inhibited by the higher substrate concentrations, as has been observed amongst other NHases (Cantarella *et al.*, 2003; Wang *et al.*, 2007). Avoiding substrate inhibition has been a challenge in design of bioconversion systems that are related to nitrile hydration using NHases, but is commonly averted by diluting the substrates. However, this would compromise the quantities of amide products achievable at industrial scale (Nagasawa *et al.*, 1993). This issue has been addressed, in the present study, and new progress is presented in Chapter 4.

An investigation into the thermal stability of the *G. pallidus* RAPc8 NHase showed that the NHase retained 90 % of the original activity after incubation for 1 h at temperatures of 40 to 50°C and thereafter loss of catalytic activity followed with increased temperature and incubation time. Inactivation of the heterotetrameric NHase may be strongly related to dissociation of the α and β subunits leading to conformational changes in the active site, consequently affecting the catalytic activity (Fernandez-Lafuente *et al.*, 1999). Thermal stability of an enzyme is important under industrial conditions; where the enzyme is exposed to harsh process conditions. We can conclude that development of a more stable biocatalyst is of importance if the NHase is to be applied in a biocatalytic process.

The NHase activity was activated by addition Co^{2+} , Fe^{2+} , K^{+} and Mg^{2+} at various concentrations. The highest NHase activity 176 % (relative activity with respect to 100% in potassium phosphate buffer) was observed with a K^{+} concentration of 6 mM. Heavy metal ions such as Cu^{2+} were found to be inhibitory to the NHase, resulting in a significant loss of activity at all metal ion concentrations.

Determination of the kinetic parameters of the *G. pallidus* RAPc8 NHase indicated that reaction with 3-cyanopyridine had the highest rates, with a V_{max} value of $48.1 \mu\text{mol} \cdot \text{ml}^{-1} \cdot \text{min}^{-1}$. Analysis of the 2-cyanopyridine and 4-cyanopyridine kinetics showed lower values V_{max} values by 1.5-fold and 3.5-fold, respectively. The difference in position of the cyano-functional group on the pyridine ring of the substrate led to the conclusion that the *meta*-substituted substrate (3-

cyanopyridine) was favoured by NHase due to the resonance-stabilized intermediate generated in the initial stages of the nucleophilic attack.

When organic/aqueous cosolvent systems were investigated, the NHase was found to retain over 90 % of the original enzymatic activity in cosolvent systems containing 10% of selected water-immiscible organic solvents. The presence of solvents such as toluene, ethyl acetate and benzene showed the greatest effects in enhancing the NHase activity over to 100% relative activities. These results have confirmed that *G. pallidus* RAPc8 NHase has potential for use as a biocatalyst in co-solvent organic/aqueous systems with numerous potential applications.

The work reported in this chapter demonstrated the reproducibility of the preparation of *G. pallidus* RAPc8 NHase from the recombinant *E. coli* BL21 (DE3) and established the most suitable conditions for the biocatalytic application of *G. pallidus* RAPc8 NHase in production of amides. It has been shown that, under experimental conditions, the NHase was relatively stable, and active, compared to counterpart NHases from mesophilic sources. Because of the biotransformation potential of this enzyme, it was decided to investigate further improvements of the functional stability, by increasing the structural rigidity through immobilization. Immobilization systems have successfully stabilized many enzymes (Guisan, 2006), and have, in addition, reduced inactivation *via* conformational changes. Immobilization of *G. pallidus* RAPc8 NHase on a various support materials using numerous techniques is described in detail in Chapter 4.

CHAPTER 4

Development of an immobilized biocatalyst using the recombinant NHase from *Geobacillus pallidus* RAPc8

4.1 INTRODUCTION - Stabilization of the *G. pallidus* RAPc8 NHase by immobilization

Although enzymes have numerous applications in industry, many of these enzymes are not sufficiently stable in the applied processes and their stabilization remains a critical issue in biotechnology (López-Gallego *et al.*, 2005). Thus, attempts to increase enzyme stability by modifying physiological or process parameters are essential in the further development of biocatalytic processes. In the field of biocatalysis, this problem is being approached from various different perspectives, including: site-directed mutagenesis to generate highly active and stable enzymes (Burton *et al.*, 2002), use of stabilizing additives which protect enzymes against inactivation (Ye *et al.*, 1988), chemical modification of the protein by coupling a functional group to a protein resulting in improved stability and function (Inada *et al.*, 1986), manipulation of the reaction medium to achieve biocatalyst stability (Gupta, 1992), and immobilization of enzymes or whole-microbial cells (Katchalsky-Katzir, 1993). Immobilization of enzymes (or whole microbial cells) on insoluble support material has been most commonly employed for this purpose, and offers many advantages, in that the biocatalyst can be used repeatedly, easily separated from product, and used in a range of different reactors (Guisan, 2006). In addition, there may be potential to reduce effluent disposal problems, and the use of soluble enzymes may be wasteful because the enzyme generally cannot be recovered at the end of the reaction (Katchalsky-Katzir, 1993). Furthermore, underpinning the application of such immobilization methods is the observation that the immobilized enzymes often remain active for longer periods compared to their soluble counterparts.

The history of immobilization of enzymes dates back to 1916 when Nelson and Griffin accidentally found that yeast invertase, adsorbed on activated charcoal, catalysed the hydrolysis of sucrose (Krishna, 2002). Immobilized enzymes then came into commercial application in the

1960s when various enzymes such as carboxypeptidases, diastases, pepsin, and ribonucleases on polyaminostyrene resin by covalent bonding (Kalchalski-Katzir and Kraemer, 2000). Since then many investigations have been reported and numerous reviews on the stabilization of enzymes by immobilization have been published (Cao *et al.*, 2003; Minovska *et al.*, 2005; Mateo *et al.*, 2007; Guisan, 2006). Immobilization of a wide range of enzymes has been successfully performed using different methods: adsorption and ionic bonding, cross-linking, encapsulation, entrapment, and covalent bonding on numerous insoluble carriers (Malcata *et al.*, 1990). These methods are described in more detail in the next section.

4.1.1 Old and new methods for immobilization of enzymes

4.1.1.1 Adsorption and ionic binding as immobilization methods

Adsorption on a support as a method for enzyme immobilization involves weak interactions such as van der Waals, electrostatic, hydrophobic and hydrogen bonding of enzyme ligands to a solid surface. This is a low-cost procedure and generally results in retention of the native conformation of the enzyme, and thus also its intrinsic catalytic activity (Hamachi *et al.*, 1994; Bosley *et al.*, 1994). However, application of physical adsorption is less popular due to the reversible nature of the biocatalyst-support bond, which can easily dissociate under varying process conditions, such as temperature, pH, and ionic strength (Synowiecki & Wolosowska, 2006). This dissociation effect of physical adsorption, further makes it difficult to operate large-scale bioreactors as significant biocatalyst leakage could occur, which then results in loss of productivity and product contamination (Marquez *et al.*, 2008).

Greater stabilization of the biocatalyst-support linkage can be achieved by use of ionic supports. With a charged support material, a biocatalyst is considered to interact electrostatically forming a stable biocatalyst-support complex (Pessela *et al.*, 2003). Materials that act as ion-exchange resins include compounds containing amino and quarternary amino groups, sulfates, phosphates, and carboxyl groups, and these have been intensively studied to date (Klibanov, 1983; Chibata *et al.*, 1986; Gupta, 1991; Katchalski-Katzir, 1993). Typically, ion exchange resins are designed for protein purification, to desorb proteins under moderately mild conditions; when they are used for

immobilization, variations in pH and temperature may permit the release of adsorbed protein to the medium after biocatalyst use (Fuentes *et al.*, 2006). One way to avert inactivation and loss of enzyme is by coating ionically-immobilized enzymes with polymers such as dextran sulphate, dextran aspartic and polyethyleneimine (Mateo *et al.*, 2000; Albayrak *et al.*, 2002; Pessela *et al.*, 2003; Fuentes *et al.*, 2004). Further, it has been shown that addition of multivalent cations to solutions containing ionic immobilization may increase the binding of the protein onto the ionic supports (Fuentes *et al.*, 2006).

4.1.1.2 Cross-linking of enzymes as an immobilization technique

Enzymes have free surface amino- and /or carboxyl groups which can be covalently cross-linked with bi- or multi- functional reagents producing three-dimensional cross-linked insoluble enzyme aggregates. Glutaraldehyde and carbodiimide are generally the most extensively used cross-linking reagents and these reagents react with, for example, side-chains ϵ -amino of lysine residues on the enzymes. Schiff base formation (Scheme 4.1) between the enzyme and glutaraldehyde is irreversible and will remain stable even at extreme pH and temperature:



Scheme 4-1 Preparation of Schiff base cross-link between an enzyme and glutaraldehyde

Cross-linking has frequently been used in combination with other techniques, as an additional stabilization procedure, for example in enzymes or cells which have already been immobilized covalently, establishing multi-point covalent enzyme-support or enzyme-enzyme attachment (López-Gallego *et al.*, 2005). Further, a new technique of enzyme immobilization *via* step wise crystallization of protein followed by addition of a bifunctional reagent, to form strong covalent bonds between free amino groups on the protein molecule to preserve the crystalline structure, has recently been reported (Sheldon, 2007). The cross-linked enzyme crystals (CLECs) offer several advantages including: increased stability, high activity and selectivity in organic media;

high mechanical stability; easy recovery and recycle; and stability against proteolysis and self-digestion.

4.1.1.3 Covalent binding of enzymes as an immobilization technique

Covalent coupling of enzymes to reactive groups in a support is probably the most thoroughly investigated approach to immobilization (Katchalski-Katzir, 1993). The wide variety of activation and coupling reactions available has made this a generally applicable method with the following advantages: (i) enzymes do not leak or detach from the support during utilization because of covalent binding involved; (ii) the immobilized enzyme can readily contact the substrate because it is localized on the support surface; and (iii) the method produces generally yields a highly stable biocatalyst due to the strong enzyme-support interaction (Varavinit *et al.*, 2001). However, the high cost of support materials, and complicated procedures for immobilization, may restrict the practical applications of the method (Katchalski-Katzir, 1993; Schmid *et al.*, 2001).

The commercially available materials Eupergit[®]C and Eupergit[®]CM have been widely used as supports in immobilization of different enzymes. Eupergit[®]C and CM are microporous, oxirane-activated acrylic beads with a diameter of 100-250 μm formed by copolymerization of *N,N*-methylene-bis-(methacrylamide), glycidyl methacrylate, allyl glycidyl ether and methacrylamide (Fig. 4.1). Eupergit[®]C has some advantageous features, *e.g.* Eupergit[®]C is stable, both chemically and mechanically, over a pH range from 0 to 14, and does not swell or shrink even with severe pH changes. Due to the stable nature of the beads, they are highly reactor- compatible, and can be used in most forms of stirred tank, fixed bed, and fluidized bed reactors, as long as the equipment has provision to withhold the carrier particles inside the vessel. Furthermore, it does not require additional reagents during the immobilization procedure.

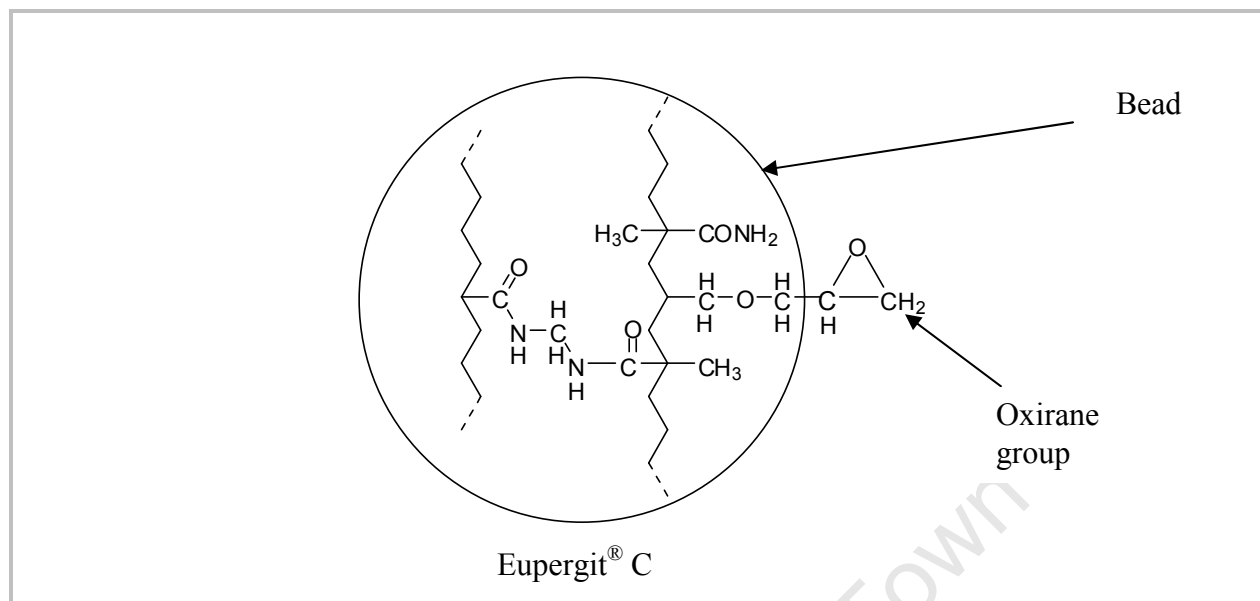


Figure 4.1: Structural representation of Eupergit® C (Katchalski-Katzir *et al.*, 2000).

It has been proposed that a two-step binding mechanism of enzyme to Eupergit® C exists (Mateo *et al.*, 2000). It is assumed that the initial step is physical adsorption of the enzyme on to the oxirane (epoxy) groups of the carrier by hydrophobic interactions. This form of binding is believed to bring amino and thiol groups of the enzyme in close proximity to the oxirane groups of the support. Under neutral and alkaline conditions, the oxirane groups react with the amino groups of the protein forming a covalent bond. The enzyme-Eupergit® C bonds are stable within a pH range of 1 to 12, with the enzyme retaining most of its activity.

While the two immobilization supports, Eupergit® C and Eupergit® CM, have similar chemical properties, they differ in their density of oxirane groups and porosity. Eupergit C has a small pore size (10nm) and an oxirane density of 600 $\mu\text{mol/g}$ dry beads; Eupergit® CM has larger pores (100 nm) and a lower oxirane density of 300 $\mu\text{mol/g}$ dry beads. Thus, Eupergit® C allows many sites for immobilization which is, in itself, considered advantageous for the high loading of enzymes to its surface.

Eupergit® C has been widely used for the preparation of large quantities of biocatalysts for industrial biotransformations, largely due its compatibility with a wide range of different enzymes and conditions for biotransformation processes. While several classes of enzyme

immobilization on Eupergit[®]C have been reported (Boller *et al.*, 2002), it was recently applied in our laboratory for the stabilization of an amidase from *G. pallidus* RAPc8 strain (Makhongela *et al.*, 2007).

4.1.1.4 Entrapment of enzymes as an immobilization technique

Entrapment is achieved when a solution containing the enzyme is involves a chemical or physical solidification, trapping the biocatalyst (in its active form) in a water-insoluble matrix polymer network. For an efficient immobilization process of enzymes, the matrix need to have a pore size that is sufficiently small to prevent leaching of the enzyme, but allowing diffusion of substrates and products (Sakai *et al.*, 2008). Various methods are available to obtain particles containing entrapped enzymes or cells including polymerization, thermal gelation, and precipitation. Entrapment in alginate gel has been used most extensively in the immobilization of enzymes or microbial cells and to date a large body of work has been published (Catana *et al.*, 2005). The biocatalyst is entrapped when a polyvalent cation such as Ca^{2+} binds to two neighboring guluronic acid residues (Fig. 4.2), which subsequently form a cross-linked polymer chain. Enzyme entrapment, as an immobilization method, is advantageous as it does not involve any modification of the enzyme and, therefore, may not adversely affect activity. However, the technique can be susceptible to leaching of enzymes out of the matrix by diffusion when pore diameters are larger than the enzyme.

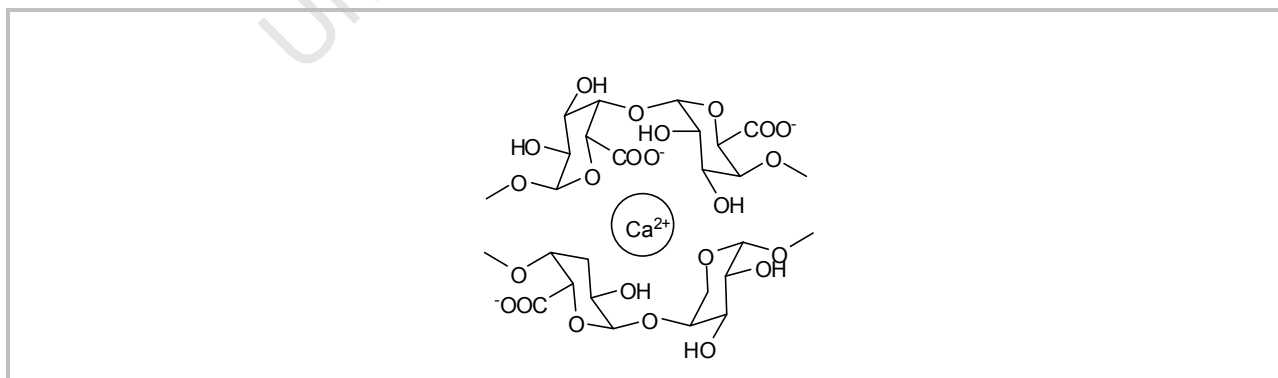


Fig. 4.2 Calcium alginate: chemical and macroscopical structure (Gerbsch & Buchholz, 1995).

4.1.1.5 Metal-chelating of enzymes as an immobilization method

This method, based on the chelating properties of most transition metals, can be employed to couple enzymes, using the protein side chain groups such as free carboxyl groups, phenolic hydroxyl groups (of tyrosyl residues), sulfhydryl groups (from cysteinyl residues), and ϵ -amino groups (from lysyl residues), which can replace ligands on the metal ions. However, it may be difficult to achieve effective enzyme immobilization in this fashion due to the fact that there may be limitations on the availability in the enzyme molecule of residual groups which can act as ligands, and steric factors may preclude such groups to come in contact with the metal compound. Commonly, bivalent transition metals (Ni^{2+} , Zn^{2+} , Co^{2+} , Cu^{2+}) are pre-loaded on to support material modified with a chelating compound such as iminodiacetic acid (IDA) (Fig. 4.3) permitting interaction between activated M^{n+} -chelate complex with surface accessible amino acid residues of the enzyme (Porath, 1992).

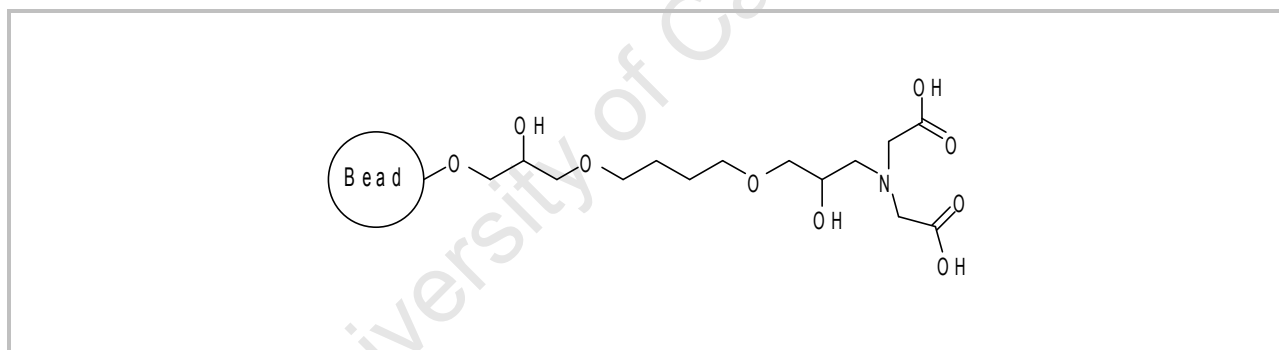


Figure 4.3: Iminodiacetic acid activated bead used in enzyme immobilization
(<http://www.piercenet.com/products/browse.cfm?fidID=02050204>)

In the present work, various support materials including Eupergit[®]C and CM, EDA-activated Amberlite XAD 4, GA-activated Amberlite XAD4, DEAE-Sephadex, SE-Sephadex, Dowex[®]50WX8, Super-Q-Toyopearl, Sepabeads EC-series, controlled pore glass, Biobeads and sodium alginate using the above-mentioned immobilization techniques were investigated. The immobilization was conducted under different conditions depending on the technique involved. The results obtained from immobilization studies were expected to provide information regarding the effect of immobilization and its effect on the operation of biocatalyst process. In

the biochemical studies of the immobilized NHase, a comparative study with the soluble enzyme was also conducted. Moreover, the batchwise hydration of 3-cyanopyridine to nicotinamide in potassium phosphate buffer was employed as the model reaction in order to investigate the properties of the immobilized *G. pallidus* RAPc8 NHase (Fig. 3.1.1). To elucidate the influence of NHase immobilization to overall hydration performance, the effects of varying pH, temperature, thermal stability and substrate concentrations were studied, using the established protocols to identify possible inhibitors to the enzyme activity. The varying effects on the operational and storage stability of the enzyme were investigated and studies to characterize the deactivation of immobilized NHase were also conducted.

4.1.2 Estimation of deactivation kinetics for the *G. pallidus* RAPc8 NHase

The study of deactivation kinetics for a newly immobilized enzyme is necessary to determine its deactivation characteristics. Numerous approaches to the study of deactivation kinetics for enzymes have been reported, for example, Knezevic *et al.* (2006) studied deactivation of a *Candida rugosa* immobilized on Eupergit® C, using a first-order model.

Assuming that in the deactivation, the active enzyme (A_0) is directly converted to inactive form (A) without producing any significant amount of intermediates. Therefore, the first-order deactivation equation is expressed as:

$$\frac{dA}{dt} = -k_d [A_0] \quad (4.1)$$

where A is the enzyme activity at time t , A_0 the initial enzyme activity, t the treatment time, and k_d the deactivation rate constant. Taking natural logarithms of Equation 4.1.

$$\ln \left(\frac{A}{A_0} \right) = -k_d t + C_1 \quad (4.2)$$

From a linear regression analysis of the graph $\ln (A/A_0)$ versus t , the slope gives the value of the deactivation rate constant k_d (Owusu & Berthelon, 1993).

4.1.2.1 The half-life of *G. pallidus* RAPc8 NHase

The half-life of an enzyme, defined as the time required by the enzyme to lose half of its initial activity, is calculated from values of thermal deactivation constants at different temperatures (Calsavara *et al.*, 2000), following the equation:

$$t_{1/2} = \frac{\ln 2}{k_d} \quad (4.3)$$

4.1.2.2 Activation energy (E_a) determination for deactivation of *G. pallidus* RAPc8 NHase

The activation energy of deactivation for NHase from *G. pallidus* RAPc8 and its immobilized derivative was estimated by using data for thermal stability studies. For these studies, the Arrhenius-type Equation 4.4 was used to calculate the activation energy required for deactivation as described previously by Lamb & Stuckey (2000).

$$k_d = Ae^{\left(\frac{-E_a}{RT}\right)} \quad (4.4)$$

where E_a is the energy of thermal activation, R universal gas constant ($8.31451 \text{ J.K}^{-1}.\text{mol}^{-1}$) and T the absolute reaction temperature (Kelvin). Taking natural logarithms of Equation 4.4:

$$\ln k_d = \ln A - \left(\frac{E_a}{R}\right) \frac{1}{T} \quad (4.5)$$

The E_d and $\ln A$ values were calculated from the slope and intercept, respectively of the plot of $\ln k_d$ vs $1/T$ respectively.

4.2 MATERIALS AND METHODS

4.2.1 Materials

Various carrier materials for immobilization were used which included: Eupergit[®]C and CM (RÖHM, Pharma Polymers, Germany), SEPABEADS Series EC (Resindion, Mitsubishi Chemicals Corporation, Japan), SE and DEAE-Sephadex A 50 (Pharmacia), Dowex (Serva Feinbiochemica), and Super-Q-Toyopearl (Tosoh Corporation), Glass beads (Supelco), and Bio-Beads (Bio-Rad). Other reagents included 50% glutaraldehyde (Aldrich), 3-aminopropyltriethoxysilane (Sigma), ethylenediamine (EDA) (Aldrich), 1-ethyl-3-(dimethylamino-propyl) carbodiimide (EDAC) (Aldrich) trichloroacetic acid (Saarchem), ZnSO₄ (Aldrich), Ag₂SO₄ (Saarchem), CoCl₂ (NT laboratories Suppliers) and CuCl₂ (Holpro analytics (Pty) LTD).

4.2.2 Methods

4.2.2.1 Immobilization of NHase by entrapment in Calcium alginate beads (Won *et al.* 2005)

Sodium alginate solution [2 and 4% (w/v)] was mixed with purified NHase solution (prepared as described in Section 3.3.2.4), containing 10 mg protein in different ratios of enzyme solution (in mL) vs sodium alginate solution (in mL) (9:1, 8:2, 7:3, and 6:4) and each of the mixtures was stirred thoroughly to ensure complete mixing. The mixed solution was dropped with a syringe from a height of approximately 20 cm into an excess (100 mL) of 200 mM CaCl₂ solution and Ca-alginate beads were immediately formed. A needle producing beads of 0.5-2 mm in diameter was used. Beads were stirred in CaCl₂ solution for another 30 min to harden, and then collected by filtration using a glass filter. The beads were then washed thoroughly on the same filter with 3 x 20 mL of 50 mM potassium phosphate pH 7.2 and stored at 4°C. The filtered CaCl₂ solution and the three washings were collected for loading efficiency determination.

4.2.2.2 Immobilization of NHase by covalent binding on Eupergit®C and CM (Martin *et al.*, 2003).

Eupergit®C (oxirane acrylic beads) (5 g) was added to 20 mL of purified NHase solution (10 mg protein, 21.3 U) in 50 mM potassium phosphate buffer, pH 7.2, and mixed by gentle shaking in a flask. The flask was then sealed and allowed to stand at room temperature for 72 - 96 h without additional shaking. The beads were collected on a Buchner funnel with filter paper, and the remaining solution was removed by vacuum. The beads were washed thoroughly on the filter with 3 x 15 mL portions of 50 mM potassium phosphate buffer pH 7.2. The beads were stored at 4 °C until used.

4.2.2.3 Immobilization of NHase by covalent binding on Eupergit®C followed by cross-linking with glutaraldehyde and EDAC (Bulawayo *et al.*, 2007)

Eupergit®C (5 g) was incubated with 20 mL purified NHase solution (10 mg protein, 21.3 U) in 50 mM potassium phosphate buffer, pH 7.2 for 76 – 92 h as previously described in section 4.2.2.2 above. After this, the cross linking was achieved by addition of 0.5% (final concentration) of either glutaraldehyde or 1-ethyl-3-(dimethylamino-propyl) carbodiimide (EDAC). The cross linking was allowed to proceed for 3 h at room temperature. The solution was then decanted, and the Eupergit C bound NHase was washed three times with 50 mM potassium phosphate buffer, pH 7.2.

4.2.2.4 Immobilization of NHase by covalent binding on EDA-activated Amberlite XAD 4 (Spagna *et al.*, 1995)

The procedure described by Spagna and coworkers (1995) was adopted and modified. In this study, 50 g of Amberlite-XAD 4 was reacted with 30 mL of ethylene diamine (EDA) under reflux in 80 mL toluene for 5 h. The Amberlite-EDA conjugate was washed with 50 mL absolute methanol and dried overnight in a vacuum dessicator to remove excess EDA. Then 20 mL purified NHase solution (10 mg protein, 21.3 U) in 50 mM potassium phosphate buffer, pH 7.2 was treated with 5 g of EDA-activated Amberlite-XAD 4 for 72 – 96 h. The immobilized NHase

was recovered by filtration, washed three times with 15 mL of 50 mM potassium phosphate buffer, pH 7.2.

4.2.2.5 Immobilization of NHase by covalent binding on glutaraldehyde-activated Amberlite XAD 4 (Spagna *et al.*, 1995)

Amberlite-XAD-4 (5 g) was treated with 2.5 % (v/v) glutaraldehyde for 30 min. The glutaraldehyde-Amberlite conjugate was washed with distilled water to remove excess glutaraldehyde. Then 5 mL purified NHase solution (10 mg protein, 21.3 U) in 50 mM potassium phosphate buffer, pH 7.2 was treated with 1 g of glutaraldehyde-activated Amberlite-XAD 4 for 72 – 96 h. The immobilized NHase was recovered by filtration, and washed three times with 15 mL of 50 mM potassium phosphate buffer, pH 7.2.

4.2.2.6 Immobilization of NHase on Sepabeads EC-series (Pessela *et al.*, 2003)

NHase was immobilized on a range of Sepabeads of the EC series, having a variety of functional groups on the surface, by methods described below:

4.2.2.6.1 Immobilization of NHase on epoxy Sepabeads (EC-EP) support

Sepabeads (EC-EP) (5 g) were suspended in 20 mL of NHase solution (10 mg protein, 21.3 U) in 50 mM potassium phosphate buffer, pH 7.2 at room temperature with gentle shaking. After 48 h of incubation, the supernatant was decanted, immobilized NHase washed with 3 x 15 mL of 50 mM potassium phosphate buffer, pH 7.2 and stored at 4°C.

4.2.2.6.2 Immobilization of NHase on amino-epoxy Sepabeads (EC-HFA) support

Sepabeads (EC-HFA) (5 g) were suspended in 20 mL of NHase solution (10 mg protein, 21.3 U) in 50 mM potassium phosphate buffer, pH 7.2 as previously described in Section 4.2.2.6.1. The mixture stirred at 150 rpm (shaker) for 72 h and the immobilized NHase was filtered, washed by using 3 x 15 mL of 50 mM potassium phosphate buffer pH 7.2 and stored at 4°C.

4.2.2.6.3 Immobilization of NHase on ethylenediamino-Sepabeads (EC-EA) support

Ethylenediamino-Sepabeads (EC-EA) supports (5 g) were prepared by being suspended in 50 mL of 50 mM potassium phosphate buffer, pH 7.2 under stirring (150 rpm) for 15 min at 25°C. The pH was checked, since it was required to be in the range of 7.2 ± 0.2 . The carrier settled and the supernatant was decanted. A solution of 20 mL glutaraldehyde (2% v/v in 50 mM potassium phosphate buffer 50mM pH 7.2 ± 0.2) was added. The slurry was stirred for 60 min at 25°C. The activated-Sepabeads were filtered, washed by 3 x 15 ml of 50 mM potassium phosphate buffer pH 7.2.

Sepabeads (EC-EA)-glutaraldehyde conjugate (5 g) was added to 20 mL of NHase solution (10 mg protein, 21.3 U) in 50 mM potassium phosphate buffer, pH 7.2. The mixture was stirred at a speed of 150 rpm at 25°C for an initial period of 20 h and then supernatant was decanted; the beads washed with 3 x 20 mL of 0.5 M NaCl and 3 x 20 mL of 50 mM potassium phosphate buffer, pH 7.2.

4.2.2.6.4 Immobilization of NHase on hexamethylenediamino-Sepabeads (EC-HA) support

Hexamethylenediamino-Sepabeads (EC-HA) (5 g) as before suspended in 50 mL of 50 mM potassium phosphate buffer, pH 7.2 under stirring (150 rpm) for 15 min at 25°C as previously described in section 4.2.6.1. The pH was checked, since it was required to be in the range of 7.2 ± 2 . The carrier settled and the supernatant was decanted. A solution of 20 mL of glutaraldehyde (2 % v/v in 50 mM potassium phosphate buffer 50mM pH 7.2) was added. The slurry was stirred for 60 min at 25°C. The activated-Sepabeads were filtered, washed by 3 x 15 mL of 50 mM potassium phosphate buffer pH 7.2.

Sepabeads (EC-HA)-glutaraldehyde conjugate (5 g) was added to 20 mL of NHase solution (10 mg protein, 21.3 U) in 50 mM potassium phosphate buffer, pH 7.2 as previously described in section 4.2.6.2. The mixture was stirred at a speed of 150 rpm at 25°C for an initial period of 20 h and then supernatant was decanted; the beads washed with 3 x 20 ml of 0.5 M NaCl and 3 x 20 ml of 50 mM potassium phosphate buffer, pH 7.2.

4.2.2.6.5 Immobilization of NHase onto iminodiacetic-Sepabeads (EC-IDA) support (Vançan *et al.*, 2002)

Iminodiacetic-Sepabeads (EC-IDA) (5 g) were rinsed with 40 mL of 20 mM potassium phosphate buffer at pH 7.0 under stirring (150 rpm). The supernatant was then decanted and 20 mL of 0.5 M metal solution (Ag^{2+} , Zn^{2+} , Cu^{2+} or Co^{2+}) was added and stirred for 2-3 h until equilibrium. The supernatant was decanted, the activated Sepabeads rinsed under stirring with 20 mM of 0.5 M NaCl in 50 mM potassium phosphate buffer, pH 7.2 for 30 min. The Sepabeads were filtered, washed with 2 x 40 mL of 20 mM potassium phosphate buffer, pH 7.0.

Sepabeads (EC-HA)-glutaraldehyde conjugate (5 g) was added to 20 mL of NHase solution (10 mg protein, 21.3 U) in 50 mM potassium phosphate buffer, pH 7.2 as previously described in section 4.2.6.2. The mixture was stirred at a speed of 150 rpm at 25 °C for a period of 48 h. The supernatant was decanted, and 2.0% w/v glutaraldehyde solution in 50 mM potassium phosphate buffer, pH 7.2 was added followed by stirring for 1 h. The supernatant was decanted, immobilized NHase washed with 50 mM potassium phosphate buffer, pH 7.2.

4.2.2.7 Immobilization of NHase on anionic exchanger resins Dowex[®] and DEAE-Sephadex (Minovska *et al.*, 2005).

The anion exchangers (Dowex[®] and DEAE-Sephadex) (5 g) was previously equilibrated with 0.5 M HCl, washed with distilled water and then equilibrated in 50 mM potassium phosphate buffer pH 7.2, agitation (100 r.p.m) for 2 h at room temperature. After that, the phosphate buffer was decanted, and the activated resins washed with 2 x 15 mL of the same buffer.

Activated anionic exchanger resins Dowex[®] and DEAE-Sephadex (5 g), separately, were added to 20 mL of NHase solution (10 mg protein, 21.3 U) in 50 mM potassium phosphate buffer, pH 7.2. The mixture was stirred at a speed of 150 rpm at 25°C for a period of 48 h. The supernatant was decanted, and the immobilized NHase was washed with 50 mM potassium phosphate buffer, pH 7.2 and stored at 4°C.

4.2.2.8 Immobilization of NHase on cationic exchanger resins Super-Q-Toyopearl and SE-Sephadex C 50

The cationic exchangers (Super-Q-Toyopearl and SE-Sephadex) (5 g) was previously equilibrated with 0.5 M NaOH, washed with distilled water and then equilibrated with 50 mM potassium phosphate buffer pH 7.2 under agitation (100 rpm) for 2 h at room temperature. After that, the phosphate buffer was decanted, and activated resins were washed with 2 x 15 mL of the same buffer.

Activated anionic exchanger resins Super-Q-Toyopearl and SE-Sephadex (5 g), separately, were added to 20 ml of NHase solution (10 mg protein, 21.3 U) in 50 mM potassium phosphate buffer, pH 7.2. The mixture was stirred at a speed of 150 rpm at 25 °C for a period of 48 h. The supernatant was decanted, and the immobilized NHase was washed with 50 mM potassium phosphate buffer, pH 7.2 and stored at 4°C.

4.2.2.9 Immobilization of NHase on Glass and Bio-beads

Glass or Bio beads (5 g) were refluxed with 10 % (v/v) solution of 3-aminopropyltrimethoxysilane in toluene for 24 h. The aminated glass or bio beads were then washed with 2 x 50 ml distilled water and another 2 x 50 ml of 50 mM potassium phosphate buffer, pH 7.2. 5 ml glutaraldehyde solution (2.0% w/v) was added and the mixture was stirred for 3 h at constant speed (150 rpm) at room temperature. The glass or bio beads was washed with 2 x 20 mL distilled water and 2 x 20 mL of 50 mM phosphate buffer solution with pH 7.2.

Activated glass or bio beads (5 g), separately, was added to 20 mL of NHase solution (10 mg protein, 21.3 U) in 50 mM potassium phosphate buffer, pH 7.2 as previously described in section 4.2.6.2. The mixture was stirred at a speed of 150 rpm at 25°C for a period of 48 h. The supernatant was decanted, and the immobilized NHase washed with 50 mM potassium phosphate buffer, pH 7.2 and stored at 4°C.

4.2.2.10 Determination of immobilized NHase activity

The activity of immobilized NHase were determined by adding of immobilized NHase biocatalyst (0.14 mg protein, approximately 5.6×10^{-2}) into a reaction mixture (3 mL total volume) consisting 50 mM of 3-cyanopyridine and 50 mM potassium phosphate buffer, pH 7.2.

The mixture was incubated in a 50°C water bath, with stirring at 150 rpm, for 5 min. Sample aliquots (1 mL) were drawn from the reaction mixture, 200 μ L of 3 M HCl added, the mixture was centrifuged and the supernatant was analyzed by HPLC as described in Section 3.2.2.8.

4.2.2.11 Characterisation of immobilized NHase biocatalysts

Following immobilization of the *G. pallidus* RAPc8 NHase on various support materials, it was necessary to identify the effects of the immobilization on the biochemical properties (this was done in comparison to the soluble enzyme). Throughout the study, Eupergit®C-immobilized plus EDAC crosslinked NHase was selected for further studies, since it had the highest immobilization efficiency. Details of the experimental procedures in the comparative study of the soluble and immobilized NHase are given below.

4.2.2.11.1 Estimation of the loading and immobilization efficiencies of immobilized NHase

The amount of protein bound to the carrier material was expressed in terms of percentage protein loading (total protein loading) after the immobilization was complete. The protein loading efficiency was calculated as:

$$\text{Loading efficiency \%} = \left(\frac{C_i V_i - C_f V_f}{C_i V_i} \right) \times 100 \quad (4.6)$$

where C_i (mg/mL) is the initial protein concentration, V_i (mL) the initial volume of protein solution, C_f (mg/mL) the protein concentration in total filtrate, and V_f (mL) the total volume of filtrate.

The amount of enzyme activity immobilized was determined by measuring the enzyme activity before and after the immobilization and expressed in terms of percent immobilization efficiency. The immobilization efficiency was calculated as:

$$\text{Immobilization efficiency} = \left(\frac{a_{\text{imm}}}{a_{\text{free}}} \right) \times 100 \quad (4.7)$$

where a_{imm} is specific activity of immobilized enzyme (U/mg protein) and a_{free} specific activity of soluble enzyme (U/mg protein).

4.2.2.11.2 Comparison of the effect of pH optima for the soluble and immobilized *G. pallidus* RAPc8 NHase

The effect of pH on the activity of the immobilized NHase were compared using 3-cyanopyridine as substrate. NHase activity was studied in the pH range of 4 to 12, using the following buffers: 0.05 M acetic acid/sodium acetate, pH (4 to 6), 0.05 M potassium phosphate pH (6 to 8), and 0.05 M Tris-HCl pH (8 to 10), and 0.05 M NaHPO₄-NaOH (pH 10 to 12). Immobilized NHase (0.14 mg protein, approximately 5.6×10^{-2} U) was added to 3.0 mL of 50 mM buffer of specified pH. The mixture was pre-incubated at 50°C for 1 min and 50 mM final concentration of 3-cyanopyridine was added, the reaction mixture incubated for a further 5 min. 1 sample was drawn from the reaction mixture, and reaction was stopped by addition of 200 μ L of 3 M HCl. The product formed was analyzed by HPLC, and the enzyme activity was calculated as described previously (Section 3.2.2.7). Relative activity was expressed as a percentage of the highest activity measured, which was at pH 7.

4.2.2.11.3 Comparison of the effect of temperature on soluble and immobilized NHase

To compare the optimum temperature on both the soluble and immobilized NHase activities, reactions were carried out at different temperatures (20, 40, 50, 60 and 70°C). Soluble or immobilized NHase (0.14 mg protein, approximately 5.6×10^{-2} U) was added to 3.0 mL of 50 mM phosphate buffer, pH 7.2 and the reaction mixture was then pre-incubated for 1 min at the desired temperature. 3-cyanopyridine was then added to give a final concentration of 50 mM and the reaction was further incubated for 5 min. 1 mL sample of reaction mixture were taken, and reaction terminated by adding 200 μ L of 3 M HCl. The product formed was analyzed by HPLC, and the enzyme activity was calculated as described previously (Section 3.2.2.7). Relative activity was expressed as a percentage of the highest activity measured, which was at 50°C.

4.2.2.11.4 Comparison of the effect of water-miscible and immiscible organic co-solvents on NHase activity

To compare the effect of biphasic organic/aqueous solvent systems on NHase activity, immobilized NHase (0.14 mg, approximately 5.6×10^{-2} U) were each added to 3.0 mL of 50 mM potassium phosphate buffer, pH 7.2 containing the specified organic solvent at 10 v/v %. The mixture was pre-incubated for 1 min and 3-cyanopyridine was then added to a final concentration of 50 mM and further incubated for 5 min. 1 mL sample of reaction mixture was taken and reaction terminated by adding 200 μ L of 3 M HCl. The product formed was analyzed by HPLC, and the enzyme activity was calculated as described previously (Section 3.2.2.7). The residual activity in the samples without organic solvent (only potassium phosphate buffer) was taken as 100 %.

4.2.2.11.5 Investigation thermostability of the Eupergit®C- immobilized NHase

Thermal stability was examined by pre-incubating immobilized NHase (containing 0.14 mg protein, 5.6×10^{-2} U) in 50 mM potassium phosphate buffer, pH 7.2 at 40°C, 50°C, 60°C, and 70°C for different times between 10 min and 2 h. Periodically, 100 μ L samples were taken, cooled and added to 3 mL of reaction mixture containing 50 mM of 3-cyanopyridine solution in 50 mM potassium phosphate buffer, pH 7.2. 1 mL sample of reaction mixture was taken and reaction terminated by adding 200 μ L of 3 M HCl. The product formed was analyzed by HPLC, and the enzyme activity was calculated as described previously (Section 3.2.2.7). Relative activity is expressed as percentage of the activity prior to incubation taken as 100 %.

4.2.2.11.6 Investigation of reusability and recycled use of the immobilized NHase

The operational stability of the immobilized NHase was measured by conducting repeated experiments with single batches of Eupergit®C-immobilized biocatalyst (5g, 1.88 U), at 50°C using 3-cyanopyridine. Reactions were maintained for 5 min with gentle stirring (150 rpm). After each cycle of 5 min, immobilized NHase was washed with 50 mM potassium phosphate buffer, pH 7.2 and resuspended into 50 mM potassium phosphate buffer. After each cycle, a 1 mL sample of reaction mixture was taken and the reaction terminated by adding 200 μ L of 3 M HCl. The product formed analyzed by HPLC, and the enzyme activity was calculated as

described previously (Section 3.2.2.7). Relative activity was expressed as percentage of the NHase activity on the first batch reaction, taken as 100 %.

4.2.2.11.7 Determination of the effect substrate concentration on the Eupergit®C- immobilized *G. pallidus* RAPc8 NHase

The effect of substrate concentration on activity of the Eupergit®C-immobilized (plus EDAC cross-linked) biocatalyst was measured using different concentrations of 3-cyanopyridine (5 to 500 mM) in 50mM potassium phosphate buffer (pH 7.2) incubated at 50°C for 5 min. 1 mL sample of reaction mixture was taken and reaction terminated by adding 200 μ L of 3 M HCl. The product formed analyzed by HPLC, and the enzyme activity was calculated as described previously (Section 3.2.2.7). Relative activity was expressed as percentage of the highest NHase activity, taken as 100%.

4.2.2.11.8 Kinetic analysis of immobilized *G. pallidus* RAPc8 NHase using 3-cyanopyridine as substrate

The kinetic constants, K_m and V_{max} of the Eupergit® C-immobilized NHase were determined at 50 °C using 3-cyanopyridine as substrate. The method was similar to that previously described in Section 3.2.2.9.9. Initial rate values, using a substrate concentration range 5 to 100 mM, were obtained over 5 min. 1 mL of sample was withdrawn from the reaction mixture every 30 sec and NHase activity was terminated by adding 200 μ L of 3 M HCl and the solution was immediately assayed for quantity of nicotinamide. The Michaelis-Menten constants K_m and V_{max} were calculated by using linear Hanes-Woolf plot, due to their high R-squared values (uniformity in error distribution).

4.2.2.11.9 Estimation of deactivation rate constant (k_d) and half-life time ($t_{1/2}$) for *G. pallidus* RAPc8 NHase

The deactivation parameters, namely, the thermal-decay constant (k_d), the half-life ($t_{1/2}$), and the activation energy of thermal inactivation (E_a), of the NHase from *G. pallidus* RAPc8 and its immobilized derivatives, were estimated by using data from thermal stability studies as described in Sections 3.3.5.6 and 4.3.5.4. The data were fitted to first-order plots and analyzed. The first-order rate constant (k_d) was determined by linear regression of $\ln(V)$ versus time of incubation

(*t*) (Sadana *et al.*, 1995). Half-life values were then calculated from values of thermal deactivation constants at different temperature using Equation 4.3. The activation energy (E_a) was estimated using Arrhenius equation Equation 4.5 for the temperature range of 40 to 70 °C. The value of E_a was determined from the slope of the plot of $\ln(k_d)$ versus $1/T$ (Lamb & Stuckey, 2000).

4.3 RESULTS AND DISCUSSION

An investigation into the immobilization of the *G. pallidus* RAPc8 NHase was conducted having in view the potential commercial viability of the NHase as a biocatalyst. Immobilization of the NHase on various supports was carried out first, in order to find the best immobilization support and technique, based on immobilization efficiency. It was appropriate also to test ways of stabilizing the quaternary structure of the heterotetrameric enzyme by using intersubunit cross linking bifunctional reagents (glutaraldehyde and EDAC). Details of the results are given below.

4.3.1 Immobilization by covalent bonding

The covalent binding of the NHase was carried out by incubating the support materials, including Eupergit® C, Eupergit® CM, Amberlite-XAD-4, ethylenediamino-activated Sepabeads (EC-EA), amino epoxy-activated Sepabeads (EC-HFA), epoxy-activated Sepabeads (EC-EP), and hexamethylenediamino-activated Sepabeads (EC-HA), with enzyme solution for periods between 48 and 96 hours as appropriate. All experiments were conducted at room temperature (since the NHase is known to be stable under these conditions), and results were expressed as loading and immobilization efficiency (%) (Section 4.2.2.11.1). The total protein loading efficiencies for all the immobilized NHases are shown in Figure 4.4. The best supports were hexamethylenediamino-activated Sepabeads (EC-HA), (total protein loading of 10 mg and loading efficiency, 100%), amino epoxy-activated Sepabeads (EC-HFA) (loading efficiency, 96.2%), ethylenediamino-activated Sepabeads (EC-EA) (loading efficiency, 91.5%) and Eupergit C (loading efficiency, 90.5%), respectively. The total protein loading for glutaraldehyde-activated Amberlite XAD-4 and EDA-activated Amberlite XAD-4 were lower than for all support materials tested, being 15.5% and 18.5 %, respectively. The explanation for this might

be that the Sepabead supports present long spacer arms which could afford increased accessibility for the NHase to bind.

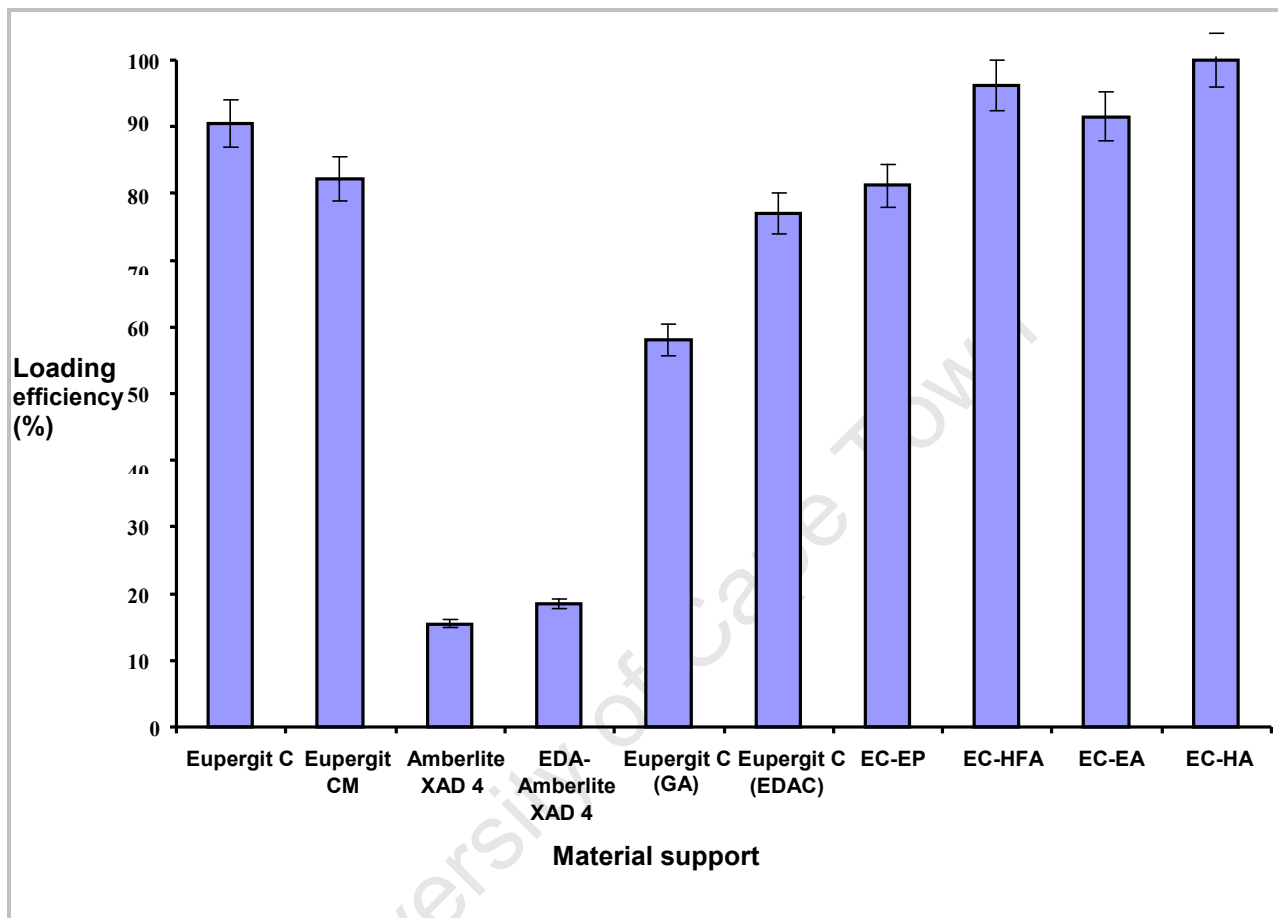


Figure 4. 4: Evaluation of loading efficiency of NHase protein on support carriers. Loading conditions: 20 mL NHase solution (10mg), 5 g support-carrier, room temperature for 72 – 96 hours. Loading efficiency expressed as percentage of amount of bound protein relative to the initial amount before immobilization (Section 4.2.2.11.1).

However, the total protein loading did not correlate with the immobilization efficiencies calculated based on the activity of the NHase. From the results of the immobilization efficiencies shown in Figure 4.5, it can be seen that Eupergit®C with EDAC cross-linking and Eupergit®C with glutaraldehyde were the best among the support materials tested, with immobilization efficiencies of 92.3 % and 83.4 % respectively, achieved with low enzyme loadings of 7.71 mg and 5.8 mg. The activation effect of coupling agents on Eupergit®C immobilized NHase resulted

in 1.7-fold and 1.5-fold increase in its immobilization efficiency from 53.1% (Fig. 4.5). The improved immobilization efficiencies for the biocatalysts might be due to the stronger stabilization of the interaction between subunits. The additional capacity for multi-point attachments introduced by cross-linkers led to increased conformational stability of the enzyme. EDAC is well known for its ability to cross-link through formation of amide between terminal carboxylic groups of Asp and Glu residues which are prominent in the NHase structure (Huang *et al.*, 1997). It has been shown that there is always a significant increase in the rigidity of the enzyme molecules by cross-linking, which would, consequently, reinforce interactions of the subunits and hence maintain catalytic activity of these enzymes (Betancor *et al.*, 2006; Mateo *et al.*, 2006). The glutaraldehyde and EDAC employed in this study, most likely, facilitated a similar cross-linking effect in the heterotetrameric structure of the NHase (Hernaiz *et al.*, 2000).

In covalently immobilized preparations without cross-linking, modest to appreciably better immobilization efficiency was observed: EDA-activated Amberlite XAD-4 (65.4 %), glutaraldehyde-activated Amberlite XAD-4 (53.5 %), and Eupergit[®] C (53.1 %), in spite of very low protein loading, particularly EDA-activated Amberlite XAD-4 and glutaraldehyde-activated Amberlite XAD-4 which had loadings 1.85 mg and 1.15 mg, respectively. Sepabead preparations gave very low immobilization efficiencies (30.1% to 24.6 %) under similar conditions, even though the total protein loading was high (81.2 to 100 %). The possible reason for low immobilization efficiencies at high protein loading in Sepabeads (EC series) may be close packing of enzyme on the support surface, which might limit the access of the substrate molecules.

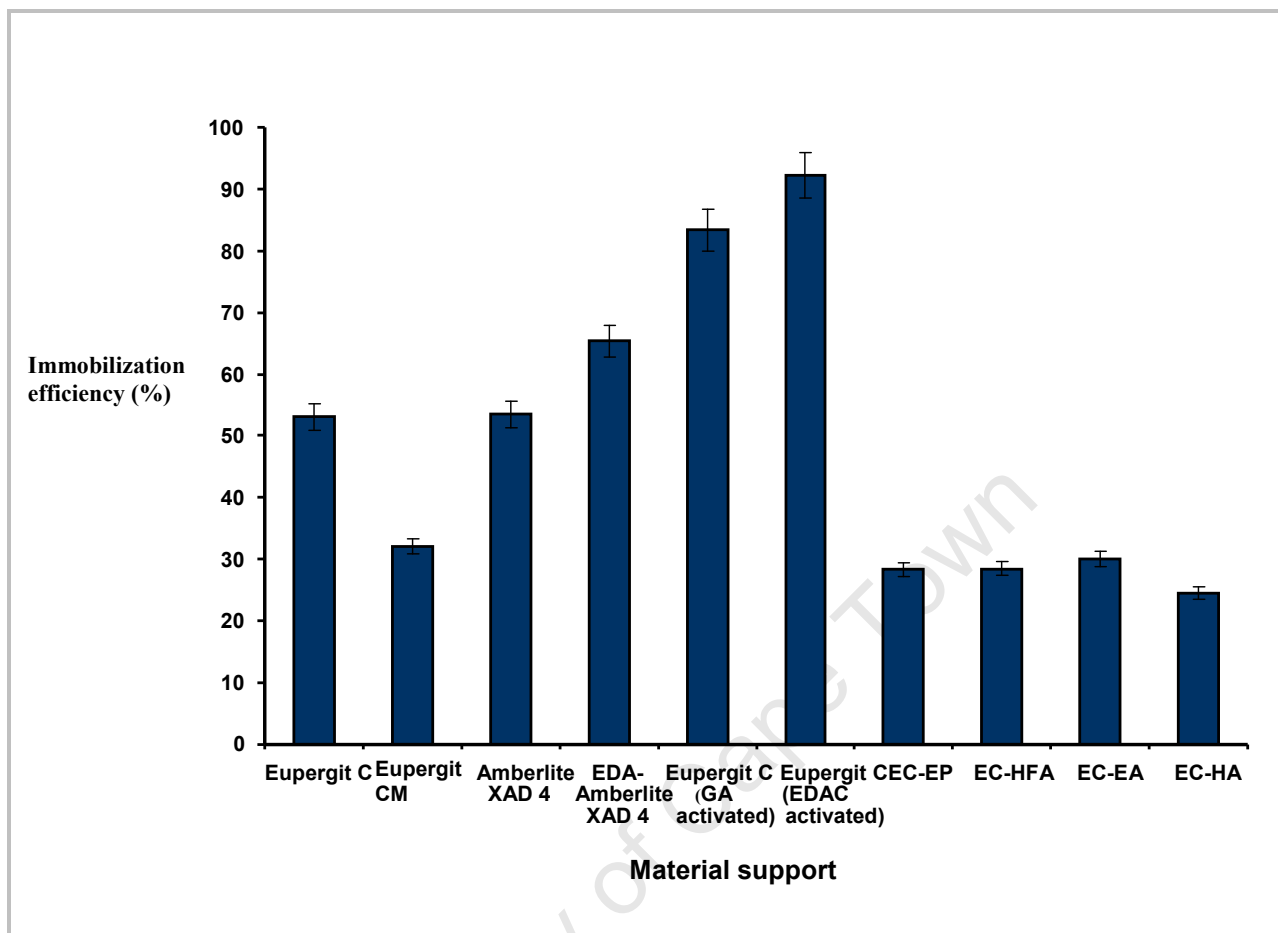


Figure 4. 5: Evaluation of the immobilization efficiency of NHase on support carriers. Immobilization conditions: 20 mL NHase solution (10 mg protein, 21.3 U), 5 g support material, room temperature for 72 – 96 hours. Immobilization efficiency expressed as percentage of specific activity of immobilized NHase to initial specific activity before immobilization (Section 4.2.2.11.1).

4.3.2 Immobilization of NHase by ionic binding

The ionic adsorption of NHase was achieved by initial equilibration of four ion exchange resins, two cationic resins (Super-Q-Toyopearl and SE-Sephadex) and two anionic resins (Dowex[®] and DEAE-Sephadex A 50) at pH 7.2. Enzyme solution was then mixed with each of the resins, the mixtures were incubated for 2 h, to allow the enzyme to reversibly displace the counter-ions and thereby to achieve ionic binding. Except for the DEAE-Sephadex C 50 support, (loading efficiency 35.2%), the other supports demonstrated high total protein loading efficiencies of 95.2

%, 73.6 % and 72.2 % for Super-Q-Toyopearl, Dowex[®] and SE-Sephadex C 50, respectively (Fig. 4.6).

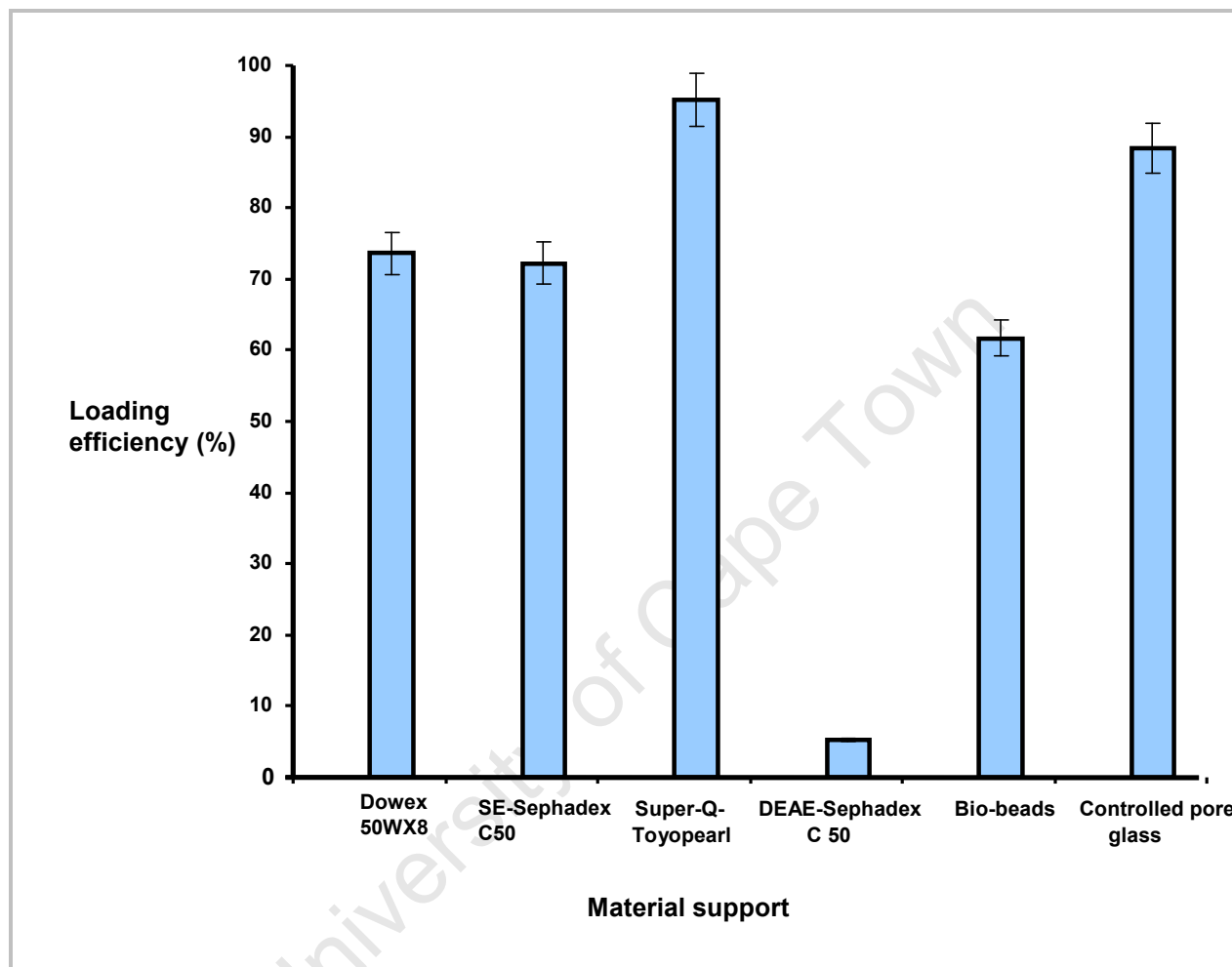


Figure 4. 6: Evaluation of the loading efficiency of NHase protein on ion exchange support carriers. Loading conditions: 20 mL NHase solution (10mg protein), 5 g support-carrier, room temperature for 72 – 96 h, and pH 7.2. Loading efficiency expressed as percentage of amount of bound protein to the initial amount before immobilization (Section 4.2.2.11.1).

Fig. 4.7 shows the results of the immobilization efficiencies of each biocatalyst. DEAE-Sephadex-A-50 and SE-Sephadex-A-50 exhibited rather modest adsorptive properties of 47.2 % and 42.8 %, respectively. Dowex[®] and Super-Q-Toyopearl gave relatively low immobilization efficiencies of 36.9 % and 20.9 %, respectively. Factors that might have affected the immobilization of NHase would include the ability of the protein to replace the exchangeable

counter-ions of the resins, the support materials having highly substituted surfaces and repulsive electrostatic interaction due to similar charges. Of these factors only the repulsion of similar charges would be likely to result in such low immobilization efficiency. The observation that the NHase surface and ionic exchange resin may contain similar charges, would suggest the strength of the electrostatic effects such as positive-to-positive repulsion or negative-to-negative charge may be the factor that control the ultimate immobilization. This would depend at least partially on the pI of the enzyme which should be determined in future studies.

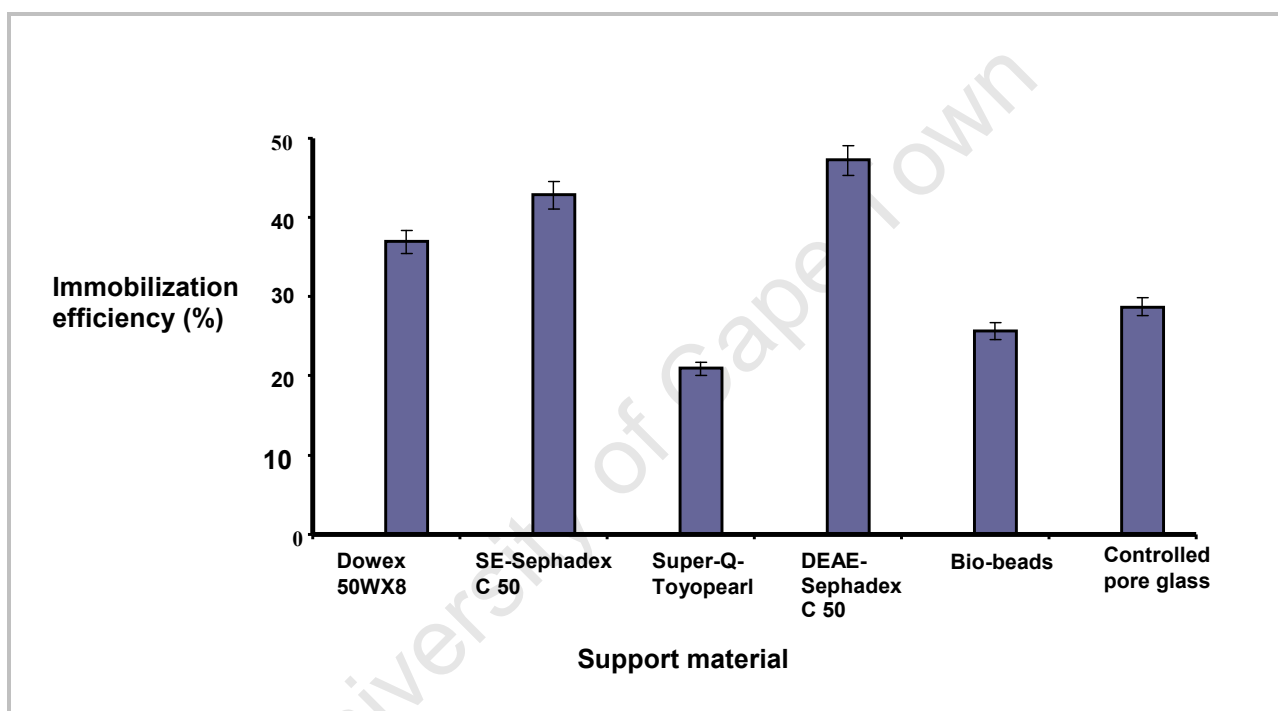


Figure 4. 7: Evaluation of the immobilization efficiency of NHase on ion exchange carriers. Immobilization conditions: 20 mL NHase solution (10mg protein), 5 g support-carrier, room temperature for 72 – 96 hours. Immobilization efficiency expressed as percentage of specific activity of immobilized NHase to initial specific activity before immobilization (Section 4.2.2.11.1).

4.3.3 Immobilization of NHase by metal chelation

Immobilization of NHase by metal chelation was carried out by treating iminodiacetic-activated Sepabeads (EC-IDA) with 0.5 M metal solutions (Ag^{2+} , Zn^{2+} , Cu^{2+} and Co^{2+} solutions) for 2-3 h and equilibration at pH 7.2. The activated carriers were then incubated with NHase solution for 48 h. The results of total protein loading of the various metal ion-activated iminodiacetic

Sepabeads (EC-IDA) are shown in Fig. 4.8. Except for iminodiacetic-activated Sepabeads (EC-IDA)-Co²⁺, the others demonstrated relatively high protein loading efficiencies: Sepabeads EC-IDA-Ag, (loading efficiency, 80 %), Sepabeads (EC-IDA)-Zn, (loading efficiency, 76%), and Sepabeads (EC-IDA)-Cu, (loading efficiency, 86 %), respectively when 10 mg of NHase was added. These results may be explained in terms of the principles of binding of proteins to metal ions. In this regard, proteins bind to metal ions based on their interaction between an electron-donating ligands on the protein surface and a metal ion (Sosnitza *et al.*, 1998). Thus, this tendency might be responsible for the high protein loading the *G. pallidus* RAPc8 NHase.

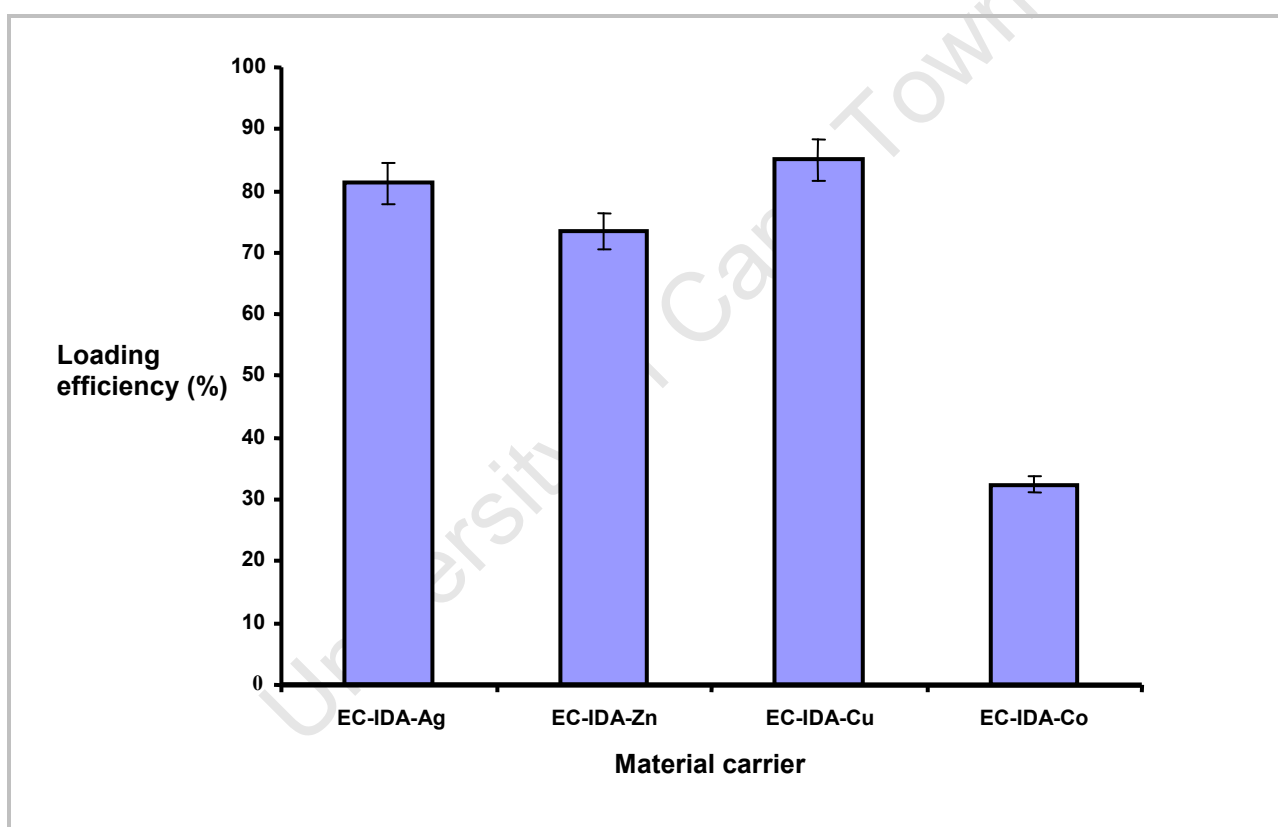


Figure 4. 8: Evaluation of the loading efficiency of NHase protein on metal chelating carriers. Loading conditions: 20 mL NHase solution (10mg protein), 5 g support-carrier, room temperature for 72 – 96 hours. Loading efficiency expressed as the percentage of amount of bound protein to the initial amount before immobilization (Section 4.2.2.11.1).

The immobilization efficiency results for immobilization of *G. pallidus* RAPc8 NHase on metal ion-activated Sepabeads are shown in Fig. 4.9. The four iminodiacetic-activated Sepabeads

(EC-IDA) containing metal ions Ag^{2+} , Co^{2+} , Zn^{2+} and Cu^{2+} were poor carriers for the NHase. Their remarkably low chelation capacity with NHase is shown by the immobilization efficiencies of 34.6 %, 32.0 %, 24.8 % and 24 %, respectively (Fig. 4.9). The low efficiency of immobilized NHase observed here may be attributed to transformation of essential active site amino acid residues including cysteine; because the cysteine residue in NHase is essential for substrate recognition and binding (Huang *et al.*, 1997), any metal-binding to it may subject it to unique modifications (such as oxidation) with deleterious consequences such loss of enzymatic activity (Cramp *et al.*, 1997).

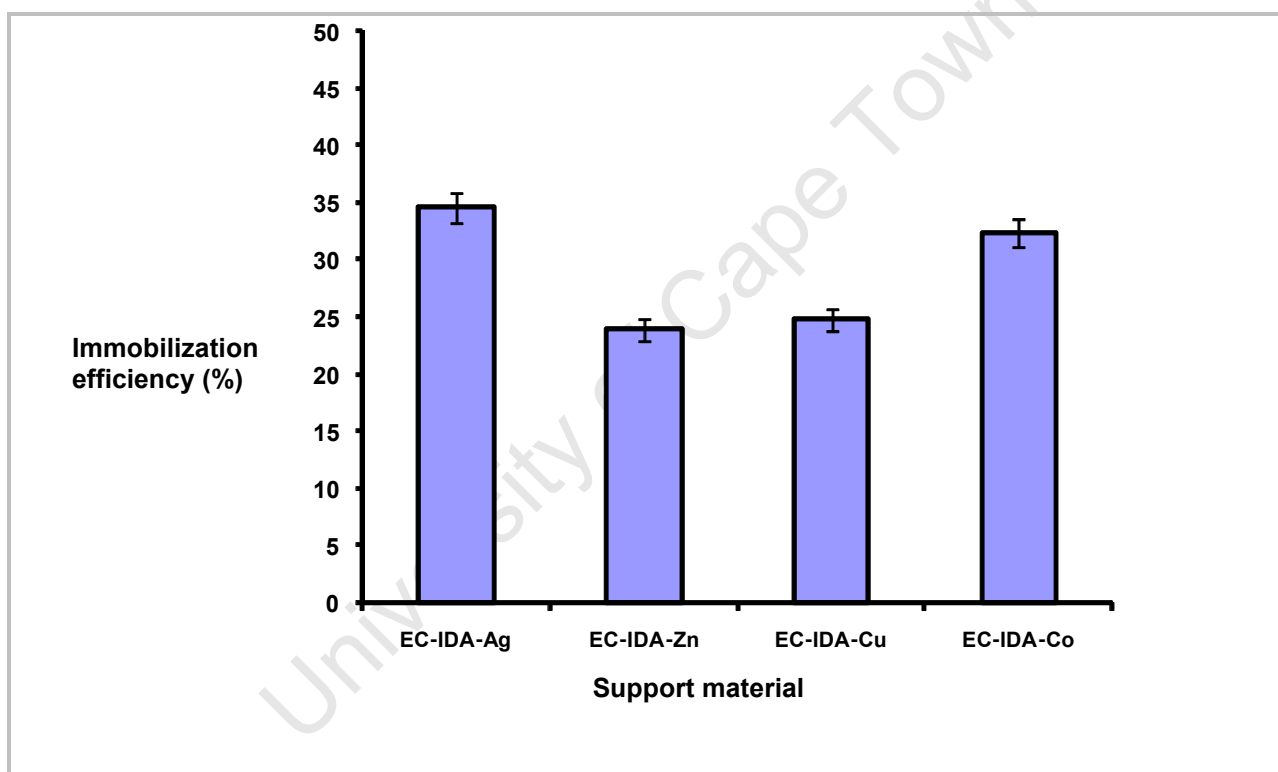


Figure 4. 9: Evaluation of the immobilization efficiency of NHase on metal chelating carriers. Loading conditions: 20 mL NHase solution (10mg protein), 5 g support-carrier, room temperature for 72 – 96 hours. Immobilization efficiency expressed as the percentage of specific activity of immobilized NHase to initial specific activity before immobilization (Section 4.2.2.11.1).

4.3.4 Alginate entrapment of *G. pallidus* RAPc8 NHase

Immobilization of *G. pallidus* RAPc8 NHase in Ca-alginate was investigated by using varying ratios of sodium alginate-to-enzyme concentration. Fig. 4.10 shows the protein loading efficiency values obtained using the varying concentrations of sodium alginate. The maximum loading capacity of (95.8%) was observed with 4 % alginate solution suggesting that the higher concentration of sodium alginate assisted in cross-linking between alginate and Ca^{2+} ions leading to better loading of the enzyme. The enzyme activity of immobilized NHase was not determined because the biocatalyst was found to be damaged at temperatures above 40 °C in the reaction mixture. It has been found that coating the surface of Ca-alginate gel beads with chitosan or silicate can improve the stability of alginate beads (Won *et al.*, 2005). However, coating alginate gel beads was not attempted in this study due to reported morphology changes that occur to the beads and the additional cost of coating materials, since one of the aims of the study was to find the most economical immobilization method.

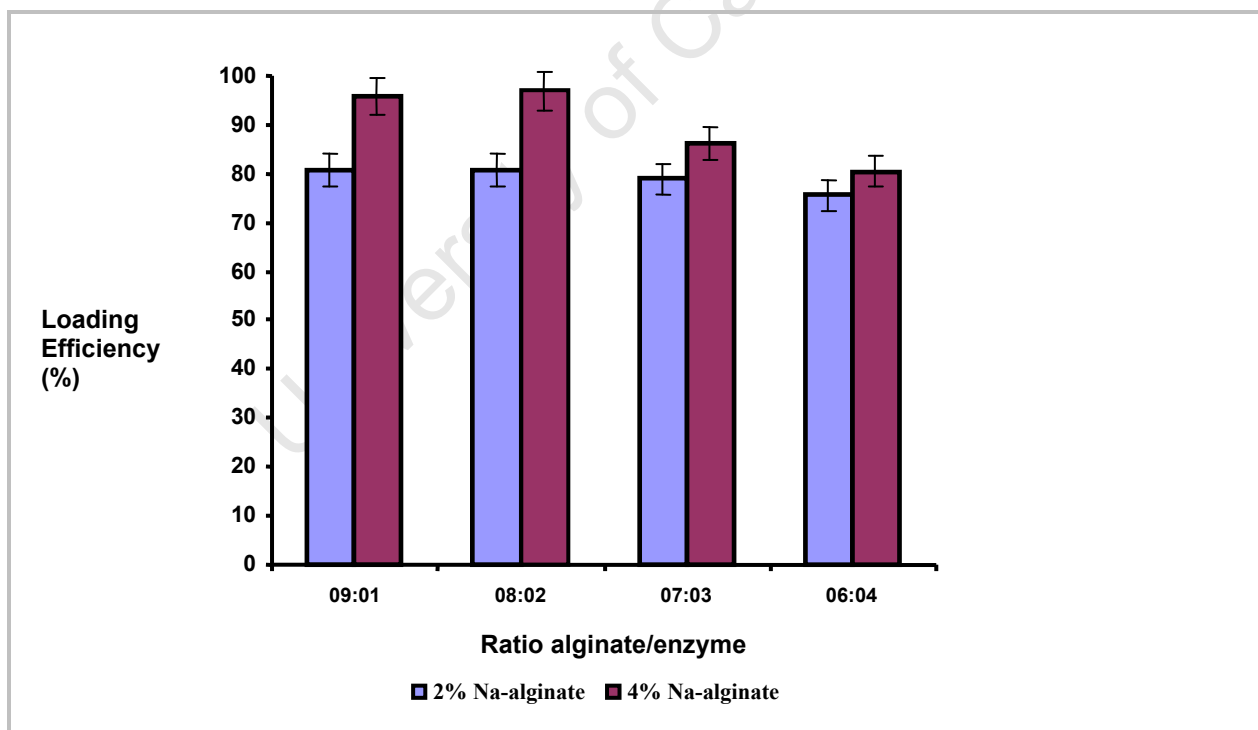


Figure 4.10: Evaluation of the loading efficiency of NHase protein in Ca-alginate. Loading conditions: 20 mL NHase solution (10mg protein), 5 g support-carrier, room temperature for 72 – 96 hours. Loading efficiency expressed as the percentage of amount of bound protein to the initial amount before immobilization.

To date, no reports of immobilization of NHases in their purified form have been published. However, the immobilization of a semi-purified NHase from *Rhodococcus erythropolis* A4 in CLEAs has been described (Kubáč *et al.*, 2008). In the present study, immobilization by particularly covalent of NHases was found to be an effective method of immobilization of *G. pallidus* RAPc8. The ability of *G. pallidus* RAPc8 NHase to retain activity up to 93 % was a novel result, since no other report have been made on covalent immobilization. A summary of the loading and immobilization efficiencies for all supports tested is given in Table 4.1.

University of Cape Town

Table 4. 1: A summary of loading and immobilization efficiencies of *G. pallidus* RAPc8 NHase * Not determined

Support	Technique	Protein loading mg/support (g)	Loading ^a efficiency (%)	Immobilization ^b efficiency (%)
Eupergit® C (EDAC)	Covalent	7.7	77.1	92.3
Eupergit® C (GA)	Covalent	5.8	58	83.4
EDA-Amberlite XAD 4	Covalent	1.8	18.5	65.4
GA-Amberlite XAD 4	Covalent	1.6	15.5	53.5
Eupergit® C	Covalent	9.1	90.5	53.1
DEAE-Sephadex A 50	Anionic	3.5	35.2	47.2
SE-Sephadex A 50	Cationic	7.2	72.2	42.8
Eupergit® CM	Covalent	8.2	82.3	32.1
Dowex® 50WX8	Cationic	7.4	73.6	36.9
Sepabeads EC-IDA-Ag	Metal chelation	8.1	81.2	34.6
Sepabeads EC-IDA-Co	Metal chelation	3.3	32.5	32.4
Sepabeads EC-EA	Covalent	9.2	91.5	30.1
Controlled pore glass	Simple adsorption	8.8	88.4	28.7
Sepabeads EC-HFA	Covalent	9.6	96.2	28.5
Sepabeads EC-EP	Covalent	8.1	81.2	28.4
Bio-beads	Simple adsorption	6.2	61.7	25.6
Sepabeads EC-IDA-Cu	Metal chelation	8.5	85	24.8
SepabeadsEC-HA	Covalent	10	100	24.6
Sepabeads EC-IDA-Zn	Metal chelation	7.3	73.2	24
Super-Q-Toyopearl	Anionic	9.5	95.2	20.9
4 % sodium alginate	Entrapment	9.6	95.8	nd*
2 % Sodium alginate	Entrapment	8.1	80.8	nd

^a Loading efficiency (%) = $\left(\frac{C_i V_i - C_f V_f}{C_i V_i} \right) \times 100$ where C_i is the initial protein concentration, V_i the initial volume of protein solution, C_f the protein concentration in total filtrate, and V_f the total volume of filtrate.

^b Immobilization efficiency (%) = $\left(\frac{a_{\text{imm}}}{a_{\text{free}}} \right) \times 100$ where a_{imm} is specific activity of immobilized enzyme (U/mg protein) and free specific activity of free enzyme (U/mg protein).

4.3.5 Optimization of conditions for biocatalytic hydration of 3-cyanopyridine by immobilized *G. pallidus* RAPc8 NHase

Based on the percentage immobilization efficiency as a criterion for efficient biocatalyst activity, the biocatalyst produced using Eupergit®C to immobilize the NHase, cross-linked with EDAC, was selected as the best biocatalyst (See Table 4.1) and this was subjected to further investigations. The objective was to identify and assess the functional and catalytic capacity of the newly developed biocatalyst, particularly in its role in bioconversion of 3-cyanopyridine to nicotinamide. All activity parameters were compared with those of the soluble NHase and investigations were carried out in batch reactions in aqueous medium, unless stated otherwise.

4.3.5.1 Comparison of effects of pH on activity of the soluble and immobilized NHase

The effects of pH on the activities of soluble and immobilized *G. pallidus* RAPc8 NHase were compared by conducting experiments at different pH values (4.11) using different buffers. The immobilized NHase showed an optimum pH of 7.0 similar to that of the soluble NHase, but the immobilized NHase exhibited a broadening of pH-activity peak as compared with that of the soluble NHase in the alkaline regions (Fig. 4.11). In the range of pH 7 to 9, the relative activity of the immobilized NHase was much higher than that of the soluble NHase, especially at pH 8, while that of the soluble NHase was low. This pattern was also observed in the range of pH 9 to 12, where the relative activity of the immobilized NHase was again higher. There have been reports suggesting the occurrence of both a shift of optimal pH (Hernaiz *et al.*, 2000) and broadening of the pH-activity (Martin *et al.*, 2003; Li *et al.*, 2007) when Eupergit®C is employed in enzyme immobilization. The latter was observed in this study and could have been due to the effect of the Eupergit®C support which presumably influenced the NHase activity in one or more of three possible ways: induced conformational changes in the NHase, enhanced enzyme /substrate binding affinity, or improved stability of the enzyme in subunit association. On the other hand, immobilization could also have influenced the microenvironment surrounding the NHase, making the pH higher than in the bulk solution than in the biocatalyst (Pajić-Lijaković *et al.*, 2007).

The results of this investigation indicated that the broadening of the apparent pH peak for the immobilized NHase would be advantageous for an industrial process. Normally, enzymes that are able to operate over a wider range of conditions have the robust biocatalyst nature that can withstand the demands of industrial processes. At the same time, the apparent pH of the immobilized NHase was still around physiological pH (pH 7.0), which would allow for hydration of nitriles without complications and is useful for productivity.

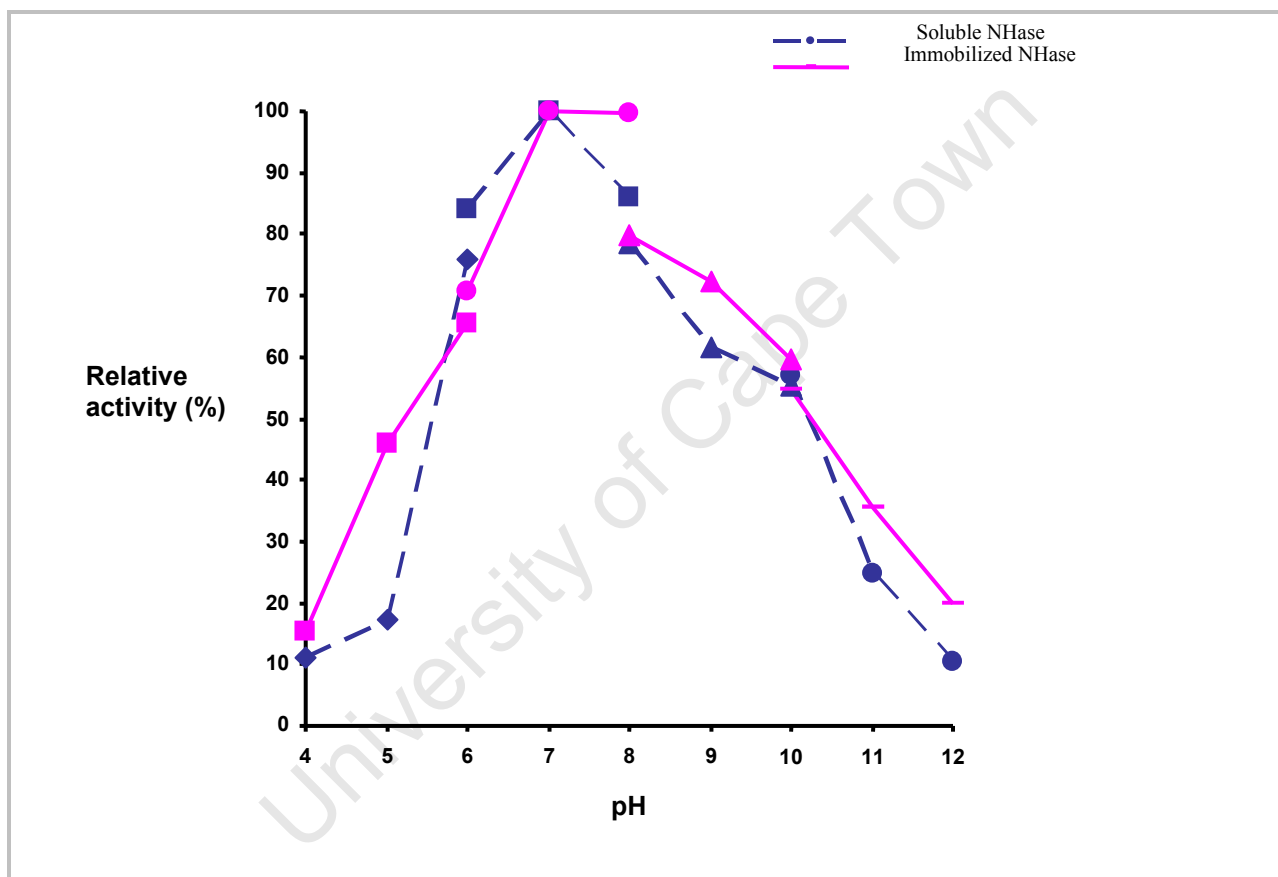


Figure 4. 11: Comparison of the dependence of the hydrolytic activity of the soluble and immobilized NHase on pH. Acetic acid-sodium acetate buffer (pH 4 to 6), potassium phosphate buffer (pH 6 to 8), Tris-HCl buffer (pH 8 to 10), and NaHPO₄-NaOH buffer (pH 10 to 12). Relative activity was expressed as a percentage of the highest activity measured, at pH 7.

4.3.5.2 Comparison of the effects of temperature on activity of the soluble and immobilized NHase

The effect of temperature on the activity of the soluble and Eupergit® C immobilized NHase was investigated in 50 mM phosphate buffer at pH 7.2, in the temperature range of 20 to 70°C. At each temperature, a 3 mL reaction mixture was incubated with 0.14 mg soluble or immobilized NHase for 5 min. The temperature profiles for both biocatalysts are shown in Fig.4.12. The maximum temperature of enzyme activity for both the soluble and the immobilized enzyme was at 60 °C, comparing very well with the optimum growth temperature of the native microorganism (Pereira *et al.*, 1998). In terms of the maximum temperature range, the immobilized biocatalyst had a broader peak (40 to 70°C) than for the soluble enzyme. Particularly, at 50°C, the relative activity value of the immobilized NHase was 98 %, while that of the soluble NHase was only 94 %. Similarly, at 70 °C the relative activity of immobilized NHase 80 %, when for the soluble NHase was observed at 64 %. The results indicate that the immobilized NHase had higher heat tolerance than that of the soluble enzyme. The increased temperature range may arise from stabilization of the conformational structure of the NHase upon covalent binding of enzyme to Eupergit® C, *via* amino groups coupled with EDAC cross-linking.

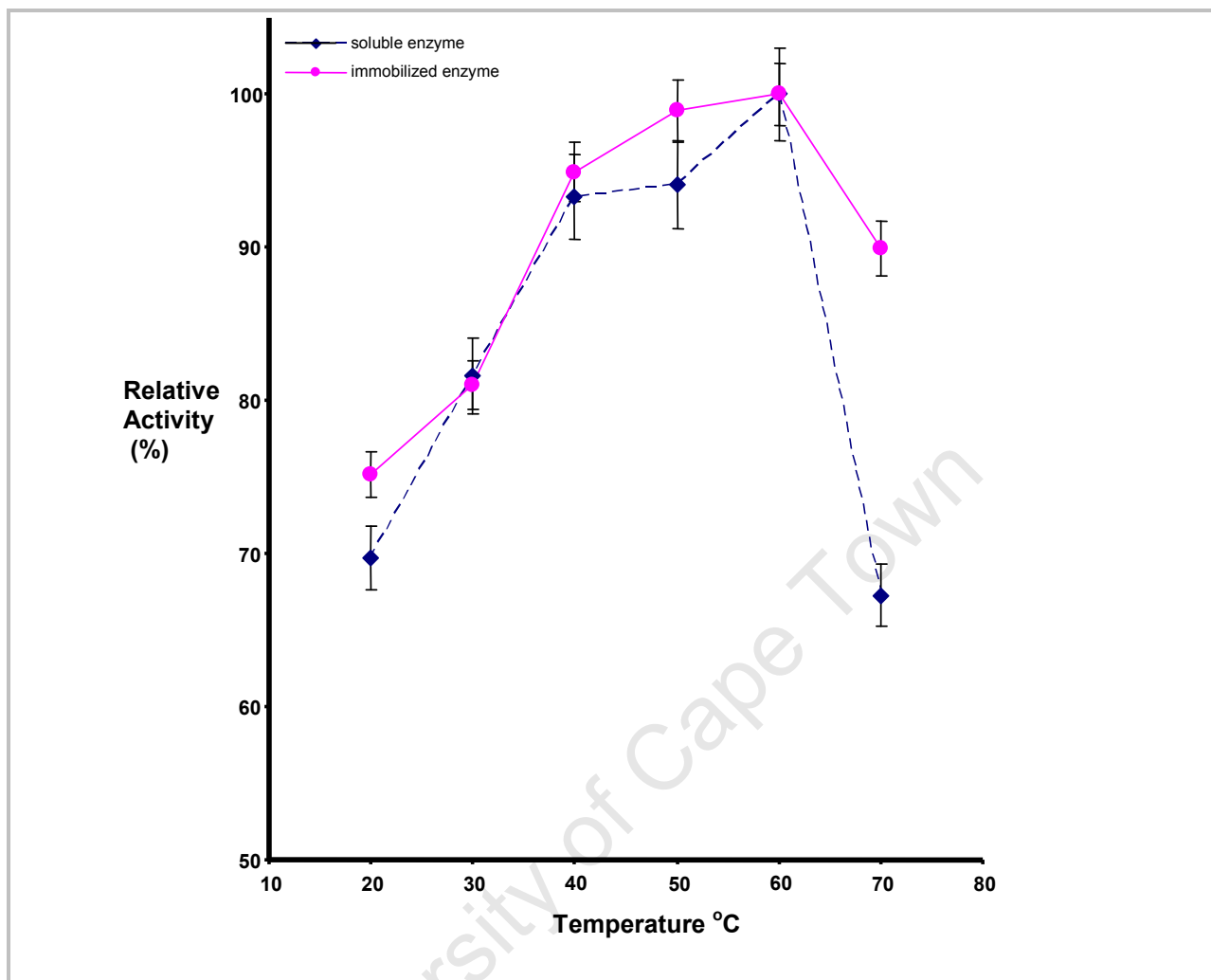


Figure 4.12: Comparison of temperature dependence of the activity of the soluble and immobilized NHase at pH 7.2. Reaction was carried out at different temperatures in 50 mM potassium phosphate buffer, for 5 min. Relative activity was calculated at the temperature at which the enzyme showed maximum activity (60 °C) , taken as 100 %.

4.3.5.3 Effect of 10 % (v/v) organic co-solvent systems on the immobilized *G. pallidus* RAPc8 NHase activity

4.3.5.3.1 Comparison of the soluble and immobilized NHase activity in presence of water-miscible and immiscible cosolvents

There has been important progress, in the recent years, towards understanding the correlation between enzyme thermal stability and resistance to denaturation by organic solvents (Owusu *et al.*, 1989; Klibanov, 2001). A wide variety of processes utilise enzymes in the presence of organic solvents (either miscible or immiscible) which have facilitated the solubility of reaction substrates or products, altered the specificity of an enzyme, or improved the activity of the overall enzyme (Serdakowski *et al.*, 2008). Further, one of the interesting properties of enzymes in anhydrous organic solvents is that they have a 'pH memory' (their catalytic activity reflects the pH of the last aqueous solution to which they were exposed) (Zaks & Klibanov, 1985; Zaks & Klibanov, 1988). Nonetheless, in some cases the activity of the enzymes has been compromised by organic solvents with high hydrophobicity (Klibanov, 1997).

In this study the role of immobilization of NHase on Eupergit[®]C, coupled with EDAC cross-linking, was studied in relation to the influence of a range of water-miscible (methanol, ethanol, propanol, ammonia, formaldehyde, acetone, 1,4-dioxane and tetrahydrofuran) and immiscible (ethyl acetate, dichloromethane, chloroform, benzene, toluene, cyclohexane and n-hexane) organic solvents. While media containing low and high percentages of cosolvents have been previously reported involving nitrile-converting microbes, this study focused on using the isolated enzyme with 10% organic solvent/potassium phosphate buffer mixture.

Immobilized NHase was incubated for 5 min in different organic/aqueous cosolvent systems at 50°C, pH 7.2, using 3-cyanopyridine as substrate. Table 4.2 shows the effect of selected solvents of varying hydrophobicity (shown as *log P*, where *P* is the partition coefficient between water and n-octanol) on the catalytic activity of *G. pallidus* RAPc8 NHase. The results obtained using Eupergit[®]C-immobilized NHase showed a marked difference from those obtained in soluble enzyme, under identical experimental conditions. Generally, the relative activities were higher than observed for the free enzyme, except for reactions in formaldehyde and propanol in which activity was much lower with relative activity % values of 56 % and 55.8 %, respectively. The highest enhanced effect was observed in the case of ethyl acetate, where the relative activity was

132 %, followed by acetone (106.0 %) and methanol (104.5 %) which is rather unexpected as methanol and acetone possess rapid inactivation effects on enzymes (Laane *et al.*, 1987). The activities in the presence of 1, 4-dioxane, ethanol, tetrahydrofuran, toluene and cyclohexane were slightly above 100 % relative to the NHase activity in potassium phosphate buffer. The relative activities in the presence of dichloromethane (97.9 %), chloroform (92.6 %), benzene (94.6 %), and n-hexane (98.3 %) were high probably due to their marginal stability effects on many enzymes reported previously (Laane *et al.*, 1987).

These results provide an excellent illustration of the contribution of an immobilization matrix to minimizing the adverse influence of organic solvents on protein structure. The mechanism underlying this resistance, especially to the more polar organic solvents (methanol, ethanol and acetone) may arise from resistance to unfolding of the cross-linked multimeric structure of the *G. pallidus* RAPc8 NHase and avoidance of disruption of critical active site water residues (Klibanov *et al.*, 1989). Thus, the immobilization process could have retained water in the microenvironment of NHase biocatalyst essential of the initiation of hydration by its nucleophilic attack on the nitrile carbon (Huang *et al.*, 1997). The ability of immobilized *G. pallidus* RAPc8 NHase to function in the presence of a range of mono- and bi-phasic aqueous/organic solvent systems would offer new opportunities to explore a wide range of nitrile substrates with varying properties, thus widening the spectrum of commercial amide products. It is worthy to note that this results have not been reported previously in literature and will be hopely published in the due course.

Table 4.2: Comparison of the influence of 10 % (v/v) organic solvent on the soluble NHase and Eupergit®C-immobilized NHase activity. The NHase activity is expressed in relative activity (%) taking the activity in potassium phosphate buffer as 100 %.

	Soluble Nhase	Immobilized NHase
Phosphate buffer	100.00	100.00
n-Hexane(3.5)	94.09	98.34
Cyclo hexane(3.2)	94.45	101.42
Toluene (2.5)	103.29	102.17
Benzene (2)	112.77	94.02
Chloroform (2)	74.01	92.63
Dichloromethane (1.25)	80.91	97.91
Ethyl acetate (0.71)	106.11	132.03
Tetrahydrofuran (0.53)	46.37	101.29
Propanol (0.34)	93.49	55.80
Acetone (-0.21)	39.92	106.66
Ethanol (-0.24)	58.04	102.74
1,4-Dioxane(-0.27)	79.35	101.09
Methanol (-0.76)	69.91	104.47
Formaldehyde (-1)	20.02	56.30

4.3.5.3.2 Effect of log P value of solvents on NHase activity

The effect of presence of different organic solvents on the NHase hydration reactions was also investigated in terms of *log P* values. It is worthy noting that most solvents are best described by their *log P* values which have direct influence on enzyme activity (Learne *et al.*, 1987). The effect of *log P* on the relative NHase activities of the soluble and immobilized enzyme is shown in Fig. 4.13. The relative activities of immobilized NHase were considerably higher at all the *log P* values tested than that for the soluble enzyme, but were highest (132%) at the *log P* 0.5. The question of the precise role of immobilization in the biocatalysis reaction in organic solvents remains. Neither a satisfactory explanation nor reproducibility of the results was investigated further in this study. However, it can be concluded that the use of immobilized NHase in nitrile hydration has the advantages that the process can be performed under a range of organic solvents

with varying log P values, thus broadening the number substrates and subsequently amide products. The many of enzymes in the literature have been reported to be active only at higher log P value (Learne *et al.*, 1987).

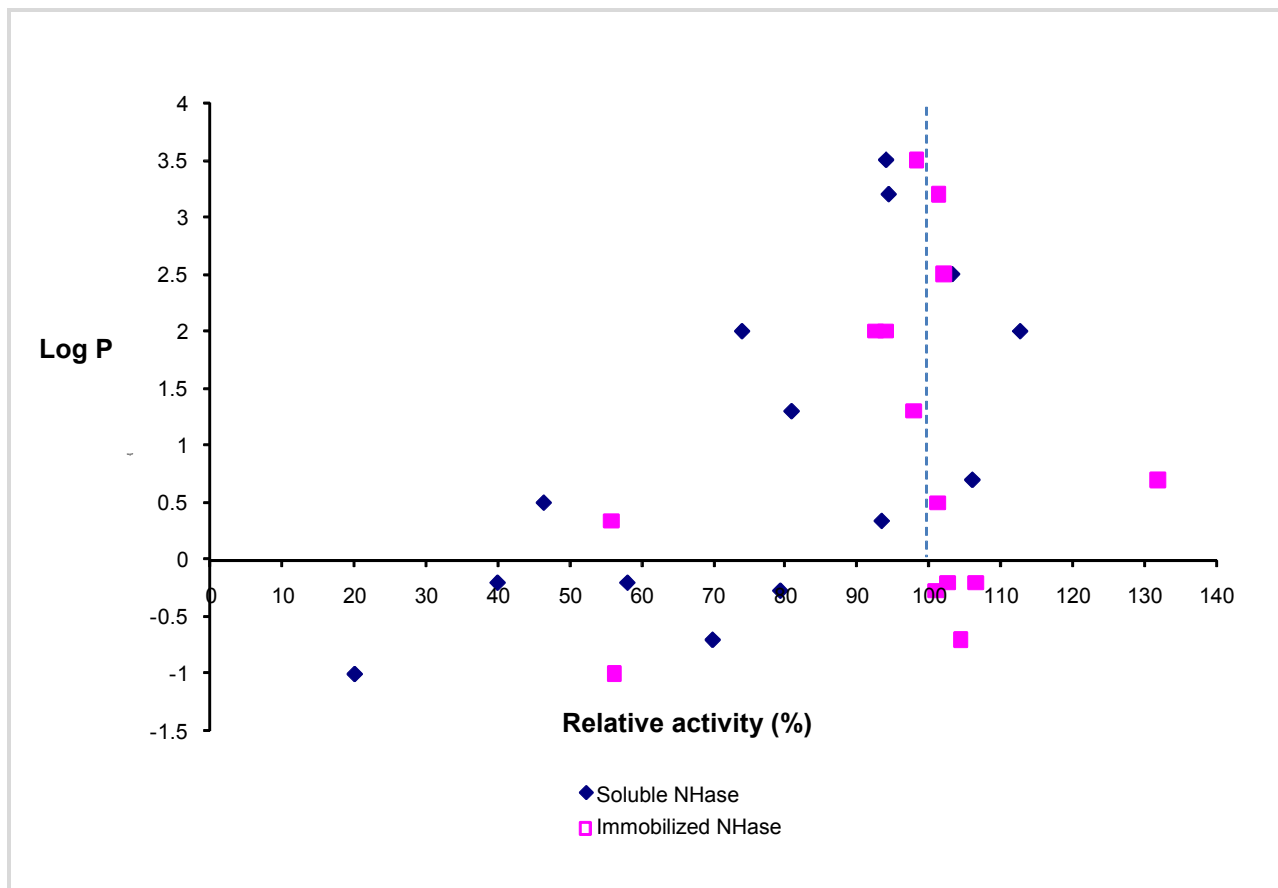


Fig. 4.13 Comparison of log P values for organic solvents with the relative activities of the soluble and immobilized NHase. The relative activity for the reaction without organic solvent (potassium phosphate buffer only), was taken as 100%.

4.3.5.4 Evaluation of the thermal stability of the immobilized *G. pallidus* RAPc8 NHase

The thermal destabilization of the immobilized NHase was quantitatively analyzed and compared with that of the soluble NHase in the temperature range of 40 to 70°C in 50 mM potassium phosphate buffer, pH 7.2. The biocatalysts were incubated at these temperatures for varying time intervals and then assayed for activity. The experiments showed that the immobilized enzyme were thermally stable at temperature range 40 °C to 60°C for at least 80 min of incubation (Fig. 4.14). These results show that the immobilized NHase was superior, in terms of resistance against elevated temperatures, over the soluble NHase (Section 3.3.5.6). Since the immobilized NHase could retain up to 80% of initial activity at 60°C for 80 min, this means that immobilization resulted in expanded range of operating conditions, which is important for industrial applications of the enzyme, providing a number of possible process advantages such as: reduced risks of microbial contamination, decreased viscosity, improved conversion rates and improved substrate solubility (Bruins *et al.*, 2004; Luckarift *et al.*, 2004). Thermostability studies of Eupergit®C-immobilized NHase have not been reported previously; therefore, these results are novel.

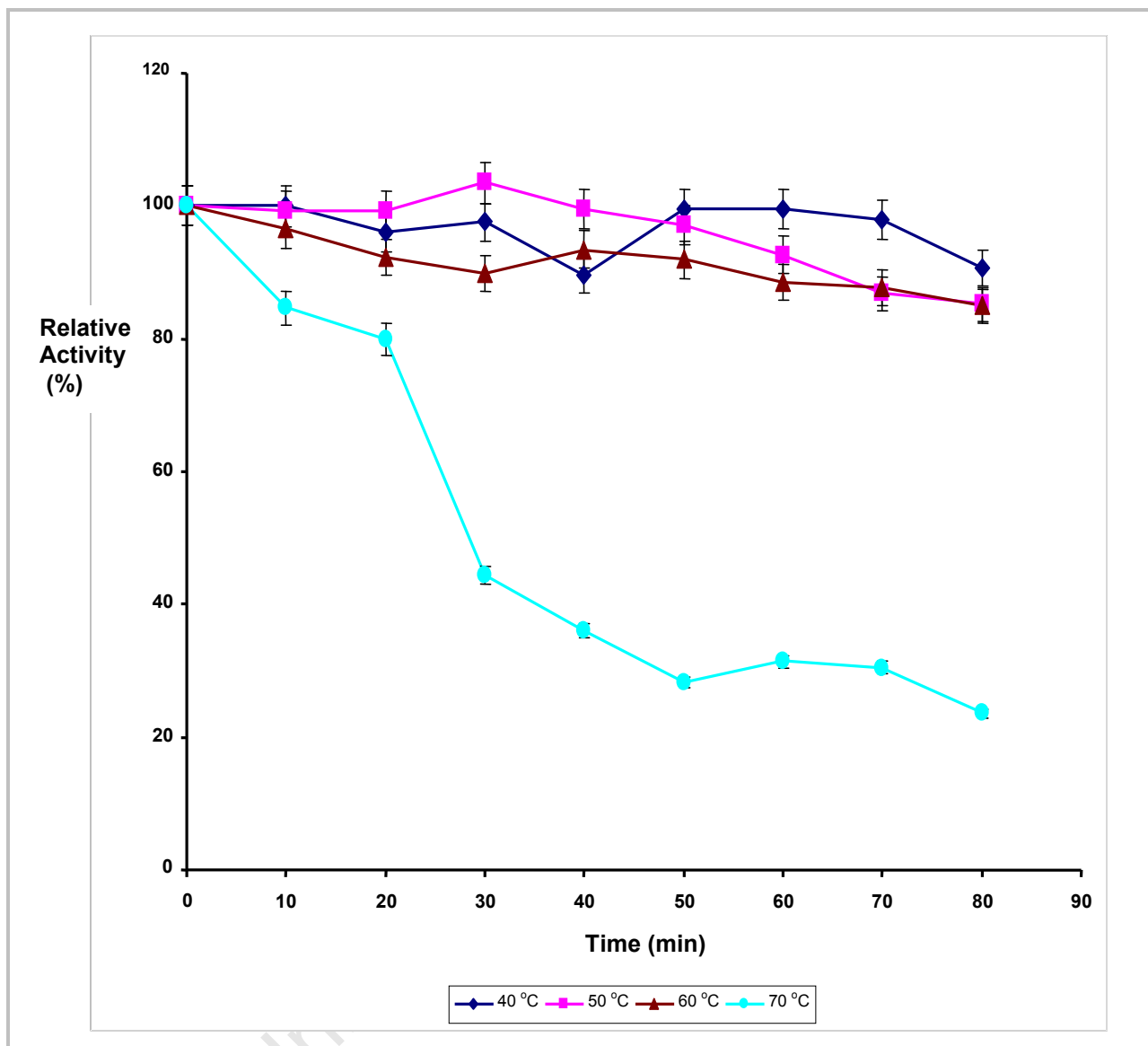


Figure 4.14: Evaluation of thermal stability of Eupergit® C immobilized NHase. The enzyme was assayed at temperatures 40 °C, 50 °C, 60 °C and 70 °C in 50 mM potassium phosphate buffer, pH 7.2 for 80 min. At time intervals of 10 min, aliquots were withdrawn and NHase activity assayed. Relative activity was calculated taking initial activity (time = 0) as 100 %.

4.3.5.5 Investigation of the reusability or recycled use of the Eupergit®C-immobilised NHase

The potential for recycling of the biocatalyst was investigated by conducting repeated reactions with the same batch of biocatalyst under consistent conditions of 50 mM phosphate buffer, pH

7.2 at 50°C. Results are shown for eight cycles, during which time the immobilized NHase activity decreased by 3.3 % and 13.8%, based on the initial activity, in the second and third cycles, respectively (Fig. 4.15). The residual activity, thereafter, remained at 85% of the original, after the eight cycles. The results indicate that the NHase immobilized on Eupergit®C was still active, and thus had excellent activity retention, under the operating conditions, suggesting that immobilization of the *G. pallidus* RAPc8 NHase significantly enhanced its stability. The ability to retain enzyme activity after reuse would provide a number of process advantages such as continuous operation in a packed-bed reactor or continuous stirred tank reactor. Moreover, these important results are the first to be achieved using known NHases, and are anticipated to lead to their application in new areas of nitrile conversions.

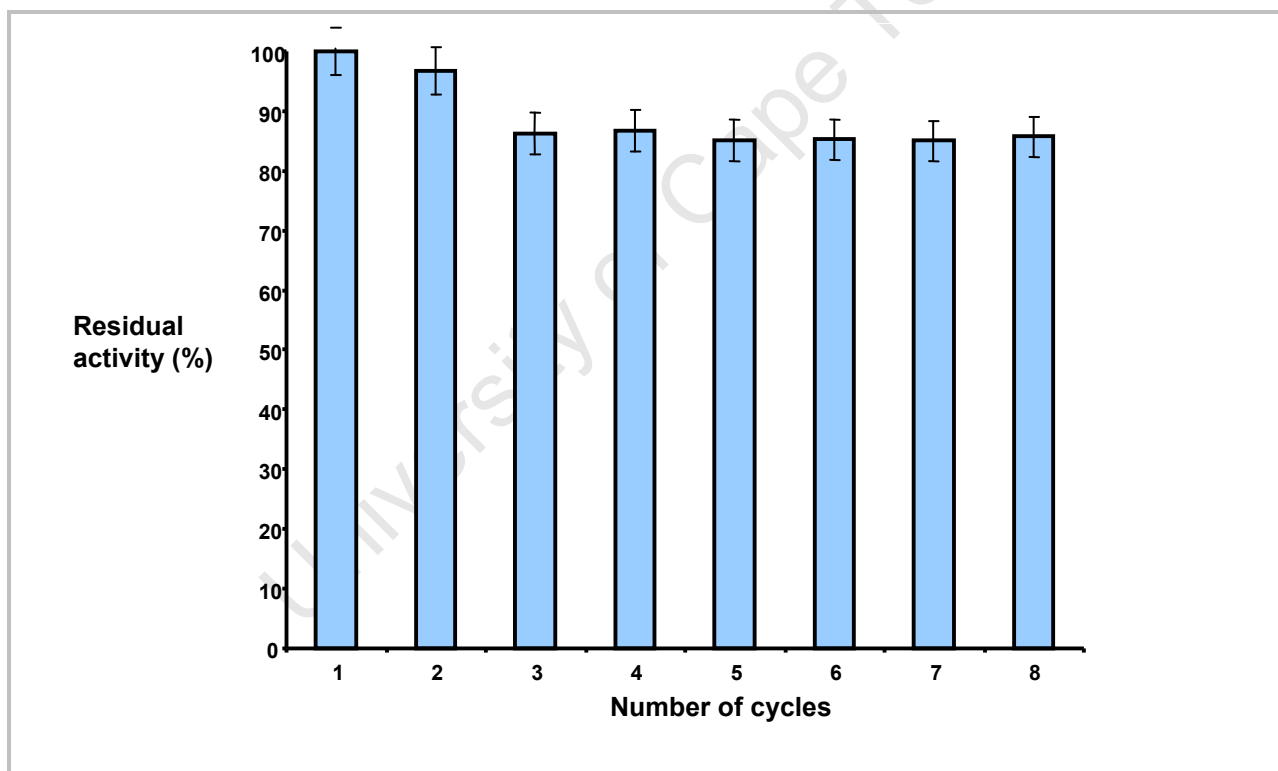


Figure 4.15: Effect of repeated use of Eupergit®C-immobilized NHase for hydration of 50 mM 3-cyanopyridine solution. Biotransformation batch runs (5 min) were performed at 50°C in potassium phosphate pH 7.2. Relative activity was calculated taking the initial enzyme activity (cycle 1) as 100 %.

4.3.5.6 Investigation of effects of substrate concentration on the Eupergit®C-immobilized NHase activity

The maximum substrate concentration for the NHase activity was studied by incubating the soluble enzyme and the immobilized NHase biocatalyst with varying 3-cyanopyridine concentrations (5 to 500 mM) for 5 min in 50 mM potassium phosphate buffer (pH 7.2), at 50°C. A typical profile of the substrate inhibition for both soluble and immobilized biocatalyst is shown (Fig. 4.16). The maximum concentration tolerance was found to be 100 mM for the soluble NHase, and above this concentration there was a decline in relative activity, for example, relative activity decrease to 93.5% at 200 mM, 61.2% at 300 mM, 46.5% at 400 mM and 17.1% at 500 mM concentration of 3-cyanopyridine. Similar results on loss of enzyme activity at elevated substrate concentrations have been reported for NHase from *R. rhodochrous* J1 (Nagasawa *et al.*, 1993).

Experiments using the immobilized *G. pallidus* RAPc8 NHase over the same substrate range (5 to 500 mM), exhibited a maximum substrate concentration of up to 300 mM, demonstrating more than 2-fold improvement in substrate concentration tolerance compared to its soluble counterpart (Fig. 4.16). The mechanism by which immobilized *G. pallidus* RAPc8 NHase can be made more resistant to higher concentrations of substrate might be complex and should be the subject of further study, particularly by investigating the docking of the substrate in the immobilized enzyme active site. The stabilization achieved for Eupergit®C-immobilized NHase seems to be responsible for the prevention of conformational changes that occur in the NHase structure during substrate-enzyme binding process (Tsekoa, 2005), particularly at higher substrate concentrations. Previous results showed that a related microorganism, *Bacillus pallidus* Dac521, immobilized in calcium alginate, gave activity at concentrations of 3-cyanopyridine up to 300 mM in the production of nicotinic acid (Almatawah & Cowan, 1999). Considering these results, it is apparent that immobilization of enzymes or whole-microbial cells would be useful in order to achieve high substrate conversion.

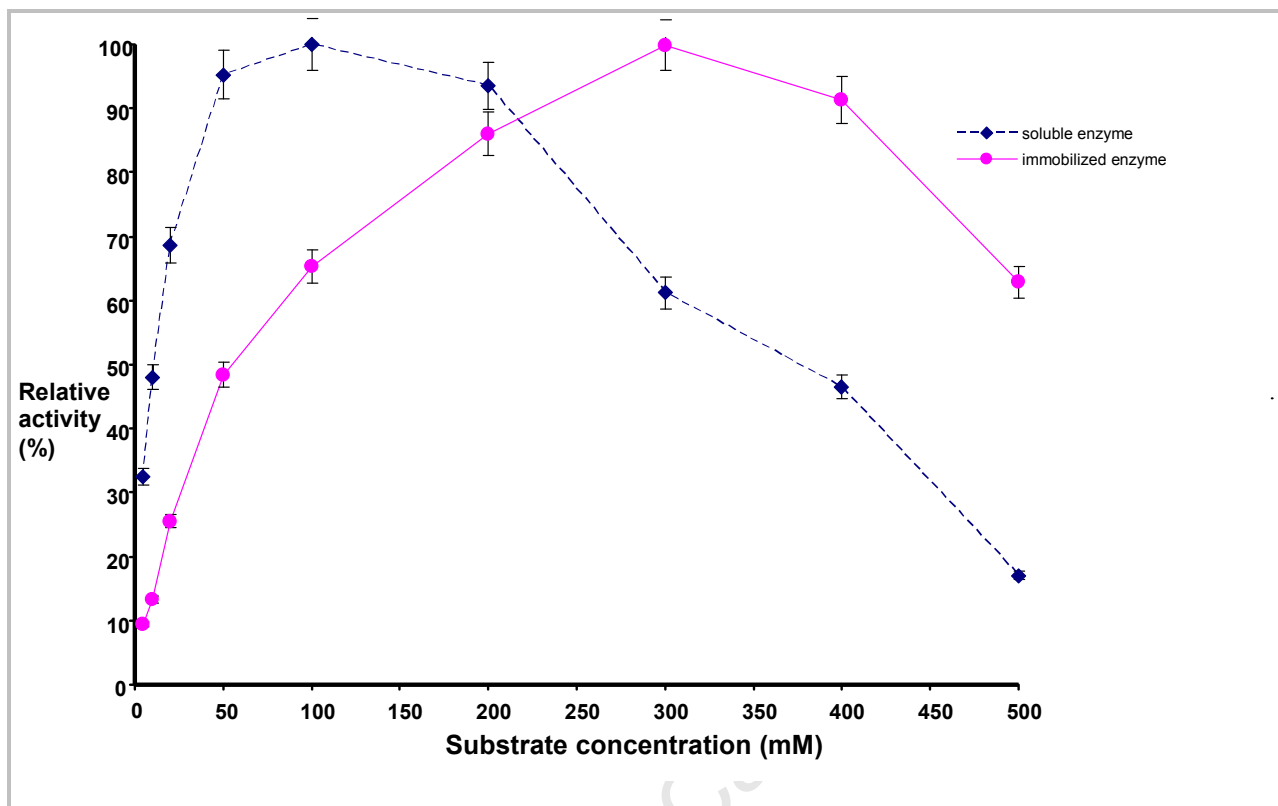


Figure 4.16: Comparison of the effects of different concentrations of 3-cyanopyridine substrate on the activity of soluble and immobilized NHase. The enzyme activity was measured in 50 mM potassium phosphate buffer, pH 7.2. Experiments were conducted at 50°C, with incubation for 5 min. Enzyme amount of 0.14 mg. Relative activity was calculated at the concentrations at which enzyme activity showed maximum activity.

4.3.5.6.1 Evaluation and comparison of the substrate inhibition constant, K_i , for the Eupergit® C-immobilized and soluble NHases using Haldane's model

The substrate inhibition constants for both soluble and immobilized NHase were estimated from a plot of NHase activity versus substrate concentration. The Software Graphpad prism 5 (Hearne Scientific Software) was used to fit the hydrolysis substrate inhibition model Equation 4.8 (Chung *et al.*, 2005) to the data from Section 4.3.5.6 at each substrate concentration.

$$v_{\max} = \frac{v_{\max} S}{K_m + S + \frac{S^2}{K_i}} \quad 4.8$$

where S is the substrate concentration (mM), v_{max} the maximum reaction rate, K_m is substrate affinity constant (mM) and K_i is the substrate-inhibition constant.

The model with the best fit lines to the data from the soluble NHase and immobilized NHase are shown in Fig. 4.17a and Fig. 4.17b, respectively. The calculated values for the substrate inhibition constants were soluble enzyme ($K_i = 101.1$ mM) and Eupergit® C-immobilized NHase ($K_i = 194.7$ mM). The results revealed a significant increase in the substrate concentration tolerance by immobilized NHase compared to the soluble NHase. It can be concluded that the use of immobilized NHase in nitrile hydration has the advantages that the process can be performed under relatively high substrate concentrations.

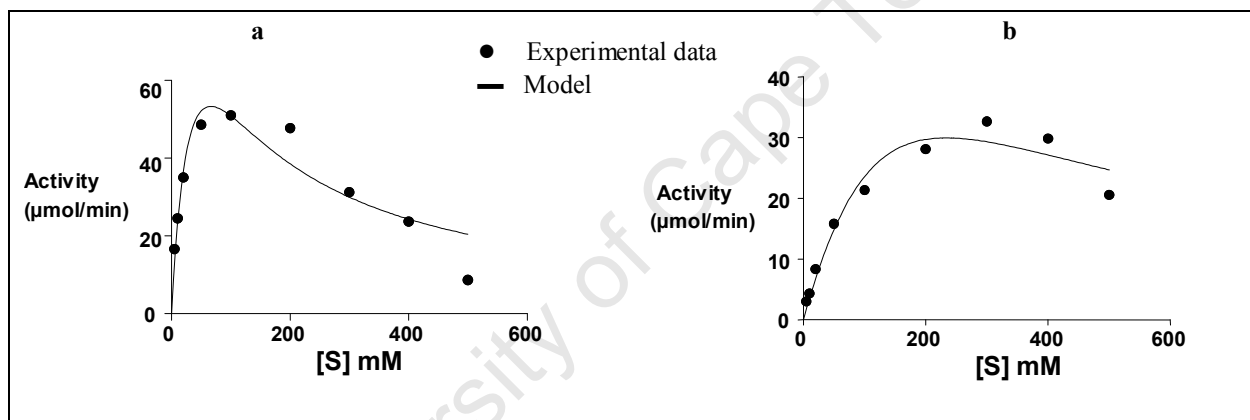


Fig.4.17 A non-linear regression Haldane's Model was fitted to substrate inhibition data of soluble (a) and Eupergit® C-immobilized *G. pallidus* RAPc8 NHase (b) using Graphpad Prism 5 Software (Hearnes Corporation), K_i (soluble NHase) = 101.1 mM, $R^2=0.857$ and $Sy. x=1$ 2.8 and K_i (immobilized NHase) = 194.7 mM, $R^2=0.9504$ and $Sy. x = 2.85$.

4.3.5.7 Measurement of kinetic parameters of immobilized *G. pallidus* RAPc8 NHase

Using 3-cyanopyridine at different concentrations, from 5 to 100 mM, the initial reaction rates (Fig. 4.18) of NHase-catalysed conversion was assayed at 50°C and pH 7.2. The kinetic data was fitted to the Michaelis-Menten equation, and the kinetic parameters maximum rate (V_{max}) and the Michaelis-Menten constant (K_m) were estimated from the Hanes-Woolf plot (Fig.4.19).

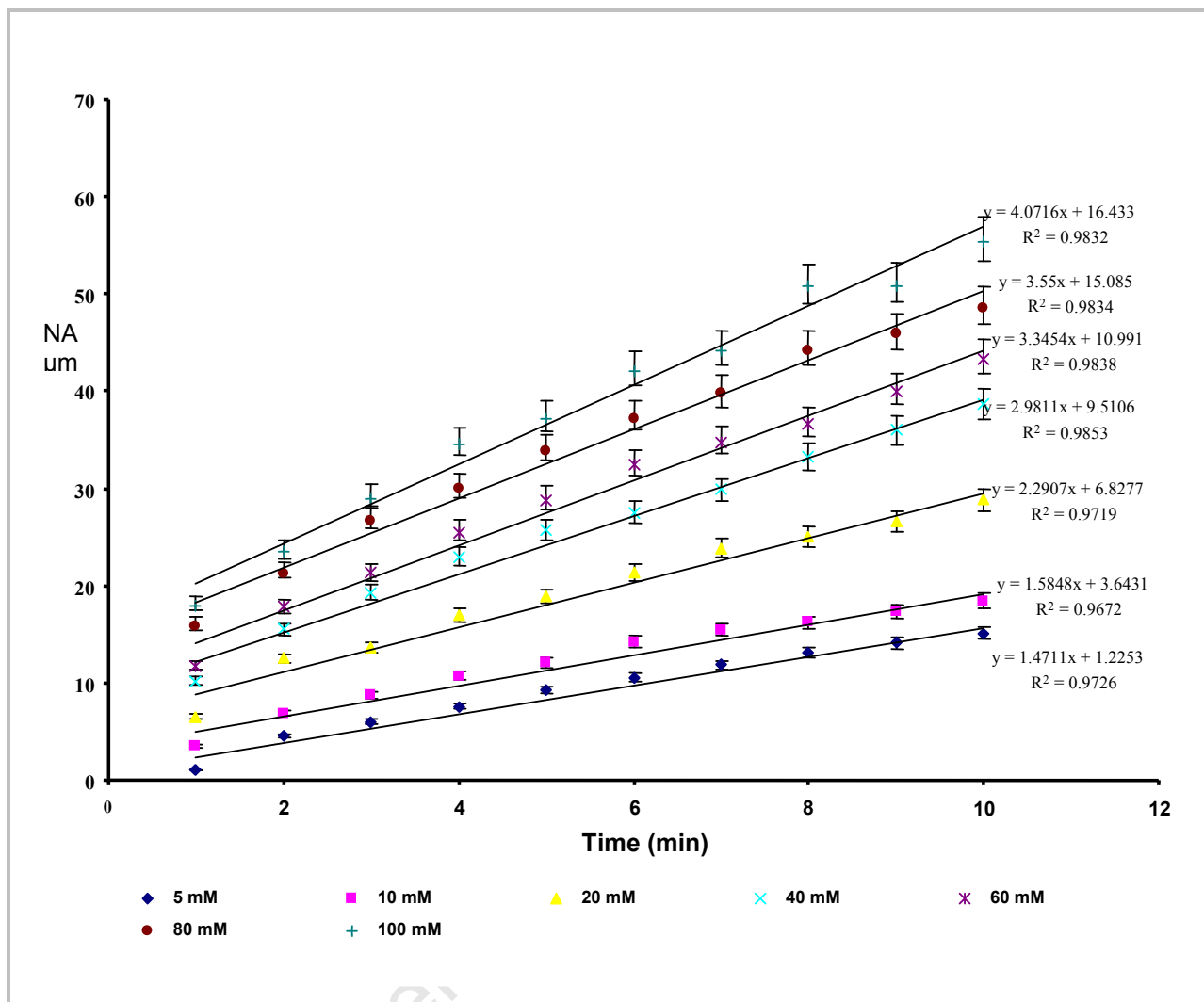


Figure 4.18: Effect of incubation time on nicotinamide production using different concentrations of 3-cyanopyridine. Immobilized NHase was incubated for 5 min at 50°C in 3 mL of activity assay system containing 50 mM KH₂PO₄-K₂HPO₄ buffer (pH 7.2) and final concentration of the enzyme 0.14 mg.

The kinetic parameters K_m and V_{max} values for the immobilized NHase in the reaction converting 3-cyanopyridine are presented in Table 4.3. The Michaelis constant for the immobilized NHase was determined to 17.7 mM which was higher than that of the soluble enzyme (Section 3.3.5.9.3), indicating that the immobilized enzyme had a lower enzyme-substrate affinity. This is a typical phenomenon generally observed for immobilized enzymes, mainly attributable to the mass transfer resistance between the substrate and enzyme (Pifferi *et al.*, 1989). The maximum reaction velocity (V_{max}) for the immobilized *G. pallidus* RAPc8 NHase is also shown in Table

4.3. The V_{\max} obtained was $4.5 \mu\text{mol}.\text{ml}^{-1}.\text{min}^{-1}$, which is 10-fold lower than the value measured using soluble NHase. This is also characteristic of immobilized biocatalysts, and the decrease in V_{\max} could be due to diffusional limitations or steric hindrances imposed by the support on the substrate and enzyme active site (Knezevic *et al.*, 2006).

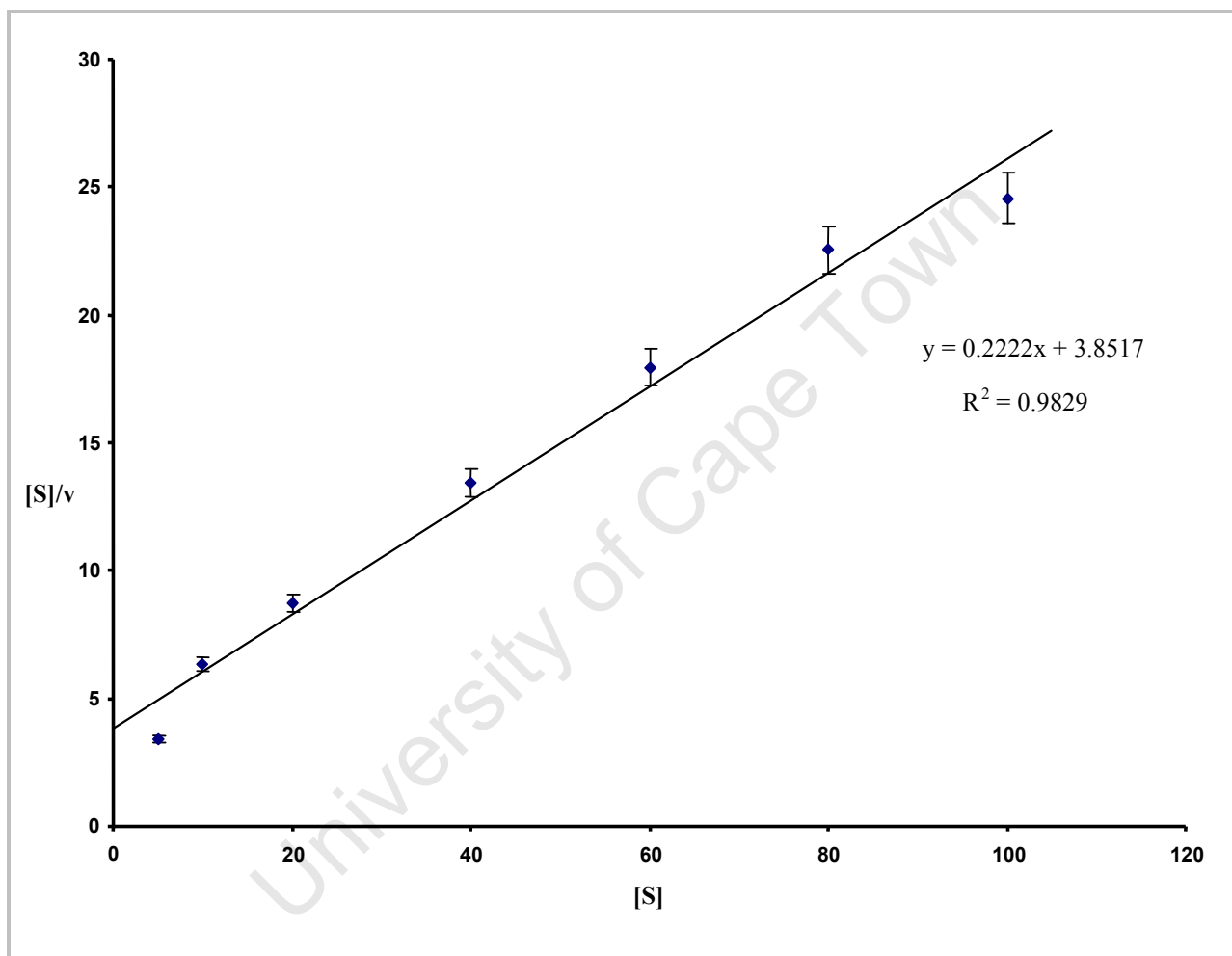


Figure 4.19: Determination of kinetic constants by the Hanes-Woolf graphical method. Substrate concentration ranges (5 to 100 mM) were used and initial velocities were measured using linear equation described in Fig. 4.18.

Table 4. 3: Summary of kinetic parameters for Eupergit® C- immobilized *G. pallidus* RAPc8 NHase

Substrate	V_{\max} ($\mu\text{mol.ml}^{-1}\text{-min}^{-1}$)	K_m (mM)	k_{cat} (s^{-1})	R^2
3-cyanopyridine	4.5	17.33	54.1	0.983

4.3.5.8 Determination of the deactivation parameters for the Eupergit®C-immobilized *G. pallidus* RAPc8 NHase

One important step towards the development of a biotechnological process is understanding the deactivation pattern of the biocatalyst of interest (Panda *et al.*, 1999). Although it is difficult to adequately predict factors that may affect the stability of the enzyme in a process, it is well known that loss of enzyme activity under operational conditions is attributable to thermal deactivation and majority of enzymes are effectively modelled as a first order reaction (previously described in Section 4.1.2) (Sadana, 1995). Thus, based on this model, the thermal deactivation and thermodynamic constants can be estimated.

4.3.5.8.1 Estimation of the deactivation constant (k_d) and enzyme half-life ($t_{1/2}$) for *G. pallidus* RAPc8 NHase

Thermal deactivation rate constants of soluble and immobilized NHase were measured from the data collected with the thermal deactivation tests (Section 3.3.5.6 and 4.3.5.4) in the temperature range 40 to 70 °C. The deactivation rate constants (k_d) were calculated at each temperature from the plot of the \ln of percentage relative activity of NHase as a function of the incubation time. The half life ($t_{1/2}$), which is the time period necessary for the enzymatic activity to decrease to half of its initial value, of the NHase at different temperatures was also calculated. A summary of calculated values of k_d and $t_{1/2}$ are given in Table 4.4 for all the temperatures tested. Generally, the k_d values increased with increasing temperature for both the soluble enzyme and the immobilized biocatalyst. At each temperature, the immobilized NHase gave a lower value compared to its soluble counterpart meaning that immobilization protected the enzyme against

thermal inactivation. For example, the deactivation rate constant (k_d) was calculated at 40°C were 0.0019 and 0.0006 min⁻¹ for the soluble and immobilized NHase, respectively. At 70 °C for the immobilized NHase showed $k_d = 0.0166$ min⁻¹, which is lower than that of the soluble enzyme (0.0186 min⁻¹). Thus, the deactivation process was found to be slower at higher temperatures for the immobilized NHase.

The half-life time of the immobilized NHase, for each temperature, was higher than the free enzyme by 3, 3, 6 and 1.2-fold at 40, 50, 60, and 70 °C, respectively, (Table 4.4). This again indicated that immobilization increased the thermostability of *G. pallidus* RAPc8 NHase. From the view point of biotechnological application, half-life values of a biocatalyst are important as they provide good indication of effect of temperature on activity (Busto *et al.*, 1999). It appears that immobilization of the NHase by covalent binding to Eupergit®C was a good strategy to improve biocatalyst stability.

Table 4. 4: Comparison of the deactivation coefficient (k_d) and half-life ($t_{1/2}$) values for soluble and Eupergit®C immobilized *G. pallidus* RAPc8 NHase

Temperature (°C)	k_d (min ⁻¹)		$t_{1/2}$ (min)	
	Soluble	Immobilized	Soluble	Immobilized
40	0.0019	0.0006	364.8	1155.2
50	0.0049	0.0017	141.5	407.7
60	0.0127	0.0021	54.6	330.1
70	0.0186	0.0166	37.3	41.8

4.3.5.8.2 Determination of the activation energy E_a for the *G. pallidus* RAPc8 NHase

The values of the NHase deactivation rate constant k_d at each temperature were used to determine the activation energy for deactivation of the enzyme (E_a). Fig. 4.20 is a plot of the deactivation constants for the soluble and immobilized NHase, $\ln(k_d)$, as a function of the inverse of the absolute temperature (K^{-1}). The energy of activation (E_a) values were calculated from the slope = E_a/R and were obtained as 1011 J.mol⁻¹ and 1306 J.mol⁻¹ for the soluble and immobilized NHase, respectively. There was a 19.3 % increase in the energy of activation for

deactivation of the immobilized NHase. This further confirms that the enzyme in immobilized form is more stable which, in turn, gives the higher value of E_a (Saleem *et al.*, 2005).

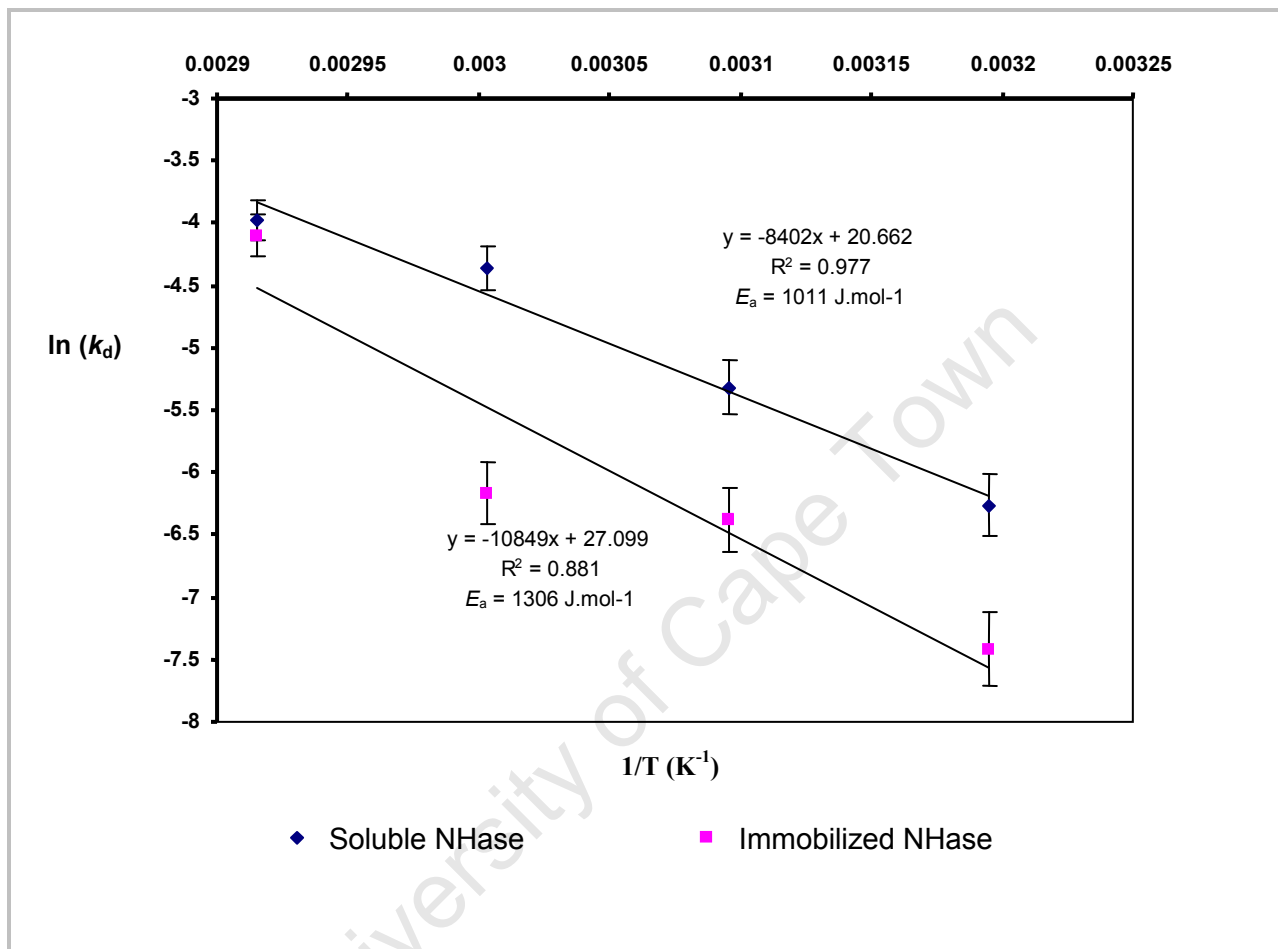


Figure 4.20: Determination of energy of activation E_a for *G. pallidus* RAPc8 NHase using Arrhenius plot between $\ln(k_d)$ and $1/T$. E_a was calculated from the slope ($-E_a/R$), using Equation 4.5.

4.4 CONCLUSIONS

Numerous immobilization methods were investigated for their potential in stabilization of *G. pallidus* RAPc8 NHase. In this chapter, the feasibility of immobilizing cell-free *G. pallidus* RAPc8 NHase on various carriers, using different techniques including covalent, adsorption, entrapment and cross-linking was demonstrated. It was also demonstrated that the soluble enzyme could readily be immobilized at physiological conditions (pH 7.2) and room

temperature. To our knowledge, this is the first example of isolated and purified NHase being immobilized on so many supports and techniques and this is the first time that successful immobilization of cell free NHase on a range of supports is reported.

It was found that, among the methods tested, the use of Eupergit®C with EDAC cross-linking gave an immobilized NHase biocatalyst with the highest immobilization efficiency, presumably because the NHase structure contained side-chains in good orientation for covalent bonding with epoxy group of the support material, and the cross-linker increased the multipoint interaction, stabilizing the heterotetrameric structure further. The protein loading efficiency of each material carrier was evaluated, but did not show any meaningful correlation with immobilization efficiency. This was attributed to the effects such as the length of spacer-arm between the bead surface and functional group, which bind to the NHase ligands.

An investigation of the properties of the soluble NHase compared with those of immobilized biocatalyst under identical reaction conditions showed significant differences between them. Using of the conversion of 3-cyanopyridine to nicotinamide as a model reaction, the biocatalysts activities were investigated in terms of optimal pH, temperature, thermostability, reusability, the effect of organic solvents and reaction kinetics. Significantly improved operational parameters were noted for the immobilized *G. pallidus* RAPc8 NHase, and this demonstrates the important potential of stabilization of the soluble enzyme by immobilization.

The operational stability of the *G. pallidus* RAPc8 NHase was significantly enhanced; after a number of recycled uses, no major decrease in activity was observed. The small losses in activity of the immobilized NHase from the initial to the third cycle were attributed to possible desorption from Eupergit®C beads, loss of enzyme stability (Alkorta *et al.*, 1996) or by washing of the immobilized enzyme.

Substrate inhibition in the NHase catalysed hydration reaction is one of the major obstacles to achieving the requirements of industrial processes of for high concentration of product. Using immobilization, we demonstrated increased tolerance of the NHase to higher substrate concentration (300 mM). The high substrate concentration utilized by the *G. pallidus* RAPc8

NHase could be further enhanced by using the biocatalyst in packed-bed reactor (PBR) systems, since PBRs are preferred reactors in processes involving substrate inhibition, product inhibition or reaction reversibility (<http://www.lsbu.ac.uk/biology/enztech>).

A clear correlation between the activity of the immobilized *G. pallidus* RAPc8 NHase and the presence of water-miscible or water-immiscible solvent systems was observed. The relationship suggests that the enzymes are generally inactivated by water-miscible organic solvent systems, but little affected and even enhanced by water-immiscible solvent systems. Nonetheless, the activity of the immobilized NHase did not depend on the nature of organic solvent in the reaction mixture, since an overall enhancement in enzyme activity was observed.

Immobilized NHase was conformationally more stable and retained up to 80 % of activity after 80 min of operation. Half-lives and deactivation constants displayed by the immobilized enzyme indicated the thermostability of the NHase by immobilization. Thermodynamic characterisation supported the conclusion that immobilization improved the energy of activation, thus, confirming the superiority of immobilized NHase over the soluble form and other known NHases.

The V_{\max} for the immobilized NHase system were lower than that of the enzyme, indicating a lowering of activity of NHase on account of immobilization. The K_m value calculated was higher than that of the free enzyme, which may be due to the diffusional resistances or conformational changes in the enzyme from immobilization.

The enhancement in the performance of the immobilized *G. pallidus* RAPc8 NHase and its ability to be reused, suggest a potential benefit for conducting repeated applications in a continuous reactor. This is an important issue of the chemical industry. Therefore, the biocatalyst of Eupergit[®]C immobilized *G. pallidus* RAPc8 NHase with EDAC cross-linking was used in a small scale process for the production of nicotinamide in a model packed-bed reactor. Details of the operations and optimization of the process are described in Chapter 5.

CHAPTER 5

Design, performance and analysis of a packed-bed reactor containing Eupergit®C-immobilized *Geobacillus pallidus* RAPc8 NHase

5.1 INTRODUCTION

The general characteristics of the immobilized *G. pallidus* RAPc8 NHase were investigated as reported in Chapter 4. The selection of immobilization strategies were based on the envisaged process requirements for the NHase which included such parameters as enzymatic activity, stability, reusability, deactivation and the ability to act in the presence of organic solvents. The advantages of immobilized enzymes are numerous, and have been discussed in terms of batch-wise reactions, but they are most markedly evident in continuous reactor systems, as investigated in work reported in this Chapter. The performance of the Eupergit®C-immobilized NHase was investigated for suitability in a packed-bed column reactor based on the model reaction, hydration of 3-cyanopyridine. A continuous packed bed reactor process was expected to allow an effective improvement in nicotinamide production.

A wide variety of continuous reactor systems are used in chemical, pharmaceutical and bio-based processes. The reactor type that can be used for a particular purpose generally depends upon factors such as: (i) the number and types of reaction phases, (ii) heat transfer and mass transfer phenomena, (iii) mixing, (iv) the expected commercial production rate, (v) the required temperature, pressure and pH, and (vi) materials for construction to achieve an economically viable operation. Packed-bed reactors (PBRs), consisting of tubular columns packed with solid catalyst particles, are most widely used for solid-catalyst, heterogeneous, reactions such as those involving immobilized enzymes or microbial cells.

In PBRs, the substrate solution is pumped through the reactor while the immobilized enzyme is contained in the vessel. This can result in greater productivity (compared to other types of reactors) from a fixed amount of enzyme, packed-bed reactors (PBRs) are known for their (i)

higher average reaction rates (Mammarella *et al.*, 2006), (ii) ease of product separation, (iii) ease of biocatalyst recovery and reuse without the need of prior separation, (iv) simple handling and operation, (v) consistent product quality, and (vi) suitability for long-term and industrial-scale operation (Balcao *et al.*, 1996).

In the presence of a single mobile phase, the two most well known modes of operation for PBRs involve either downward flow of substrate that takes advantage of gravitational forces, or upward flow operation. The upward operational mode is common, because such an arrangement permits reduced backmixing and avoids extensive bypassing. In the case of multiphase liquid systems, two streams may flow through the reactor in opposite directions (countercurrent flow) with more dense phase flowing downwards (Kosugi *et al.*, 1990) or in same direction (co-current flow) (Lamine *et al.*, 1996).

5.1.1 Theory and model for packed-bed reactor design and operation

The plug flow reactor model has been previously described in a continuous flow system of immobilized enzymes to estimate key reactor variables. The key assumptions in a plug-flow reactor, the entire substance stream flows at the same velocity, parallel to the reactor axis with no back-mixing. All materials present at any given reactor cross-sectional area have an identical residence time, with all product emerging with the same residence time, and substrates molecules all having similar opportunity for reaction (Mammarella *et al.*, 2006).

Various mathematical models based on the concept of ideal plug flow are known (Bhattacharya *et al.*, 2004) and have been adapted to allow prediction of the behavior of chemical reactors, so that key variables such as the best dimensions of the reactor, can be estimated. The mass balance equation for any enzymatic reaction in a tubular reactor is given by the plug-flow reactor model:

$$u \frac{ds}{dz} = -v \quad 5.1$$

where u is superficial fluid velocity in the reactor, s the substrate concentration, z length of section in the reactor, and v is the initial reaction rate of the enzyme catalysed reaction.

Several factors are taken into account when modeling immobilized enzyme reactors. Assuming Michaelis-Menten enzyme type kinetics without substrate inhibition, and negligible intra-particle and external mass transfer resistances, the steady state equation for the material balance of a cross-sectional area of the reactor can be written as:

$$u \frac{ds}{dz} = - \left(\frac{1-\varepsilon}{\varepsilon} \right) \frac{v_{\max} s}{K_m + s} \quad 5.2$$

In a reactor with void fraction ε , assuming negligible intra-particle, external mass transfer resistances and inhibition, the equation can be solved analytically to obtain the design equation for the reactor over mean residence time (τ):

$$\tau = \frac{\varepsilon}{1-\varepsilon} \left\{ \frac{K_m}{V_{\max}} \ln \left(\frac{S_o}{S} \right) + \frac{S - S_o}{V_{\max}} \right\} \quad 5.3$$

For a continuous plug flow reactor under steady state, in terms of fractional substrate conversion and in the absence of the axial and radial diffusion, the design equation becomes:

$$\tau = \frac{\varepsilon}{1-\varepsilon} \left\{ - \frac{K_m}{V_{\max}} \ln(1-\delta) + \frac{S_o \delta}{V_{\max}} \right\} \quad 5.4$$

where τ is the mean residence time of the liquid, defined based on interstitial velocity, δ is the substrate conversion. The modified plug-flow reactor (PFR) model can then be used in design and simulation of flowing systems to estimate key design parameters such as mean residence time, flow rate and length of a packed-bed reactor (Bhattacharya *et al.*, 2004).

The aim of the work reported in this Chapter was to: (i) characterise important hydrodynamic parameters with respect to packed bed reactor application (parameters such as minimum fluidization flow rate, void fraction and steady-state were experimentally determined), (ii) investigate a possible optimization of the continuously operated packed-bed immobilized enzyme

reactor *via* modification of the initial substrate concentration, flow rate (or mean residence time), bed-height, operation temperature and bed height, (iii) conduct a detailed investigation of performance of the packed bed reactor under prolonged use (operational stability) and to ascertain the deactivation constants. The results of the PBR were compared with those for the same reaction in a CSTR.

5.2 MATERIALS AND METHODS

5.2.1 Materials

The packed-bed reactor was constructed from borosilicate 3, 3-type glass, initially purchased from Glasschem, Stellenbosch (South Africa). All chemicals were purchased from Sigma-Aldrich (SA), Aldrich-SA and Fluka. Eupergit®C was purchased from Röhm Pharma Polymers (Darmstadt, Germany) and the immobilized NHase biocatalyst was prepared as previously described using Eupergit®C and EDAC cross-linking (prepared as described in Section 4.2.2.3). The physical characteristics of the biocatalyst are given in Table 5.1. Solvents were purchased from Merck-SA. All other chemicals were also obtained commercially and were of analytical grade.

Table 5.1: Properties of the Eupergit®C-immobilized NHase used in the experiments.

Property	Value
Physical state	Solid
Density (g/mL)	0.6
Activity of immobilized enzyme (U) per reactor	27.6
Void fraction	0.35
Total protein concentration per reactor (mg/mL)	22.7

5.2.2 Equipment and experimental methods.

5.2.2.1 Packed bed reactor (PBR)

The reactor was a jacketed Pyrex-glass column, 2 cm in internal diameter and 18 cm in height, with a catalyst bed height of 16 cm. The reactor had a bottom support of perforated glass. Eupergit® C-immobilized NHase were aseptically introduced into the reactor and packed above the bottom disc. A perforated Teflon disc was placed over the beads to prevent bed expansion during operation (Fig. 5.1). The void fraction of the reactor was 0.35 (calculated from experiments in Section 5.2.3.1). The reactor was equipped with a temperature controlled water jacket and operated at 50°C. The inlet and outlet flow rates were kept equal to maintain the liquid level constant at just above the bed level. The reactor was equilibrated by running at the desired feed rate and substrate concentration, for a minimum of 3 reactor volumes before studying the nicotinamide production.

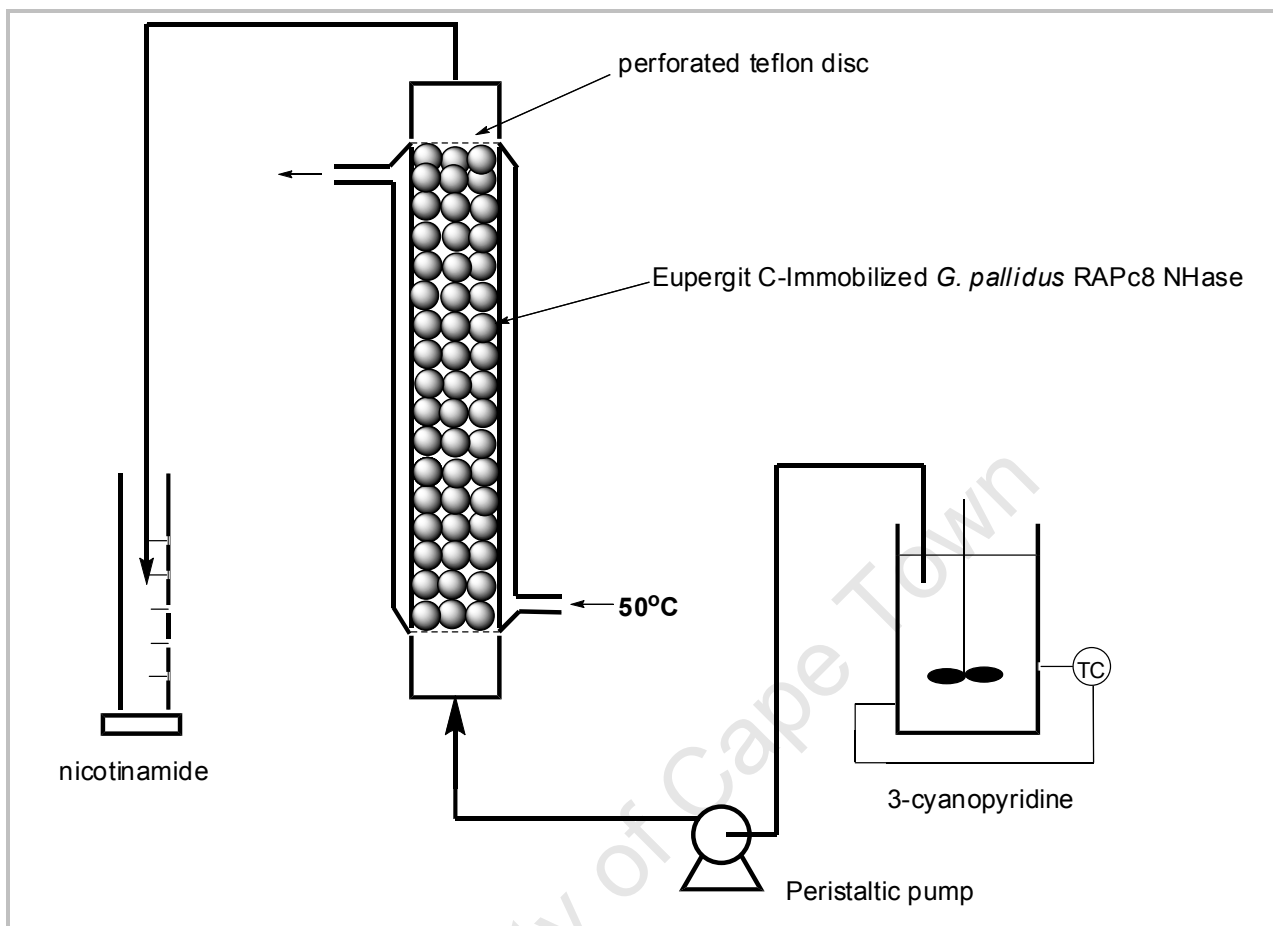


Figure 5. 1: A schematic representation of the equipment used for continuous hydration of 3-cyanopyridine to nicotinamide in a PBR. Bed diameter: 20mm, substrate: 3-cyanopyridine, Buffer: 50 mM potassium phosphate buffer, pH 7.2, Bed density: 0.6g/mL, Total biocatalyst weight: 5g total biocatalyst, Flow rate: 3 mL/min.

5.2.2.1.1 Investigation of the effects of flow rate on packed bed fluidization

When a packed bed reactor with immobilized enzyme is subjected to a sufficiently high upward flow of liquid, the particles become freely suspended or fluidized. To determine the minimum fluidization flow rate, the packed bed reactor containing 15 g of biocatalyst was subjected to increasing flow rates by adjusting the pump setting in range 0 to 10. As the flow rate was increased further, the bed started to fluidize. This is when the upward force exerted by the fluid on the particle is sufficient to enable the particle float and taken as the minimum fluidization flow rate.

5.2.2.1.2 Estimation of the void fraction (ϵ) for the packed bed reactor containing 15 g of Eupergit®C-immobilized NHase.

The void fraction in packed-bed reactors was estimated experimentally with the method described by mathematical expressed as:

$$\epsilon = \frac{\text{volume not occupied by biocatalyst}}{\text{total volume of reactor}} = \frac{\text{total volume of reactor} - \frac{\text{mass of biocatalyst}}{\text{density of biocatalyst}}}{\text{total volume of reactor}}$$

5.2.2.1.3 Steady-state determination of 3-cyanopyridine conversion in the packed bed reactor

The packed-bed reactor column was mounted vertically on a suitable stand (Fig. 5.1). The immobilized NHase in potassium phosphate buffer (pH 7.2) was then poured into the column. The column was connected to a tank containing substrate (3-cyanopyridine) solution of appropriate concentration and the column outlet was adjusted with a flow controller (stopcock) to a value close to 3 mL/min. The effluent solution, containing nicotinamide and unconverted 3-cyanopyridine, was collected in a beaker. Product samples (1 mL) were taken straight from the reactor every 30 min and analyzed for nicotinamide and unconverted substrate content. Steady-state conditions were assumed to be achieved when nicotinamide concentrations of consecutive samples were the same, after three residence times (three column volumes).

5.2.2.1.4 Determination of the performance of Eupergit®C-immobilized NHase in the packed-bed reactor (PBR)

The 3-cyanopyridine substrate solution was equilibrated to reaction temperature (50°C) and fed from the bottom of the column by a peristaltic pump with a fixed feed rate. Substrate conversion was analyzed by taking samples at each column volume (or one residence time). The substrate 3-cyanopyridine solution, at concentrations 0.5 g/L (equivalent of 5 mM), 5.4 g/L (equivalent of 50 mM), 10.4 g/L (equivalent of 100 mM) and 15.6 g/L (equivalent of 150 mM), was used for the study. For each concentration, the reactor was run at three different flow rates (0.7, 1.9 and 3.0 mL/min) and at each flow rate the reactor was operated continuously for a minimum of 1 residence time. Samples were withdrawn, and product and unconverted substrate in the effluent stream were analyzed by the HPLC method. From these data, the volumetric productivity and substrate conversion efficiency of the reactor were calculated.

5.2.2.2 Investigation of the operational stability of the Eupergit®C-immobilized NHase in a continuous stirred tank reactor (CSTR)

Continuous stirred tank experiments were performed using a 500 mL beaker. Temperature was controlled at 50 °C on a magnetic hot plate and the working volume was 30 mL. The substrate in potassium phosphate buffer was fed at a flow rate of 3.0 mL/min with a peristaltic pump and effluent was received by another pump at the same speed (Fig. 5.2). The immobilized NHase (15 g, 5.63 U) was placed in a jacketed cylindrical vessel (4.5 cm internal diameter, 6 cm height) and agitated at 150 rpm with magnet stirrer. The substrate mixture (5 mM 3-cyanopyridine in potassium phosphate buffer) was stirred at 150 rpm by magnetic stirrer and introduced into continuous stirred tank reactor (CSTR) with a peristaltic pump. The reaction was maintained at 50°C by heating the vessel. The substrate mixture was introduced to the top of the vessel at flow rate of 3 mL/min and the product was removed at the bottom of the vessel by a peristaltic pump.

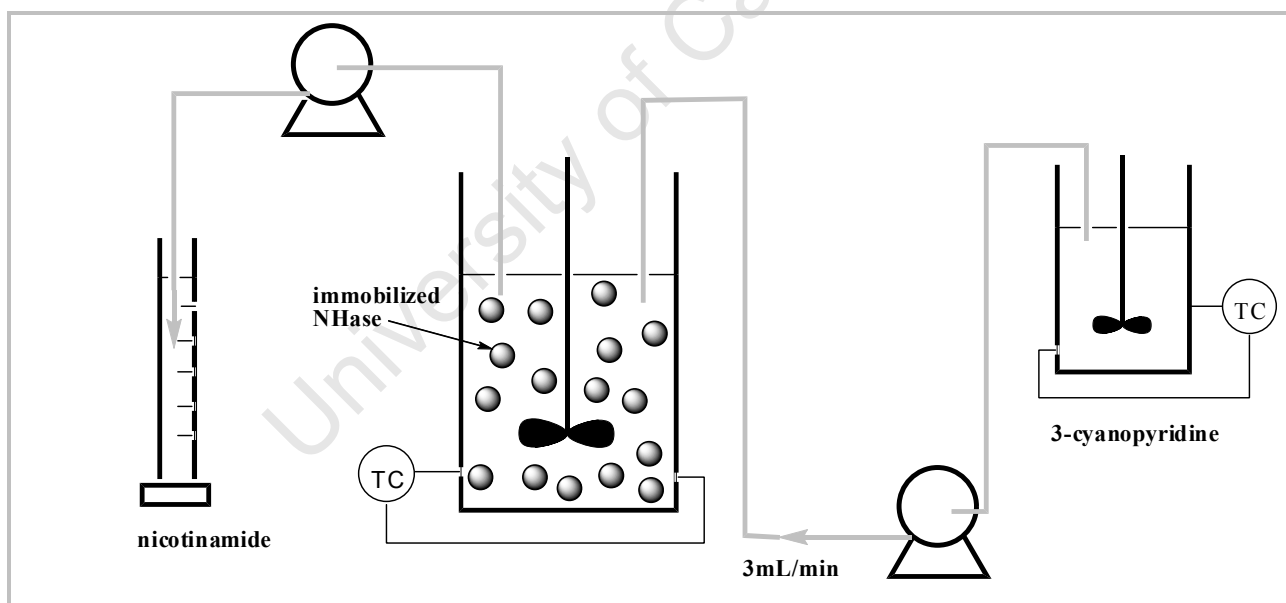


Figure 5.2: Schematic representation for continuous hydrolysis of 3-cyanopyridine by Eupergit®C immobilized *G. pallidus* RAPc8 NHase at 50 °C with stirring speed of 150 rpm. Bed diameter: 20m, Bed density: 0.6, substrate: 3-cyanopyridine, Buffer: 50 mM potassium phosphate buffer, pH 7.2, Flow: 3 ml/min Total biocatalyst weight: 15g, Total biocatalyst volume in reactor: 7.5cm³.

5.2.2.3 Analytical methods

The conversion of 3-cyanopyridine to nicotinamide were measured by HPLC using a reverse phase column with 10 mM $K_2HPO_4/KH_2PO_4-H_3PO_4$ as previously described in Section 3.2.2.8. The conversion fraction was calculated using the Eq. 5.5 (described in Section 5.3.2) and volumetric productivity was calculated using Eq. 5.6 (described in Section 5.3.2).

5.3 RESULTS AND DISCUSSION

The preliminary investigations consisted of three separate experiments. The first experiment was performed to establish design parameters such as the void fraction, flow rate and steady state. In the second experiments, design parameters were applied to investigate the optimum conditions for maximum substrate conversion and volumetric productivity. In the third experiment, operation stability of the packed-bed reactor containing Eupergit®C-immobilized NHase was investigated in comparison with its performance in a continuous stirred tank reactor and deactivation constants were determined. The results presented here is the first report of a packed-bed reactor system utilising the cell-free immobilized NHase for conversion of 3-cyanopyridine to nicotinamide.

5.3.1 Investigation of the effect of flow rate on bed fluidization

The flow rate expected to fluidize the biocatalyst was determined by investigating the influence of the flow rate on the bed height. As is shown in Fig. 5.3, there was a steady increase in bed height with an increase in the flow rate (the bed expansion responded as a linear function of the flow rate). The graph shows a steep increase in bed height (indicating fluidization) above the flow rate of 3 mL/min. Therefore, 3 mL/min was found to be the minimum fluidization flow rate for the packed bed reactor and was taken as the maximum flow rate to be applied in the study.

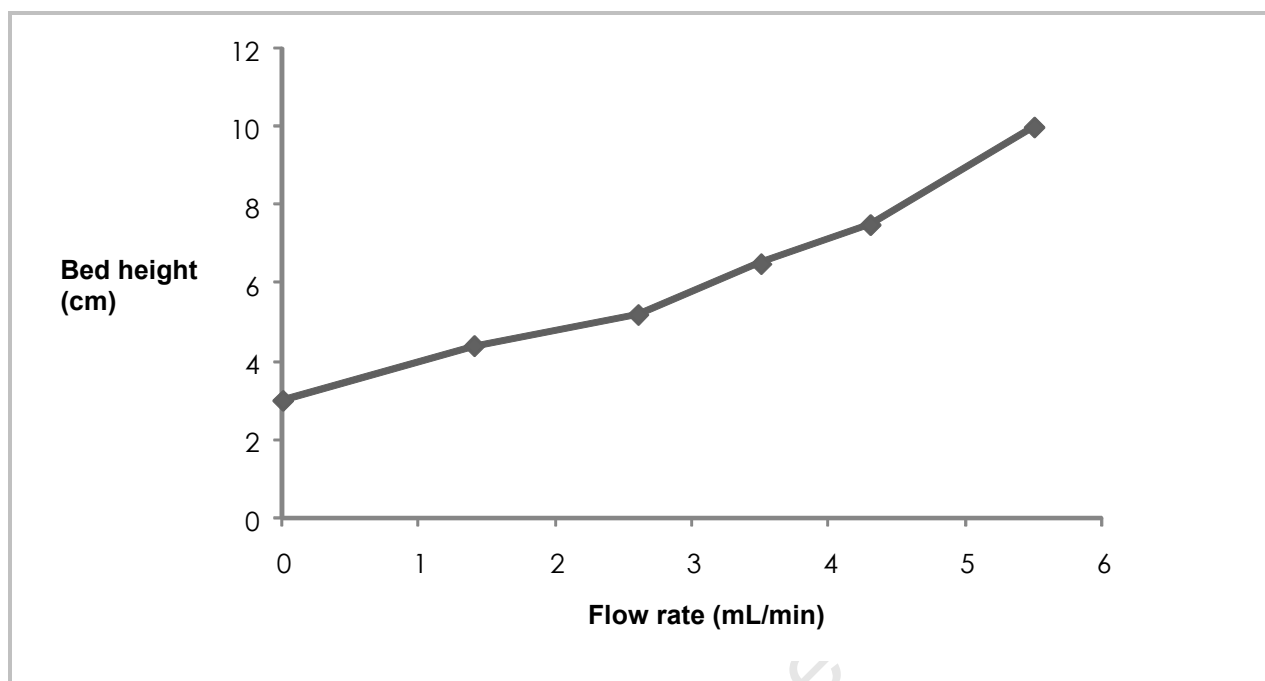


Figure 5.3: Investigating the effects of flow rate on bed fluidization by determining variations in bed heights with increasing feed flow rates.

5.3.2 Investigation of the performance of Eupergit®C-immobilized *G. pallidus* RAPc8 NHase in the packed-bed column reactor

The performance of the Eupergit®C immobilized NHase reactor were evaluated as a function of numerous parameters, such as flow rate of the reaction mixture, initial substrate concentration, bed height (varying amounts of biocatalyst), and operational stability. The performance of the packed bed reactor was assessed based on substrate conversion and volumetric productivity. Substrate conversion is a convenient variable and it is often used in place of concentration. It is calculated as a percentage of the total moles of substrate converted into product and the total moles of the initial substrate fed into the reactor per unit time for a continuous reactor, expressed mathematically as:

$$\delta = \frac{[S] - [S_0]}{[S_0]} \quad (5.5)$$

in which $[S]$ is the substrate concentration at $t = x$, $[S_0]$ is substrate concentration at $t = 0$.

Volumetric productivity Q_p of a bioprocess is defined as the amount of product per unit volume and time. Thus, the volumetric productivity is more useful measure of efficiency of the bioprocess at a given time point and is defined as:

$$Q_p = \frac{P}{V.t} \quad (5.6)$$

where P is amount of product (g), V is volume of reactor, and t is time at the end of an operation.

5.3.2.1 The effect of substrate concentration on fractional conversion and volumetric productivity of the PBR.

The effect of substrate concentration on the reaction of immobilized enzyme in a packed-bed reactor was investigated using 3-cyanopyridine at a concentration range of 0.5 to 15.6 g/L (5 mM to 150 mM). Starting with the substrate concentration of 0.5 g/L, the feed concentration was increased step wise while keeping the flow rate and reactor volume constant at 3mL/min and 17.6 mL, respectively. As shown in Fig. 5.4, the substrate conversion decreased with an increase in substrate feed concentration. The highest substrate conversion (94 %) was obtained at a very low substrate concentration of 0.5 g/L and the lowest conversion (17%) was obtained at feed concentration of 15.6 g/L. The decrease in fractional conversion rate with increasing substrate concentration could be due to declining enzymatic activity with increasing concentration of 3-cyanopyridine. The substrate molecules could be occupying the active pocket in a manner which inhibits the binding of other substrates at very high substrate concentrations, resulting in substrate inhibition. Tsekoa (2005) reported that the *G. pallidus* RAPc8 NHase had channels accessible to the bulk solution, probably the active-site pocket. Thus, when substrate molecules bind, they would not only to attach to catalytic sites, but also nearby sites, affecting the reaction rate, hence decreasing the overall reaction rate. Similar results were reported when the *G. pallidus* RAPc8 NHase was applied in batch reactions (see Section 3.3.5.2).

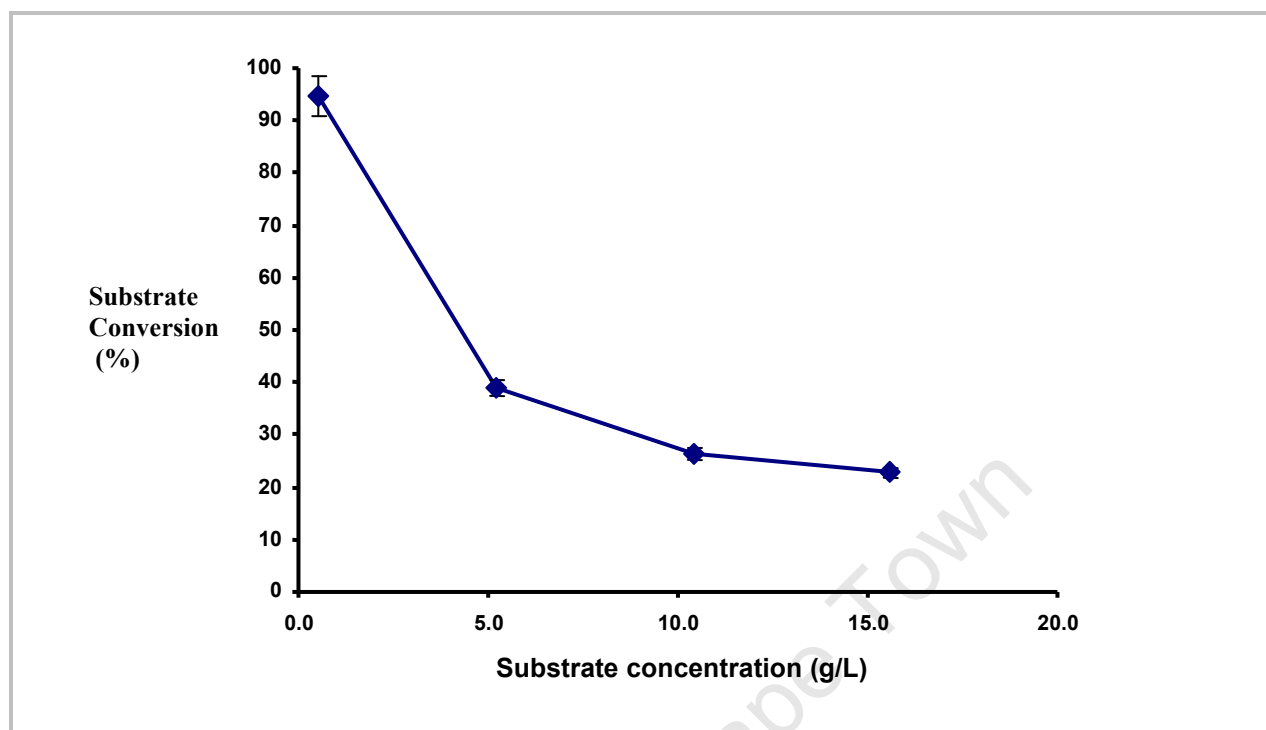


Figure 5. 4: Relationship between the concentration of 3-cyanopyridine in the feed stream and substrate conversion (%) at a flow rates of 3 mL/min, using fixed amount of biocatalyst. Substrate conversion is calculated as a percentage of the total moles of substrate converted into product and the total moles of the initial substrate fed into the reactor per unit time for a continuous reactor.

On the other hand, a change in the substrate concentration resulted in an increase in the volumetric productivity. The profile of the volumetric productivity with varying substrate concentrations but constant flow rate and reactor volume (3 mL/min and 17.6 cm³) is shown (Fig. 5.5). The highest volumetric productivity of 48.8 g/L/h was obtained at the highest substrate concentration of 15.6 g/L at the given flow rate. The results suggest that availability of substrate in the reaction medium was an important factor to achieve higher volumetric productivity (Leng *et al.*, 2006), thus increasing the substrate guaranteed higher volumetric productivity. The results show a promising way for efficient production of nicotinamide, although it is conceivable that overall activity of biocatalyst may be compromised at extreme high substrate concentration.

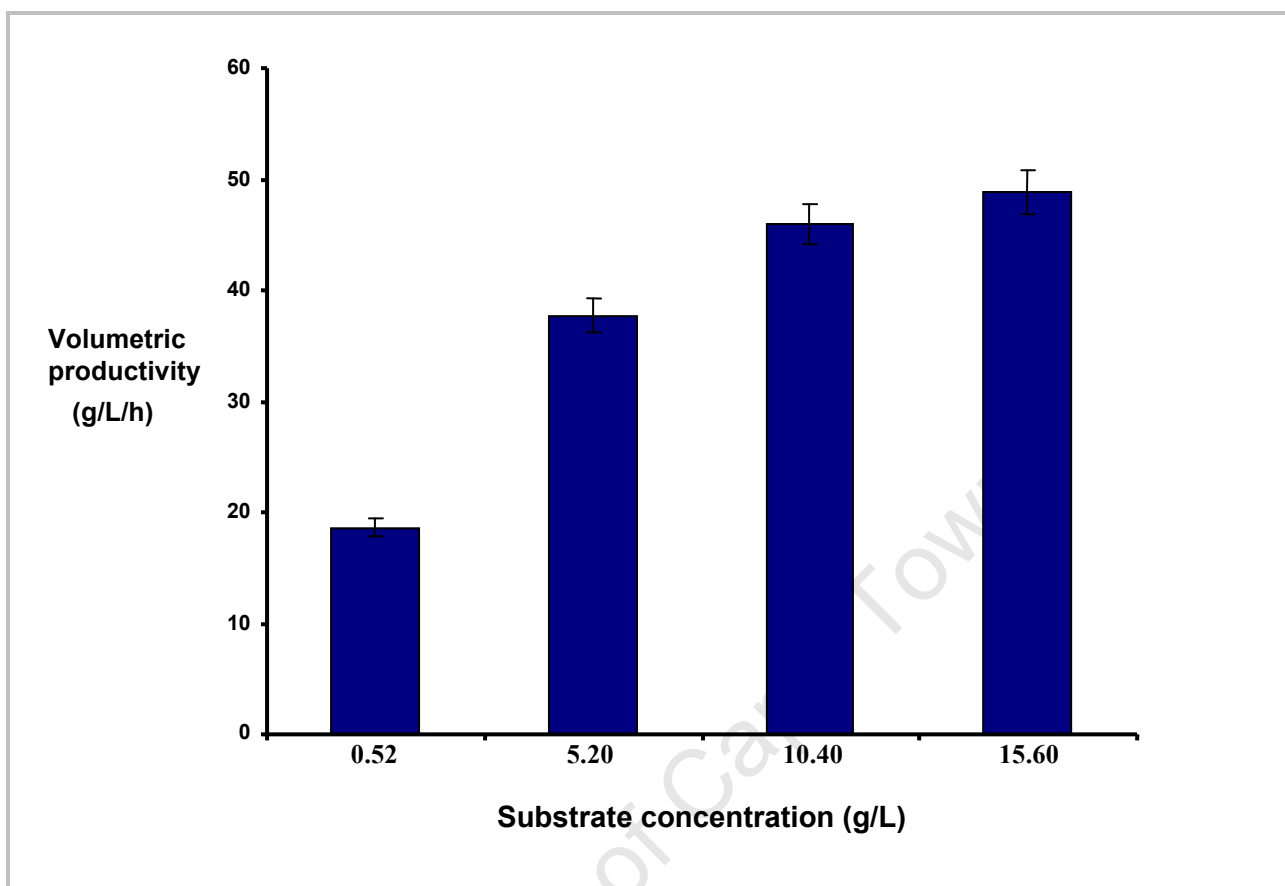


Figure 5. 5: Relationship between the concentration of 3-cyanopyridine in the feed stream and volumetric productivity (g/L/h) at a constant flow rate (3mL/min) and reactor volume (17.6 cm³). The volumetric productivity Q_p is defined as the ratio of is amount of product P (g) to is volume of reactor V , (L) and time t (h) at the end of an operation.

5.3.2.2 The effect of flow rate (mean residence time) on substrate conversion and volumetric productivity of the PBR

The substrate conversions of the packed-bed reactor were investigated by varying the flow rate of the substrate feed. This subsequently affected the residence time for the 3-cyanopyridine in a packed-bed reactor. Flow rate of feed was changed from 0.7 to 3.0 mL/min corresponding to a mean residence time range of 0.186 to 0.042 h, respectively. The variations in the PBR observed with respect to flow rate are shown in Fig. 5.6. As expected, the fractional conversion declined with increasing flow rate in the continuous reactor for all the substrate concentrations tested.

Higher conversion could be achieved by correspondingly reducing the flow rate at any given substrate concentration, because the contact time between the substrate and immobilized enzyme would then increase with a lower flow rate.

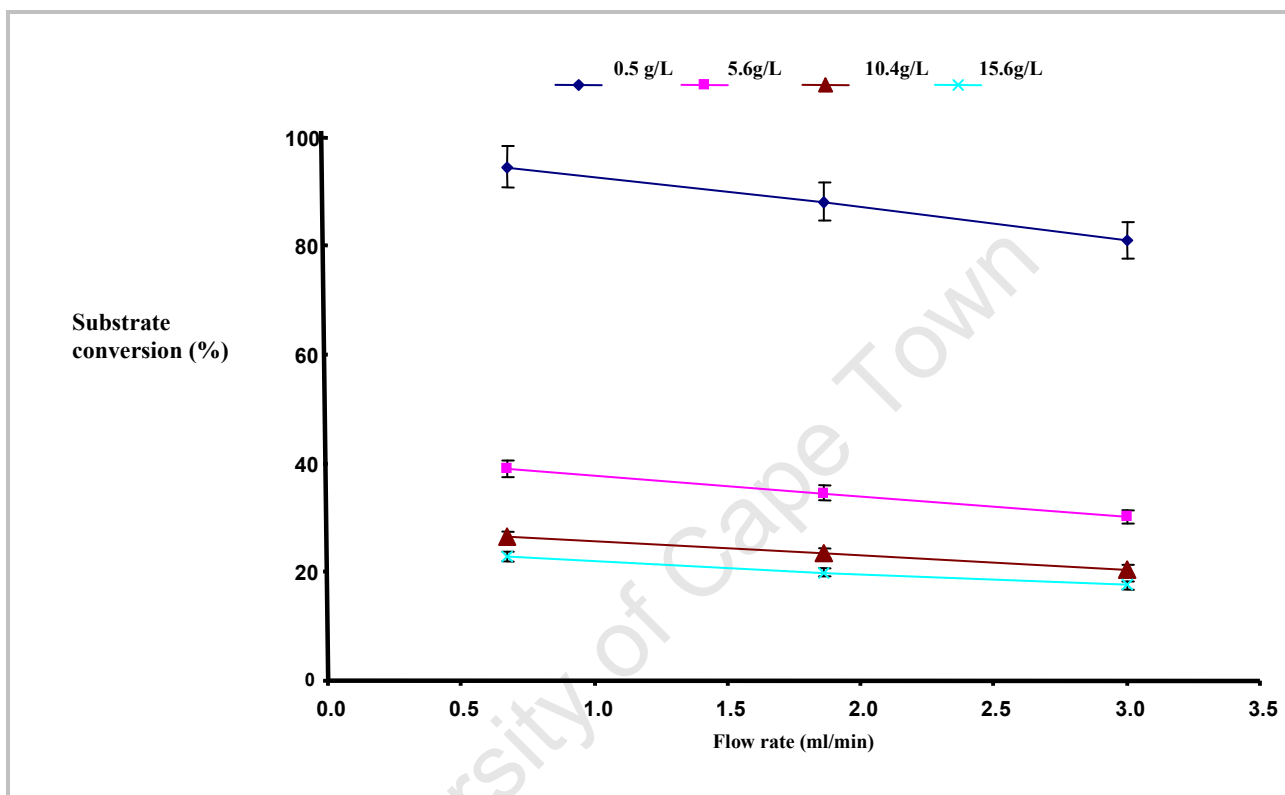


Figure 5.6: Effects of flow rates of the feed on the substrate conversion in packed-bed reactor at 50°C at constant reactor volume, but varying substrate concentrations. Substrate conversion is calculated as a percentage of the total moles of substrate converted into product and the total moles of the initial substrate fed into the reactor per unit time for a continuous reactor.

Experiments at various flow rates of the substrate feed were carried out to obtain the relationship between the volumetric productivity and the flow rates of feed substrate. The volumetric productivity of the PBR increased with increasing flow rate for all substrate concentrations to a maximum volumetric productivity of 48.8 g/L/h at flow rate of 3 mL/min and residence time of 2.5 min (Fig. 5.7). The volumetric productivity values are comparable with values reported in literature bioconversion processes and occurred at substrate concentrations far from the inhibitory concentration (300 mM) for the immobilized *G. pallidus* RAPc8 NHase. The results mean that

significant amounts of desired product were obtained at 3 mL/min, which gave a relatively short residence time that could be of industrial significance. Generally, it may be concluded that a substrate feed rate (flow rate) could be used as a control parameter for the continuous production of nicotinamide in a packed bed reactor.

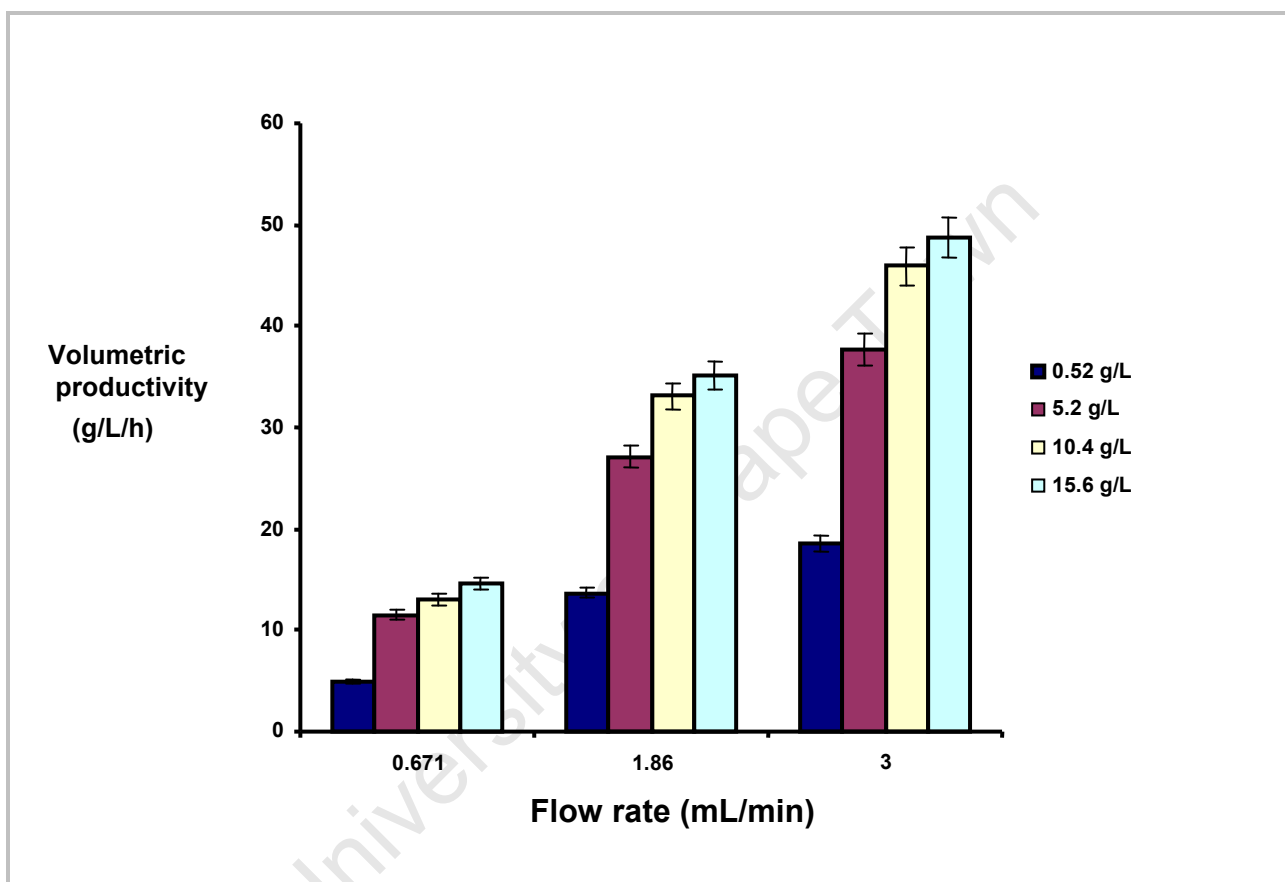


Figure 5.7: Effects of flow rates on volumetric productivity in packed-bed reactor at 50°C at different substrate concentrations (0.52, 5.2, 10.4 and 15.6 g/L). The volumetric productivity Q_p is defined as the ratio of is amount of product P (g) to is volume of reactor V , (L) and time t (h) at the end of an operation.

A summary of effects of substrate concentration and flow rate (mean residence time) on substrate conversion and volumetric productivity is presented in Table 5.2. Overall, despite increase in the volumetric productivity of the packed bed reactor in all experiments conducted, the percentage substrate converted per reaction was declining. A number of factors may be considered in order to improve the conversion rate of the system. The low conversion, therefore, may be improved by

increasing the biocatalyst loading in the reactor that will increase the bed height. The effect of increasing the biocatalyst load in the PBR was subsequently investigated and details of the results on varying amounts of biocatalyst loading are discussed in Section 5.3.2.3.

Table 5. 2: Effects of substrate concentration and flow rate (mean residence time) on substrate conversion and volumetric productivity.

Substrate g/L	Substrate mM	Flow rate, F (mL/min)	Residence time (h ⁻¹)	% substrate conversion	Volumetric productivity g/L/h
0.5	5	0.7	0.186	94	4.9
		1.9	0.068	88	13.7
		3.0	0.042	81	18.6
5.2	50	0.7	0.186	39	11.5
		1.9	0.068	34	27.1
		3.0	0.042	30	37.7
10.4	100	0.7	0.186	26	13.0
		1.9	0.068	23	33.1
		3.0	0.042	20	45.9
15.6	150	0.7	0.186	22	14.5
		1.9	0.068	19	35.1
		3.0	0.042	17	48.8

5.3.2.3 The effect of bed height (enzyme loading) on volumetric productivity of the PBR.

The effect of bed height was investigated by varying the amounts of immobilized biocatalyst packed into the column reactor. Masses, 5 g (1.88 U), 10 g (3.75 U) and 15 g (5.63 U) of immobilized biocatalyst were packed into the reactor resulting in different bed heights 2.4 cm,

4.5 cm and 5.6 cm, respectively. A substrate concentration of 15.6 g/L (equivalent to 150 mM) was chosen for the study and was pumped through the packed-bed reactor at 3mL/min (corresponding to a residence time of 0.042 h). As observed in Fig. 5.8, the volumetric productivity decreased with increased bed height. A maximum volumetric productivity (45.9 g/L/h) was observed at a bed height of 2.4 cm (corresponding to a 5 g mass of biocatalyst), and the lowest volumetric productivity (31.7 g/L/h) was recorded at bed height of 5.6 cm (equivalent to 15 g biocatalyst). These results indicate that the majority of the biocatalytic activity was occurring within a small portion of the PBR between the inlet and the length < 2.4 cm, which could have been enough to attain a nearly complete conversion in 0.042 h (2.5 min). The upper section above 2.4 cm of the reactor, was thus only contributing marginally to total product formation and this represents an inefficient use of the bioreactor volume under the operating conditions. In literature, similar effects have been observed in cases when a packed bed reactor was used. For example, Xi & Xu (2005) observed a decrease in volumetric productivity with increase bed height during preparation of enantiopure (S)-ketoprofen by immobilized *Candida rugosa* lipase in a packed bed reactor. In a separate finding, Chen *et al.* (2005) also reported a decline in the azo-dye decolorization in a continuous packed bed bioreactor when the bed length containing gel-entrapped cells of *Pseudomonas luteola*, was increased. Lastly, Mandaavilli (2000) presented a model that predicted ethanol production in a packed bed reactor and showed that as the product concentration increased along the length of the reactor, the kinetic rate and overall conversion efficiency decreased, and thus concluded that highest conversions are expected at the reactor inlet where the substrate concentrations are high and product inhibition is minimal. Moreover, the mass transfer resistance and higher pressure drop due to increase in bed length may also have influenced the reactor productivity. Therefore, it was concluded that, up to a certain height (approximately 2.4 cm) through the packed bed reactor, the biocatalyst remained under-utilized at the given flow rate. The apparent increase in biocatalyst loading should have been followed by adjustment in flow rates to allow for the mass transfer resistances through long bed heights.

Overall, the decreased bed height would lead to a smaller length-to-diameter ratio that is normally advantageous for an industrial process where smaller reactor volumes are favoured over longer ones, which perhaps affords a long retention times.

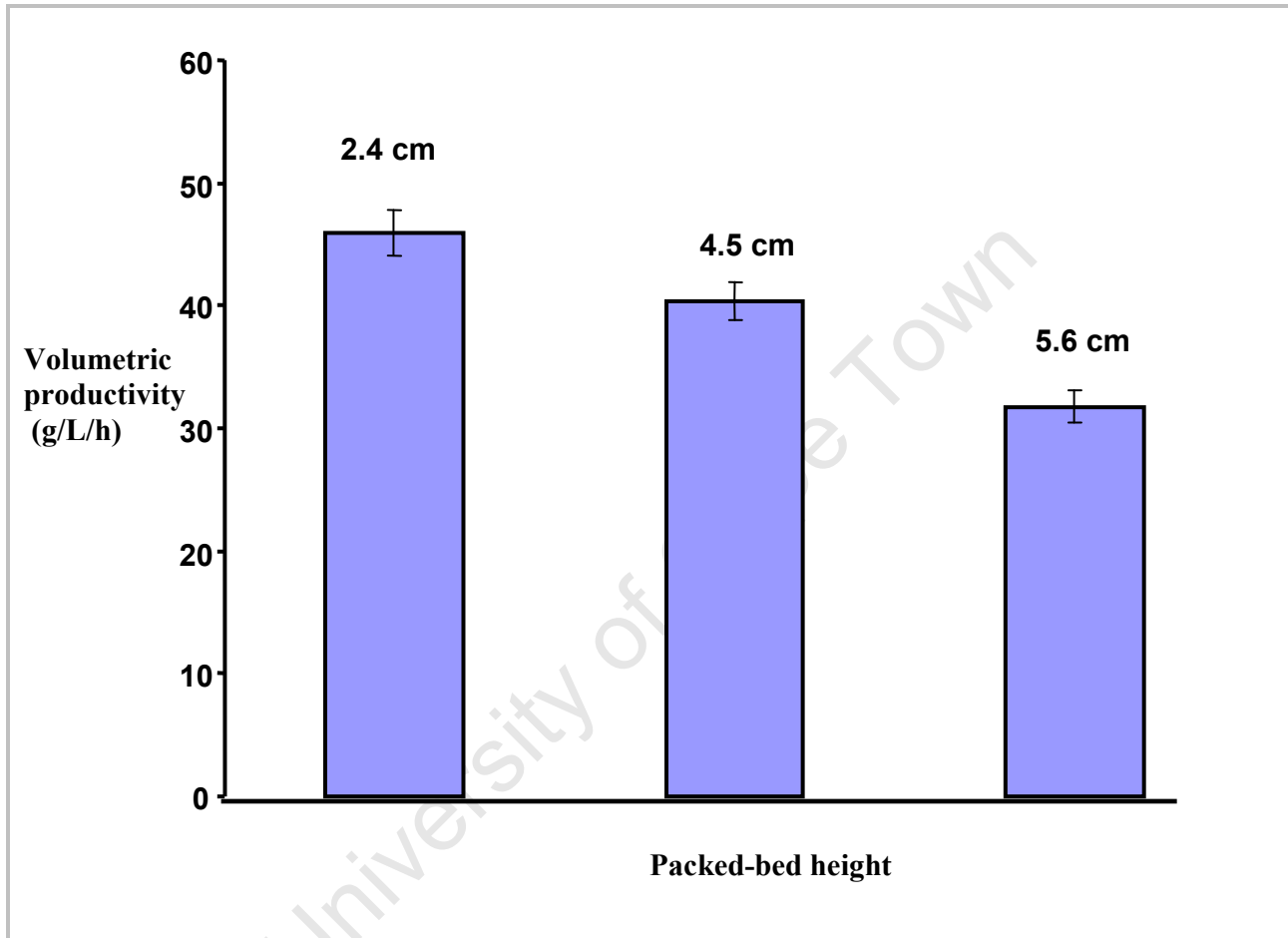


Figure 5. 8: Volumetric productivity at various bed heights. Maximal productivity 45 g/L/h obtained at a height 2.4 cm (5 g mass biocatalyst), while the productivity declined with the increase in amount of biocatalyst added to the column. The volumetric productivity Q_p is defined as the ratio of is amount of product P (g) to is volume of reactor V , (L) and time t (h) at the end of an operation

5.3.2. 4 Investigation of the effect of temperature on the volumetric productivity of the PBR

One important operational variable in bioreactor design is the operational temperature as it affects both the reaction rate and the solubility of substrates. As observed earlier in the study, the NHase

gave higher conversion rate at elevated temperatures. Thus, it was important that the effect of temperature be investigated for the packed-bed reactor. In this study, the temperature was changed between 25 and 50°C while keeping substrate concentration, flow rate and amount of biocatalyst constant. As shown in Fig. 5.9, improved biocatalytic reactions were obtained at 50°C for each time period tested. However, in the case of lower temperature, at 25°C, the product concentration became very low and about 40 % decrease in product concentration was observed at each time period. The higher operation temperature of the immobilized-NHase PBR system would be advantageous for the application of the biocatalyst in an industrial process, since higher temperatures would improve the solubility of 3-cyanopyridine and subsequently, other less aqueous soluble substrates.

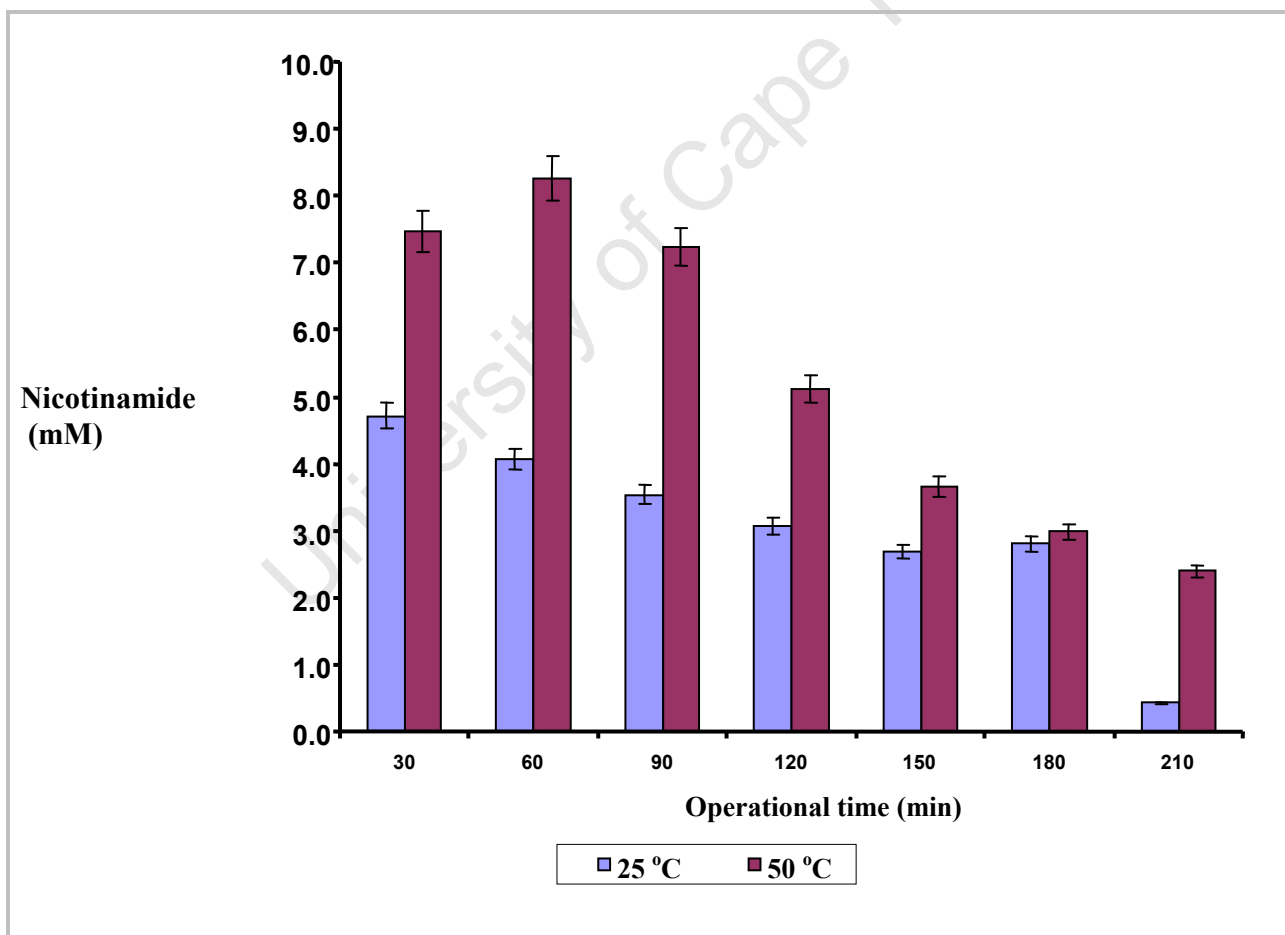


Figure 5. 9: The effect of temperature on the activity of the Eupergit®C immobilized *G. pallidus* RAPc8 NHase in a packed-bed reactor (5 g, 1.88 U) at 0.5g/L substrate feed, and flow rate of 3mL/min.

5.3.2. 5 Comparison of the operational stability of the immobilized RAPc8 NHase in the PBR and a CSTR

Earlier experiments in Section 5.3.2.1, 5.3.2.2 and 5.3.2.3 showed that the PBR was capable of high volumetric productivities under the operation conditions of high substrate concentration (15.6 g/L), short mean residence time (0.042 h^{-1}) and small reactor volume (7.5 cm^3). The objective of this experiment were to evaluate sustained operation under this set of conditions ($S=15.6\text{ g/L}$, $\text{time}=0.042\text{ h}^{-1}$, $V=7.5\text{ cm}^3$) and to evaluate the relationship between substrate conversion and biocatalyst deactivation. To provide a comparison, the process was also operated in a CSTR of volume 30 mL, incorporating the same amount of biocatalyst (5 g)

Thus, 3-cyanopyridine substrate (15.6 g/L or 150 mM) was continuously fed at 3.0 mL/min into the PBR and CSTR, respectively, and the reactors were run for 3 residence times before achieving steady state. The substrate conversion–time course plots are shown in Fig.5.10. It is clear that substrate conversions were nearly constant with time for the first one and half hours for both PBR and CSTR, and the levels of substrate conversion were reasonably similar. While the packed bed reactor showed a highest conversion of 85%, the CSTR gave a higher conversion for the first 120 min (the spikes in substrate conversion for the CSTR were attributable to temporary product accumulation due to blockages of the product outlet tubing in the reactor). The substrate conversion in both reactors decreased with increasing operation time; for example, the substrate conversion was observed to be 67.7 % and 58 % for the PBR and CSTR respectively, after 420 min of operation. This represents a considerable decrease in the NHase activity and was likely to have been due to deactivation of the enzyme under the somewhat stringent conditions. In the CSTR, these would include shear stress in addition to the increasing concentration of product and relative ly high operational temperature. It is significant that the decline in conversion was lower in PBR.

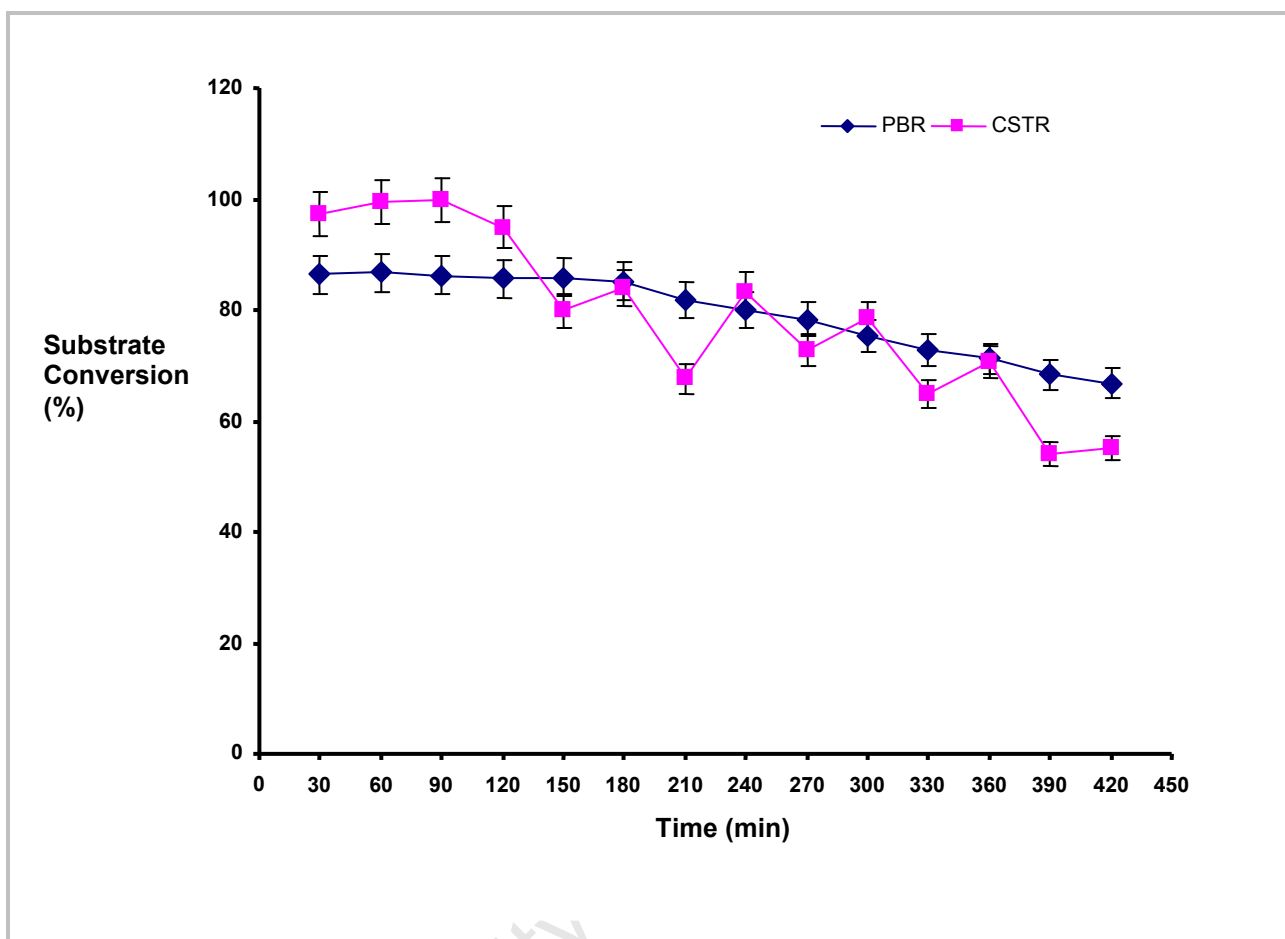


Figure 5. 10: Comparison in operational performance between the PBR and CSTR in production of nicotinamide at 50°C by immobilized *G. pallidus* RAPc8 NHase. Substrate concentration of 0.56 g/L, bed height of 2.4 cm, and flow rate of the feed solution at 3 mL/min.

5.3.2.6 Determination of the deactivation constant of immobilized *G. pallidus* RAPc8 NHase in packed bed reactor

Because the biocatalyst stability is a fundamental aspect in reactor performance, investigating the deactivation of the immobilized NHase in the packed bed reactor was of great importance. Several factors that may lead to activity loss of an immobilized enzyme include unfolding of the protein structure, permanent blockage of enzyme active sites, steric hindrance, or effects of immobilization (Henley *et al.*, 1986). The operational stability of a biocatalyst is commonly estimated by the half-life and the thermal deactivation constant, k_d (Owusu & Berthelon, 1993;

Calsavara *et al.*, 2000). Biocatalyst inactivation in the packed bed reactor for the NHase system was therefore estimated by determining the deactivation constant and half-life using the natural log of relative activity % against time plot (Fig. 5.11). For the NHase in the packed-bed reactor, a k_d value of 0.007 was obtained, and an apparent half-life value of 990 min (16.5 h) was determined.

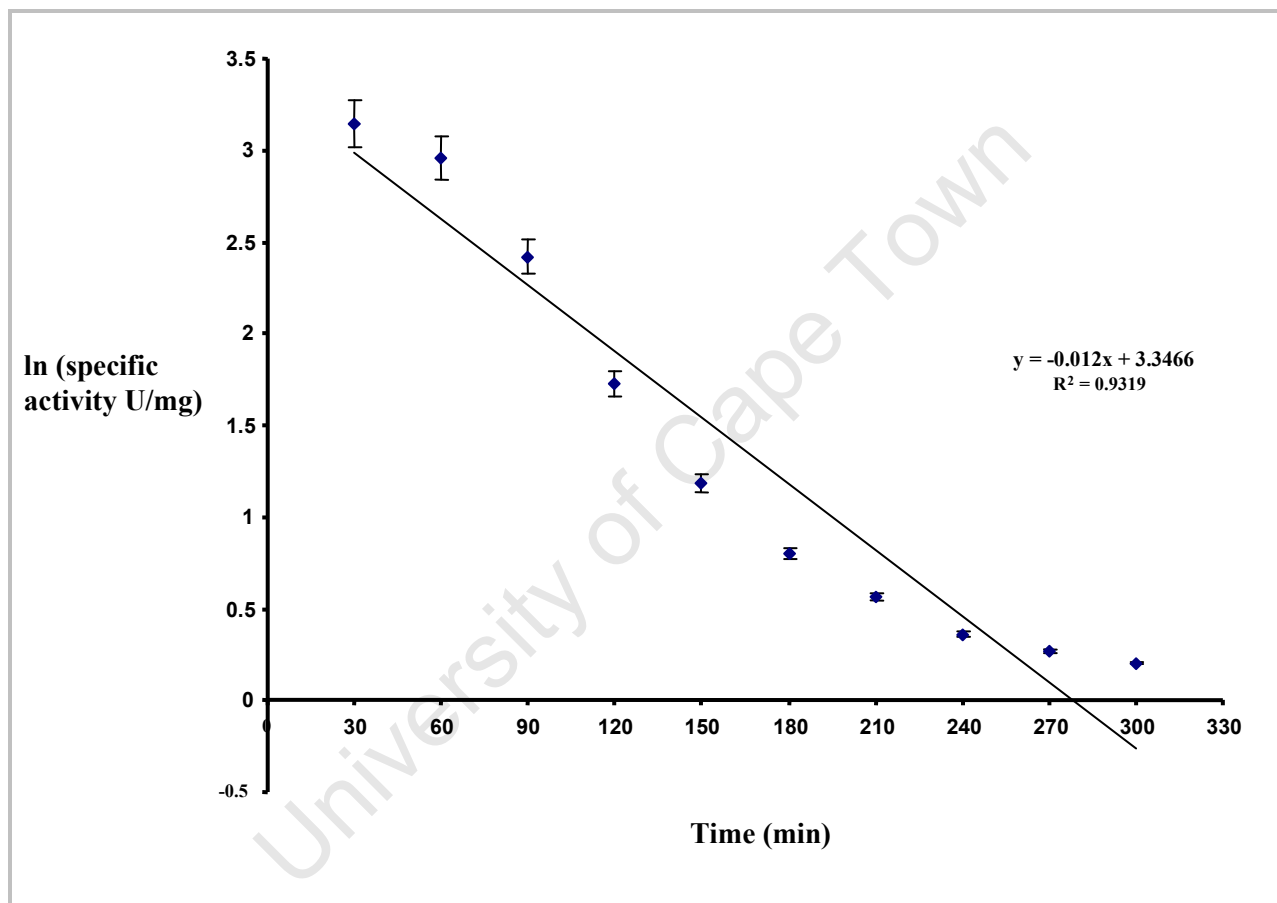


Figure 5. 11: Semilog plot of ln (relative activity) against time for the optimal condition from the reactor performance analysis. E_a was calculated from the slope ($-E_a/R$), using Equation 4.5.

5.4 CONCLUSIONS

In this study, the Eupergit®C-immobilized *G. pallidus* RAPc8 NHase was characterised in order to determine the optimal biocatalytic conditions in a packed-bed reactor. The percentage substrate conversion and volumetric productivity of the NHase-catalysed conversion of 3-cyanopyridine in the PBR were found to be dependent on substrate concentration, flow rate, amount of biocatalyst (or bed height), and operating temperature. The optimum reaction time required for optimal NHase activity was found to be 0.042 h. The apparent optimum flow rate of the immobilized NHase in the packed bed reactor used here was 3 mL/min, while the optimum biocatalyst loading was 5 g (which translated to the shortest bed height of 2.4 cm). The apparent temperature optimum for the Eupergit®C-immobilized NHase in the packed bed reactor was 50°C. The volumetric productivity increased with increased substrate concentration, and volumetric productivity as high as 48.8 g/L/h was attainable. The study demonstrated that a substantial increase in volumetric productivity can be obtained at increased substrate feed concentrations. For example, an increase of almost 3-fold in volumetric productivity was obtained with respect to substrate concentration increment from 0.5 to 15.6 g/L (or 5 mM to 150 mM). On the other hand, percentage substrate conversion decreased with increasing substrate concentration and this can be attributed to a decline in enzyme activity at high substrate concentrations. In bioprocess engineering, volumetric productivity is a useful term for describing efficacy of a process, as it indicates the average production capacity per unit volume and time of the bioreactor. The standard method of using substrate conversion does not indicate the physical amount of product in a bioreactor, but rather a ratio, so it is less useful. Overall, these results indicate an improvement in the volumetric productivity over values reported in the literature for the continuous production of nicotinamide when the immobilized whole cells were used (Table 2.2).

The process using the immobilized NHase was found to favour a PBR with a shorter bed height (< 2.4 cm). The volumetric productivity in the packed bed reactor having longer bed heights were low due to mass transfer resistance and higher pressure drops caused by increase in bed length. It was deduced that the productivity of the system could be improved by using a combination of increased flow rates and length-to-diameter ratio of the bioreactor. Since it is known that liquid flow conditions inside the packed bed column reactor dictate how it performs, thus the flow rate

is an important variable for improving the packed bed reactor performance (Gostick *et al.*, 2004). A detailed study of the varying amounts of the biocatalyst in the packed bed reactor could be addressed further in possible future work.

The operational stability of Eupergit®C-immobilized NHase in the PBR was compared in a performance of CSTR at a similar flow rate, volume and substrate concentration. The average substrate conversions of the NHase in both the PBR and CSTR declined steadily with time. A rigorous comparison between the PBR and CSTR is difficult due the existence of external mass transfer limitations in the latter. However, the PBR was found to be somewhat more effective (as it exhibited a more steady, albeit declining, activity) than the CSTR which had a rapid erratic loss in enzyme activity. This observation underlines the importance of the PBR system. The reactor seems a promising alternative for the hydration of nitrile by immobilized NHase from *G. pallidus* RAPc8. This system could be improved by further investigating properties of the biocatalyst including, (i) increase in the beads size of the biocatalyst which allows for the loading per unit volume to be maximized while retaining a low pressure drop through the reactor, thus offering good accessibility of the substrate to the biocatalyst surface (Lathouder *et al.*, 2004) and (ii) a higher flow rate to minimise mass transfer resistance (Gostick *et al.*, 2004).

In this chapter, different possibilities were explored in the design, operation and analysis of the packed bed reactor. Considerable progress has been achieved in the application of an immobilized NHase application in a continuous reactor system. To date, no such system involving isolated and immobilized NHase has been reported in literature. The most important conclusions to be drawn from these results include demonstration that optimization of packed bed reactor in terms of substrate concentration, flow rates, bed height and operation temperature could further improve productivity. The technical and operational feasibility of using isolated NHase immobilized on Eupergit®C has been conclusively established for the packed-bed reactor and this study has therefore shown the potential to provide a practical, cost effective bioconversion process for the production of nicotinamide.

CHAPTER 6

GENERAL DISCUSSION AND CONCLUSION

The primary aim of the work reported in this thesis was to investigate the application of the thermostable *G. pallidus* RAPc8 NHase as an isolated immobilized enzyme for the production of nicotinamide as a model product which could potentially be used industrially. The work focused mainly on optimization of the conditions for the use of the enzyme. *G. pallidus* RAPc8 NHase was chosen as the source of enzyme, based on the biochemical characteristics of the NHase that favoured its ease of development into an industrial biocatalyst. First, the NHase was isolated from a moderate thermophilic bacterium which meant the enzyme was thermostable. Biocatalyst thermostability would enable operation outside the bacterial cell and at higher operation temperature that would be advantageous for industrial process due to higher reaction rates, increased substrate solubility leading to higher space-time yields, lower viscosity and reduced risks of contamination (Bruins *et al.*, 2003). Second, the *G. pallidus* RAPc8 NHase was reported to have a higher preference for 3-cyanopyridine (the substrate in the nicotinamide synthesis) compared to other reported NHases (Cameron & Cowan, 2005). Given the industrial importance of nicotinamide, it was of interest to further investigate its effective production. Thirdly, the broader substrate preference for the *G. pallidus* RAPc8 NHase offers potential for production of numerous amides.

In the development of a bioprocess, the biocatalyst should be produced from large quantities of the biomass with high levels of enzyme activity in a host organism that is easy to culture in a simple medium. The isolation, cloning and overexpression of *G. pallidus* RAPc8 NHase in *E. coli* BL21 (DE3) strain had been subject of earlier studies (Pereira *et al.*, 1998; Cameron & Cowan, 2005). In previous work, the *G. pallidus* RAPc8 NHase was partially characterized, analysis of its molecular catabolism operon had been conducted, and crystallization for X-ray structure analysis has been achieved (Tsekoa *et al.*, 2004). In this study, it was shown that production of *G. pallidus* RAPc8 NHase was possible through adapting previously reported protocols, to automated fermentation. Recombinant *E. coli* BL21 (DE3) harbouring the NHase genes was cultivated using LB medium in a 1L shake flask and a 5L BioFlo fermenter. Comparison of

growth in the two vessels showed that 5L BioFlo fermenter provided a similar biomass yield (3.26 g/L) compared to the 1L shake flask (3.40 g/L) on the basis of wet cell weight, which meant that the enzyme production had the potential of being scaled up reproducibly. *G. pallidus* RAPc8 NHase expression in *E.coli* BL21 (DE3) is known to be activated by addition of 0.1 mM cobalt ions 30 min prior to induction. Addition of cobalt ions to the culture medium is necessary for both catalytic activity and synthesis of NHase (Cameron & Cowan, 2005). Recombinant protein expression was induced with IPTG to 0.4 mM final concentration. For laboratory-scale production, IPTG-inducible promoters are widely used. However, they are expensive and future work might focus on finding an alternative method of induction more suitable for large scale production.

The NHase was purified by using the procedures described in literature (Pereira *et al.*, 1998; Cameron & Cowan, 2005). Although the overall purification of the enzyme was successful, with a yield of 67%, this still indicates that part of the activity was lost due to inactivation of the NHase. Generally, multi-step enzyme purification procedures result in relatively low yield of active enzyme partly due to its susceptibility to oxidizing conditions and proteases degradation. However, the heat treatment method provides a stable and nearly pure NHase in high concentration, and this could be useful in purification of industrial biocatalyst; it would be cost-effective since very pure enzyme may not be necessary in the industry.

The purified *G. pallidus* RAPc8 was characterised in terms of its molecular weight and number and size of subunits. SDS-PAGE analysis revealed two protein bands representing subunits of molecular weight 28 kDa and 29 kDa for the α and β -subunits of the NHase, respectively. NHases typically exist as $\alpha\beta$ dimers, and the NHase has a relative molecular mass of approximately 110 kDa. This result supports earlier work on the same enzyme in its native host (Pereira *et al.*, 1998).

One of the objectives of this study was to identify the optimal reactions conditions for the *G. pallidus* RAPc8 NHase. Firstly identification and analysis methods for the products and unreacted substrate were achieved by use of HPLC. Thus, single peaks of different retention times (3.86 min for nicotinamide and 6.38 min for 3-cyanopyridine) were found, and analysis of

the products and substrates was possible by combination of use of appropriate wavelength (235 nm) and mobile phase (acetonitrile-10 mM KH_2PO_4 - H_3PO_4) buffer (1:4 v/v). These results show that 3-cyanopyridine was successfully converted to nicotinamide without carboxylic acid as by-products. To date, all industrial process which use NHases, apply immobilized whole cells in their processes (Thomas *et al.*, 2002). The use of whole cell biocatalysts has the disadvantages of mass transfer transport limitations of substrates and products through the cell membrane (Ni and Chen, 2004). Furthermore, the use of whole microbial cells leads to formation of a number of secondary metabolites which may lead to product contamination (Yin *et al.*, 2000). The use of purified NHases could thus avoid some of these shortcomings of the whole cell processes and it offers potential for development of a cost-effective process, since there will be no purification of products required.

Further studies were conducted to establish the exact amount of enzyme, reaction time and substrate concentrations to be used in characterization and optimization investigations. Under these conditions, assays using purified enzyme (100 μL , 0.14 mg) in 3 mL test solutions, 50 mM substrate (3-cyanopyridine) and 5 min reaction time were established and used in further investigations.

After the preliminary reaction conditions had been optimised, various experiments to give the information regarding the intrinsic properties of the NHase and its stability were conducted. The optimal temperature for the activity of NHase during the biocatalytic reaction was found to 60°C and the optimal pH was found to be 7. Thermal stability studies on the NHase showed considerable stability up to from 20°C to 50°C. This stability profile is similar to that reported by others for thermophilic NHase from *G. pallidus* Dac521 (Cramp *et al.*, 1997). The higher temperature optimum is favourable for industrial processes, as solubility of substrate (e.g. 3-cyanopyridine) is increased, promoting a higher rate of substrate conversion. In the investigations of optimal substrate concentration, the NHase activity increased with initial substrate concentration (0 to 100 mM), but at higher concentrations the rate of reaction declined significantly. The substrate inhibition effect was a significant challenge to the research in terms of productivity.

The role of various monovalent and bivalent metal ions in the activity and stability of the NHase were studied. It was found that the addition of low molecular weight metal ions such K^+ , Mg^{2+} and Ba^{2+} , and other ions including Co^{2+} and Fe^{2+} to the reaction medium induced higher enzyme activity, while transition metal ions Mn^{2+} , Zn^{2+} and Cu^{2+} inhibited the activity of the NHase. Generally, the inhibition and stabilization of the NHase by the metal ions were concentration-dependent, with most cations exerting their effects above 8 mM. Nonetheless, metal ion inhibition can occur when the metal ions, such as Cu^{2+} and Zn^{2+} , interact with the cysteine residue in the NHase active site and interfere with its catalytic function.

Application of NHases in nonaqueous media has been reported by a number of researchers (Kobayashi & Shimizu, 2000). In our study, the *G. pallidus* RAPc8-catalysed reactions were most successful in presence of water-immiscible organic solvents. The marked increase and retention of activity in the presence of the water-immiscible co-solvents was an important result for the *G. pallidus* RAPc8 NHase since it has a remarkably broad substrate range (Cameron & Cowan, 2005) and could be used in a range of processes, including with non-aqueous soluble substrates and/or products.

The kinetic parameters were determined in order to develop some understanding of the performance characteristics of the NHase. The V_{max} and K_m values estimated for 2-cyano, 3-cyano and 4-cyanopyridine substrates by initial rates of reaction (differential) method and data fitted to linearised Hanes-Woolf. Of these, the least-square fits were compared, and the Hanes-Woolf plot was selected on basis of the minimal deviation from linearity in the data. The Michaelis constants K_m were found to be: 2-cyanopyridine (2.46 mM), 3-cyanopyridine (8.61 mM), 4-cyanopyridine (4.5 mM). The V_{max} values for the soluble NHase were estimated as 45.6, 31.3, and 13.1 $\mu\text{mol}.\text{ml}^{-1}.\text{min}^{-1}$ respectively for substrate 3-cyanopyridine, 2-cyanopyridine, and 4-cyanopyridine. The results of these kinetic studies show that 3-cyanopyridine is a better substrate for the *G. pallidus* RAPc8 NHase than other heteroaromatic substrates. These kinetic data may be useful in future studies, in predicting the performance of a process for the synthesis of nicotinamide, and other potential products. The second aim was investigation to understand the basis for such a difference in substrate specificity of the *G. pallidus* RAPc8 NHase on the heteroaromatic cyanopyridine substrates. The insight into substrate specificity of *G. pallidus*

RAPc8 NHase thus will help select the best positioned amino moiety in the heteroaromatic ring of nitrile substrates.

Various immobilization materials and methods were investigated to further improve the stability of the NHase. Results from the immobilization of the *G. pallidus* RAPc8 NHase demonstrated the importance of covalent binding and cross-linking for improving the performance of the biocatalyst. For example, among the six techniques applied in NHase immobilization, it was found that only covalent immobilization provided enhanced enzyme activity. Further, the Eupergit®C-immobilized NHase coupled with EDAC cross-linking showed the highest immobilization efficiency of 92.3 %. The biocatalyst was re-used in 8 cycles while maintaining 85.7% of its initial activity. It was also found to be more thermostable up to 60°C for 120 min, retaining 80% of its initial activity. The half-life of the immobilized NHase was found to be 1155 min (19.3 h) at 40°C as compared with the soluble form which had a half-life of only 364.8 min (6.1 h) under the same conditions. Furthermore, the immobilized preparation showed increased tolerance to higher substrate concentration from 100 mM to 300 mM for the free and immobilized NHase, respectively. However, it was also useful to perform a more detailed characterization of substrate inhibition kinetics, both of the free and of the immobilized preparation. Overall, these results showed a very significant increase in thermostability of the immobilized NHase compared to the free enzyme and other NHases studied, and present positive implications for the potential feasibility of nicotinamide synthesis from NHase-catalysed hydration of 3-cyanopyridine.

After the conditions for use of the immobilized enzyme were optimised, some of the parameters under batch mode for nicotinamide production from 3-cyanopyridine were incorporated into the continuous production studies. In the case of other parameters such as flow rate, these were estimated by using a packed-bed reactor design equation.

The Eupergit®C-immobilized *G. pallidus* RAPc8 NHase was used in a packed-bed reactor (PBR), in continuous operation mode which is novel and has not been reported in literature. Using a substrate concentration of 15.6 g/L, the Eupergit®C-immobilized NHase biocatalyst demonstrated a volumetric productivity of 48.8 g/L/h (residence time = 0.042 h; 5 g biocatalyst).

The volumetric productivity achieved in this study falls within the range of values reported in literature (4 to 80 g/L/h) for biotransformation processes involving amide production (Straathof *et al.*, 2002), which is important result considering that no such report of purified immobilized NHase used in a packed-bed reactor has previously been made. The volumetric productivities obtained in literature were achieved using more complex whole cell systems and included recycle loops and pH controllers (Thomas *et al.*, 2002). These results indicate the scope of utilising Eupergit®C-immobilized NHase for continuous commercial production of nicotinamide from 3-cyanopyridine.

Investigations into the varying bed height of the PBR system, on the other hand, resulted in decreased volumetric productivity as the bed height increased. This has been attributed to external transport limitation and high pressure drop across the reactor with increase in the length of the bed. However, such operational constraints are generally reduced by increasing the flow rates of the substrate through the column and changing the column reactor height-to-diameter ratio that subsequently increase the linear velocity. From a practical view point, it would be advantageous to have a process having a relatively smaller bed height (smaller reactor volume) and higher volumetric productivity.

The steady decline in substrate conversion, observed after 150 min of application of the *G. pallidus* RAPc8 NHase in the packed-bed reactor, indicated that the NHase activity was insufficient for prolonged use. The loss in substrate conversion observed could be a problem associated with enzymatic reactions in continuous reactors, which might result from a number of factors such as biocatalyst leakage from support carrier, denaturation of enzyme due to effect of pH and temperature, and substrate or product inhibition. One of the disadvantages of biocatalyst application in industrial processes is that they lose catalytic power during the reaction. However, the operation stability of a biocatalyst in a continuous reactor system is easily estimated by its half-life (the time at which the catalytic activity is reduced by half). The economic feasibility of a process may hinge on the useful life time of the enzyme biocatalyst. The Eupergit®C-immobilized NHase had a half-life of 16.5 h under operation, indicating a good stability comparable to other biocatalysts reported in the literature for the production of amides (Cowan *et al.*, 2003). An alternative investigation in the operational stability of the *G. pallidus* RAPc8

NHase in a CSTR under similar experimental conditions with the PBR, over the same period of time, did not yield significantly better results from those reported before in this study for the PBR.

In conclusion, this thesis has described the characterisation and development of a biocatalyst for the synthesis of nicotinamide from 3-cyanopyridine. The study was planned to design an effective process through development of a biocatalyst with improved catalytic properties coupled with enhanced stability. The enhancement in the performance of the immobilized *G. pallidus* RAPc8 NHase, namely, the facility for re-use, increased stability and increased substrate tolerance, suggested that the efficient hydration of higher than previously used concentrations of 3-cyanopyridine in a continuous packed-bed enzyme reactor would be feasible. Since the immobilization of purified NHase and its subsequent use in a packed-bed reactor have not been reported before, it is envisaged that data generated in this thesis will contribute towards effective biocatalytic production of nicotinamide and other amide commodities. In order to apply this system in a scaled-up, cost-effective industrial process, certain draw-backs in the system would need to be addressed in future work which is suggested in the next section.

FUTURE WORK

Due to the preliminary nature of some of the work in this study, further work may be conducted in several areas that remain open for exploration. Future work would likely progress in the following direction:

1. *E. coli* BL21 (DE3) cell production and enzyme expression

Further study in the production of a high cell density of recombinant *E. coli* BL21 (DE3) and achieving a high expression of the NHase is required as the batch cultures fermentation was previously seen to produce low cell density and specific activity. In order to increase the *E. coli* BL21 (DE3) cell density biomass and specific activity of NHase, fed-batch techniques are proposed in cultivation and can be used for the purpose. The cultivations by fed-batch will have to be supplemented adding growth medium (yeast extracts and tryptone as sources of C and N, respectively) during the fermentation. A number of considerations could be made to the design and operation of the fed-batch fermentor, in particular:

- Different nutrient feed rate to be investigated in the cultivations of *E. coli* (BL21) DE3 and the results to be compared by looking at the maximum specific activities and high cell biomass.
- Care to be taken to reduce viscosity during addition of nutrients to the culture.
- Improved oxygen transfer by increase agitation and strong aeration.
- Strategic plan for continuous addition of inducer (IPTG) and activator metal ions (Co^{2+}) also need to be considered.

Fed-batch fermentations have successful been employed in industrial processes involving production of recombinant proteins, thus a significant improvement in *G. pallidus* RAPc8 NHase production is expected.

2. Stabilization of NHase by chemical modification method

It would be of interest to attempt to stabilize the *G. pallidus* RAPc8 NHase by chemical modification or cross-linking. For example, chemical modification of selected amino acid residues on the NHase surface that do not form part of the active-site, would enhance the enzyme stability. This method might be especially revealing for *G. pallidus* RAPc8 NHase as it exists as a heterotetrameric structure. Several bifunctional reagents can be used in the stabilization the heterotetrameric NHase against dissociative deactivation by intra-molecular and inter-molecular subunit cross-linking that subsequently lead to formation of aggregates of water-insoluble enzymes. In particular the following can be considered in future studies:

- In this study typical reagents such as glutaraldehyde, carbodiimine, dicarboxylic acids and anhydrides can be tested for the chemical modification as they have been previously described in the chemical modification of many enzymes.
- Glutaraldehyde can be used to couple side-chain ϵ -amino group of lysine residues on the NHase surface. Alternatively, a carbodiimide could be linked to a carboxyl group on the protein surface to form intermediates that would be subsequently be coupled to various amino groups such as diethyl amine.
- Numerous bifunctional reagents with varying spacer arm length can be used to stabilize the NHase and the stabilization efficiencies compared.

Chemical modification of residues on the NHase surface would introduce high density of chemical functional groups (primary amino and carboxyl groups) that can be later permit a wider range of support linkages and general stabilization of the enzyme structure.

3. Coating the calcium alginate-immobilized NHase beads

Renewed attempts to obtain a better stabilized calcium alginate entrapped *G. pallidus* RAPc8 NHase can be studied by coating the biocatalyst with a polymeric capsules γ carrageenan or chitosan to stabilize it against reactions at higher temperatures. Since using encapsulation (or coating) method has large influences on the enzyme performance, attention to be paid to the following:

- the nature of monomer used in coating,

- the thickness of the membrane might lead to diffusion constraints, and
- the pore sizes are to be carefully controlled. Control of the degree of coating is accomplished by adjusting the cross-linking conditions of the coating components and using appropriate materials. For example, materials such as 1, 6-hexane diamine, piperidine, polyphenol, 2, 2-bis (4-hydroxyphenyl) propane, PAA, PEI and chitosan, have successfully been used for many enzymes (Cao and Schmid 2006).

Often, coating is used to enhance the entrapped enzymes by improving stability against mechanical, thermal and deactivation by organic solvents. The NHase would be expected to have high thermostability than previously observed in this study.

4. Further studies on the NHase activity in co-solvent aqueous/organic solvent

The insight into the biocatalysis of the *G. pallidus* RAPc8 NHase in aqueous/organic co-solvents and its higher activities in non-polar co-solvents (*log P* 2 to 4) can be used to investigate whether it is likely that the NHase would perform much better in the presence of organic co-solvents with *log P* values greater than 4. The following further work can be considered:

- Varying percentages of organic solvent in phosphate buffer from 20 to 100% (v/v), reflecting the progressive decreasing water content, could be used to investigate the hydrolytic activity of NHase.
- Promising non-polar organics such as octane (*log P* 4.5), isooctane (*log P* 4.3), n-decane (*log P* 5.6), n-dodecane (*log P* 6.6), tetradecane (*log P* 7.6), and n-hexadecane (*log P* 8.8) can to be investigated.
- The effect of the *log P* values on the *G.pallidus* RAPc8 NHase kinetic parameters. Thus the correlation between the influence of *log P* of a solvent on the V_{\max} , K_m and k_{cat} to be sought.
- the hydrolytic activity of NHase and its stability in organic co-solvents can also be assessed by incubating the NHase in varying aqueous/organic co-solvents (10 to 100% v/v) for a given duration of time upon which the residual activity will be determined at different time intervals.
- The relationship of residual activity against time can then be used to estimate the half-lives of the co-solvents.

Thus, information about the NHase hydrolytic activity, its stability and half-lives in organic media will greatly expand NHase-catalysed transformations in bi-phasic media.

5. Further work on the operational stability of NHase in the packed-bed reactor

Further refinement of immobilized NHase in the packed bed reactor to be studied as the biocatalyst was hardly used higher volumetric productivity for prolonged period. Further investigations in the area would initially need detailed theoretical equations to be developed that will include Michaelis-Menten rate expression to predict the time course of conversion due to enzyme deactivation. Perhaps the following can be considered in future work:

- Multiple mode immobilized reactors such as two-stage, three-stage and four-stage reactors to be considered, and immobilized enzyme deactivation, product yields, substrate conversion, and volumetric productivity are compared among the reactor modes.
- The reactor system with lowest enzyme deactivation and highest productivity can be chosen for future investigations.

This will help in achieving high volumetric productivities as multi-stage reactor systems have shown to be better than single unit reactors if only the temperature control can be provided along the reactor columns.

6. Studies regarding reactor scale-up

It would be of interest to check the industrial feasibility of the immobilized NHase packed-bed reactor by looking at its scale-up. This will require appropriate reactor design to maintain optimal operating conditions in the reactor and provide homogeneous reaction without large pressure drops and heat transfer within the bed. In addition, particular attention should be paid to amount of immobilized biocatalyst to be used, reactor volume, and flow rate and residence time of substrate within the reactor. Typically, the following can be done:

- The amount of biocatalyst can be increased 10 times, and it is likely the increase in size would favour higher product yield;
- While smaller reactor volumes are normally desirable for improved productivity, the length and diameter of the packed bed reactor can be doubled;

- Increase in the reactor size entail increased flow rate (this is important when a reactor is scaled-up as the complex hydrodynamics of the substrate flow and immobilized enzyme differ dramatically at different sizes).
- The maximum residence time of substrate in the reactor has to be maintained as that derived in this study.

Scale-up, though is very much associated with economical view-point, will guide in the establishment of a pilot plant and commercialization of the immobilized-*G. pallidus* RAPc8 NHase process.

7. Studies into the economic feasibility of the NHase packed-bed reactor

An extensive economic feasibility (cost estimation) of nicotinamide production from 3-cyanopyridine using an immobilized enzyme packed-bed reactor involving *G. pallidus* RAPc8 NHase can be conducted. This assessment will build on the scale-up work to check its viability for an industrial process. The primary consideration will be the capital (set up of a plant) and operating cost (running costs). Capital cost includes the price of equipment purchases which would also include upstream units such as autoclaves, inoculum bioreactors, main reactor and auxiliary equipment (pumps, heat exchanges, storage tanks, connectors, and air supplier) and total cost will depend on the number of reactors planned to be used. On the other hand, operational costs will especially include:

- Cost of pre-processing of raw material (3-cyanopyridine) involves chemical conversion of 2-methyl-1, 5-diaminopentane to 3-methylpyridine and its ammoxidization to 3-cyanopyridine,
- Cost of media (Tryptone, yeast extract and sodium chloride),
- Cost of waste product handling,
- Cost immobilization of the NHase is estimated by calculate the cost of support material per kilogram of enzyme (SAR/kg enzyme),
- Productivity cost (kg nicotinamide/kg enzyme) can also be estimated, and
- General expenses which include plant operating labour, administrative, taxes and insurance.

- Another important factor in nicotinamide production is the economical recovery from solution. Among several techniques, evaporation has been more attractive because it separates nicotinamide from reaction mixture has been reported in literature. I recommend that using evaporation recovery on nicotinamide recovery should be used in future studies as it is economically viable.

The overall economic analyses of the immobilized NHase packed bed reactor are possible to answer the questions whether they would provide advantages over conventional processes in the industry today. A detailed economical analysis of a packed bed reactor will determine whether commercialization of the process is possible.

University of Cape Town

APPENDICES

APPENDIX A

Appendix A. 1: Potassium Phosphate ($\text{KH}_2\text{PO}_4/\text{K}_2\text{HPO}_4$) Buffer

1 M potassium dihydrogen orthophosphate (KH_2PO_4). Weigh 68.05 g and dissolve in 500 ml dH_2O

1 M di-Potassium Hydrogen Phosphate (K_2HPO_4). Weigh 87.09 g dissolve in 500 ml dH_2O

Make up separately, autoclave.

Table A.1: Mixture of monobasic dihydrogen phosphate and dibasic monohydrogen phosphate yielding varying range of buffers pH.

pH	Volume of 1 M K_2HPO_4 (mL)	Volume of 1 M KH_2PO_4 (mL)
5.8	8.5	91.5
6.0	13.2	86.8
6.2	19.2	80.8
6.4	27.8	72.2
6.6	38.1	61.9
6.8	49.7	50.3
7.0	61.5	38.5
7.2	71.7	28.3
7.4	80.2	19.8
7.6	86.6	13.4
7.8	90.8	9.2
8.0	94.0	6.0

Table A.2: Mixture of monobasic dihydrogen phosphate and dibasic monohydrogen phosphate yielding varying range of buffers pH.

pH	Volume of 1 M Na ₂ HPO ₄ (mL)	Volume of 1 M NaH ₂ PO ₄ (mL)
5.8	7.9	92.1
6.0	12.0	88.0
6.2	17.8	82.2
6.4	25.5	74.5
6.6	35.2	64.8
6.8	46.3	53.7
7.0	57.7	42.3
7.2	68.4	31.6
7.4	77.4	22.6
7.6	84.5	15.5
7.8	89.6	10.4
8.0	93.2	6.8

APPENDIX B

Appendix B.1: 0.1 M stock solution of IPTG

0.238 g of IPTG dissolved in sterile water to 10 L. Filter sterilize store in 20 x 50 µL aliquots.

Appendix B. 2: 100 µg/mL stock of Ampicillin

0.1 g in 1 mL of dH₂O or 1.0 g in 10 mL of dH₂O

Filter sterilize with 0.22 µm filter. Make up the 10 mL of aliquot into 500 µL each.

APPENDIX C

Appendix C. 1: 30% acrylamide monomer stock for separation and stacking gels

29.2 g acrylamide (PAGE quality) + 0.8 g bis-acrylamide (DGGE + PAGE quality).

Weigh out in 250 mL glass beaker and add 50 mL of dH₂O. Stir or sonicate until fully dissolved. Make up to 100 mL and store in 100 mL schoff bottle at 4 °C in foil. Mark as dangerous.

Appendix C. 2: 10 % Ammonium Persulfate stock for SDS.

Dissolve 0.1 g Ammonium persulfate in 1 ml dH₂O in an epidoff. Store at -20 °C for a short periods i.e. less than 2 months.

Appendix C. 3: Dye for SDS PAGE.

Bromophenol blue dye for SDS Page: (0.1 % Bromophenol Blue), 0.2 g Bromophenol Blue

Add 1.5 ml, 0.1 M NaOH solution (0.1 g NaOH in 25 ml). Make up to 100 ml with dH₂O. Aliquot in 10 mL qualities.

Appendix C. 4: SDS (20%)

Dissolve 20 g SDS in 100 mL sterile water in sterile bottle (weigh out in fume cupboard / wear mask). Filter through 0.22 µm filter into 4 x 25 mL sterile bottles. Label. Do not autoclave or reffridgerate.

Appendix C. 5: Staining solution for SDS Page.

0.125 % Coomassie Blue, 50 % MeOH, 10 % Acetic Acid. Make stock solution by dissolving 2 g Coomassie Blue R250 in 200 ml dH₂O. Filter through whatman No. 1 paper in long stem funnels. Make working solutions by taking 62.5 ml stock, 250 ml MeOH and 50 ml Acetic Acid. Make up to 500 ml adding 137.5 ml dH₂O.

Appendix C. 6: Destaining solution for SDS Page

5mL methanol, 7.5mL acetic acid . Make up to 100 ml with dH₂O.

Appendix C. 7: Electrode Buffer for SDS Page

Electrode buffer for SDS Page: (0.025 M Tris; 172 mM glycine; 0.1 % SDS; pH 8.3). In a 1 L volumetric flask weighed out:

6.06 g Tris base

28.8 g Glycine

1 g SDS or 10 mL of 20 % SDS solution.

Make up to 1 L and pour into 2.5 L brown glass bottle. Add another dH₂O for 2L final volume. No need to check pH.

Table C.1: Preparation of 10%, 12%, and 15% separating gels for PAGE

	Separating Gels		
% Acrylamide	10 %	12 %	15 %
	Volume (mL)		
Distilled H ₂ O	7.9	6.6	4.6
1.5 M Tris-HCl, pH 8.8	5	5	5
20 % (w/v) SDS	0.2	0.2	0.2
Acrylamide/Bis-acrylamide (29.2%/0.8%w/v)	6.7	8.0	10
10 % (w/v) ammonium persulfate	0.2	0.2	0.2
TEMED	0.01	0.01	0.01
Total volume	20	20	20

Table C. 2: Preparation of stacking gels for PAGE.

Stacking gel	
	Volume (mL)
Distilled H ₂ O	2.80
0.5 M Tris-HCl, pH 6.8	1.25
20 % (w/v) SDS	0.05
Acrylamide/Bis-acrylamide (30%/0.8% w/v)	0.85
10 % (w/v) ammonium persulfate	0.05
TEMED	0.005
Total volume	5.005

APPENDIX D

Appendix D. 1: Ammonium sulphate fractionation

Final concentration of ammonium sulphate, % saturation																	
10	20	25	30	33	35	40	45	50	55	60	65	70	75	80	90	100	
Gram solid ammonium sulphate to be added to 1 L of solution																	
0	56	114	144	176	196	209	243	277	313	351	390	430	472	516	561	662	767
10		57	86	118	137	150	183	216	251	288	326	365	406	449	494	592	694
20			29	59	78	91	123	155	189	225	262	300	340	382	424	520	619
25				30	49	61	93	125	158	193	230	267	307	348	390	485	583
30					19	30	62	94	127	162	198	235	273	314	356	449	546
33						12	43	74	107	142	177	214	252	292	333	426	522
35							31	63	94	129	164	200	238	278	319	411	506
40								31	63	97	132	168	205	245	285	375	469
45									32	65	99	134	171	210	250	339	431
50										33	66	101	137	176	214	302	392
55											33	67	103	141	179	264	353
60												34	69	105	143	227	314
65													34	70	107	190	275
70														35	72	153	237
75															36	115	198
80																77	157
90																	79

APPENDIX E

Table E. 1: Initial rate of reaction for *G. pallidus* RAPc8 NHase using 2-cyanopyridine

	2-cyanopyridine concentrations						
Time (min)	5 mM	10 mM	20 mM	40 mM	60 mM	80 mM	100 mM
0.17	6.76	7.72	9.98	11.58	13.46	13.77	16.76
0.33	12.11	13.07	13.99	19.71	17.69	19.43	23.20
0.50	16.18	18.01	19.30	25.62	24.54	27.17	31.10
0.67	20.03	23.45	24.06	30.26	32.25	32.28	37.06
0.83	23.97	27.88	28.07	35.33	36.49	37.55	42.27
1.00	28.17	33.39	33.75	39.69	40.23	43.07	47.81
1.17	30.81	35.60	37.25	42.55	43.67	48.41	53.25
1.33	32.56	39.06	42.09	48.22	48.81	52.16	58.72
1.50	36.28	43.74	44.49	50.76	50.72	57.24	63.00
1.67	39.16	46.20	47.75	59.62	56.02	60.12	67.55

Table E. 2: Initial rate of reaction for *G. pallidus* RAPc8 NHase using 3-cyanopyridine

	3-cyanopyridine concentrations						
time (min)	5 mM	10 mM	20 mM	40 mM	60 mM	80 mM	100 mM
0.167	2.38	9.52	10.31	14.81	17.47	19.65	24.48
0.333	7.20	12.52	18.59	19.93	24.41	26.36	29.83
0.500	10.08	17.90	25.95	28.30	31.43	34.27	39.93
0.667	13.39	21.97	32.99	34.77	39.44	42.65	47.72
0.833	15.80	26.69	38.83	41.09	47.27	51.52	57.36
1.000	19.13	29.43	42.56	46.35	53.51	60.96	64.97
1.167	21.55	33.17	47.98	52.66	59.20	66.03	71.60
1.333	23.88	37.48	51.71	59.67	65.04	73.52	76.72
1.500	27.63	41.22	58.43	63.77	68.94	77.43	82.71
1.667	29.70	44.83	61.06	68.71	75.00	84.21	88.36

Table E. 3: Initial rate of reaction for *G. pallidus* RAPc8 NHase using 4-cyanopyridine

	4-cyanopyridine concentrations				
Time (min)	5 mM	10 mM	20 mM	40 mM	60 mM
0.17	3.54	4.55	7.08	12.06	17.69
0.33	4.74	6.01	8.47	14.27	19.59
0.50	6.08	7.75	11.14	16.77	20.39
0.67	7.19	9.36	12.38	19.03	24.24
0.83	8.45	10.57	13.94	21.07	26.65
1.00	9.65	11.44	15.70	22.21	27.51
1.17	10.66	12.86	17.06	24.60	31.07
1.33	12.02	14.18	18.92	25.86	33.94
1.50	12.96	15.77	20.54	28.21	35.25
1.67	14.08	17.90	21.71	29.64	38.56

Table E. 4: Initial rate of reaction for immobilized *G. pallidus* RAPc8 NHase using 3-cyanopyridine

	3-cyanopyridine concentrations						
Time (min)	5 mM	10 mM	20 mM	40 mM	60 mM	80 mM	100 mM
1	1.02	3.47	6.55	10.20	11.80	16.10	18.24
2	4.60	6.91	12.53	15.54	17.80	21.61	23.74
3	6.01	8.74	13.70	19.30	21.29	26.99	29.30
4	7.57	10.75	17.03	22.97	25.67	30.27	34.75
5	9.23	12.05	18.90	25.74	29.04	34.19	37.46
6	10.57	14.23	21.30	27.54	32.66	37.53	42.38
7	11.86	15.40	23.87	29.85	35.03	40.01	44.50
8	13.12	16.21	25.01	33.24	36.88	44.49	51.07
9	14.11	17.36	26.55	36.00	40.24	46.11	51.15
10	15.07	18.46	28.82	38.70	43.50	48.79	55.68

APPENDIX F

Table F. 1: Semilog plot of \ln (relative activity) against t at different temperatures for the estimation of k_d and $t_{1/2}$.

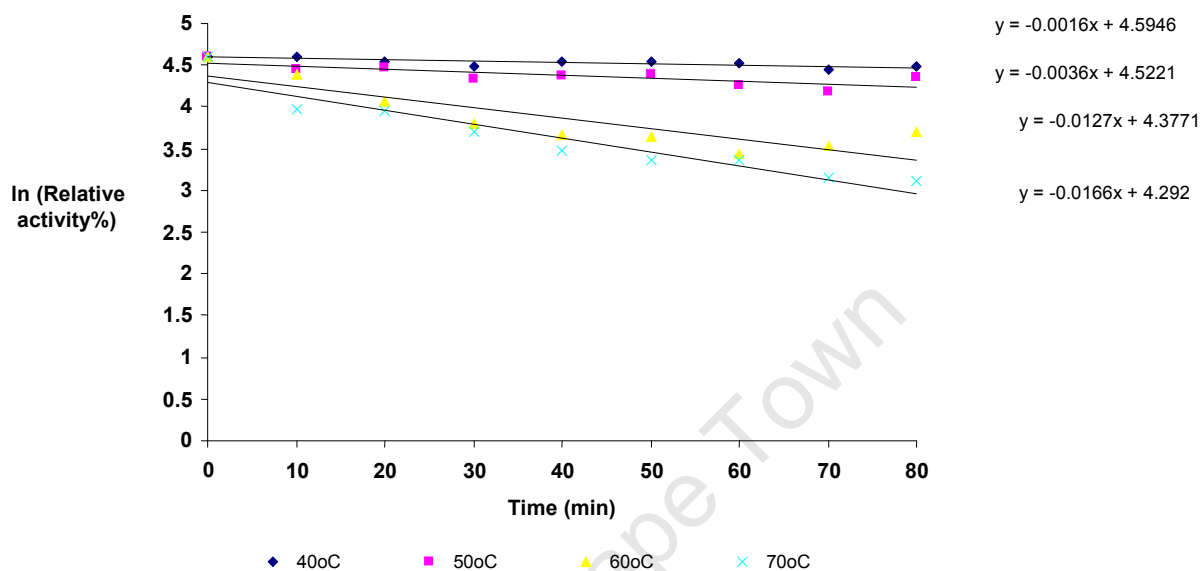
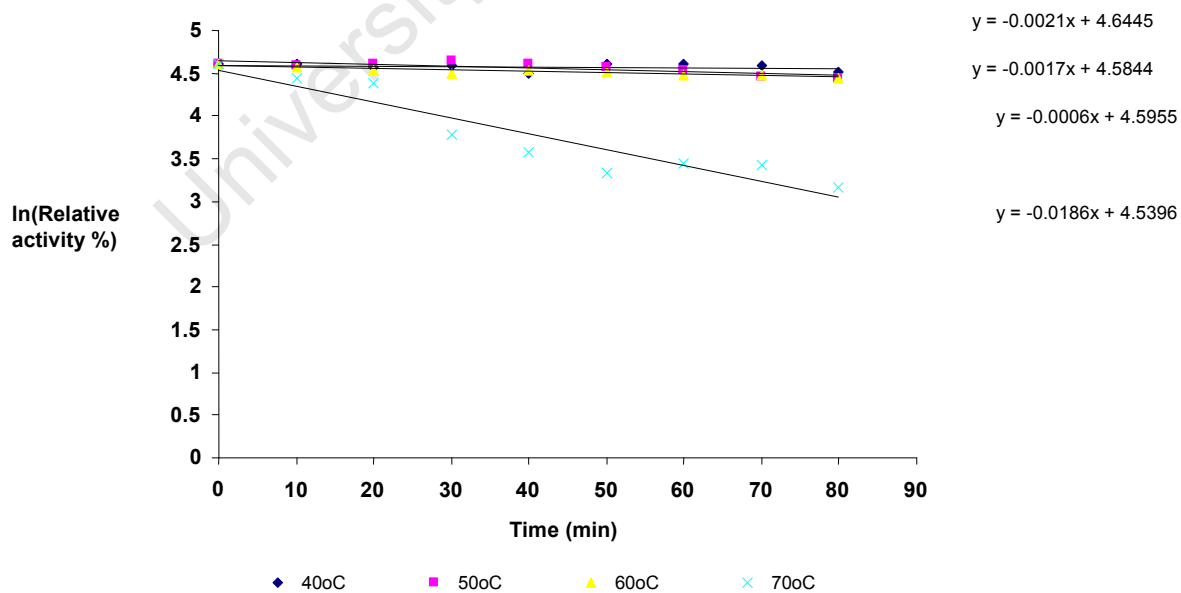


Table F. 2: Semilog plot of \ln (relative activity) against t at different temperatures for the estimation of k_d and $t_{1/2}$. Reactions were conducted at 50 °C as described in standard assay.



APPENDIX G

K_{cat} Calculation

3-cyanopyridine

$$\begin{aligned}
 1 \text{ mole enzyme} &= 110\,000 \\
 0.14 \text{ mg enzyme} &= \frac{0.14 \times 10^{-3} \text{ g}}{110\,000 \text{ g/mol}} \\
 &= 1.27 \times 10^{-9} \text{ moles enzyme} \\
 48.08 \text{ } \mu\text{mol/mL-min} &= 48.08 \times 10^{-6} \text{ mol/mL-min} \\
 \text{Turnover number} &= \frac{48.08 \times 10^{-6} \text{ mol/mL-min}}{1.27 \times 10^{-9} \text{ mol/mL}} \\
 &= \underline{37777.1 \text{ min}^{-1}}
 \end{aligned}$$

REFERENCES

- Adamczak M and Krishna H. S. (2004) Enzymes for efficient biocatalysis. *Food Technol. Biotechnol.* 42: 251-264.
- Albayrak N. and Yang S. (2002) Immobilization of β -galactosidase on fibrous matrix by polyethyleimine for production of galactooligosaccharides from lactose, *Biotechnol. Prog.* 18: 240-251.
- Alkorta I., Garbisu C., Llama M. J., Serra J. L. (1996) Immobilization of pectinlyase from *Penicillium italicum* by covalent binding to nylon. *Enzyme Microb. Technol.* 18: 141-146.
- Almatawah Q. A., and Cowan D. A. (1999) Thermostable nitrilase catalysed production of nicotinic acid from 3-cyanopyridine. *Enzyme Microb. Technol.* 25: 718-724.
- Balcão V. M., Paiva A.L., Malcata F.X. (1996) Bioreactor with immobilized lipases: State of the art. *Enzyme Microb. Technol.* 18:391-416.
- Banerjee A., Sharma R., Banerjee U. C. (2002) The nitrile-degrading enzymes: Current Status and future prospects. *Appl. Microbiol. Biotechnol.* 60: 33-44.
- Bauer R, Hirrlinger. B, Layl N, Stolz A, Knackmuss H. J. (1994) Enantioselective hydrolysis of racemic 2-phenylpropionitrile and other (r,s)-2-arylpropionitriles by a new bacterial isolate, *Agrobacterium tumefaciens* strain d3. *Appl. Microbiol. Biotechnol.* 42:1-7.
- Bauer R., Stolz A., Knackmuss H. J. (1998) Enantioselective hydrolysis of racemic 2-arylpropionitriles by a nitrile hydratase from *Agrobacterium tumefaciens* strain d3. *Microbiol. Biotechnol.* 49: 89-95.

- Battistel E., Bernandi A., Maestri P. (1997) Enzymatic decontamination of aqueous polymer emulsions containing acrylonitrile. *Biotechnol. Lett.* 19: 131-134.
- Becker P. (1997) Determination of the kinetic parameters during continuous cultivation of the lipase producing thermophile *Bacillus* sp. 1H1-91 on olive oil. *Appl. Microb. Biotechnol.* 48:148-190.
- Beilen J. B. and Li Z. (2002) Enzyme technology: an overview. *Curr. Opin. Biotechnol.* 13, 338-344.
- Belenky P., Bogan K. L., Brenner C. (2007) NAD⁺ metabolism in health and disease. *Trends. Biotechnol.* 32: 12-19.
- Betancor L., López-Gallego F., Alonso-Morales N., Dellamora G. Mateo C., Fernandez-Lafuente R, Guisan J. M. (2006) Glutaraldehyde in protein immobilization: A versatile reagent. *Methods Biotechnol.* 22: 57-64.
- Bhattacharya S., Nayak A., Gomes J., Bhattacharya S.K. (2004) A continuous process for production of D-ribulose-1, 5-bisphosphate from D-glucose. *Biochem. Eng. J.* 19: 229-235.
- Blanco R. M., Calvete J. J., Guisan J. M. (1989) Immobilization–stabilization of enzymes; Variables that control the intensity of the trypsin (amine)-agarose (aldehyde) multi-point covalent attachment. *Enzyme Microb. Technol.* 11: 353-359.
- Bogin O., Peretz M., Hacham Y., Korkhin Y., Frolow F., Kalb (Gilbon) A. J., Burstein Y. (1998) Enhanced thermal stability of *Clostridium beijerinckii* alcohol dehydrogenase after strategic substitution of amino acid residue with proline from the homologous thermophilic *Thermoanaerobacter brockii* alcohol dehydrogenase. *Protein Sci.* 7: 1156-1163.
- Boller T., Meier C., Meuzler S. (2002) Eupergit Oxirane Acrylic Beads: How to make enzymes fit for biocatalysis. *Org. Process Res. Dev.* 16: 509 – 519.

Bommarius A. S and Riebel B. R., *Biocatalysis: Fundamentals and Applications*, Wiley-VC, 2004.

Bosley J. A., Clayton J. C. (1994) Blueprint for lipase support: Use of hydrophobic controlled-pore glass as a model system. *Biotechnol. Bioeng.* 43: 934-938

Bozell J. J. (2008) Feedstocks for the future-Biorefinery production of chemicals from renewable carbon. *Acta Hydroch. Hydrob.* 36: 641-647.

Bradford M. M (1976) A rapid and sensitive method for quantitation of microgram quantities of protein utilizing the principle of protein dye binding. *Anal Biochem.* 72:248-254.

Brandão P. F. and Bull A. T. (2002) Nitrile hydrolysing activities of deep-sea and terrestrial mycolate actinomycetes. *Antonie Van Leeuwenhoek* 84: 89-98

Brennan B. A., Cummings J. G., Chase D. B. Turner I. M. Jr., Nelson M. (1996) Raman spectroscopy of nitrile hydratase, a novel iron-sulfur enzyme. *Biochemistry.* 35: 10068-10077.

Bronzino J. D. (2000) *The biomedical Engineering Handbook*, 2nd Ed. IEEE press.

Bruins M. E., Janssen A. E. M., Boom R. M. (2001) Thermozyms and their applications: a review of the recent literature and patents. *Appl. Biochem. Biotechnol.* 90: 155-186.

Bulawayo B. T., Dorrington R. A., Burton S. G. (2007) Enhanced operational parameters for amino acid production using hydantoin-hydrolysing enzymes of *Pseudomonas putida* strain RUKM3s immobilized in Eupergit C. *Enzyme Microb. Technol.* 40: 533-539.

Burton S. G. (2001) Development of bioreactors for application of biocatalysts in biotransformations and bioremediation. *Pure Appl. Chem* 73: 77-83

Burton S. G, Cowan D. A, Woodley J. M. (2002) The search for the ideal biocatalyst. *Nature* 20:37-45.

Busto M. D., Apenten R. K. O., Robinson D. S., Casey R., Wu Z., Hughes R. K. (1999). Kinetics of thermal inactivation of pea seed lipoxygenases and the effect of additives on their thermostability. *Food Chem.* 65:323-329.

Calsavara L. P. V., Moraes F. F. Zain G. M (2000) Thermal stability and energy of deactivation of free and immobilized cellobiase. *Brazilian J. Chem. Eng.* 48: 4-7.

Cameron R. A (2002). Nitrile degrading enzymes from extreme environment. PhD thesis, University of London, London, UK.

Cameron R. A, and Cowan D. A. (2005) Molecular analysis of the nitrile catabolism operon of the thermophile *Bacillus pallidus* sp. RAPc8. *Biochim. Biophys. Acta* 1725: 35-46.

Cantarella M., Spera A., Alfani F. (1998) Characterisation in UF-Membrane Reactors of Nitrile Hydratase from *Brevibacetrium imperialis* CBS 489-74 Resting cells. *Ann. N.Y. Acad. Sci.* 864:224-227.

Cantarella M., Canterella L., Alfani F. (1991) Hydrolytic reactions in two-phase systems. Effect of water-immiscible organic solvents on stability and activity of acid phosphatase, β -glucosidase and β -fructo furanosidase. *Enzyme. Microb. Technol.* 13: 547-553.

Cantarella M., Cantarella L., Gallifuoco A., Frezzini R., Spera A., Alfani F. (2003) A study in UF-Membrane reactor on activity and stability of nitrile hydratase from *Microbacterium imperiate* CBS 498-74 resting cells for propionamide production. *J. Mol. Catal. B: Enzym.* 29: 1-6.

Cao L., (2006) Carrier-bound immobilized enzymes: Principles, Application and Design. Wiley-VCH Press,

- Cao L, Langen L and Sheldon R. A. (2003) Immobilized enzymes: carrier-bound or carrier-free? *Curr.Opin. Biotechnol.*14: 387-394.
- Catana R., Ferreira B. S., Cabral J. M. S., Fernandez P. (2005) Immobilization of inulinase for sucrose hydrolysis. *Food Chem.* 91: 517-520.
- Chen B., Chen S., Chang J. (2005) Immobilized cell fixed-bed bioreactor for wastewater decolorization. *Process Biochem.* 40: 3434-3440.
- Chibata T., Sato T., Sato Tosa. (1986) Biocatalysis: immobilized cells and enzymes. *J. Mol. Catal.*37: 1-24.
- Cho S., Shin D., Ji G. E., Heu S., Ryu S. (2005) High-level recombinant protein production by overexpression Mlc in *Escherichia coli*. *J. Biotechnol.* 119: 197-203.
- Chung T., Wu C., Jang R. (2005) Improved dynamic analysis on cell growth with substrate inhibition using two-phase models, *Biochem. Eng. J.* 25: 209-217.
- Cowan D. A. (2000) Microbial genomes – the untapped resources. *Trends Biotechnol.* 18: 14-16
- Cowan. D. A., Cameron R.A., Tsekoa T. L. (2003) Comparative biology of mesophilic and thermophilic nitrile hydratases. *Adv. Appl. Microbiol.* 52: 123-158.
- Cowan D, Cramp R, Pereira R, Graham D, Almatawah Q. (1998) Biochemistry and biotechnology of mesophilic and thermophilic nitrile metabolizing enzymes. *Extremophiles.* 2: 207-216.
- Cramp R., Gilmour M., Cowan D. A. (1997) Novel thermophilic bacteria producing nitrile-degrading enzyme. *Microbiol.* 143:2313-2320.
- Cramp R. A. and Cowan D. A. (1999) Molecular characterisation of a novel thermophilic nitrile hydratase. *Biochim. Biophys. Acta Protein Struct. Mol. Enzymol* 1431: 249.

Davey J. and Lord M. (2003) *Essential cell biology: A practical approach*, Oxford University press, Demirjian D., Moris-Varas F., Cassidy C. (2001). *Curr. Opin. Chem. Biol.* 5:144.

Demirjian D., Moris-varas F., Cassidy C. (2001). Enzymes from extremophiles. *Curr. Opin. Chem. Biol.* 5: 144-151.

Desai L. V., Zimmer M. (2004) Substrate selectivity and conformational space available to bromoxynil and acrylonitrile in iron nitrile hydratase. *Dalton Trans.*, 2004:872-877.

DeVito C. S. (2007) Nitriles, Kirk-Othmer Encyclopedia of Chemical Technology, John Wiley & Sons . Inc.

Dort R., (2004) *The Engineering Handbook*. 2nd Ed. CRC Press, New York. Prentice Hall.

Duran R, Chion C, Bigey F, Arnaud A, Galzy P. (1992) The N-terminal amino acid sequences of *Brevibacterium sp.* R312 nitrile hydratase. *J. Basic Microbiol.* 32: 13-19.

Duran R., Nishiyama M., Horinouchi S., Beppu T. (1993) Characterisation of nitrile hydratase genes cloned by DNA screening from *Rhodococcus erythropolis*, *Biosci. Biotechnol. Biochem.* 57: 1323-1328.

Endo I., Nojiri M., Tsujishima M., Nakasako S., Nagashima S., Yohda M., Odaka M. (2001) Fe-type nitrile hydratase. *J. Inorg. Biochem.* 83: 247-253.

Endo T. and Watanabe I. (1989) Nitrile hydratase of *Rhodococcus sp.* N-774: purification and amino acid sequences. *FEBS Lett.* 243: 61-64.

Eyal J. and Charles M. (1990) Hydration of 3-cyanopyridine to nicotinamide by whole cell nitrile hydratase. *J. Ind. Microbiol.* 5: 71-78.

Fan D. D., Luo Y., Mi Y., Ma X. X., Shang L. (2005) Characteristics of fed-batch cultures of recombinant *E. coli* containing human-like collagen cDNA at different specific growth, *Biotechnol. Lett.* 27: 865-870.

Fernández-Lafuente R., Rosell C. M., Alvaro G., Guisan J. M. (1992) Additional stabilization of penicillin G-acylase-agarose derivatives by controlled chemical modification. *Enzyme Microb. Technol.* 17: 366-372.

Fernández-Lafuente R., Cowan D. A., Wood A. N. P. (1995) Hyperstability of a thermophilic esterase by multipoint covalent attachment. *Enzyme Microb. Technol.* 17: 366-372.

Fernández-Lafuente R., Rosell C. M., Rodriguez V., Guisan J. M. (1995) Strategies for enzyme stabilization by intramolecular cross linking with bifunctional reagents. *Enzyme Microb. Technol.* 17: 517-523.

Fernández-Lafuente R., Rodriguez V., Mateo C., Penzol G., Hernández-Justiz O., Irazoqui G., Villarino A., Ovsejevi K., Batista F., Guisan J. (1999) Stabilization of multimeric enzymes via immobilization and post-immobilization techniques. *J. Mol. Cat B: Enzym.* 7: 181-189.

Fuentes M., Pessela B. C. C., Maquiese J. V., Ortiz C., Segura R. L., Palomo J. M. (2004) Reversible and strong immobilization of proteins by ionic exchange on supports coated with sulphate-dextran, *Biotechnol. Prog.* 26: 1134-1139.

Fuentes M., Maquiese J. V., Pessela R. T., Torres R., Grazú V., Fernández-Lafuente R., Guisan J. M., Mateo C. (2006) Use of polyvalent cations to improve the adsorption strength between adsorbed enzymes and support coated with dextran sulphate. *Enzyme Microb. Technol.* 39: 332-336.

Gerbsch N and Buchholz R. (1995) New processes and actual trends in biotechnology. *FEMS Microbiol. Rev.* 16: 259-269.

Gorman L. A. S., Dordick S. J. (1992) Organic solvents strip water off enzymes. *Biotechnol. Bioeng.* 39: 392-397.

Gostick J., Pritzker M., Lohi A., Doan H. D. (2004) Mass transfer variation within a packed bed and its relation to liquid distribution. *Chem. Eng. J.* 100: 33-41.

Guisan J. M. Immobilization of enzymes and cells. Methods Biotechnology, 2nd Ed., New York: Humana Press Inc, 2006.

Guisan J. M., Bastida A., Cuesta C., Fernandez-Lufuente R. (1991) Immobilization-stabilization of α -chymotrypsin by covalent attachment to aldehyde-agarose gels. *Biotechnol. Bioeng.* 38: 1144 -1152.

Gupta M. N. (1991) Thermostabilization of proteins, *Biotechnol. Appl. Biochem.* 14: 1-11.

Gupta M. (1992) Enzyme function in organic solvents. *Eur. J. Biochem.* 203:25-32.

Haki G. D., Rakshit S. K. (2003) Developments in industrially important thermostable enzymes: a review. *Bioresour. Technol.* 89:17-34.

Hamachi I., Fujita A., Kunitake T. (1994) Enhanced N-Demethylase Activity of Cytochrome c Bound to a phosphate-Bearing Synthetic Bilayer Membrane. *J. Am. Chem. Soc.* 116: 8811-8812.

Hann E. C, Eisenberg A, Susan K. F, Perkins N. E, Gallagher F. G, Cooper S. M, Gavagan J. E, Stieglitz B, Hennessey S. M and DiCosimo R. (1999) 5-Cyanovaleramide production using immobilized *pseudomonas chlororaphis* B23. *Bioorg. Med. Chem.* 7: 2239-2245.

Haney P., Konisky J., Koretke K. K., Luthey-Schulten Z., Wolynes P. G. (1997) Structural basis for thermostability and identification of potential active site residues for adenylate kinases from archaeal genus *Methanococcus*. *Protein* 28: 117-130.

Hanning G. and Marides S. C. (1998) Strategies for optimizing heterologous protein expression in *Escherichia coli*. *Trends Biotechnol.* 16: 54-60.

Harborne J. B. (1993) Introduction to Ecological Biochemistry, Ed 4, Academic Press, London.

Henley S. and T. Sadana (1986) Deactivation theory, *Biotechnol. Bioeng.* 28:1277–1285.

Hernaiz M. J. and Crout D. H. G. (2000) Immobilization on Eupergit C of the galactosidase from *B. circulans* and a galactosidase from *Aspergillus oryzae*. *Enzyme Microb. Technol.* 27: 26-32.

Hill E. M. (2007) Benign tunable solvents for improved processing of pharmaceutically relevant products and catalyst. PhD thesis, Georgia Institute of Technology, School of Chemical and Biomolecular Engineering, Georgia.

Hourai S., Ishii, T., Miki M., Takashima Y., Mitsuda S., Yonagi K. (2005) Cloning, purification, crystallization and preliminary X-ray diffraction analysis of nitrile hydratase from thermophilic *Bacillus smithii* SC-J05-1. *Acta Crystallogr. Sect.F. Struct. Biol. Cryst. Commun.* 61:974-977.

Howaldt M. W., Kulbe K. D., Chmiel H. (1986) Choice of reactor to minimize enzyme requirements: 1. Mathematical model for one-substrate Michaelis-Menten type kinetics in continuous reactors. *Enzyme Microb. Technol.* 8 627-631.

<http://www.atp.nist.gov/atp/97wp-cat.htm>

<http://www.lsbu.ac.uk/biology/enztech>

http://www.ambion.com/techlib/spec/sp_9462.pdf

<http://www.piercenet.com/products/browse.cfm?fldID=02050204>

Huang W, Jia J, Cumming J, Nelson M, Schneider G, Lindqvist Y. (1997) Crystal structure of nitrile hydratase reveals a novel iron centre in a novel fold. *Structure* 5: 691-699.

Hwang J. S., Chang H. N. (1989) Biotransformation of acrylonitrile to acrylamide using whole cells of *Brevibacterium* CH1 in a recycle fed-batch reactor. *Biotech. Bioeng.* 34:380-386.

Inada Y., Yoshimoto T., Matsushima A., Saito Y. (1988) Engineering physiochemical and biological properties of proteins by chemical modifications. *Trends Biotechnol.* 4: 68-73.

Ishige T, Honda K., Shimizu S. (2005) Whole organism biocatalysis. *Curr. Opin. Chem. Biol.* 9:174-180.

Jaffe E. K., Martins J., Li. J., Kervinen J., Dunbrack Jr. R. L. (2001) The molecular mechanism of lead inhibition of human porphobilinogen synthase. *J. Biol. Chem.* 276: 1531-1537.

Jallageas J. C., Arnaud A., Galzy P. (1980) Bioconversions of nitriles and their applications. *Adv. Biochem. Eng.* 25: 1-32.

Johnson D. V., Zabelinskaja-Mackova A.A., Griengl H. (2001) Oxynitrilases for asymmetric C-C bond formation. *Curr. Opin. Chem. Biol.* 4: 103-109.

Katchalski-Katzir, E. (1993) Immobilized enzymes-learning from past successes and failures. *Trends Biotechnol.* 11: 471-478.

Katchalski-Katzir E. D., Kraemer D. M. (2000) Eupergit C a carrier for immobilization of enzymes of industrial potential. *J. Mol. Catal. B: Enzym.* 10: 157 – 176.

Kato Y, Ooi R, Asano Y. (2000) Distribution of aldoxime dehydratase in microorganisms. *Appl. Environ. Microbiol.* 66: 2290-2296.

Kaul P., Banerjee A., Banerjee U. C (2004) Biocatalysis: *Drug discovery world spring.* 80-89.

- Kimani S. W., Agarkar V. B., Cowan D. A., Sayed M. F., Sewell B. T. (2007) Structure of aliphatic amidase from *Geobacillus pallidus* RAPc8. *Acta crystallogr. D. Biol. Crystallogr.* 63: 1048-1058.
- Kim S. H and Oriel P. (2000) Cloning and expression of the nitrile hydratase and amidase genes from *Geobacillus pallidus* BR449 into *Escherichia coli*, *Enzyme Microb. Technol.* 27: 492-501.
- Kim S. H., Padamkumar P, Oriel P. (2001) Cobalt activation of Bacillus BR 449 nitrile hydratase expressed in *E. coli*, *Appl. Biochem. Biotechnol.* 93: 597-603.
- Kirk O., Borchert T. V., Fulgsang C. C. (2002) Industrial enzyme applications. *Curr. Opin. Biotechnol.* 13: 345-351.
- Klibanov A. M. (1983) Approaches to enzyme stabilization. *Biochem. Soc. Trans.* 11: 19-20.
- Klibanov A. M. (1989) Enzymatic catalysis in anhydrous organic-solvents. *Trends Biochem. Sci.* 14: 141-144.
- Klibanov A. M. (1997) Why are enzymes less active in organic solvents than water? *Trends Biotechnol.* 15: 97-101.
- Klibanov A.M., (2001) Improving enzymes by using them in organic solvents. *Nature* 409: 241 - 248.
- Knezevic Z., Milosavic N., Bezbradica D., Jakovljevic Z, Prodanovic R. (2006) Immobilization of lipase from *Candida* on Eupergit C support by covalent attachment. *Biochem. Eng. J.* 30: 269-278.
- Kobayashi M, Nishiyama M, Nagasawa T, Horinouchi s, Beppu T, Yamada H. (1991) Cloning , nucleotide sequence and expression in *Escherichia coli* of two cobalt-containing nitrile hydratase genes from *Rhodococcus rhodochrous* J1. *Biochi. Biophys. Acta.* 1129:23-33.

- Kobayashi M., Nagasawa T., Yamada H. (1992) Enzymatic synthesis of acrylamide: a success story not yet over. *Trends Biotechnol.* 10: 402-408.
- Kobayashi, M., and Shimizu, S. (1998) Metalloenzyme nitrile hydratase: Structure, regulation, and application to biotechnology. *Nat. Biotechnol.* 16:733-736
- Kobayashi M, and Shimizu S. (1999) Cobalt protein. *Eur. J. Biochem.* 261:1-9.
- Kobayashi M. and Shimizu S. (2000) Nitrile hydrolases. *Curr. Opin. Chem. Biol.* 4: 95-104.
- Komeda H, Kobayashi M, Shimizu S. (1996) A novel gene cluster including the *Rhodococcus rhodochrous* J1 nhlba genes encoding a low molecular mass nitrile hydratase (L-NHase) induced by its reaction product. *J. Biol. Chem.* 271: 15796-15802.
- Kosugi Y., Tanaka H., Tomizuka N. (1990) Continuous hydrolysis of oil by immobilized lipase in a countercurrent reactor. *Biotechnol. Bioeng.* 36: 617-622.
- Krenkova J and Svec F. (2009) Less common applications of monoliths: IV. Recent developments in immobilized enzyme reactors for proteomics and biotechnology. *J. Sep. Sci.* 32: 706-718.
- Krishna S. H. (2002) Developments and trends in enzyme catalysis in non-conventional media. *Biotechnol. Adv.* 20: 239-266.
- Kubáč D., Kaplan O., Elišáková V, Pátek M, Vejroda V., Slámová K, Tothora A., Lemaire M., Gallienne E., Lutz-Wahl S., Fischer L., Kuzma M., Pelantová H., van Pelt S., Bolte J., Křen V., Martinková L. (2008) Biotransformation of nitriles to amides using soluble and immobilized nitrile hydratase from *Rhodococcus erythropolis* A4. *J. Mol. Catal. B: Enzym.* 56: 107-113.
- Kumar S., Tsai C. J., Nussinov R. (2000) Factors enhancing protein thermostability. *Protein Eng.* 13; 179-191.

- Laemmli V. K. (1970) Cleavage of structural proteins during the assembly of the head of bacteriophage T4. *Nature* 227: 680-685.
- Lamb S. B. and Stuckey D.C. (2000) Enzyme immobilization on colloidal liquid aphrons (CLAs): the influence of system parameters on activity. *Enzyme Microb. Technol.* 26:574-581.
- Lamine A. S., Gerth L., LeGall H., Wild G. (1996) Heat transfer in packed bed reactor with co-current down flow of a gas and a liquid. *Chem. Eng. Sci.* 51: 3813-3827.
- Lathouder K. M., Bakker J., Kreutzer M. T., Kapteijn F., Moulijn J. A., Wallin S. A. (2004) Structured reactors for enzyme immobilization: advantages of tuning the wall morphology. *Chem. Eng. Sci.* 59: 5027-5033.
- Layh N. and Willetts A., (1998) Enzymatic nitrile hydrolysis in low water systems. *Biotechnol. Lett.* 20:329-331.
- Laane C, Boeren S, Vos K, Veeger C. (1987) Rules of optimisation of biocatalysis in organic solvents. *Biotechnol. Bioeng.* 30:81-87.
- Lee S. Y. (1996) High cell-density culture of *Escherichia coli*. *Trends Biotechnol.* 14: 98-105.
- Lee M. Y., Dordick J. S. (2002) Enzyme inactivation for nonaqueous media. *Curr. Opin. Biotechnol.* 13: 376-384.
- Leng Y., Zheng P., Sun Z. (2006) Continuous production of L-phenylalanine from phenylpyruvic acid and L-aspartic acid immobilized recombinant *Escherichia coli* SW0209-52. *Process. Biochem.* 41: 1669 – 1672.
- Leuenberger H. G. W. (1990) Biotransformation-A useful tool in organic chemistry. *Pure Appl. Chem.* 62: 753-768.

Li L., Zhu Y., Huang Z, Jiang Z., Chen W. (2007) Immobilization of the recombinant xylanase B (XYnB) from the hyperthermophilic *Thermotoga maritime* on metal-chelate Eupergit C250 L. *Enzyme Microb. Technol.* 41: 278-285.

Lonza: 20 years of Biotransformation, Lonza AG. Switzerland (2001).

López-Gallego F, Montes T, Fuentes M, Alonso N, Grazu V, Betancor Guisan M. J and Fernandez-Lfuentes R. (2005) Improved stabilization of chemically aminated enzymes via multipoint covalent attachment on glyoxyl supports. *J. Biotechnol.* 116:1-5.

Luckarift H. R., Spain J. C., Naik R. R., Stone M. O. (2004) Enzyme immobilization in a biometric silica support. *Nat. Biotechnol.* 22: 211-213.

Lye G. J., Woodley J. M. (1999) Application of in situ product removal techniques to biocatalytic processes. *Trends Biotechnol.* 17: 395-402.

Makhongela H. S., Glowacka A., Agarkar V., Sewell B., Weber B., Cameron R., Cowan D., Burton S. (2007) A novel thermostable nitrilase superfamily amidase from *Geobacillus pallidus* showing acyl transfer activity. *Appl. Microbiol. Biotechnol.* 75: 801-811.

Malcata F. H., Reyes H. R., Garcia H. S., Hill G. C., Amundson C.H (1990) Immobilized lipase reactors for modification of fats and oils –A review. *JAOCs.* 67: 890-909.

Mammarella E. J., Rubiolo A. C. (2006) Predicting the packed-bed reactor performance with immobilized microbial lactase. *Process Biochem.* 41: 1627-1636.

Mandavilli S. N. (2000) Performance characteristics of an immobilized enzyme reactor producing ethanol from starch. *J. Chem. Eng. Jpn.* 33: 886-890.

- Marquez L. D. S, Cabral B. V, Freitas F. F. , Cardoso V. L. and Ribeiro E. J. (2008) Optimization of invertase immobilization by adsorption in ionic exchange resins for sucrose hydrolysis. *J. Mol. Catal. B: Enzym.* 51: 86-92.
- Martin T. M., Plou F. J., Alcalde M., Ballesteros A. (2003) Immobilization of cyclodextrin glucosyltransferase (CGTase) and properties of the immobilized biocatalyst. *J. Mol. Catal. B: Enzym.* 21: 299-308.
- Martinková L. and Stolz A., Knackmass H. J. (1996) Enantioselectivity of the nitrile hydratase from *Rhodococcus equi* cells. *Biotechnol. Lett.* 17: 1219-1222.
- Martinková L., Mylerová V. (2003) Synthetic applications of nitrile converting enzymes. *Curr. Org. Chem.* 7: 1279-1295.
- Mascharak P.K (2002) Structural and functional models of nitrile hydratase. *Coord. Chem. Rev.* 225: 201-214.
- Mateo C., Fernandez-Lorente G., Abian O., Fernandez-Lafuente R., Guisan J. M. (2000) Multifunctional epoxy supports: a new tool to improve the covalent immobilization of proteins. The promotion of physical adsorptions of proteins on the supports before their covalent linkage. *Biomacromolecules.* 1:739-745.
- Mateo C., Grazú V., Pessella B. C. C, Montes T., Fernandez-Lafuente R., Guisan J. M. (2007) Advances in the design of new epoxy supports for enzyme immobilization stabilization. *Biochem. Soc. Trans.* 35: 1593-1601.
- McLeish M. J, Kneen M. M, Gopalakrishna K. N, Koo C. W, Babbitt P. C, Gerlt J. A, Kenyon G. L. (2003) Identification and Characterisation of Mandelamide Hydrolase and an NAD(P)⁺-Dependent Benzaldehyde Dehydrogenase from *Pseudomonas putida* ATCC 12633. *JB.* 185: 2456 – 2456.

McMahon H., Zoecklein B. W., Fugelsang K. and Jasinski Y. (1999) Quantification of glycosidase activities in selected yeast and lactic acid bacteria. *J. Ind. Microbiol. Biotechnol.* 23: 198-203

Medyantseva E. S., Marganita G., Budnikov K. G., Budnikov G. (1998) Metal ions on enzyme effectors. *Russ. Chem. Rev.* 67: 225-232.

Minovska V., Winkelhausen E., Kuzmanova S. (2005) Lipase immobilized by different techniques on various support materials applied in oil hydrolysis. *J. Serb. Chem. Soc.* 70: 607 – 624.

Miranda M., Murado M. A., Sanromán A., Lema J. M. (1991) Mass transfer control of enzymatic hydrolysis of poly saccharides by gluco amylase. *Enzyme Microb. Technol.* 13: 142-147.

Miyanaga A., Fushinobu S, Ito K, and Wakagi T. (2001) Crystal structure of cobalt-containing nitrile hydratase. *Biochem. Biophys. Res. Commun.* 288: 1169-1174.

Miyanaga A., Fushinobu S., Ito K., Shoun H., Wakagi T. (2004) Mutational and structural analysis of a cobalt-containing nitrile hydratase on substrate and metal binding. *Eur. J. Biochem.* 271: 429-438.

Miyazaki M. and Maeda H. (2006). Microchannel reactors and their applications for processing. *Trends Biotechnol.* 24: 463-470.

Morrison R. T., Boyd R. N. (2001) Organic Chemistry, 6th Edition, New York University press.

Mounaji K., Vlassi M., Erraiss N. E., Wegnez M., Serrano A., Soukri A. (2003). In vitro effect of metal ions on the activity of two amphibian glyceraldehydes-3-phosphate dehydrogenases: potential metal binding site. *Comp. Biochem. Physiol. B: Biochem. Mol. Biol.* 135: 241-254.

Mylerova V. and Martinkova L. (2003) Synthetic application of nitrile converting enzyme. *Curr. Org. Chem.* 7: 1-17.

Nagasawa T, Ryuno K. and Yamada H. (1986) Nitrile hydratase of *Brevibacterium* R312- purification and characterisation. *Biochem. Biophys. Res. Commun.* 139:1305-1312.

Nagasawa T, Nanba H, Ryuno K, Takeuchi K, Yamada H. (1987) Nitrile hydratase of *Pseudomonas chlororaphis* B23: Purification and characterisation. *Eur. J. Biochem.* 162: 691-689.

Nagasawa T and Yamada H. (1987) Nitrile hydratase is quinoprotein. A possible new function of pyrroloquinoline quinine: activation of H₂O in an enzymatic hydration reaction. *Biochem. Biophys. Res. Commun.* 147: 701-709.

Nagasawa T, Mathew C. D, Manger J, Yamada H. (1988) Nitrile hydratase-catalysed production of nicotinamide from 3-cyanopyridine in *Rhodococcus rhodochrous* J1. *Appl. Environ. Microbiol.* 54: 1766-1769.

Nagasawa T, Takeuchi K, and Yamada H. (1991) Characterisation of a new cobalt-containing nitrile hydratase purified from urea-induced cells of *Rhodococcus rhodochrous* J1. *Eur. J. Biochem.* 196:581-589.

Nagasawa T, Shimizu H, Yamada H. (1993) The superiority of the third-generation catalyst *Rhodococcus rhodochrous* J1 nitrile hydratase, for industrial production of Acrylamide. *Appl. Microbiol. Biotechnol.* 40:189-195.

Nagasawa T and Yamada H. (1989) Microbial transformations of nitrile. *Trends Biotechnol.* 7: 153-158.

Nagasawa T and Yamada H. (1995) Microbial production of commodity chemicals. *Pure Appl. Chem.* 67: 1241 – 1256.

Nagashima S, Nakasako M, Dohmae N, Tsujimura M, Takio K, Odaka M, Yohda M, Kamiya N, and Endo I. (1998) Novel non-heme iron center of nitrile hydratase with a claw setting of oxygen atoms. *Nat. Struct. Biol.* 5: 347-351.

Nakajima Y., Doi T., Satoh Y., Fujiwara A., Watanbe I. (1987) A photoresponsive nitrile hydratase from *Rhodococcus* N-771. *Chem. Lett.* 9: 1767-1770.

Nakasako M., Odaka M., Yohda M., Dohmac N., Takio K., Kamiya N., Endo I. (1999) Tertiary and quaternary structures of photoactive nitrile hydratase from *Rhodococcus* sp. N771: roles of hydration water molecules in stabilizing its structure and structural origin of the substrate specificity of the enzyme. *Biochemistry.* 38: 9887-9898.

Ni Y. and Chen R. R. (2004) Accelerating whole-cell biocatalysis by reducing outer membrane permeability barrier, *Biotechnol. Bioeng.* 87: 804-811.

Nishiyama M, Horinouchi S, Kobayashi M, Nagasawa T, Yamada H. (1991) Cloning and characterisation of genes responsible for metabolizing compounds from *Pseudomonas chlororaphis* B23. *J. Bacteriol.* 173: 2465-2472.

Nor Z. M., Tamer I. M., Scharer J. M., Moo-Young M., Jervis E., J. (2001) Automated fed-batch culture of *Kluyveromyces fragilis* based on a novel method for on-line estimation of cell specific growth rate. *Biochem. Eng. J.* 9: 221-231.

Owusu R. K. and Berthelon N. (1993) A test for the two-stage thermoinactivation model for chymotrypsin. *Food Chem.* 48: 223 – 235.

Owusu R. K and Cowan D. A. (1989) Correlation between microbial protein thermostability and resistance to denaturation in aqueous: organic solvent two phase systems. *Enzyme Microbiol. Technol.* 11: 568-574.

- Padmakumar R. and Oriel P. (1999) Bioconversion of acrylonitrile to acrylamide using a thermostable nitrile hydratase. *Appl. Biochem. Biotechnol.* 79: 671-679.
- Page M. J and DiCera E. (2006) Role of Na⁺ and K⁺ in enzyme function. *Physiol. Rev.* 86:1046-1092
- Pajić-Lijaković I., Bugarski D., Plavsić M., Branko B. (2007) Influence of microenvironmental conditions on hybridoma cell growth inside the alginate- poly-L-lysine microcapsule, *Process Biochem.* 42: 167-174.
- Panda T., Naidu G. S. N., Sinha J. (1999) Multiresponse analysis of microbiological parameters affecting the production of pectolytic enzymes by *Aspergillus niger*. A statistical view. *Process Biochemistry* 35: 187-195.
- Panke S. and Wubbolts M. G. (2005) Advances in biocatalytic synthesis of pharmaceutical intermediates. *Curr. Opin. Chem.* 9: 251-264.
- Papezová K., Nemec T., Chaloupková R., Glatz Z. (2007) Study of substrate inhibition by electrophoretically mediated microanalysis in partially filled capillary. *J. Chromatogr. A.* 25:327-331.
- Payne M. S., Wu S. J., Fallon R. D., Tudor G., Stieglitz B., Turner I. M., Nelson M. J. (1997) A stereoselective cobalt-containing nitrile hydratase. *Biochemistry* 36: 5447-5454.
- Pereira R. A., Graham D., Rainey F. A., Cowan D. A. (1998) A novel thermostable nitrile hydratase. *Extremophiles* 2: 347-357.
- Pessela B. C., Fernandez R, Fluentes M., Vian A., Garcia J., Carracosa A. V. (2003) Reversible immobilization of a thermophilic β -galactosidase *via* ionic adsorption on PEI-coated Sepabeads. *Enzyme Microb. Technol.* 32: 369-374.

- Pessela B. C., Fernandez-Lafuente R., Torres R., Mateo C., Fuentes M., Filho M. (2007) Production of a thermoresistant alpha-galactosidase from *Thermus* sp. Strain T2 for food processing. *Food Biotechnol.* 21: 91-103.
- Pifferi P. G., Tramontini M., Malacarne A. (1989) Immobilization of endopolygalacturonase from *Aspergillus niger* on various types of macromolecular support. *Biotechnol. Bioeng.* 33: 1258 – 1266.
- Pollard D. J., Woodley J. M. (2007) Biocatalysis for pharmaceutical intermediates: the future is now. *Trends Biotechnol.* 25: 66-73.
- Porath J. (1992) Immobilized metal ion affinity chromatography protein expression and purification. *Protein Expr. Purif.* 3: 263 -281.
- Prasad S., Raj J., Bhalla T. C. (2007) Bench scale conversion of 3-cyanopyridine to nicotinamide using resting cells of *Rhodococcus rhodochrous* PA-34. *Indian J. Microb.* 47: 34-41.
- Přepechalová I., Martinkova L., Stolz A., Ovesna M., Bezouska K., Kopecky J., Křen V. (2001) Purification and characterisation of the enantioselective nitrile hydratase from *Rhodococcus equi* A4. *Appl. Microbiol. Biotechnol.* 55: 150-156.
- Radledge C. and Kristiansen B. Basic biotechnology, Cambridge University Press, New York, 2006.
- Ran N., Zhao L., Chen Z., Tao J. (2008) Recent applications of biocatalysis in developing green chemistry for chemical synthesis at the industrial scale. *Green Chem.* 10: 361-372
- Rios G. M., Belleville M. P., Paolicci D. and Sanchez S. (2004) Progress in enzymatic membrane reactors – a review. *J. Membr. Sci.* 242: 189-196.

Rosenberg I. M., Protein Analysis and Purification: Bench-top Techniques, Birkhäuser Publishers, USA, 1996.

Ross A. C., Bell G., Halling P. J. (2000) Organic solvent functional group effect on enzyme inactivation by interfacial mechanism. *J. Mol. Catal. B: Enzym.* 8: 183-192.

Rozkov A., Larsson B., Gillstrom S., Bjomestedt R., Schmidt S. R. (2006) Large-scale production of endotoxin-free plasmids for transient expression in mammalian cell culture. *Biotechnol. Bioeng.* 99: 557-566

Russell R. J., Ferguson J. M., Hough D. W., Danson M. J., Taylor G. L. (1997) The crystal structure of citrate synthase from the hyperthermophile archaea *Pyrococcus furiosus* at 1.9 Å resolution. *Biochemistry* 36: 9983-9994.

Sadana A. Biocatalysis: Fundamentals of deactivation kinetics, Prentice-Hall, Englewood Cliffs, 1995.

Sakai S., Antoku K., Yamaguchi T., Kawakami K. (2008) Transesterification by Lipase Entrapped in Electrospun Poly(Vinyl Alcohol) Fibers and Its Application to a Flow-Through Reactor, *J. Biosci. Bioeng.* 105: 687-689.

Saleem M., Rashid M. H., Jabbar A., Perveen R., Khalid A. M, Rajoka M. I.(2005) Kinetic and thermodynamic properties of an immobilized endoglucanase from *Arachniotus citrinus*. *Process Biochem.* 40; 849-855.

Salminen T., Teplyakov A., Kankare J., Cooperman B. S., Lahti R., Goldman A. (1996) An unusual route of thermostability disclosed by the comparison of *Thermus thermophilus* and *Escherichia coli* inorganic pyrophosphatases. *Protein Sci.* 5: 1014-1025.

Scarrow R. C., Brennan B. A. Cummings J. G., Jin H., Duog D. J. Kindt J. T., Nelson M. J. (1996) X-ray spectroscopy of nitrile hydratase. *Biochemistry.* 35: 10078-10088.

- Schmid A, Dordick J. S, Hauer B, Kiener A, Wubbolts M, Witholt B. (2001) Industrial biocatalysis today and tomorrow. *Nature* 409: 258-268.
- Schmid A., Hollmann F., Park B. J., Buhler B. (2002) The use of enzymes in chemical industry in Europe. *Curr. Opin. Biotechnol.* 13: 359-366.
- Schoemaker H. E, Mink D., Wubbolts M. G. (2003) Dispelling the Myths-Biocatalysis in Industrial Synthesis. *Science*. 299:1694-1697.
- Sellek G. A., Chandhuri J. B. (1999) Biocatalysis in organic media using enzymes from extremophiles. *Enzyme Microb. Technol.* 25: 471-482.
- Serdakowski A. L. and Dordick J. S. (2008) Enzyme activation for organic solvent made easy. *Trends Biotechnol.* 26: 48-54.
- Sharma S. K., Husain M., Kumar R., Samuelson L. A., Kumar J., Watterson A. C., Parmar V. S. (2005) Biocatalytic routes towards pharmaceutically important precursors and novel polymeric systems. *Pure Appl. Chem.* 77: 209-226.
- Sheldon R.A., (2007) Cross-linked enzyme aggregates (CLEAs): stable and recyclable biocatalysts. *Biochem. Soc. Trans.* 35: 1583-1587.
- Spagna G., Pifferi P. G., Tramontini M. (1995) Immobilization and stabilization of pectinlyase on synthetic polymers for application in beverage industry. *J. Mol. Catal. A: Chem.* 101: 99-105.
- Sosnitza P., Farroqui M., Saleemuddin M., Ulber R., Scheper T. (1998) Application of reversible immobilization techniques for biosensors. *Ana Chim. Acta.* 368: 197 – 203.
- Straathof A. J. J. (2002) The production of fine chemicals by transformation. *Curr. Opin. Biotechnol.* 13: 548-556

Sugiura Y., Kuwahara J., Nagasawa T., Yamada H. (1987) Nitrile hydratase: the first non-heme iron enzyme with a typical low-spin Fe (III)-active center. *J. Am. Chem. Soc.* 109: 5848-5850.

Svec F., Tennikova T. B., Deyl Z. (2003) Monolithic Materials: Preparation, Properties and Applications. *J. Chrom. Libr.* 67: 1-73.

Synowieck J. and Wolosowska S. (2006) Immobilization of thermostable β -glucosidase from *Sulfolobus shibatae* by cross-linking with transglutaminase. *Enzyme Microb. Technol.* 39: 1417-1422.

Takashima Y., Yamaga Y., Mitsuda S. (1998) Nitrile hydratase from a thermophilic *Bacillus smithii*. *J. Ind. Microbiol. Biotechnol* 20:220.

Tamagnini P., Axelsson R., Lindberg P., Oxelfelt F., Wünschiers R., Lindblad P. (2002) Hydrogenases and hydrogen metabolism of cyanobacteria. *Microbiol. Mol. Rev.* 66: 1-20.

Tan Y., Wang Z, X., Marshall K. C. (1996) Modelling substrate inhibition of microbial growth. *Biotechnol. Bioeng.* 52: 602-608.

Techapun C., Poosaran N., Watanabe M., Sasaki K. (2003) Thermostable and alkaline-tolerant microbial cellulose-free xylanases produced from agricultural wastes and the properties required for use in pulp bleaching bioprocessing: a review. *Process Biochem.* 38: 1327-1340.

Tehrany E.A., Fournier F., Desobry S. (2004) Simple method to calculate octanol-water partition coefficient of organic compounds. *J. Food Eng.* 64: 315-320.

Thomas J. M., Raja R. (2005) Designing catalysts for clean technology, green chemistry and sustainable development. *Annu. Rev. Mater. Res.* 35:315-350.

Thomas S. M., DiCosimo R., Nagarajan V. (2002) Biocatalysis: application and potentials for the chemical industrial. *Trends Biotechnol.* 20: 238-242.

- Thompson L., Knowles C., Linton E. (1988) Microbial biotransformations of nitriles. *Chem. Br.* 24: 900.
- Tittmann K., Proske D., Spinka M., Ghisha S., Rudolph R., Hübner G., Kern G. (1998). Activation of Thiamine Diphosphate and FAD in phosphate dependent pyruvate oxidase from *Lactobacillus plantarum*. *J. Biol. Chem.* 273: 12929-12934.
- Tsekoa T. L., Sayed M. F., Cameron R. A., Sewell B.T. and Cowan D.A. (2004) Purification, crystallization and preliminary X-ray diffraction analysis of thermostable nitrile hydratase. *S. Afr. J. Sci.* 100: 488-490.
- Tsekoa T. L. (2005) Structure, enzymology and genetic engineering of *Bacillus* sp. RAPc8 Nitrile Hydratase. PhD thesis, University of the Western Cape, Cape Town.
- Turner N. and Schneider (2000) Biocatalysis and Biotransformation Editorial Overview: Biocatalysis: - molecular, structural and synthetic advances, *Curr. Opin. Chem. Biol.* 4: 65-67.
- VanÇan S., Miranda E. A., Bueno S. M. A. (2002) IMAC of human IgG: studies with IDA – immobilized copper, nickel, zinc and cobalt ions and different buffer systems. *Process Biochem.* 37: 573-579.
- Varavinit S., Chaokasem N., Shobsngob S. (2001) Covalent immobilization of a glucoamylase to bagasse diadehyde cellulose. *World J. Microbiol. Biotechnol.* 17: 721-725.
- Vogt G., Argos P. (1997) Protein thermal stability: hydrogen bonds or internal packing? *Fold. Des.* 2:S40-46.
- Vogt G. Woells Argos P. (1997) Protein thermal stability, hydrogen bonds, and ion pairs. *J. Mol. Biol.* 269: 631-643.

Wang C., Zhang C., Xu X., Li C. (2001) Inducing expression and reaction characteristic of nitrile hydratase from *Rhodococcus* sp. SHZ-1. *Chin. J. Chem. Eng.* 15: 573-578.

Wang C., Zhang C., Xu X., Li C. (2007) Inducing expression and reaction characterisation of nitrile hydratase from *Rhodococcus* sp. SHZ-1. *Chin. J. Chem. Eng.* 15: 573-578.

Watanabe K., Hata Y., Kizaki H., Katsube Y., Suzuki Y. (1997) The refined crystal structure of *Bacillus cereus* oligo-1, 6-glucosidase at 2.0 Å resolution: structural characterisation of proline-substitution site for protein thermostabilization. *J. Mol. Biol.* 269: 142-153.

Won K, Kim S, Kim K, Park W. H and Moon S. (2005) Optimization of lipase entrapment in Ca-alginate gel beads. *Process Dev.* 40:2149-2154.

Wu S., Fallon R., Payne M. (1997) Over-production of stereoselective nitrile hydratase from *Pseudomonas putida* 5B in *Escherichia coli*. Activity requires a novel downstream protein. *Appl. Microbiol. Biotechnol.* 48: 704-708.

Wyatt, J.M. and Knowles, C.J. (1995) Microbial degradation of acrylonitrile waste effluents: the degradation of effluents and condensates from the manufacture of acrylonitrile. *Int. Biodeterior. Biodegrad.* 227–248.

Xi W. W. and Xu J. H. (2005) Preparation enantiopure (S)-ketoprofen by immobilized *Candida* lipases in packed bed reactor. *Process Biochem.* 40: 2161-2166.

Yamada H and Kobayashi M. (1996) Nitrile hydratase and its application to industrial production of acrylamide. *Biosci. Biotech. Biochem.* 60: 1391.

Yamaki T; Oikawa T; Ito K; Nakamura T. (1997) Cloning and sequencing of a nitrile hydratase gene from *Pseudonocardia thermophila* JCM 3095. *J. Ferment. Bioeng.* 83:474-477.

Yamamoto K., Uenoy Y., Otsubo K., Yamne H., Komatsu K. I., Tani Y. (1992) Efficient conversion of dinitrile to mononitrile-monocarboxylic acid by corynebacterium sp. C5 cells during tranexamic acid synthesis. *J. Ferment. Bioeng.* 73: 125-129.

Yano T., Ozawa T., Masuda H. (2008) Structural and functional model systems for analysis of the active center of nitrile hydratase. *Chem. Lett.* 37: 672-677

Ye W., Combes D., Monsan P. (1988) Influence of additives on the thermostability of glucose oxidase. *Enzyme Microb. Technol.* 10: 498-502.

Yip K. S., Stillman T. J. Britton K. L., Artymiuk P. J. Baker P. J. Sedelnikova S. E., Engel P.C., Pasquo A., Chiaraluce R., Consalvi V. (1995) The structure of *Pyrococcus fusiosus* glutamate dehydrogenase reveals a key role for ion-pair networks in maintaining enzyme stability at extreme temperatures. *Structure* 15: 1147-1158.

Zaks A. and Klibanov A. M. (1988) The effect of water on enzyme activity in organic media. *J. Biol. Chem.* 263: 8017-8021.

Zaks A and Klibanov A. M. (1985) Enzyme-catalyzed processes in organic solvents. *Proc. Natl. Acad. Sci. USA.* 82: 3192-3196.

Zhao H. (2002) Directed evolution of enzymes and pathways for industrial biocatalysis. *Curr. Opin. Biotechnol.* 13: 104-110.

Zuber H. (1988) Temperature adaptation of lactate dehydrogenase. Structural, functional and genetic aspects. *Biophys. Chem.* 29: 171-179.

University of Cape Town